



University
of Antwerp

Faculty of Medicine and Health Sciences
Laboratory of Cell Biology and Histology
Molecular Pathology Group

Immunological biomarkers of COVID-19: response to vaccination and monoclonal antibody treatments in immunocompromised patients

Immunologische biomarkers van COVID-19: reactie op vaccinatie en monoklonale antilichaambehandelingen in immunogecompromitteerde patiënten

PhD thesis submitted for the degree of Doctor of Medical Sciences at the University of Antwerp to be defended by

Angelina Konnova

Promotors: Prof. Samir Kumar-Singh
Prof. Surbhi Malhotra-Kumar

Begeleiders: Dr. An Hotterbeekx
Dr. Matilda Berkell

Antwerp, 2023

Disclaimer

The authors allow to consult and copy parts of this work for personal use. Further reproduction or transmission in any form or by any means, without the prior permission of the authors is strictly forbidden.

Members of the doctoral jury

Prof. Samir Kumar-Singh, *Promotor*

Molecular Pathology Group, Laboratory of Cell Biology and Histology, Faculty of Medicine and Health Sciences, University of Antwerp, Belgium

Prof. Surbhi Malhotra-Kumar, *Promotor*

Laboratory of Medical Microbiology, Vaccine and Infectious disease Institute, University of Antwerp, Antwerp, Belgium

Dr. An Hotterbeekx, *Begeleider*

Molecular Pathology Group, Laboratory of Cell Biology and Histology, Faculty of Medicine and Health Sciences, University of Antwerp, Belgium

Dr. Matilda Berkell, *Begeleider*

Molecular Pathology Group, Laboratory of Cell Biology and Histology, Faculty of Medicine and Health Sciences, University of Antwerp, Belgium

Laboratory of Medical Microbiology, Vaccine and Infectious disease Institute, University of Antwerp, Antwerp, Belgium

Internal doctoral committee

Prof. Annemieke Smet, *Committee chairperson*

Laboratory of Experimental Medicine and Pediatrics, University of Antwerp, Antwerp, Belgium

Infla-Med Centre of Excellence, University of Antwerp, Antwerp, Belgium

Prof. Ingrid De Meester, *Committee member*

Laboratory of Medical Biochemistry, Department of Pharmaceutical Sciences, University of Antwerp, Antwerp, Belgium

External members of the jury

Prof. Lieve Naesens, *External jury member*

Laboratory of Virology and Chemotherapy (Rega Institute), Department of Microbiology, Immunology and Transplantation, KU Leuven, Leuven, Belgium

Prof. Charlotte Charpentier, *External jury member*

Agents infectieux et hygiène hospitalière, Hôpital Bichat, Paris, France

Prof. Wim Adriansen, *External jury member*

Head of Clinical Immunology Unit, Department of Clinical Sciences, Institute of Tropical Medicine, Antwerp, Belgium

Table of Contents

List of Abbreviations.....	- 1 -
Abstract and Aims	- 5 -
Chapter 1 (Part A):.....	- 9 -
COVID-19: Diagnosis, Prevention, and Treatment strategies.....	- 9 -
SARS-CoV-2 structure and genome organisation	- 9 -
SARS-CoV-2 detection and COVID-19 diagnosis	- 10 -
COVID-19 vaccines	- 11 -
COVID-19 treatments.....	- 15 -
References.....	- 17 -
Chapter 1 (Part B):.....	- 21 -
COVID-19 and Cancer: Understanding the Link through Cytokine, Chemokine, and Growth Factor Dysregulation.....	- 21 -
Abstract	- 22 -
Introduction	- 23 -
COVID-19-associated immune misfiring	- 23 -
COVID-19 related CCG dysregulation affects cancer progression	- 25 -
Post-COVID-19 syndrome (PCS) in cancer patients	- 27 -
Circulating immune biomarkers reflect vaccine induced adaptive immune responses in cancer	- 31 -
Therapeutic protection of cancer patients predicted by host immune functioning.....	- 32 -
References.....	- 33 -
Chapter 2:	- 41 -
Sample collection, management and processing within the ORCHESTRA consortium.....	- 41 -
Objectives and brief description of sub-studies within ORCHESTRA.....	- 41 -
Characterisation of SARS-CoV-2 viral variants (Task 6.2, <i>not part of this thesis</i>)	- 41 -
Characterisation of serological markers of SARS-CoV-2 infection (Task 6.3)	- 41 -
Characterisation of cellular immunity for SARS-CoV-2 infection (Task 6.4, <i>not part of this thesis</i>)...	- 42 -
Cytokinome analysis (Task 6.5)	- 42 -
Next generation sequencing (NGS) of COVID-19 cohorts (Task 6.6, <i>not part of this thesis</i>)	- 42 -
Epigenome-wide analyses (Task 6.7, <i>not part of this thesis</i>)	- 42 -
Intestinal Microbiome Profiling (Task 6.8, <i>not part of this thesis</i>).....	- 42 -
Respiratory microbiome dynamics (Task 6.9, <i>not part of this thesis</i>).....	- 42 -
Sampling timepoints	- 43 -
Sampling timepoints for COVID-19 patients (including re-infections and breakthrough infections in vaccinated individuals).....	- 43 -

Sampling timepoints for vaccinated individuals	- 43 -
Storage instructions and destination sites	- 47 -
Sample workflow, redcap instruments, and Labelling instructions	- 47 -
Study documentation	- 50 -
Shipment Manifest	- 50 -
Shipping instructions and sample reconciliation	- 51 -
Anti-IgG measurements in serum samples.....	- 51 -
ACE2 neutralization measurements in serum samples	- 54 -
Cytokine, chemokine and growth factor (CCG) measurements in plasma samples	- 55 -
Appendices.....	- 56 -
Appendix 1. Serum sample collection and storage instructions	- 56 -
Appendix 2. EDTA plasma sample collection and storage instructions.....	- 57 -
Appendix 3. Shipment Manifest	- 58 -
Appendix 4. Shipment Request Form	- 59 -
Appendix 5. Transmission Sheet – Material and Data Transfer Agreement	- 60 -
Chapter 3:.....	- 61 -
Predictive model for BNT162b2 vaccine response in cancer patients based on blood cytokines and growth factors	- 61 -
Abstract.....	- 63 -
Background	- 63 -
Methods	- 63 -
Results	- 63 -
Conclusion	- 63 -
Introduction	- 64 -
Material and Methods	- 64 -
Patient Population and study design	- 64 -
Sample collection and processing.....	- 65 -
Cytokine, chemokine and growth factor (CCG) measurements in plasma.....	- 65 -
Anti-RBD IgG measurements in serum	- 66 -
Statistics	- 66 -
Results.....	- 67 -
Activation of early immune responses by BNT162b2 in cancer patients	- 67 -
Type of cancer therapy does not majorly alter the CCG profile induced by the BNT162b2 mRNA vaccine.....	- 69 -
CRP, IL-15, IL-18, and PIGF predict a poor BNT162b2 immune response in cancer patients.....	- 70 -
Discussion	- 72 -
Declaration of Interest.....	- 73 -
Author contributions	- 73 -
Funding	- 73 -
Supplementary Methods	- 73 -
Sample collection and processing.....	- 73 -
Cytokine, chemokine and growth factor (CCG) measurements in plasma.....	- 74 -

Supplementary Figures and Tables	- 75 -
References.....	- 80 -
Chapter 4:	- 85 -
Using machine learning to predict antibody response to SARS-CoV-2 vaccination in Solid Organ Transplant Recipients: the multicentre ORCHESTRA cohort	- 85 -
Abstract	- 87 -
Objectives.....	- 87 -
Methods	- 87 -
Results	- 87 -
Conclusions.....	- 87 -
Introduction	- 88 -
Methods	- 89 -
Variables.....	- 89 -
Laboratory assays	- 90 -
Statistical analysis.....	- 90 -
Results.....	- 90 -
Characteristics of study cohort	- 90 -
Serological assessment	- 91 -
Predictors of negative antibody response	- 91 -
Discussion.....	- 95 -
ORCHESTRA-WP4 study group.....	- 96 -
Transparency declaration	- 97 -
Financial support.....	- 97 -
Author contributions.....	- 97 -
Supplementary Figures and Tables.....	- 98 -
References.....	- 112 -
Chapter 5:	- 115 -
Host immunological responses facilitate development of SARS-CoV-2 mutations in patients receiving antibody treatments.....	- 115 -
Abstract	- 116 -
Background:	- 116 -
Methods:	- 116 -
Results:	- 116 -
Conclusions:	- 116 -
Introduction	- 117 -
Results.....	- 118 -
Immunocompromised COVID-19 patients receiving early mAb therapy continue to display significantly higher viral loads compared to non-immunocompromised patients (<i>not part of this thesis</i>)	- 118 -
Immunocompromised patients display higher rates of SARS-CoV-2 Spike RBD mutations (<i>not part of this thesis</i>).....	- 122 -
Therapeutic mAb titers are not directly associated with development of Spike RBD mutations	- 125 -

Neutralizing capacities of mAbs are (co-)drivers of development of escape mutants	- 126 -
Natural adaptive T-cell immunity is associated with development of SARS-CoV-2 escape mutants (<i>not part of this thesis</i>)	- 127 -
Host immune profile as a predictor of Spike RBD escape mutants	- 129 -
Discussion	- 131 -
Material and Methods	- 134 -
Study design	- 134 -
SARS-CoV-2 viral load and variant sequencing	- 134 -
Serology.....	- 134 -
ACE2 neutralization measurements in serum	- 135 -
Measurements of circulating immune-related biomarkers (CIB) in serum.....	- 135 -
SARS-CoV-2 specific cellular responses	- 135 -
Flow cytometry	- 135 -
Statistical analysis	- 136 -
Study approval	- 136 -
Data availability.....	- 136 -
Author Contribution.....	- 137 -
Supplementary Methods	- 137 -
RNA extraction, cDNA conversion, library preparation, and SARS-CoV-2 genome sequencing	- 137 -
SARS-CoV-2 RT-qPCR.....	- 137 -
SARS-CoV-2 variant detection.....	- 137 -
SNP validation using Sanger sequencing	- 138 -
Serology.....	- 138 -
ACE2 neutralization measurements in serum	- 139 -
SARS-CoV-2 specific cellular responses	- 139 -
Flow cytometry	- 139 -
Supplemental Tables.....	- 141 -
Supplemental Figures	- 148 -
References	- 155 -
Supplementary References.....	- 160 -
Chapter 6:.....	- 163 -
Neutralization capacity of bamlanivimab with or without etesevimab, casirivimab/imdevimab, sotrovimab and tixagevimab/cilgavimab monoclonal antibodies against currently circulating SARS-CoV-2 Omicron variants.....	- 163 -
Abstract.....	- 164 -
Background	- 164 -
Methods.....	- 164 -
Results	- 164 -
Conclusions	- 164 -
Introduction	- 165 -
Material and Methods	- 166 -
Trial design and sample collection.....	- 166 -
SARS-CoV-2 viral load and confirmation.....	- 166 -
Serology.....	- 166 -
ACE2 neutralization measurements in serum	- 166 -

Measurements of circulating immune-related biomarkers (CIB) in serum	- 167 -
Statistics	- 167 -
Results	- 167 -
Tixagevimab/cilgavimab should not be recommended for the treatment of acute COVID-19	- 167 -
Casirivimab/imdevimab and sotrovimab show non-overlapping superior neutralisation of the majority of Omicron sub-variants.....	- 169 -
Macrophage-associated metabolism of mAbs affects neutralisation by casirivimab/imdevimab ..	- 172 -
Discussion.....	- 173 -
Supplementary Figures	- 175 -
References.....	- 177 -
Chapter 7:	- 179 -
Conclusions and Future Perspectives.....	- 179 -
Future perspectives and deep cytokine profiling	- 181 -
References.....	- 182 -
Academic CV – Angelina Konnova	- 185 -
Contact information	- 185 -
Education	- 185 -
Publications	- 185 -
Manuscripts in preparation/Abstracts submitted	- 187 -
Oral and poster presentations	- 188 -
Guidance in Master and Bachelor Dissertations.....	- 189 -
Grants/Awards	- 189 -
Acknowledgements	- 191 -

List of Abbreviations

AbR	Antibody Response
ACE2	Angiotensin-Converting Enzyme 2
AE	Adverse Event
ARDS	Acute Respiratory Distress Syndrome
AUROC	Area Under the Curve Receiver Operating Characteristic
BA	Balanced Accuracy
BDNF	Brain-Derived Neurotrophic Factor
bFGF	Community Acquired Pneumonia
CAP	Community Acquired Pneumonia
CCGs	Cytokines, Chemokines, and Growth factors
CIBs	Circulating Immune Biomarkers
COVID-19	Coronavirus Disease 2019
CRP	C-Reactive Protein
CRS	Cytokine Release Syndrome
CTACK	Cutaneous T-cell Attracting Chemokine
CTCAE	Common Terminology Criteria for Adverse Events
ELISA	Enzyme-Linked Immunosorbent Assay
EMA	European Medicines Agency
EMT	Epithelial-to-Mesenchymal Transition
ENA	European Nucleotide Archive
EUA	Emergency Use Authorization
FDA	US Food and Drug Administration
Flt-1	Fms-like tyrosine kinase 1
GM-CSF	Granulocyte-Macrophage Colony-Stimulating Factor

HCWs	Health Care Workers
i.m.	Intramuscularly
ICAM-1	Intercellular Adhesion Molecule 1
IFN	Interferon
IL	Interleukin
IL-1Ra	IL-1 Receptor antagonist
IL-2R α	IL-2 Receptor α
IL-6R	IL-6 Receptor
IP-10	IFN- γ Induced Protein 10
JAK	Janus kinase
KNN	k-Nearest Neighbours
LLQ	Lower Limit of Quantitation
M-CSF	Macrophage Colony Stimulating Factor
mAb	Monoclonal Antibody
MCP	Monocyte Chemoattractant Protein
MDSC	Myeloid-Derived Suppressor Cells
MIP	Macrophage Inflammatory Protein
MSD	Meso Scale Discovery
OLR	Ordinal Logistic Regression
ORF	Open Reading Frame
PBMC	Peripheral Blood Mononuclear Cell
PCS	Post-COVID-19 Syndrome
PK	Pharmacokinetics
PIGF	Placental Growth Factor
PLS-DA	Partial Least-Squares Discriminant Analysis
PRAUC	Area Under the Precision-Recall Curve

RFC	Random Forest classifiers
ROC	Receiver Operating Characteristic
SAA	Serum Amyloid A
SARS-CoV-2	Severe Acute Respiratory Syndrome Coronavirus 2
SMOTE	Synthetic Minority Oversampling Technique
SNP	Single Nucleotide Polymorphism
SOT	Solid Organ Transplant
TAM	Tumour Associated Macrophage
TGF- β	Tumor Growth Factor β
Tie-2	Angiopoietin Receptor 1
TIL	Tumour Infiltrating Lymphocyte
TNF α	Tumour Necrosis Factor- α
Treg	Regulatory T cells
TrkB	Tyrosine kinase B
TSLP	Thymic Stromal Lymphopoietin
ULQ	Upper Limit of Quantitation
VCAM-1	Vascular Cell Adhesion Molecule 1
VEGF	Vascular Endothelial Growth Factor
VOC	Variant of Concern
VOI	Variant of Interest
WHO	World Health Organisation

Abstract and Aims

COVID-19 has caused almost 7 million deaths worldwide with 768 million documented cases of SARS-CoV-2 infections. However, the burden of the pandemic could have been even higher without the development of effective COVID-19 treatments and vaccines in record time. The main objective of this thesis was to expand our understanding of immunological responses to COVID-19 and COVID-19 vaccinations with the focus on identifying immune-related blood biomarkers.

As part of my doctoral thesis, I studied multiple cohorts of immunocompromised patients with COVID-19, or at high risk of developing COVID-19, with the overall aim to build immune-related signatures to predict either development of vaccination responses or responses to treatments, such as those with anti-SARS-CoV-2 monoclonal antibodies (mAb). We hypothesised that some of the immunocompromised patients are unable to develop sufficient antibody responses despite repeated vaccinations and that blood cytokines, chemokines and growth factors (CCGs) can reflect the intrinsic immune state of immunocompromised patients, predicting these responses. Additionally, we hypothesised that the intrinsic or COVID-19-induced immune state can affect the course of COVID-19 disease or treatment, for example, affecting mutation development upon mAb treatment. Therefore, the **specific aims** of my doctoral thesis are:

1. To propose an immunological biomarker signature to identify non-responders to the COVID-19 vaccine among patients with solid and haematological malignancies.
2. To assess post-vaccination antibody response in solid organ transplant (SOT) recipients and identify clinical predictors of antibody response in this patient population.
3. To evaluate host immunological biomarkers of SARS-CoV-2 mutation development upon mAb treatment and to study the pharmacokinetics of the mAb treatment as well as the ability of different mAbs to neutralize SARS-CoV-2 variants of concern (VOCs).

In the **Introduction (Chapter 1)**, I provide a comprehensive overview of literature describing COVID-19-related immune dysregulation. In this chapter, my focus is cytokine and chemokines immunity, specifically in cancer patients, and to discuss molecular causes and consequences of COVID-19 in the context of cancer. While studying the role of CCGs in cancer and in COVID-19, I explored their dysregulation in acute COVID-19 as well as its potential long-term sequelae (post-COVID-19 syndrome). I also discussed the potential of CCGs as circulating immune biomarkers of successful vaccination response and SARS-CoV-2 mutation development. This chapter highlights the COVID-19 linked CCG dysregulation in cancer patients and the need for deep cytokine profiling in this patient group.

In **Chapter 3** and under research **Aim 1**, we proposed a blood-based signature of cytokines and growth factors that can be employed in identifying cancer patients at persistent high risk of COVID-19 despite vaccination with BNT162b2. In this chapter, we employed machine learning approaches to identify a biomarker signature based on blood cytokines, chemokines, and immune- and non-immune-related growth factors linked to vaccine immunogenicity in 199 cancer patients receiving the BNT162b2 vaccine. We identified a cytokine and growth factor profile that correctly classified patients with a diminished vaccine response with more than 80% accuracy. Amongst these, CRP showed the highest predictive value for poor response to vaccine administration. Importantly, this

unique signature of vaccine response was present at different studied timepoints both before and after vaccination and was not majorly affected by different anti-cancer treatments. These data suggest that immune signature, like the one proposed in this paper, may reflect the inherent immunological constitution of some cancer patients who are refractive to immunotherapy.

In **Chapter 4**, as **Aim 2**, we studied another vulnerable population, namely solid organ transplant (SOT) recipients, and assessed the antibody response after COVID-19 vaccination. In this chapter, SOT recipients receiving SARS-CoV-2 vaccination were prospectively enrolled (March 2021-January 2022) at six hospitals in Italy and Spain. Antibody response was assessed at first dose (t0), second dose (t1), 3±1 month (t2), and 1 month after third dose (t3). Antibody response in SOT recipients was compared to healthcare workers (HCWs) at t0, t1, and t2. This study demonstrated that the antibody levels in HCWs were significantly higher than the ones measured in the SOT population. In the SOT recipients, the kinetics showed an increase in antibody levels up to 76 days and a non-significant decrease after 118 days. Antibody response in SOT recipients was further improved upon the administration of the booster vaccine. Additionally, in collaboration with other members of our study group (EU H2020 ORCHESTRA), we showed that several clinical parameters, including age, anti-metabolites and steroid treatments, time since transplantation, and type of transplantation, significantly affect antibody response in SOT recipients. However, unfortunately, the best ML model we found only reached a moderate prediction accuracy. Therefore, these data suggest that clinical covariates provide only limited information about potential post-vaccine antibody development in SOT recipients.

Given the inability of some immunocompromised patients to develop sufficient antibody responses to COVID-19 vaccines that was discussed in Chapters 3 and 4, it is important to assess currently available treatment and prophylaxis options. Therefore, subsequent chapters of this thesis focus on mAb treatments, which are used for the treatment and prophylaxis of COVID-19. Specifically, as part of **Chapter 5** and addressed as **Aim 3**, we evaluated the effect of mAb treatments and of host immune factors on Spike mutation development. This chapter describes a prospective, observational, monocentric ORCHESTRA cohort study, conducted between March 2021 and November 2022, in which mild-to-moderately ill COVID-19 patients receiving bamlanivimab, bamlanivimab/etesevimab, casirivimab/imdevimab, or sotrovimab were longitudinally studied over 28 days for viral loads, de novo Spike mutations, mAb kinetics (part of my thesis), seroneutralization against infecting variants of concern (part of my thesis), T-cell immunity and cytokine immunity (part of my thesis). Overall, our data suggest that patients treated with various mAbs develop evasive Spike mutations with remarkable speed and high specificity to the targeted mAb-binding sites. We also showed that mAb treatment results in extremely high antibody titres, however, with more than 10,000 times ‘free’ therapeutic mAb titers measured in blood than those required for effective virus neutralization, expectedly, we did not find any direct selective pressure of therapeutic mAbs in the development of SARS-CoV-2 Spike RBD mutations. Instead, we showed that an anti-inflammatory and healing-promoting host milieu facilitates development of Spike mutations, where 4 CIBs identified patients at high risk of developing escape mutations against therapeutic mAbs with high accuracy. These data demonstrated that host-driven immune and non-immune responses are essential for development of mutant SARS-CoV-2 and supported point-of-care decision-making in reducing the risk of mAb treatment failure and improving mitigation strategies for possible dissemination of escape SARS-CoV-2 mutants.

Continuing into mAb research, as part of **Chapter 6**, we studied neutralizing capacity of bamlanivimab, bamlanivimab/etesevimab, casirivimab/imdevimab, sotrovimab or tixagevimab/cilgavimab against SARS-CoV-2-CoV-2 variants of concern (VOCs). Studying seroneutralization response against 32 VOCs at Day 2, casirivimab/imdevimab combination was the most effective therapy against the majority of variants, including de-escalated, Delta and Omicron (BA.2, BA.2L452M, BA.2.12, BA.2.75, BA.4.,6 and BF.7) sub-variants. However, for other sub-variants (BA.1, BA.1L452R, BA.1R346K, BA.2L452R, BA.2.75.2, BA.3, BQ.1, BQ.1.1, and XBB.1), sotrovimab demonstrated a superior neutralization capacity. Additionally, for BA.4 and BA.5, casirivimab/imdevimab, sotrovimab, and tixagevimab/cilgavimab demonstrated comparable neutralization. Additionally, we observed that specific mutations, such as L452R, can be drivers of mAb resistance. Our data suggest that clinicians should take the circulating variant into consideration while prescribing different mAbs.

I believe that the work performed during my doctoral thesis has provided us with useful insights into our understanding of the molecular pathology of COVID-19 and would also form the basis for future research in the development of effective treatments and prevention strategies for COVID-19.

Chapter 1 (Part A): COVID-19: Diagnosis, Prevention, and Treatment strategies

At the end of 2019, a new coronavirus emerged in Wuhan, China, causing severe respiratory syndrome and a lethal form of pneumonia and, 3 months later, the World Health Organization characterized the outbreak as a pandemic called Coronavirus disease 2019 (COVID-19). The pandemic caused by the novel coronavirus termed Severe Acute Respiratory Syndrome Coronavirus 2 (SARS-CoV-2) has led to a profound impact on medical care systems, economic progress, and social cohesion around the world. As of July 20, 2023, there were almost 7 million reported deaths and 768 million cases of COVID-19, as reported by the World Health Organisation (WHO). However, the burden of the pandemic could have been even higher without the development of effective COVID-19 treatments and vaccines in record time.

SARS-CoV-2 structure and genome organisation

SARS-CoV-2 genome organisation is shared with other betacoronaviruses, including 79% genome sequence identity with SARS-CoV and 50% with MERS-CoV ¹. The six functional open reading frames (ORFs) are arranged in order from 5' to 3' end and include *Replicase (ORF1a/ORF1b)*, *Spike*, *Envelope*, *Membrane*, and *Nucleocapsid*. Additionally, seven putative ORFs encoding accessory proteins are interspersed between the structural genes ² (**Figure 1A**).

The SARS-CoV-2 virion is thus made up of four structural proteins: Spike, Envelope, Membrane, and Nucleocapsid (**Figure 1B**). Most of these structural proteins of SARS-CoV-2 share more than 90% amino acid identity with SARS-CoV, except for the Spike protein, which diverges ¹. Similar to some other coronaviruses, Spike protein of SARS-CoV-2 is cleaved in S1 and S2 subunits during their biosynthesis in the infected cells, while in some other coronaviruses, Spike protein is cleaved only when they reach the next target cell ³. Apart from the structural proteins, SARS-CoV-2 genome contains the *Replicase* gene, which encodes a large polyprotein (pp1ab) that is proteolytically cleaved into 16 non-structural proteins involved in transcription and virus replication. Like the majority of structural proteins, most of these SARS-CoV-2 non-structural proteins have greater than 85% amino acid sequence identity with SARS-CoV ².

Spike protein is an essential protein for the SARS-CoV-2 entry into the host cell, since the S1 subunit of the Spike protein binds the host angiotensin-converting enzyme 2 (ACE2) and the S2 subunit anchors the Spike protein to the membrane. The primary role of ACE2 in normal physiology is to convert angiotensin I and angiotensin II into angiotensin-(1–9) and angiotensin-(1–7), respectively, regulating vasoconstriction and blood pressure. Afterwards, cleavage of an additional site internal to the S2 subunit is performed by the host TMPRSS2 protein at the cell surface or by Cathepsin L in the endosomal compartment, causing conformational changes and promoting viral entry ³.

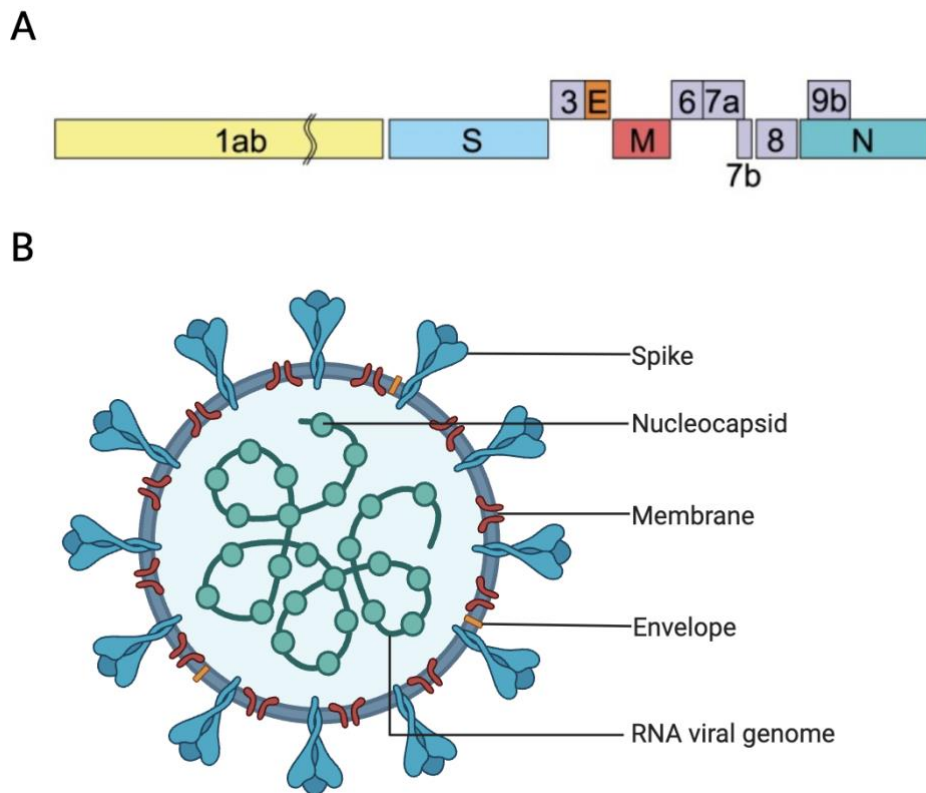


Figure 1. Structure of the SARS-CoV-2 virus. (A) Schematic representation of SARS-CoV-2 genome organisation adapted from ². (B) Structural proteins of the SARS-CoV-2 virion. Figure was made in BioRender.

SARS-CoV-2 detection and COVID-19 diagnosis

Understanding of SARS-CoV-2 genome and virion structure has led to rapid development of diagnostic methods. SARS-CoV-2 detection technologies mainly target either specific viral nucleic acids (RT-PCR-based molecular testing), proteins (antigen testing), or anti-SARS-CoV-2 antibodies (serological testing). The choice between each of these tests depends on the purpose of the test, biological sample availability, and sampling time ⁴. Additionally, it is important to consider patient's medical history, symptoms, and general clinical picture for a successful outcome of the diagnostic test.

However, the emergence of novel SARS-CoV-2 variants, including variants of interest (VOIs) and high-risk VOCs, has change the course of the pandemic, including effectiveness of the abovementioned diagnostic tools. VOIs and VOCs include variants with accumulated mutations that affect receptor binding, treatment efficacy, immune evasion, disease severity, and transmissibility ⁵. Evolution of SARS-CoV-2 variants in Belgium and Italy (from where most of the samples utilized in the study emerged) is summarised in **Figures 2 and 3**, respectively. Due to the accumulation of a large number of mutations, VOIs and VOCs are occasionally able to avoid original diagnostic methods, highlighting the importance of new versatile diagnostic technologies ⁵.

COVID-19 vaccines

One of the biggest milestones throughout the pandemic was the development of efficient COVID-19 vaccines capable of decreasing the number of infections and preventing development of severe COVID-19. The nine leading vaccines – manufactured by Pfizer/BioNTech (BNT162b2), Moderna/NIAID (mRNA-1273), Oxford/AstraZeneca (AZD1222), Janssen/Johnson&Johnson (Ad26.CoV.S), Gamaleya (Sputnik V), Novavax/CEPI (NVX-CoV2373), Sinopharm (BBIBP-CorV), Bharat Biotech (Covaxin), and Sinovac (CoronaVac) – have been developed against the wild-type Wuhan strain ⁶ (**Table 1**). These vaccines utilised different technologies, including innovative mRNA vaccines encoding full-length Spike protein (BNT162b2, mRNA-1273), adenoviral vector vaccines containing Spike protein (Sputnik V, AZD1222, Ad26.COVS), inactivated SARS-CoV-2 virus vaccines (BBIBP-CorV, CoronaVac, Covaxin), and Spike protein subunit vaccine (NVX-CoV-2373) ⁶. Overall, COVID-19 vaccines were able to provide impressive protection against symptomatic COVID-19 with efficiency ranging from 51 to 96% ⁶.

However, vaccine efficacy was jeopardised by the rapid emergence and spread of SARS-CoV-2 VOCs (Figures 2 and 3) that could escape vaccine-induced neutralising antibodies and cell-mediated immune responses. After full immunization, mRNA vaccine effectiveness against symptomatic disease was 88–100% against Alpha, 76–100% against Beta/Gamma, and 47.3–88% against Delta variants ⁷. Reduction of effectiveness for the AZD1222 vaccine was even more pronounced with effectiveness against disease caused by Alpha variants being 74.5% and by Delta being 67% ⁷. Smaller studies indicated that CoronaVac effectiveness was reduced to 36.8–73.8% against the disease caused by Alpha/Gamma/D614G SARS-CoV-2 variants ⁷. However, despite a significant decrease in efficiency against symptomatic infections, effectiveness of mRNA, AZD1222, and CoronaVac vaccines against hospitalization and death upon infections with Alpha, Beta, Gamma and Delta variants remained relatively high (80-95%) ⁷.

Upon the emergence of the Omicron variant, studies have shown that protection provided by various vaccines against hospitalization and death from severe COVID-19 disease is decreasing slowly after a two-dose vaccination ⁸. Specifically, Both BA.1 and BA.2 have been shown to evade neutralizing antibodies elicited by a primary series of mRNA (mRNA-1273 or BNT162b2), vector-based (Ad26.CoV.S, Sputnik V, or AZD1222), subunit (NVX-CoV2373), and inactivated (BBIBP-CorV) vaccines, although some activity is retained from mRNA or ChAdOx1 nCoV-19 vaccination ⁹. Later Omicron sub-lineages, such as BA.4, BA.5, and BA.2.12.1, escape original vaccine-elicited neutralizing antibodies to an even greater extent than BA.1 and BA.2 ^{10,11}. Several events were able to improve immune responses against these VOCs. Specifically, administration of booster vaccines, BA.1- or BA.4/5-specific boosters, and infection with SARS-CoV-2 were able to increase neutralizing antibody titres against Omicron variants ¹². However, most recent Omicron sub-variants, such as BA.2.75.2, BQ.1, BQ.1.1, and XBB.1, have been shown to exhibit an even lower neutralization sensitivity than BA.4/BA.5, indicating further neutralization escape with newly emerging sub-lineages ¹³⁻¹⁵.

Finally, new COVID-19 vaccine types are looking into ways to prevent an infection from becoming established in the first place, rather than only curtailing infection and protecting against the development of disease symptoms. Specifically, mucosal vaccines provide an interesting opportunity to induce adaptive immune responses at mucosal sites, involving antibody secretion and activation

Belgium

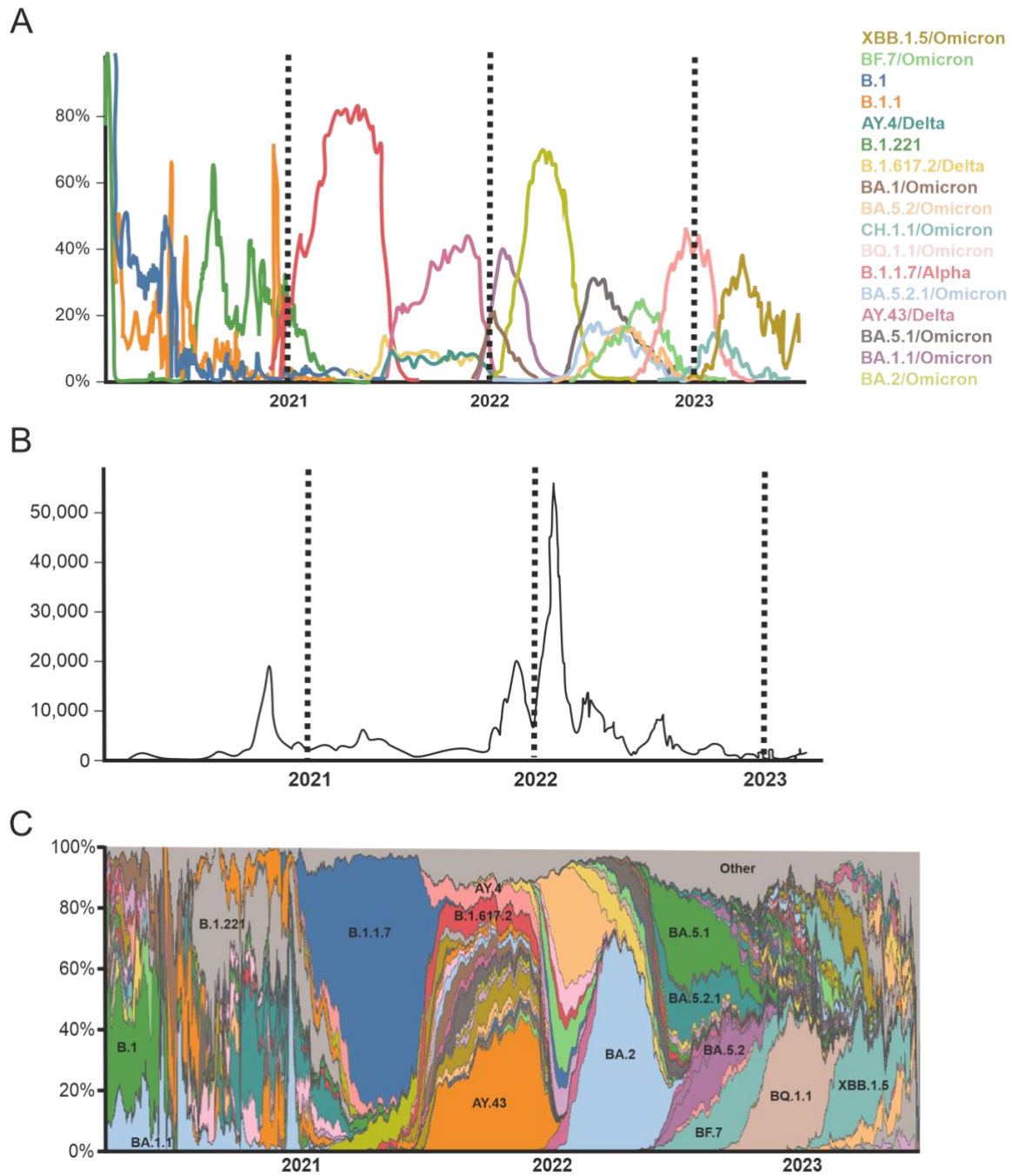


Figure 2. Evolution of viral variants in Belgium. (A) Schematic representation of the longitudinal prevalence of the dominant SARS-CoV-2 PANGO lineages. (B) Number of infections with SARS-CoV-2. (C) Composition of SARS-CoV-2 infections in terms of SARS-CoV-2 PANGO lineages. Adapted from <https://outbreak.info>.

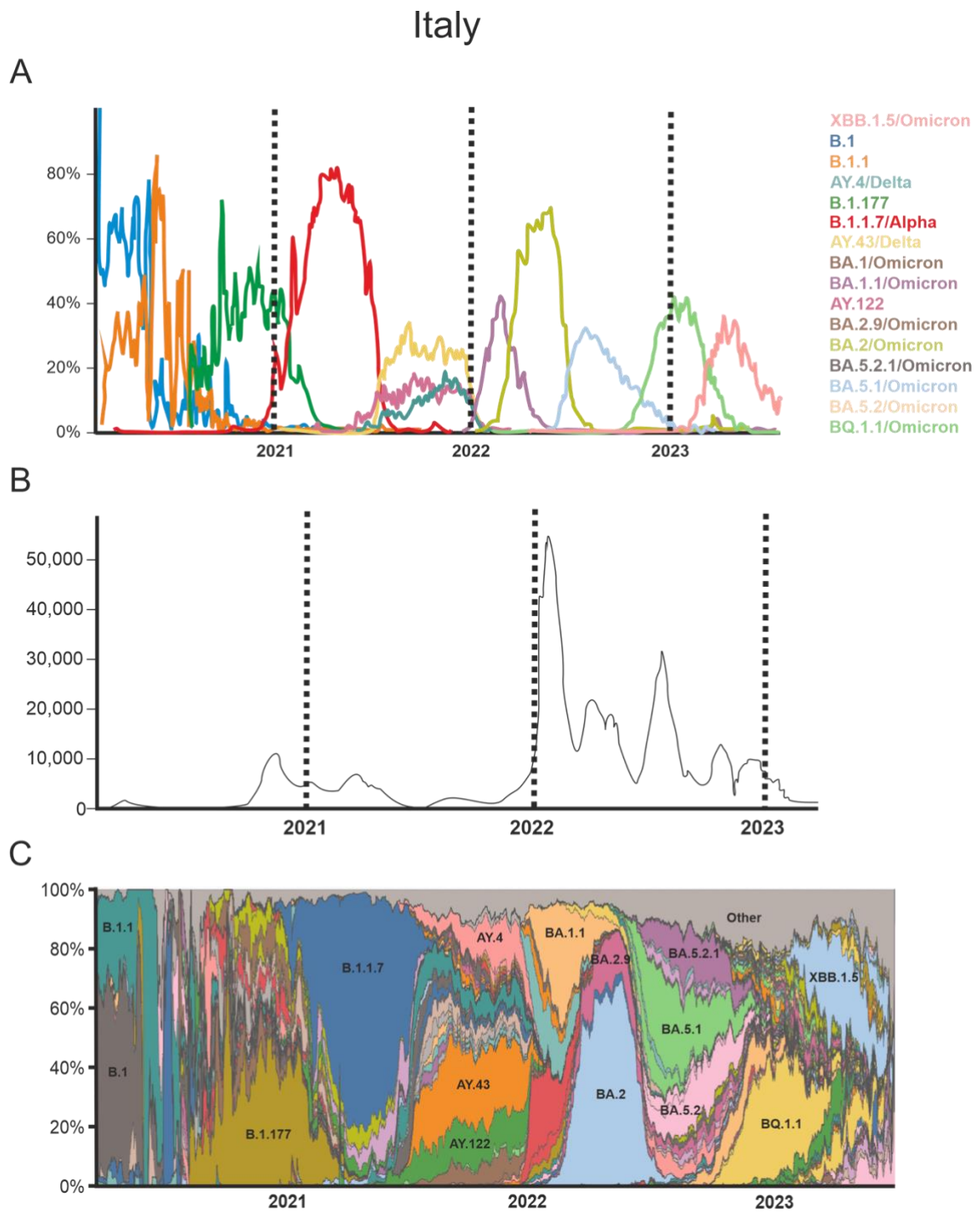


Figure 3. Evolution of viral variants in Italy. (A) Schematic representation of the longitudinal prevalence of the dominant SARS-CoV-2 variants. (B) Number of infections with SARS-CoV-2. (C) Composition of SARS-CoV-2 infections in terms of SARS-CoV-2 PANGO lineages. Adapted from <https://outbreak.info>.

Table 1. Characteristics of nine lead vaccines. Adapted from ⁶.

	BNT162b2	mRNA-1273	AZD1222	Ad26.COV2.S	Sputnik V	BBIBP-CorV	CoronaVac	Covaxin	NVX-CoV-2373
Developer	Pfizer/ BioNTech	Moderna/ NIAD	University of Oxford/ AstraZeneca	Janssen/ Johnson & Johnson	Gamaleya	Sinopharm	Sinovac Biotech	Bharat Biotech	Novavax and CEPI
Type	mRNA	mRNA	Chimpanzee adenoviral vector	Human adenoviral vector	Human adenoviral vectors	Inactivated virus	Inactivated virus	Inactivated virus	Protein subunit
Antigen	S protein	S protein	S protein	S protein	S protein	Whole virus	Whole virus	Whole virus	S protein
Dosages	Two	Two	Two	One	Two	Two	Two	Two	Two
Interval	21 days apart	28 days apart	12 weeks apart		21 days apart	21 days apart	14 days apart	28 days apart	21 days apart
Efficacy	95%	94%	81%	66%	92%	78%	51%	78%	96%
Most common side effects	Local post- injection pain, fatigue, headache	Local injection-site reactions, fever, fatigue, headache	Injection site pain, fever, headache	Injection site pain, headache, fatigue, muscle pain, nausea	Injection site pain, hyperthermia, headache, asthenia, muscle and joint pain	Injection site pain, fever, headache, fatigue	Injection site pain, headache, fatigue	Injection site pain, headache, fatigue, fever	Injection site pain and tenderness, fatigue, headache, muscle pain
Safety concern	Anaphylaxis, myocarditis	Anaphylaxis, myocarditis	Thrombosis and thrombocytopen ia syndrome	Anaphylaxis, TTS, CVST, GBS, myocarditis			Pityriasis rosea, reactive arthritis		

of tissue-resident T cells, eliminating the need for transfer of antibodies and cells through the mucosal barrier. However, mucosal vaccines have not yet been licenced for the use against COVID-19, mostly due to the fact that recent advances, including RNA and DNA vaccines, have not yet been successfully translated to mucosal vaccines ¹⁶.

In this thesis, we have studied the efficacy of COVID-19 vaccination specifically in vulnerable populations, such as patients with solid or haematological malignancies and solid organ transplant recipients. Additionally, using machine learning algorithms, we have identified clinical and molecular biomarkers of COVID-19 vaccine response.

COVID-19 treatments

During the COVID-19 public health emergency, the Food and Drug Administration (FDA) and European Medicines Agency (EMA) issued Emergency Use Authorization (EUA) for various new drugs and medical products without full agency approval. Currently, antivirals, neutralising antibodies, convalescent plasma, anti-inflammatory agents, and some common drugs together with combination therapies are used for inhibition, treatment, or supportive care of COVID-19 patients¹⁷⁻¹⁹.

Importantly, antivirals, monoclonal antibodies (mAb), and convalescent plasma treatments are used as a first-line treatment in patients at high risk of developing severe COVID-19 ^{18,19}. Common mAbs utilised in COVID-19 are summarized in **Table 2**.

Table 2. Characteristics of monoclonal antibodies studied in this thesis

	Mode of administration	Dosing	Designed against	FDA authorisation	EMA authorisation
Bamlanivimab	Intravenously	700mg	SARS-CoV-2 (2020)	No	No
Bamlanivimab/ Etesevimab	Intravenously	700mg, 700mg	SARS-CoV-2 (2020)	No	No
Casirivimab/ Imdevimab (Ronaprev)	Intravenously	600mg, 600mg	SARS-CoV-2 (2020)	No	Yes
Sotrovimab (Xevudy)	Intravenously	500mg	SARS-CoV	No	Yes
Tixagevimab/ Cilgavimab (Evusheld)	Intramuscularly	150mg, 150mg	SARS-CoV-2 (2020)	No	Yes

However, mAb therapies rely heavily on timely administration and are mostly ineffective in severe and critical cases. Moreover, mAbs, specifically tixagevimab/cilgavimab, are used prophylactically prior to exposure to SARS-CoV-2 in fragile patients unable to develop sufficient antibody responses post vaccine administration. Unfortunately, similarly to vaccines, emergence of new SARS-CoV-2 VOCs with mutations in mAb binding sites compromised efficiency of mAb therapies. Mutations observed in the BA.1 (Omicron) variant as well as binding sites of clinically relevant mAbs that are affected by these mutations are summarised in **Figure 4**. In this thesis, mAbs efficiency against different SARS-CoV-2 variants is discussed in more details in **Chapter 6**.

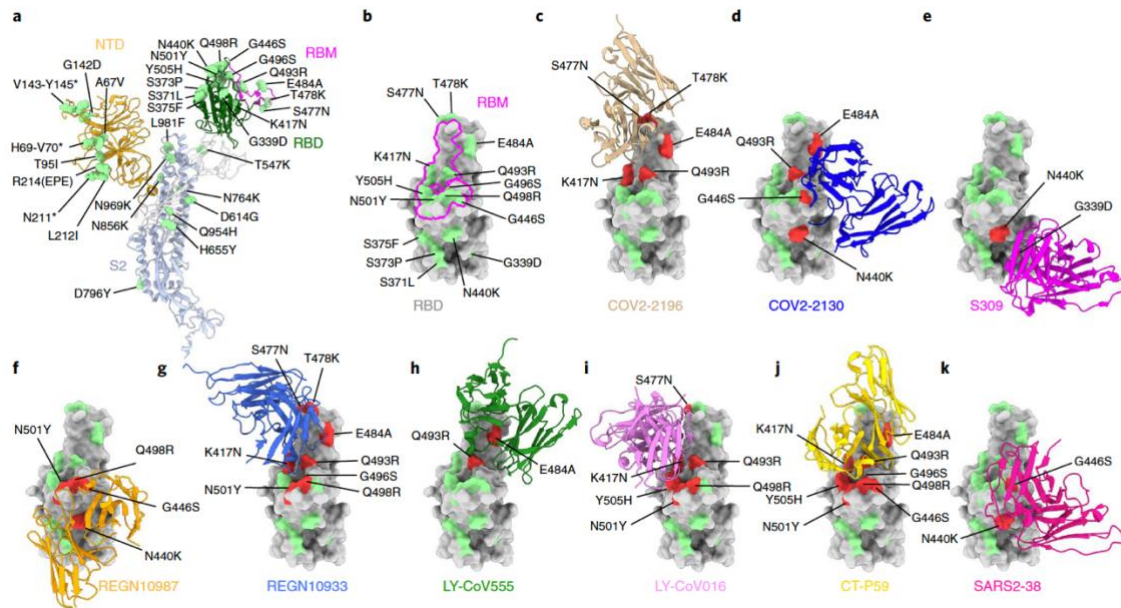


Figure 4. Summary of BA.1 mutation and MAb binding sites. (A, B) SARS-CoV-2 spike trimer (PDB: 7C2L and PDB: 6W41). One spike protomer is highlighted, showing the NTD in orange, RBD in green, RBM in magenta and S2 portion of the molecule in blue (A). Close-up view of the RBD with the RBM outlined in magenta (B). Amino acids that are changed in B.1.1.529 compared to WA1/2020 are indicated in light green (A, B), with the exception of N679K and P681H, which were not modeled in the structures used. (C-K) SARS-CoV-2 RBD bound by the following mAbs: COV2-2196, tixagevimab (PDB: 7L7D) (C); COV2-2130, cilgavimab (PDB: 7L7E) (D); S309, sotrovimab (PDB: 6WPS) (E); REGN10987, imdevimab (PDB: 6XDG) (F); REGN10933, casirivimab (PDB: 6XDG) (G); LY-CoV555, bamlanivimab (PDB: 7KMG) (H); LY-CoV016, etesevimab (PDB: 7C01) (I); CT-P59, regdanvimab (PDB: 7CM4) (J); and SARS2-38 (PDB: 7MKM) (K). Residues mutated in the B.1.1.529 RBD and contained in these mAbs' respective epitopes are shaded red, whereas those outside the epitope are shaded green. Adapted from ²⁰.

On the other hand, anti-inflammatory and immunosuppressive drugs, such as corticosteroids, IL-6 receptor blockers, and Janus kinase (JAK) inhibitors, are strongly recommended by WHO to be used in severe and critical cases of COVID-19 ²¹. These drugs are effective in curbing the overactivation of immune system upon SARS-CoV-2 infection, which is followed by the release of proinflammatory cytokines and chemokines, called cytokine release syndrome (CRS). In severe COVID-19, CRS has been characterized by increased secretion of Interleukin (IL)-6, Tumour

Necrosis Factor- α (TNF α), IL-8, Monocyte Chemoattractant Protein (MCP)-1, and Vascular Endothelial Growth Factor (VEGF) (discussed in more details in **Chapter 1 (Part B)**)^{22,23}. After several randomized clinical trials, corticosteroids, IL-6 receptor blockers, and JAK inhibitors have been proved to be able to improve survival in severe COVID-19^{18,19,24,25}.

All the above-mentioned treatments with different advantages or disadvantages targeting the virus or hyperimmune response were very beneficial to tackle the pandemic before effective vaccines and targeted anti-SARS-CoV-2 therapies were developed. In this thesis, five different monoclonal antibodies are studied in more details in terms of their effect on the SARS-CoV-2 virus evolution and effectiveness at the current stage of the pandemic (discussed in more details in **Chapters 4 and 5**). ORCHESTRA consortium

Development of effective treatments and vaccines has been a result of multiple successful collaborations. Several international consortia were established to tackle the pandemic with collaborative efforts. The research presented in this thesis was partially conducted within the ORCHESTRA consortium (<https://orchestra-cohort.eu>). ORCHESTRA is a three-year international research project aimed at tackling the COVID-19 pandemic. ORCHESTRA is led by the University of Verona and involving 26 partners (extending to a wider network of 37 partners) from 15 countries: Argentina, Belgium, Brazil, Congo, France, Gabon, Germany, India, Italy, Luxemburg, Netherlands, Romania, Slovakia, Spain, Venezuela. The goal of the project was to establish an international large-scale cohort for the conduct of retrospective and prospective studies in order to generate rigorous evidence to improve the prevention and treatment of COVID-19 and to be better prepared for future pandemics. ORCHESTRA project was funded by the European Union's Horizon 2020 research and innovation programme under the ERA vs CORONA Action Plan which was developed jointly by Commission services and national authorities.

Within the ORCHESTRA consortium, UAntwerpen acts as a central processing laboratory. FGGW mVISION Laboratory of Cell Biology and Histology–Molecular Pathology Group studied specifically the immunological responses to COVID-19 and COVID-19 vaccination in patients with and without immunocompromising conditions while the viral variant sequencing and viral loads were studied by Laboratory of Medical Microbiology. We focused on the identification of immunological biomarkers and development of prediction models that are described in more details in Chapters 1B, 2 and 3.

References

1. Lu, R., *et al.* Genomic characterisation and epidemiology of 2019 novel coronavirus: implications for virus origins and receptor binding. *Lancet* **395**, 565-574 (2020).
2. Chan, J.F., *et al.* Genomic characterization of the 2019 novel human-pathogenic coronavirus isolated from a patient with atypical pneumonia after visiting Wuhan. *Emerg Microbes Infect* **9**, 221-236 (2020).
3. Jackson, C.B., Farzan, M., Chen, B. & Choe, H. Mechanisms of SARS-CoV-2 entry into cells. *Nat Rev Mol Cell Biol* **23**, 3-20 (2022).
4. Falzone, L., Gattuso, G., Tsatsakis, A., Spandidos, D.A. & Libra, M. Current and innovative methods for the diagnosis of COVID-19 infection (Review). *Int J Mol Med* **47**(2021).

5. Fernandes, Q., *et al.* Emerging COVID-19 variants and their impact on SARS-CoV-2 diagnosis, therapeutics and vaccines. *Ann Med* **54**, 524-540 (2022).
6. Hadj Hassine, I. Covid-19 vaccines and variants of concern: A review. *Rev Med Virol* **32**, e2313 (2022).
7. Fiolet, T., Kherabi, Y., MacDonald, C.J., Ghosn, J. & Peiffer-Smadja, N. Comparing COVID-19 vaccines for their characteristics, efficacy and effectiveness against SARS-CoV-2 and variants of concern: a narrative review. *Clin Microbiol Infect* **28**, 202-221 (2022).
8. Chenchula, S., Karunakaran, P., Sharma, S. & Chavan, M. Current evidence on efficacy of COVID-19 booster dose vaccination against the Omicron variant: A systematic review. *J Med Virol* **94**, 2969-2976 (2022).
9. Bowen, J.E., *et al.* Omicron spike function and neutralizing activity elicited by a comprehensive panel of vaccines. *Science* **377**, 890-894 (2022).
10. Cao, Y., *et al.* BA.2.12.1, BA.4 and BA.5 escape antibodies elicited by Omicron infection. *Nature* **608**, 593-602 (2022).
11. Hachmann, N.P., *et al.* Neutralization Escape by SARS-CoV-2 Omicron Subvariants BA.2.12.1, BA.4, and BA.5. *N Engl J Med* **387**, 86-88 (2022).
12. Pather, S., *et al.* SARS-CoV-2 Omicron variants: burden of disease, impact on vaccine effectiveness and need for variant-adapted vaccines. *Front Immunol* **14**, 1130539 (2023).
13. Wang, Q., *et al.* Alarming antibody evasion properties of rising SARS-CoV-2 BQ and XBB subvariants. *Cell* **186**, 279-286.e278 (2023).
14. Kurhade, C., *et al.* Low neutralization of SARS-CoV-2 Omicron BA.2.75.2, BQ.1.1 and XBB.1 by parental mRNA vaccine or a BA.5 bivalent booster. *Nat Med* **29**, 344-347 (2023).
15. Miller, J., *et al.* Substantial Neutralization Escape by SARS-CoV-2 Omicron Variants BQ.1.1 and XBB.1. *N Engl J Med* **388**, 662-664 (2023).
16. Lavelle, E.C. & Ward, R.W. Publisher Correction: Mucosal vaccines - fortifying the frontiers. *Nat Rev Immunol* **22**, 266 (2022).
17. Drożdżal, S., *et al.* An update on drugs with therapeutic potential for SARS-CoV-2 (COVID-19) treatment. *Drug Resist Updat* **59**, 100794 (2021).
18. Niknam, Z., *et al.* Potential therapeutic options for COVID-19: an update on current evidence. *Eur J Med Res* **27**, 6 (2022).
19. Yuan, Y., Jiao, B., Qu, L., Yang, D. & Liu, R. The development of COVID-19 treatment. *Front Immunol* **14**, 1125246 (2023).
20. VanBlargan, L.A., *et al.* An infectious SARS-CoV-2 B.1.1.529 Omicron virus escapes neutralization by therapeutic monoclonal antibodies. *Nat Med* **28**, 490-495 (2022).
21. Agarwal, A., *et al.* A living WHO guideline on drugs for covid-19. *Bmj* **370**, m3379 (2020).
22. Moore, J.B. & June, C.H. Cytokine release syndrome in severe COVID-19. *Science* **368**, 473-474 (2020).

23. Hu, B., Huang, S. & Yin, L. The cytokine storm and COVID-19. *J Med Virol* **93**, 250-256 (2021).
24. Zhang, W., *et al.* The use of anti-inflammatory drugs in the treatment of people with severe coronavirus disease 2019 (COVID-19): The Perspectives of clinical immunologists from China. *Clin Immunol* **214**, 108393 (2020).
25. Sterne, J.A.C., *et al.* Association Between Administration of Systemic Corticosteroids and Mortality Among Critically Ill Patients With COVID-19: A Meta-analysis. *Jama* **324**, 1330-1341 (2020).

Chapter 1 (Part B): COVID-19 and Cancer: Understanding the Link through Cytokine, Chemokine, and Growth Factor Dysregulation

Angelina Konnova^{1,2}, Fien HR De Winter^{1,2}, Akshita Gupta^{1,2}, Yana Debie^{3,4}, An Hotterbeekx¹, Lise Verbruggen³, Timon Vandamme^{3,4}, Surbhi Malhotra-Kumar², Evelina Tacconelli⁵, Marc Peeters^{3,4**}, Peter van Dam^{3,4**}, Samir Kumar-Singh^{1,2*}

¹Molecular Pathology Group, Laboratory of Cell Biology & Histology, Faculty of Medicine and Health Sciences, University of Antwerp, Antwerp, Belgium

²Laboratory of Medical Microbiology, Vaccine & Infectious Disease Institute, University of Antwerp, Antwerp, Belgium

³Multidisciplinary Oncologic Centre Antwerp (MOCA), Antwerp University Hospital, Wilrijkstraat 10, Edegem, B-2650, Belgium

⁴Center for Oncological Research (CORE), Integrated Personalized and Precision Oncology Network (IPPON), University of Antwerp, Universiteitsplein 1, Wilrijk, B-2610, Belgium

⁵Division of Infectious Diseases, Department of Diagnostics and Public Health, University of Verona, P.le L.A. Scuro 10, 37134, Verona, Italy

Angelina Konnova is the primary author of this review. Together with the senior authors (Prof. Marc Peeters, Prof. Peter van Dam, and Prof. Samir Kumar-Singh), she conceptualised the review, performed literature search and wrote the manuscript.

**Shared senior authors

*Corresponding author: samir.kumarsingh@uantwerpen.be

Manuscript under review in Critical Reviews in Oncology / Hematology

Abstract

COVID-19 pandemic has had a significant impact on global health, particularly in individuals with cancer, who are at increased risk for severe disease and death. COVID-19 is known to cause severe immune dysregulation, potentially affecting cancer incidence and/or progression. Despite the promising results of vaccination in reducing the risk of severe outcomes, studies have shown that following both SARS-CoV-2 infection and vaccination, antibody titres in certain cancer patients remain very low. Here, we describe the role of cytokines, chemokines, and growth factors (CCGs) in cancer and COVID-19, exploring their dysregulation in acute COVID-19 as well as in post-COVID-19 syndrome (PCS), also called Long Covid, seen in up to 30% of cancer patients that experienced acute COVID-19. We also discuss the potential of CCGs as circulating immune biomarkers of successful vaccination response and SARS-CoV-2 mutation development. Overall this review highlights the need of deep cytokine profiling to study CCG dysregulation in cancer patients with COVID-19 or PCS to better understand key targetable steps in this patient group to improve the patient outcomes, including health-related quality of life. Also, as several of CCGs change concurrently, in order to better evaluate the net effect of these changes, it is important to understand the function of each of these CCGs.

Introduction

The COVID-19 pandemic has had a devastating impact on global health, and individuals with cancer have been at an increased risk of severe disease and death from SARS-CoV-2 infection [1-4]. While vaccination has shown promise in reducing the risk of infection and severe outcomes in the general population, previous studies have shown that antibody titres in patients with certain cancers, including but not limited to, advanced cancers and B cell haematological malignancies, are either absent or low not only after SARS-CoV-2 infection, but also after SARS-CoV-2 vaccination [5-14]. However, in addition to the direct threat of the disease and delay of diagnosis and treatment observed mostly in the beginning of the pandemic, COVID-19 can cause severe immune dysfunction, potentially affecting both carcinogenesis and cancer progression. Immune system plays a vital role in recognizing and eliminating cancer cells and can contribute to the development of an inflammatory microenvironment that promotes angiogenesis, cancer progression, and metastasis [15].

In this review, we provide an in-depth analysis of the role of cytokines, chemokines, and certain growth factors (CCGs) linked to both cancer and COVID-19. We discuss CCGs involved in acute COVID-19 and their dysregulation for an extended period after recovery, highlighting the potential long-term consequences of COVID-19 infection in cancer patients. Furthermore, we explore the potential of CCGs as predictors of vaccination and therapy efficiency, the latter in terms of SARS-CoV-2 mutation development in response to anti-SARS-CoV-2 treatments. We also investigate the role of CCGs dysregulation in cancer impacting cancer progression. We call for further research to elucidate the underlying mechanisms of CCG dysregulation in SARS-CoV-2-infected cancer patients and the development of targeted interventions to optimise patient outcomes.

COVID-19-associated immune misfiring

COVID-19 is a complicated disease that involves dysregulation of multiple components of the immune system. A severe degree of dysregulation of the immune system can lead to cytokine release syndrome (CRS) in severe COVID-19 cases [16, 17]. CRS is caused by large, rapid release of cytokines into the blood by immune cells responding excessively to infection or to certain therapies [18]. CRS is characterized by increased secretion of Interleukin (IL)-6, Tumour Necrosis Factor- α (TNF α), IL-8, Monocyte Chemoattractant Protein (MCP)-1, and Vascular Endothelial Growth Factor (VEGF) [16, 19].

IL-6 is widely considered to be the primary hallmark of severe MERS-CoV-2 and SARS-CoV-2 infections and is found in particularly high levels in blood of severe and critical cases of COVID-19 [20-23]. Studies have also shown that IL-6 upregulation occurs in the very early stage of COVID-19 and then declines rapidly [20, 22]. Moreover, several clinical trials have shown that tocilizumab, a humanized mAb against IL-6 receptor (IL-6R), reduces the risk of mechanical ventilation and mortality in hospitalised COVID-19 patients [24-27], although a smaller Brazilian randomised control study showed that tocilizumab is not superior to the standard care alone [28].

TNF- α , also referred to as cachectin, is produced by many different cell types and is important in the induction of expression of genes responsible for immune activation, including initiation of inflammatory responses of the innate immune system. Increased TNF- α levels were shown to be related to COVID-19 disease severity [20, 21, 29-32]. Furthermore, after initial high levels, a fast

decrease of TNF- α was shown in patients with moderate COVID-19, whereas the levels in severely ill patients remained high over a longer period [20].

IL-8, also known as CXCL8, is another commonly elevated cytokine observed in COVID-19 patients. IL-8 is a chemoattractant that attracts neutrophils to the site of infection and is consistently detected in COVID-19 patients, which might be related to COVID-19 disease severity. In this regard, a significant difference between disease severity groups has been reported by several groups [20, 21, 33], with the highest levels observed at the time of critical disease [29, 30, 34, 35]. However, this might not be specific to COVID-19 as the levels of IL-8 in COVID-19 patients admitted to the ICU are not significantly different from the levels measured in ICU-admitted patients with community acquired pneumonia (CAP) [36]. It is also not clear whether IL-8 is beneficial in pneumonia resolution as hyper increased neutrophil recruitment could cause high collateral host tissue damage resulting from a prominent pro-inflammatory IL-8 induced response [37].

Like IL-8, MCP-1 is yet another chemoattractant shown to be elevated in COVID-19 patients. MCP-1 is most potent in rapidly attracting most types of monocyte to the site of infection, but also declines fast post-COVID-19 recovery [38, 39], suggesting that MCP-1 could serve as both an early and a prognostic marker of COVID-19 disease severity [21, 29, 33-35, 40-42]. Additionally, a few studies have also shown correlations of MCP-1 with kidney failure [43] and with mortality [43, 44].

Finally, VEGF is an important contributor to CRS. VEGF facilitates blood vessel growth and remodelling, providing mitogenic and survival stimuli to endothelial cells, and influences the immune system in several different ways [45, 46]. In COVID-19, VEGF induces vascular permeability and contributes to pulmonary oedema development. Clinical and *in vivo* experimental model studies show that VEGF dysregulation is associated with acute respiratory distress syndrome (ARDS) [47-49]. However, VEGF also mediates angiogenesis and is a key factor in tissue repair processes. Specifically, in COVID-19 patients, VEGF-A and VEGF-C levels appear to be higher compared to the healthy controls, while VEGF-D levels are lower compared to the healthy controls [21, 39, 50-52]. VEGF-A and VEGF-D levels in COVID-19 patients correlate with disease severity or duration (i.e. hospitalization time) and can be used as prognostic markers [29, 33, 42, 53]. Additionally, VEGF isotypes potentially play an important role in brain inflammation causing neurological COVID-19 symptoms and participates in 'silencing' of pain via subversion of VEGF-A/NRP-1 signalling that may underlie increased disease transmission in asymptomatic individuals [54, 55].

Currently, only limited data exists on the associations between specific CCGs and the severity of COVID-19 in cancer patients. Specifically, Fendler *et al.* have demonstrated that IL-6, IL-8, Interferon (IFN)- γ , IL-18, Interferon Gamma Induced Protein (IP)-10, pleiotropic cytokine IL-9, and Macrophage Inflammatory Protein (MIP)-1 β are elevated in cancer patients with acute COVID-19, in which these markers also correlate with disease severity [13]. Correlation between COVID-19 severity in cancer patients and IFN-related proteins, such as type-II interferons (IFN- γ), interferon gamma inducing factor (IL-18), and downstream effector of IFN- γ (IP-10) highlights the importance of IFN responses against SARS-CoV-2 viral infection [13]. Interestingly, in non-cancer COVID-19 patients, IL-18 and IP-10 also highly correlate with COVID-19 disease severity in some studies [21, 22, 29, 33], but not all [21, 22, 29, 33]. Additionally, IL-9 is also upregulated in cancer-free COVID-19 patients, compared to healthy controls, and correlates with disease severity [21, 29, 56]. These

observations highlight the need for further studies comparing acute COVID-19 responses in cancer patients versus non-cancer patients.

COVID-19 related CCG dysregulation affects cancer progression

Although COVID-19 is largely an immune mediated acute disease, SARS-CoV-2 related chronic inflammation is a potential contributor to the development of cancer but could also lead to the progression and development of metastases of primary tumours [57-60]. Especially in solid tumours, infiltration of immune cells into the tumour mass produces a repertoire of cytokines and chemokines that can either support or subvert immune evasion. It is therefore unclear how CCG dysregulation caused by SARS-CoV-2 infection would affect cancer progression and treatment, although it has previously been hypothesised that prolonged elevation of cytokine levels or CRS may have a severe impact on cancer patients leading to increased mortality, especially in the early pandemic [61-64]. Additionally, it has been shown *in vivo* that other infections, such as acute Influenza A, can reprogram tumour microenvironment and induce long-term pro-tumoural effects [65]. In order to evaluate the impact of CCG dysregulation on cancer patients, we further focus here on cancer-specific functions of the most important CCGs observed to be altered in COVID-19 or involved in COVID-19-associated CRS.

A major marker of CRS, IL-6, is a highly expressed cytokine that facilitates the crosstalk between cancer cells and tumour microenvironment, creating conditions favourable for immune evasion and tumour growth. IL-6 regulates multiple signalling pathways, including survival, apoptosis, proliferation, angiogenesis, invasiveness, metastasis and metabolic remodelling, besides contributing to therapy resistance [66, 67].

TNF- α , is present in very low amounts or even absent in healthy individuals but can be found in several cancers, such as chronic lymphocytic leukaemia and prostate cancer, and are indicative of a poor prognosis (reviewed in reference [68]). Depletion of TNF- α leads to the profound resistance to inflammation-induced cancer, as shown in chemical carcinogenesis models [68]. Moreover, TNF- α is involved in activation, function, and differentiation of immune regulatory cells, including myeloid-derived suppressor cells (MDSCs) and regulatory T cells (Treg) and triggers activation-induced cell death of CD8+ tumour infiltrating lymphocytes (TILs), which create a favourable tumour microenvironment and facilitate tumour growth [69]. Additionally, TNF- α has a direct effect on the survival, dedifferentiation and epithelial-to-mesenchymal transition (EMT) of cancer cells [70], leading to the decreased immunogenicity and tumour relapse [68, 69]. However, the role of TNF- α in cancer is context- and concentration-dependent. While low levels of TNF- α sustain cancer development, high levels of this cytokine sometimes impede tumour growth [69]. Delivering high concentrations of TNF- α in tumours induces tumour necrosis and enhances immunotherapy efficacy [69].

Another CCG highly expressed in the tumour microenvironment and involved in CRS, as discussed above, is IL-8. IL-8 is a chemokine that correlates to the mass of the tumour and has a role in angiogenesis, survival signalling, and myeloid cell attraction that together enable tumour growth and local immune suppression. Furthermore, IL-8 promotes EMT, which contributes to the tumours ability to metastasise [71, 72].

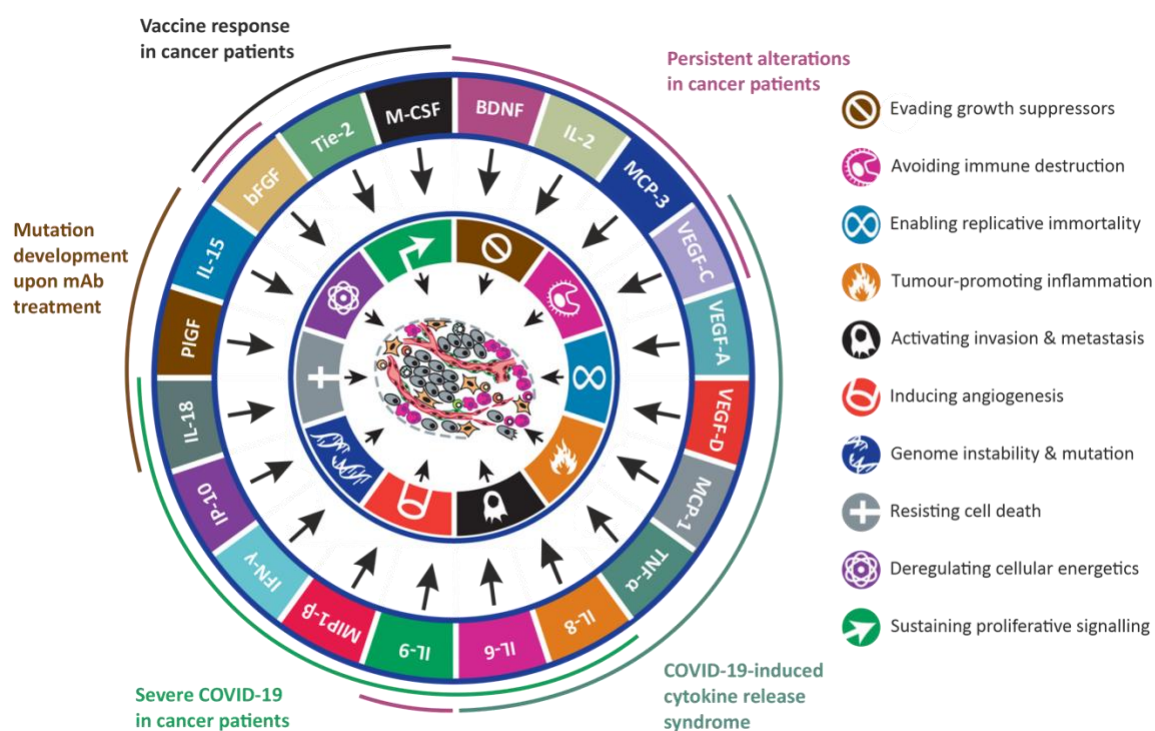
The role of MCP-1 is also well described in cancer, where it is mostly thought to contribute to the recruitment of tumour associated macrophages (TAMs) to the tumour microenvironment, enabling immune evasion [73]. Similarly, MIP-1 β (CCL4) is also reported to be upregulated in cancer patients infected with SARS-CoV-2 [74]. MIP-1 β acts as a chemoattractant for T cells, NK cells, and monocytes in the site of inflamed or damaged tissue. Multiple studies indicate that MIP-1 β can promote tumour development and progression by recruiting Treg cells and pro-tumourigenic macrophages to the tumour site as well as by facilitating pro-tumourigenic capacities of other resident cells, such as fibroblasts and endothelial cells. On the other hand, MIP-1 β can enhance tumour immunity by recruiting Tc cells and macrophages with phagocytic ability, suggesting context-dependent role of MIP-1 β in determining tumour microenvironment [75].

VEGFs are the main mediators of angiogenesis and vascular permeability in cancer, which are essential for tumour growth and invasion ability. VEGF facilitates blood vessel growth and remodelling, provides mitogenic and survival stimuli to endothelial cells, and influences the immune system in several different ways [45, 46]. In line with these data, we have reported a significant increase in VEGF-A in plasma of patients with different solid tumours [76].

In cancer, IFNs, like several other cytokines, have ambiguous function and can contribute to both immune responses against cancers (and thus utilised as anti-cancer therapy) and tumour immune evasion and growth, especially when expressed locally in low levels. Specifically, IL-18 is well known to be anti-tumourigenic through its pro-inflammatory function as a strong inducer of IFNs. Nonetheless, IL-18 can also help tumours to escape immunity and facilitate metastasis and angiogenesis. Generally, high IL-18 levels can be found in cancer patients and can be related to poor prognosis [77]. Another cytokine upregulated upon SARS-CoV-2 infection in COVID-19 patients, IFN- γ , is a double-edged sword in cancer. On the one hand, its apoptotic functions prevent cancer formation, and its chemoattractant functions aid in tumour mass reduction. On the other hand, cell death in the tumour can release small amounts of IFN- γ enabling immune evasion of the tumour [78, 79]. Similarly, the role of IP-10 in cancer is also not well understood, and while it is suggested as a cancer therapy because of its role as an immune cell chemoattractant, there are also reports that IP-10 can promote tumour angiogenesis and metastasis [80].

Lastly, IL-9 is produced predominantly by helper T cells, importantly T_{H2} and a new class of helper T cells (T_{H9}) [81]. and has both direct and indirect effects on hematopoietic progenitor cells, lymphocytes, mast cells, as well as airway smooth muscle cells and epithelial cells [81]. Since IL-9 was originally described as a T cell growth factor with cell growth promotion potential, it is not surprising that IL-9 is involved in pathogenesis of multiple cancer types, including lung cancer, leukaemia, breast cancer, thyroid cancer, colon cancer and lymphoma [81]. On the other hand, IL-9 might also have indirect anti-cancer effect in other cancers, such as melanoma [81].

Thus, it is clear that acute infection with SARS-CoV-2 alters levels of several CCGs that directly impact tumour cell proliferation, reduced antitumour immunity, and enhanced immunosuppression leading to increased tumour growth, invasion, and metastasis. This highlights the need for further investigation into the acute effects of COVID-19 on cancer patients, specifically on the immune system that can have a long-term impact as a post-COVID sequelae (PCS) in cancer patients (**Figure 1**).



Adapted from Hanahan and Weinberg (Cell, 2011)

Figure 1. Schematic representation of the effects of COVID-19 and COVID-19-associated CCGs on cancer. The figure is based on the Hallmarks of Cancer proposed by Hanahan and Weinberg [82], which include evading growth suppressors, avoiding immune destruction, enabling replicative immortality, tumour-promoting inflammation, activating invasion and metastasis, inducing angiogenesis, genome instability and mutation, resisting cell death, deregulating cellular energetics, and sustaining proliferative signaling (clockwise from the top).

Post-COVID-19 syndrome (PCS) in cancer patients

While the immediate impact of COVID-19 in cancer patients seems to be rather understood, how the early effects of SARS-CoV-2 infection on tumour and immune biology drives PCS occurring in 15-30% of cancer patients infected with SARS-CoV-2 [83, 84] is not understood. While studies linking PCS in cancer patients with specific CCGs are awaited, we have shown that SARS-CoV-2 infection in cancer patients could lead to long-term alterations of the CCG profile that could sustain for up to 6 months. Specifically, in patients with solid tumours, we showed that exposure to SARS-CoV-2 can induce significant long-lasting upregulation of inflammatory markers CRP and SAA as well as immune cell activators IL-2 and MCP-3 [76].

IL-2 is produced mainly by T cells, particularly CD4+ helper cells [85]. Signals from the IL-2 receptor activate the transcription factors STAT5 and NF- κ B, which promote cell survival, proliferation and EMT [70, 85]. IL-2 can potently induce expansion of effector T cells, making IL-2 essential for fighting infections [86]. In COVID-19, mostly patients with as severe disease show

higher levels of IL-2 and it seems that over the course of disease IL-2 keeps increasing in patients with severe disease [21, 39]. One report even shows IL-2 as a marker for mortality [87]. Additionally, due to its role in the proliferation and differentiation of effector and memory T cells as well as the potential to boost the cytolytic activity of NK cells and lymphokine-activated killer cells, IL-2 was proposed to be used in the treatment of cancer patients to boost anti-cancer immune responses [85]. However, this treatment was not sufficiently effective and safe to be widely adopted, potentially due to the critical role of IL-2 in the development and peripheral expansion of CD4⁺CD25⁺ regulatory T cells, which promote self-tolerance by suppressing T cell responses [85].

Another CCG upregulated for a long period after COVID-19 infection in cancer patients is MCP-3 [76]. Like MCP-1, MCP-3 is responsible for attracting monocytes. However, unlike MCP-1, the role of MCP-3 is less well described in cancer, although it was observed that higher MCP-3 expression can lead to better or worse prognoses, depending on the context [88]. As a chemoattractant, MCP-3 can help in anti-tumour immunity through the recruitment of TILs, but it is also associated with infiltration of tumour associated macrophages (TAMs), which help in immune evasion, and tumour-associated angiogenesis [88, 89].

Additionally, SARS-CoV-2 exposure in cancer patients can also result in a significant reduction of several CCGs, such as angiogenesis factors VEGF-C, basic Fibroblast Growth Factor (bFGF), and Brain-Derived Neurotrophic Factor (BDNF), as well as IL-9, whose role is described above, and total Transforming Growth factor (TGF)- β , which is a CCG involved in intracellular signalling that can promote tumourigenesis, metastasis and chemoresistance in the later stages of cancer [90].

VEGF-C, bFGF, and BDNF are some of the main mediators of angiogenesis and vascular permeability in cancer. Together, they facilitate blood vessel growth and remodelling, provide mitogenic and survival stimuli to endothelial cells, and influence the immune system in several different ways [45, 46, 91]. In particular, basic FGF (bFGF) or FGF2, which is elevated in multiple cancers, is a survival factor that acts by inhibiting apoptosis [76, 91]. Also, bFGF is responsible for non-specific mitogenesis and angiogenesis signals [92]. Additionally, BDNF and its receptor, tyrosine kinase B (TrkB) receptor, are upregulated in many solid cancer types, conferring aggressive phenotypes and chemotherapy resistance [93]. Their pro-tumourigenic effect is modulated by the downstream targets of the TrkB receptor, which include the well-characterised pro-inflammatory, anti-apoptotic and pro-survival PI3K/Akt signalling pathway [93]. However, despite the oncogenic effect of BDNF administration *in vitro*, it was shown that *in vivo* administration of BDNF may support anti-tumour immune responses [93]. A potential explanation for the controversial role of BDNF in cancer might be the presence of multiple TrkB receptor isoforms, which along with the tissue origin of the cancer ultimately govern the effect BDNF has on various cellular activities [93]. Currently, there is no evidence that COVID-19 has any direct influence on the therapeutic effectiveness of PI3K inhibitors or other drugs, but theoretically this may be possible. Altogether, these cytokine alterations suggest that even asymptomatic COVID-19 infections can have a significant impact on cancer progression and treatment outcomes in cancer patients (**Table 1**). Whether some of these cytokines are also linked with PCS development and sustenance in cancer patients remains to be studied.

Table 1. The effect of CCGs dysregulated upon COVID-19 in cancer. *—Evidence available in cancer patients.

Cytokine	Cancer	Acute COVID-19	Cancer with post-acute COVID-19 (up to 6m)	Potential effect on cancer patients
IL-6	↑ (colorectal adenomas, gastric carcinomas, hepatocellular carcinomas, oesophageal carcinomas, breast carcinomas, ovarian carcinomas) [66, 67]	↑* [13, 20, 22]	Not altered	Bad [66, 67]
TNF-α	↑ (ovarian cancers, renal cancers, prostate cancers, chronic lymphocytic leukaemia) [68]	↑ [20]	Not altered	Bad [68, 69]
IL-8	↑ (melanomas, mesotheliomas, brain cancers, breast cancers, lung cancer, Hodgkin's lymphomas, acute myeloid leukaemias) [71, 72]	↑* [13, 29, 30, 34, 35]	Not altered	Bad [71, 72]
MCP-1	↑ (breast cancers, non-small-cell lung cancers) [73]	↑ [38, 39]	Not altered	Bad [73]
VEGF-A	↑ (glioblastomas, renal cancers, haematological malignancies) [45, 46]	↑ [21, 39, 50-52]	Not altered	Bad [45, 46]
VEGF-C	↑ (non-small lung cancers, breast cancers) [45, 46]	↑ [21, 39, 50-52]	↓* [76]	Unclear [45, 46]

VEGF-D	↑ (breast cancers) [45, 46]	↓ [21, 39, 50-52]	Not altered	Bad [45, 46]
IFN-γ	↑ (hepatocellular carcinomas, colon cancers, fibrosarcomas) - 30 - ↓ (hepatomas, mammary adenocarcinomas, melanomas) [78, 79]	↑* [13]	Not altered	Unclear [78, 79]
IL-18	↑ (hepatocellular carcinomas, ovarian cancers) ↓ (colorectal cancers) [77]	↑* [13]	Not altered	Unclear [77]
IP-10	↓ (melanomas, myelomas, mesotheliomas, lung cancers, gliomas) [80]	↑* [13, 20]	Not altered	Potentially good [80]
MIP-1β	↑ (breast cancers) [75]	↑* [13]	Not altered	Bad [75]
IL-2	↓ (renal cell carcinomas, melanomas) [85]	↑ [21, 39]	↑* [76]	Potentially good [85]
MCP-3	↑ (gliomas, lung cancers, head and neck cancers) ↓ (liver cancers, breast cancers, endometrial cancers) [88, 89]	↑ [22]	↑* [76]	Unclear [88, 89]
bFGF	↑ (non-small lung cancers) [76, 91]	↑ [20, 21, 29, 52, 94]	↓* [76]	Unclear [91, 92]
BDNF	↑ (lung cancers, colon cancers, ovarian cancers) [93]	↓ [95]	↓* [76]	Unclear [93]
IL-9	↑ (chronic lymphoid leukaemias, colon cancers, lymphomas)	↑* [13, 21, 29, 56]	↓* [76]	Unclear [81]

	↓ (melanomas) [81]			
TGF-β	↑ (gliomas, thymomas, melanomas, breast cancers) [90]	↑ [56]	↓* [76]	Unclear [90]

Circulating immune biomarkers reflect vaccine induced adaptive immune responses in cancer

Given the long-term consequences of COVID-19, cancer patients require additional protection to prevent CCG alterations that can affect cancer progression or successful treatment. Despite successful vaccination in healthy populations, the limited ability of some cancer patients to develop a protective antibody response [6-11, 96] highlights the importance of identifying unique signatures in cancer patients that can differentiate good from poor responders to COVID-19 vaccination. In healthy population, transient increases in IL-15 and IFN-γ levels are shown to be biomarkers for a good anti-SARS-CoV-2 IgG response [97]. In cancer patients, upregulated CRP, IL-15, IL-18, and Placental Growth Factor (PIGF) were identified as the best predictors of a poor response to COVID-19 vaccine (discussed in more details in **Chapter 3**) [15]. Moreover, this signature was maintained until day 28 after the administration of the primer dose, suggesting that it is driven by an inherent difference between cancer patients.

One of the main predictors of vaccine response, IL-15, is a cytokine with a structural similarity to IL-2, a cytokine also upregulated upon COVID-19. IL-15 is essential for NK, NKT and memory CD8+ T cell development and function, one of the main functions employed to eradicate virus infected cells [98]. Therefore, IL-15 is essential for viral clearance and infection suppression, and thus has been suggested to be utilized as a treatment against COVID-19 infection [99]. Several large cohort studies have shown IL-15 associated not only with disease severity [39, 100, 101] but also with mortality [87]. In cancer, IL-15 agonism is mostly being considered as an immunotherapy agent. However, the cellular mechanisms of IL-15-mediated anti-tumour activity depends on the nature of the tumour [98]. For example, anti-tumour activity of IL-15 agonism is driven by NK cells in metastatic melanoma, but tumour-specific CD8+ T cells in multiple myeloma, and both NK and CD8+ T cells in metastatic breast and colon cancers [98]. Nonetheless, it is important to note that in T-cell leukemia, IL-15 can promote tumour cells [102].

Another predictor of vaccine response, IL-18, originally described as an interferon gamma inducing factor, is involved in inflammasome formation and pyroptosis of infected cells. Accordingly, IL-18 is a marker and mediator of tissue damage [103, 104]. Several studies have reported a correlation between IL-18 and COVID-19 disease severity [20, 22, 33, 42]. However, as discussed above, in cancer, IL-18 plays an anti-tumourigenic role through its pro-inflammatory and inducer of IFNs function. On the other hand, IL-18 can also help tumours to escape immunity and facilitate metastasis and angiogenesis and accordingly, high IL-18 levels found in cancer patients are generally related to poor prognosis [77].

PIGF is a pleiotropic cytokine that was originally discovered in placenta and belongs to the VEGF family. In cancer, PIGF might be a useful prognostic marker for cancer progression [105, 106]. PIGF

is involved in the modification of innate and adaptive immune responses, therefore creating an environment favourable for tumour development and progression [105, 106]. Additionally, PIGF inhibits apoptosis and induces survival as well as chemoresistance through Akt and NF- κ B signaling in tumour cells. It also enhances cell motility through ERK 1/2 signaling and therefore promotes invasion [106]. Direct pro-angiogenic activity of PIGF is still subject to debate [105, 106]. Significantly higher levels of PIGF were also observed in plasma of both solid and haematological tumour patients compared to healthcare workers [76]. As demonstrated previously in preeclampsia, PIGF and its decoy receptor soluble fms-like tyrosine kinase 1 (sFlt-1) are the most prominent markers of AngII-mediated endothelial dysfunction. It was speculated that due to the elevated levels of AngII, COVID-19 patients might also exhibit a high soluble fms-like tyrosine kinase-1 (sFlt-1)/PIGF ratio and a subsequent imbalance between angiogenic and anti-angiogenic factors, causing endothelial dysfunction[107]. In fact, PIGF levels were shown to be elevated in COVID-19 positive pneumonia patients compared to healthy controls, although no difference was observed between COVID-19 pneumonia and pneumonia of other aetiology [107]. Most importantly, sFlt1/PIGF ratio is upregulated in COVID-19 pneumonia patients compared to pneumonia patients with other aetiologies and healthy controls, suggesting an imbalance between angiogenic and antiangiogenic factors specific to patients with COVID-19 pneumonia [107]. However, another study has demonstrated no difference in PIGF levels between ICU COVID-19 patients, non-ICU COVID-19 patients, and healthy controls [52].

To summarize, it is clear that CCGs discussed above exhibit an ability to predict the development of sufficient immune responses following vaccination in cancer patients, suggesting that while progress has been made in predicting immune responses to vaccines, there is a continued need for research to optimise vaccination efficacy across diverse populations and building immune-based algorithms that can identify poor immune responders for prioritization of continued booster dose administration and pre-exposure prophylaxis.

Therapeutic protection of cancer patients predicted by host immune functioning

Poor responders to the COVID-19 vaccine, as identified using the CCG signature, are at higher risk of developing severe COVID-19 infection and would need additional protection in terms of monoclonal antibodies (mAbs), either in a form of pre-exposure prophylaxis, or as a post-exposure treatment. However, the use of mAbs can also lead to the development of SARS-CoV-2 mutations. The development of mutations is dependent on various factors, including the host immune profile [108]. Specific factors such as inflammatory marker SAA and CCGs, such as bFGF, Tie-2, and Macrophage Colony Stimulating Factor (M-CSF), can influence the development of mutations, which can potentially lead to new variants of the virus (discussed in more details in **Chapter 6**) [108].

Despite the fact that this prediction was not specifically derived from cancer patients infected with SARS-CoV-2, mAb therapy should be carefully considered in cancer patients, since bFGF exhibits elevated levels in multiple cancers [76, 92]. In particular, bFGF is a survival factor that acts by inhibiting apoptosis [91]. Also, bFGF is responsible for non-specific mitogenesis and angiogenesis signals in cancer [92]. There is limited information available about the role of bFGF in infections,

although *in vitro* evidence indicates that downregulation of bFGF can accelerate H5N1, H1N1 and Zika virus replication potentially through confining IFN response [109-111]. Additionally, bFGF was elevated in H1N1-infected patients, and its overexpression mitigated influenza-induced injury [112]. The exact role of bFGF in COVID-19 patients remains unclear, although most of the studies demonstrate elevated bFGF levels in patients infected with SARS-CoV-2 compared to healthy controls [20, 21, 29, 52, 94]. Most of the current studies report no difference between severe and non-severe cases in terms of bFGF expression [20, 21, 29, 52, 94].

On the other hand, Tie-2 is typically downregulated in cancer patients, decreasing their risk for developing SARS-CoV-2 mutations upon mAb treatment. Tie-2, also called TYR2 and TYK2, is a member of the Janus kinase (JAK) family, which transduces cytokine and growth factor signalling, making it an important actor in immunity and inflammation [113, 114]. In cancer, Tie-2 is involved in angiogenesis, metabolism regulation and enabling cell death resistance [113, 114]. Dysregulation of Tie-2 activation, aberrant Tie-2 protein levels, and gain-of-function mutations in the Tie-2 gene are frequently observed in different types of cancer [114]. Upon viral infections, Tie-2 is involved in the IFN-mediated antiviral pathway, which is initiated after secretion of type I and III IFNs [115]. However, type I interferon (IFN-I) immunity has been found to be dampened in COVID-19 [115]. In fact, SARS-CoV-2 Nucleocapsid protein can bind to STAT1/STAT2 proteins, suppress their nuclear translocation and phosphorylation, and interfere with their interaction with Tie-2, leading to the inhibition of IFN-I signalling [115]. The importance of Tie-2 is further supported by the identification of a significant association of a specific single-nucleotide polymorphisms in Tie-2 [116] with critical COVID-19 cases [117].

M-CSF is another important cytokine in cancer progression. M-CSF promotes hematopoietic cell types to differentiate into macrophages, polarizing macrophages into two main types, pro-inflammatory M1 type that relieves infection and an anti-inflammatory M2 type that is more immunosuppressive. M-CSF is associated with M2 polarization, which makes it an important target in cancer therapy because of its stimulation of immunosuppressive tumour associated macrophages [118, 119]. Few studies have investigated the role of M-CSF in COVID-19 suggesting that M-CSF goes up early in infection and some report it to be related to severity [20, 22, 29, 33].

To sum up, understanding the role of cytokines in COVID-19 in cancer patients is crucial for developing effective treatment strategies. Since CCGs, like bFGF, Tie-2, and M-CSF, can drive the development of mutations upon mAb treatment and are dysregulated in cancer patients, mAb therapy should be carefully considered in this patient population and monitored to minimise the risk of developing new mutations. As research in this area continues, it is hoped that new insights will emerge, leading to better understanding of the preferred treatment of COVID-19 in cancer patients.

Deep cytokine profiling and future perspectives of CCG research in immunocompromised patients are discussed in more details in **Chapter 7**. However, we believe that CCGs could play a crucial role in developing personalised cancer treatment plans improving patient outcomes and treatment compliances.

References

1. Liang, W., et al., Cancer patients in SARS-CoV-2 infection: a nationwide analysis in China. *Lancet Oncol*, 2020. **21**(3): p. 335-337.

2. Dai, M., et al., Patients with Cancer Appear More Vulnerable to SARS-CoV-2: A Multicenter Study during the COVID-19 Outbreak. *Cancer Discov*, 2020. **10**(6): p. 783-791.
3. Sidaway, P., COVID-19: more evidence emerges. *Nat Rev Clin Oncol*, 2020. **17**(8): p. 451.
4. Sidaway, P., COVID-19 and cancer: what we know so far. *Nat Rev Clin Oncol*, 2020. **17**(6): p. 336.
5. van Dam, P.A., et al., High mortality of cancer patients in times of SARS-CoV-2: Do not generalize! *Eur J Cancer*, 2020. **138**: p. 225-227.
6. Peeters, M., et al., Reduced humoral immune response after BNT162b2 coronavirus disease 2019 messenger RNA vaccination in cancer patients under antineoplastic treatment. *ESMO Open*, 2021. **6**(5): p. 100274.
7. Massarweh, A., et al., Evaluation of Seropositivity Following BNT162b2 Messenger RNA Vaccination for SARS-CoV-2 in Patients Undergoing Treatment for Cancer. *JAMA Oncol*, 2021. **7**(8): p. 1133-1140.
8. Maneikis, K., et al., Immunogenicity of the BNT162b2 COVID-19 mRNA vaccine and early clinical outcomes in patients with haematological malignancies in Lithuania: a national prospective cohort study. *The Lancet Haematology*, 2021. **8**(8): p. e583-e592.
9. Fendler, A., et al., Adaptive immunity and neutralizing antibodies against SARS-CoV-2 variants of concern following vaccination in patients with cancer: the CAPTURE study. *Nature Cancer*, 2021. **2**(12): p. 1305-1320.
10. Linardou, H., et al., Responses to SARS-CoV-2 Vaccination in Patients with Cancer (ReCOVer Study): A Prospective Cohort Study of the Hellenic Cooperative Oncology Group. *Cancers (Basel)*, 2021. **13**(18).
11. Chung, D.J., et al., Disease- and Therapy-Specific Impact on Humoral Immune Responses to COVID-19 Vaccination in Hematologic Malignancies. *Blood Cancer Discov*, 2021. **2**(6): p. 568-576.
12. van Dam, P., et al., Immunoglobulin G/total antibody testing for SARS-CoV-2: A prospective cohort study of ambulatory patients and health care workers in two Belgian oncology units comparing three commercial tests. *European Journal of Cancer*, 2021. **148**: p. 328-339.
13. Fendler, A., et al., Functional antibody and T cell immunity following SARS-CoV-2 infection, including by variants of concern, in patients with cancer: the CAPTURE study. *Nat Cancer*, 2021. **2**(12): p. 1321-1337.
14. Overheu, O., et al., Low Serological Prevalence of SARS-CoV-2 Antibodies in Cancer Patients at a German University Oncology Center. *Oncol Res Treat*, 2022. **45**(3): p. 112-117.
15. Konnova, A., et al., Predictive model for BNT162b2 vaccine response in cancer patients based on blood cytokines and growth factors. *Front Immunol*, 2022. **13**: p. 1062136.
16. Hu, B., S. Huang, and L. Yin, The cytokine storm and COVID-19. *J Med Virol*, 2021. **93**(1): p. 250-256.

17. Que, Y., et al., Cytokine release syndrome in COVID-19: a major mechanism of morbidity and mortality. *Int Rev Immunol*, 2022. **41**(2): p. 217-230.
18. Shimabukuro-Vornhagen, A., et al., Cytokine release syndrome. *J Immunother Cancer*, 2018. **6**(1): p. 56.
19. Moore, J.B. and C.H. June, Cytokine release syndrome in severe COVID-19. *Science*, 2020. **368**(6490): p. 473-474.
20. Lucas, C., et al., Longitudinal analyses reveal immunological misfiring in severe COVID-19. *Nature*, 2020. **584**(7821): p. 463-469.
21. Huang, C., et al., Clinical features of patients infected with 2019 novel coronavirus in Wuhan, China. *Lancet*, 2020. **395**(10223): p. 497-506.
22. Yang, Y., et al., Plasma IP-10 and MCP-3 levels are highly associated with disease severity and predict the progression of COVID-19. *J Allergy Clin Immunol*, 2020. **146**(1): p. 119-127.e4.
23. Mojtavavi, H., A. Saghazadeh, and N. Rezaei, Interleukin-6 and severe COVID-19: a systematic review and meta-analysis. *Eur Cytokine Netw*, 2020. **31**(2): p. 44-49.
24. Kaye, A.G. and R. Siegel, The efficacy of IL-6 inhibitor Tocilizumab in reducing severe COVID-19 mortality: a systematic review. *PeerJ*, 2020. **8**: p. e10322.
25. Tleyjeh, I.M., et al., Efficacy and safety of tocilizumab in COVID-19 patients: a living systematic review and meta-analysis. *Clin Microbiol Infect*, 2021. **27**(2): p. 215-227.
26. McCreary, E.K. and N.J. Meyer, Covid-19 controversies: the tocilizumab chapter. *Bmj*, 2021. **372**: p. n244.
27. Gordon, A.C., et al., Interleukin-6 Receptor Antagonists in Critically Ill Patients with Covid-19 – Preliminary report. *medRxiv*, 2021: p. 2021.01.07.21249390.
28. Veiga, V.C., et al., Effect of tocilizumab on clinical outcomes at 15 days in patients with severe or critical coronavirus disease 2019: randomised controlled trial. *Bmj*, 2021. **372**: p. n84.
29. Angioni, R., et al., Age-severity matched cytokine profiling reveals specific signatures in Covid-19 patients. *Cell Death Dis*, 2020. **11**(11): p. 957.
30. Hou, H., et al., Using IL-2R/lymphocytes for predicting the clinical progression of patients with COVID-19. *Clin Exp Immunol*, 2020. **201**(1): p. 76-84.
31. Liu, Q.Q., et al., Cytokines and their relationship with the severity and prognosis of coronavirus disease 2019 (COVID-19): a retrospective cohort study. *BMJ Open*, 2020. **10**(11): p. e041471.
32. Del Valle, D.M., et al., An inflammatory cytokine signature predicts COVID-19 severity and survival. *Nat Med*, 2020. **26**(10): p. 1636-1643.
33. Chi, Y., et al., Serum Cytokine and Chemokine Profile in Relation to the Severity of Coronavirus Disease 2019 in China. *J Infect Dis*, 2020. **222**(5): p. 746-754.

34. Jøntvedt Jørgensen, M., et al., Increased interleukin-6 and macrophage chemoattractant protein-1 are associated with respiratory failure in COVID-19. *Sci Rep*, 2020. **10**(1): p. 21697.
35. Li, S., et al., Clinical and pathological investigation of patients with severe COVID-19. *JCI Insight*, 2020. **5**(12).
36. McElvaney, O.J., et al., Characterization of the Inflammatory Response to Severe COVID-19 Illness. *Am J Respir Crit Care Med*, 2020. **202**(6): p. 812-821.
37. Naumenko, V., et al., Neutrophils in viral infection. *Cell Tissue Res*, 2018. **371**(3): p. 505-516.
38. Hue, S., et al., Uncontrolled Innate and Impaired Adaptive Immune Responses in Patients with COVID-19 Acute Respiratory Distress Syndrome. *Am J Respir Crit Care Med*, 2020. **202**(11): p. 1509-1519.
39. Lucas, C., et al., Longitudinal analyses reveal immunological misfiring in severe COVID-19. *Nature*, 2020. **584**(7821): p. 463-469.
40. Haljasmägi, L., et al., Longitudinal proteomic profiling reveals increased early inflammation and sustained apoptosis proteins in severe COVID-19. *Sci Rep*, 2020. **10**(1): p. 20533.
41. Sims, J.T., et al., Characterization of the cytokine storm reflects hyperinflammatory endothelial dysfunction in COVID-19. *J Allergy Clin Immunol*, 2021. **147**(1): p. 107-111.
42. Young, B.E., et al., Viral dynamics and immune correlates of COVID-19 disease severity. *Clin Infect Dis*, 2020.
43. Bülow Anderberg, S., et al., Increased levels of plasma cytokines and correlations to organ failure and 30-day mortality in critically ill Covid-19 patients. *Cytokine*, 2021. **138**: p. 155389.
44. Chen, Y., et al., IP-10 and MCP-1 as biomarkers associated with disease severity of COVID-19. *Mol Med*, 2020. **26**(1): p. 97.
45. Carmeliet, P., VEGF as a key mediator of angiogenesis in cancer. *Oncology*, 2005. **69 Suppl 3**: p. 4-10.
46. Apte, R.S., D.S. Chen, and N. Ferrara, VEGF in Signaling and Disease: Beyond Discovery and Development. *Cell*, 2019. **176**(6): p. 1248-1264.
47. Thickett, D.R., et al., Vascular endothelial growth factor may contribute to increased vascular permeability in acute respiratory distress syndrome. *Am J Respir Crit Care Med*, 2001. **164**(9): p. 1601-5.
48. Kaner, R.J., et al., Lung overexpression of the vascular endothelial growth factor gene induces pulmonary edema. *Am J Respir Cell Mol Biol*, 2000. **22**(6): p. 657-64.
49. Epiphonio, S., et al., VEGF promotes malaria-associated acute lung injury in mice. *PLoS Pathog*, 2010. **6**(5): p. e1000916.
50. Rovas, A., et al., Microvascular dysfunction in COVID-19: the MYSTIC study. *Angiogenesis*, 2021. **24**(1): p. 145-157.

51. Ackermann, M., et al., Pulmonary Vascular Endothelialitis, Thrombosis, and Angiogenesis in Covid-19. *N Engl J Med*, 2020. **383**(2): p. 120-128.
52. Pine, A.B., et al., Circulating markers of angiogenesis and endotheliopathy in COVID-19. *Pulm Circ*, 2020. **10**(4): p. 2045894020966547.
53. Kong, Y., et al., VEGF-D: a novel biomarker for detection of COVID-19 progression. *Crit Care*, 2020. **24**(1): p. 373.
54. Yin, X.X., et al., Vascular Endothelial Growth Factor (VEGF) as a Vital Target for Brain Inflammation during the COVID-19 Outbreak. *ACS Chem Neurosci*, 2020. **11**(12): p. 1704-1705.
55. Moutal, A., et al., SARS-CoV-2 spike protein co-opts VEGF-A/neuropilin-1 receptor signaling to induce analgesia. *Pain*, 2021. **162**(1): p. 243-252.
56. Ghazavi, A., et al., Cytokine profile and disease severity in patients with COVID-19. *Cytokine*, 2021. **137**: p. 155323.
57. Grivennikov, S.I., F.R. Greten, and M. Karin, Immunity, Inflammation, and Cancer. *Cell*, 2010. **140**(6): p. 883-899.
58. Terzić, J., et al., Inflammation and colon cancer. *Gastroenterology*, 2010. **138**(6): p. 2101-2114.e5.
59. Lan, T., L. Chen, and X. Wei, Inflammatory Cytokines in Cancer: Comprehensive Understanding and Clinical Progress in Gene Therapy. *Cells*, 2021. **10**(1).
60. Mantovani, A., et al., Cancer-related inflammation. *Nature*, 2008. **454**(7203): p. 436-444.
61. Heydarian, M., et al., The effect of COVID-19 derived cytokine storm on cancer cells progression: double-edged sword. *Mol Biol Rep*, 2022. **49**(1): p. 605-615.
62. Hippisley-Cox, J., et al., Risk prediction of covid-19 related death and hospital admission in adults after covid-19 vaccination: national prospective cohort study. *Bmj*, 2021. **374**: p. n2244.
63. van Dam, P.A., et al., SARS-CoV-2 and cancer: Are they really partners in crime? *Cancer Treat Rev*, 2020. **89**: p. 102068.
64. Addeo, A. and A. Friedlaender, Cancer and COVID-19: Unmasking their ties. *Cancer Treat Rev*, 2020. **88**: p. 102041.
65. Garmendia, I., et al., Acute Influenza Infection Promotes Lung Tumor Growth by Reprogramming the Tumor Microenvironment. *Cancer Immunol Res*, 2023. **11**(4): p. 530-545.
66. Taniguchi, K. and M. Karin, IL-6 and related cytokines as the critical lynchpins between inflammation and cancer. *Semin Immunol*, 2014. **26**(1): p. 54-74.
67. Kumari, N., et al., Role of interleukin-6 in cancer progression and therapeutic resistance. *Tumour Biol*, 2016. **37**(9): p. 11553-11572.
68. Balkwill, F., TNF-alpha in promotion and progression of cancer. *Cancer Metastasis Rev*, 2006. **25**(3): p. 409-16.

69. Montfort, A., et al., The TNF Paradox in Cancer Progression and Immunotherapy. *Front Immunol*, 2019. **10**: p. 1818.
70. Huber, M.A., et al., NF-kappaB is essential for epithelial-mesenchymal transition and metastasis in a model of breast cancer progression. *J Clin Invest*, 2004. **114**(4): p. 569-81.
71. Alfaro, C., et al., Interleukin-8 in cancer pathogenesis, treatment and follow-up. *Cancer Treat Rev*, 2017. **60**: p. 24-31.
72. David, J.M., et al., The IL-8/IL-8R Axis: A Double Agent in Tumor Immune Resistance. *Vaccines (Basel)*, 2016. **4**(3).
73. Yoshimura, T., The chemokine MCP-1 (CCL2) in the host interaction with cancer: a foe or ally? *Cell Mol Immunol*, 2018. **15**(4): p. 335-345.
74. Fendler, A., et al., Functional antibody and T-cell immunity following SARS-CoV-2 infection, including by variants of concern, in patients with cancer: the CAPTURE study. *Res Sq*, 2021.
75. Mukaida, N., S.I. Sasaki, and T. Baba, CCL4 Signaling in the Tumor Microenvironment. *Adv Exp Med Biol*, 2020. **1231**: p. 23-32.
76. De Winter, F.H.R., et al., Blood Cytokine Analysis Suggests That SARS-CoV-2 Infection Results in a Sustained Tumour Promoting Environment in Cancer Patients. *Cancers (Basel)*, 2021. **13**(22).
77. Esmailbeig, M. and A. Ghaderi, Interleukin-18: a regulator of cancer and autoimmune diseases. *Eur Cytokine Netw*, 2017. **28**(4): p. 127-140.
78. Kursunel, M.A. and G. Esendagli, The untold story of IFN- γ in cancer biology. *Cytokine Growth Factor Rev*, 2016. **31**: p. 73-81.
79. Mojic, M., K. Takeda, and Y. Hayakawa, The Dark Side of IFN- γ : Its Role in Promoting Cancer Immuno-evasion. *Int J Mol Sci*, 2017. **19**(1).
80. Tokunaga, R., et al., CXCL9, CXCL10, CXCL11/CXCR3 axis for immune activation - A target for novel cancer therapy. *Cancer Treat Rev*, 2018. **63**: p. 40-47.
81. Lee, J.E., et al., The Role of Interleukin-9 in Cancer. *Pathol Oncol Res*, 2020. **26**(4): p. 2017-2022.
82. Hanahan, D. and R.A. Weinberg, Hallmarks of cancer: the next generation. *Cell*, 2011. **144**(5): p. 646-74.
83. Pinato, D.J., et al., Prevalence and impact of COVID-19 sequelae on treatment and survival of patients with cancer who recovered from SARS-CoV-2 infection: evidence from the OnCovid retrospective, multicentre registry study. *Lancet Oncol*, 2021. **22**(12): p. 1669-1680.
84. Maamar, M., et al., Post-COVID-19 syndrome, low-grade inflammation and inflammatory markers: a cross-sectional study. *Curr Med Res Opin*, 2022. **38**(6): p. 901-909.
85. Abbas, A.K., The Surprising Story of IL-2: From Experimental Models to Clinical Application. *Am J Pathol*, 2020. **190**(9): p. 1776-1781.

86. Spolski, R., P. Li, and W.J. Leonard, Biology and regulation of IL-2: from molecular mechanisms to human therapy. *Nat Rev Immunol*, 2018. **18**(10): p. 648-659.
87. Abers, M.S., et al., An immune-based biomarker signature is associated with mortality in COVID-19 patients. *JCI Insight*, 2021. **6**(1).
88. Korbecki, J., et al., CC Chemokines in a Tumor: A Review of Pro-Cancer and Anti-Cancer Properties of the Ligands of Receptors CCR1, CCR2, CCR3, and CCR4. *Int J Mol Sci*, 2020. **21**(21).
89. Okada, M., et al., Tumor-associated macrophage/microglia infiltration in human gliomas is correlated with MCP-3, but not MCP-1. *Int J Oncol*, 2009. **34**(6): p. 1621-7.
90. Colak, S. and P. Ten Dijke, Targeting TGF- β Signaling in Cancer. *Trends Cancer*, 2017. **3**(1): p. 56-71.
91. Noh, K.H., et al., API5 confers tumoral immune escape through FGF2-dependent cell survival pathway. *Cancer Res*, 2014. **74**(13): p. 3556-66.
92. Presta, M., et al., Fibroblast growth factors (FGFs) in cancer: FGF traps as a new therapeutic approach. *Pharmacol Ther*, 2017. **179**: p. 171-187.
93. Radin, D.P. and P. Patel, BDNF: An Oncogene or Tumor Suppressor? *Anticancer Res*, 2017. **37**(8): p. 3983-3990.
94. Petrey, A.C., et al., Cytokine release syndrome in COVID-19: Innate immune, vascular, and platelet pathogenic factors differ in severity of disease and sex. *J Leukoc Biol*, 2020.
95. Azoulay, D., et al., Recovery from SARS-CoV-2 infection is associated with serum BDNF restoration. *J Infect*, 2020. **81**(3): p. e79-e81.
96. Cortés, A., et al., Limited T cell response to SARS-CoV-2 mRNA vaccine among patients with cancer receiving different cancer treatments. *Eur J Cancer*, 2022. **166**: p. 229-239.
97. Bergamaschi, C., et al., Systemic IL-15, IFN-gamma, and IP-10/CXCL10 signature associated with effective immune response to SARS-CoV-2 in BNT162b2 mRNA vaccine recipients. *Cell Rep*, 2021. **36**(6): p. 109504.
98. Guo, Y., et al., Immunobiology of the IL-15/IL-15R α complex as an antitumor and antiviral agent. *Cytokine Growth Factor Rev*, 2017. **38**: p. 10-21.
99. Kandikattu, H.K., et al., IL-15 immunotherapy is a viable strategy for COVID-19. *Cytokine Growth Factor Rev*, 2020. **54**: p. 24-31.
100. Bermejo-Martin, J.F., et al., Viral RNA load in plasma is associated with critical illness and a dysregulated host response in COVID-19. *Crit Care*, 2020. **24**(1): p. 691.
101. Yang, Y., et al., Plasma IP-10 and MCP-3 levels are highly associated with disease severity and predict the progression of COVID-19. *J Allergy Clin Immunol*, 2020. **146**(1): p. 119-127 e4.
102. Yamada, Y. and S. Kamihira, Pathological roles of interleukin-15 in adult T-cell leukemia. *Leuk Lymphoma*, 1999. **35**(1-2): p. 37-45.

103. Vecchié, A., et al., IL-18 and infections: Is there a role for targeted therapies? *J Cell Physiol*, 2021. **236**(3): p. 1638-1657.
104. Carty, M., C. Guy, and A.G. Bowie, Detection of Viral Infections by Innate Immunity. *Biochem Pharmacol*, 2021. **183**: p. 114316.
105. Dewerchin, M. and P. Carmeliet, Placental growth factor in cancer. *Expert Opin Ther Targets*, 2014. **18**(11): p. 1339-54.
106. Albonici, L., et al., Multifaceted Role of the Placental Growth Factor (PlGF) in the Antitumor Immune Response and Cancer Progression. *Int J Mol Sci*, 2019. **20**(12).
107. Giardini, V., et al., Increased sFLT-1/PlGF ratio in COVID-19: A novel link to angiotensin II-mediated endothelial dysfunction. *Am J Hematol*, 2020. **95**(8): p. E188-e191.
108. Gupta, A., et al., Host immunological responses facilitate development of SARS-CoV-2 mutations in patients receiving monoclonal antibody treatments. *J Clin Invest*, 2023.
109. Wang, K., et al., miR-194 Inhibits Innate Antiviral Immunity by Targeting FGF2 in Influenza H1N1 Virus Infection. *Front Microbiol*, 2017. **8**: p. 2187.
110. Shi, J., P. Feng, and T. Gu, MicroRNA-21-3p modulates FGF2 to facilitate influenza A virus H5N1 replication by refraining type I interferon response. *Biosci Rep*, 2020. **40**(5).
111. Limonta, D., et al., Fibroblast Growth Factor 2 Enhances Zika Virus Infection in Human Fetal Brain. *J Infect Dis*, 2019. **220**(8): p. 1377-1387.
112. Wang, K., et al., Basic fibroblast growth factor protects against influenza A virus-induced acute lung injury by recruiting neutrophils. *J Mol Cell Biol*, 2018. **10**(6): p. 573-585.
113. Leitner, N.R., et al., Tyrosine kinase 2 - Surveillant of tumours and bona fide oncogene. *Cytokine*, 2017. **89**: p. 209-218.
114. Wöss, K., et al., TYK2: An Upstream Kinase of STATs in Cancer. *Cancers (Basel)*, 2019. **11**(11).
115. Mu, J., et al., SARS-CoV-2 N protein antagonizes type I interferon signaling by suppressing phosphorylation and nuclear translocation of STAT1 and STAT2. *Cell Discov*, 2020. **6**: p. 65.
116. Kern, K.A. and R.J. Rosenberg, Preoperative lymphoscintigraphy during lymphatic mapping for breast cancer: improved sentinel node imaging using subareolar injection of technetium 99m sulfur colloid. *J Am Coll Surg*, 2000. **191**(5): p. 479-89.
117. Pairo-Castineira, E., et al., Genetic mechanisms of critical illness in COVID-19. *Nature*, 2020.
118. Cannarile, M.A., et al., Colony-stimulating factor 1 receptor (CSF1R) inhibitors in cancer therapy. *J Immunother Cancer*, 2017. **5**(1): p. 53.
119. Szebeni, G.J., et al., Inflammation and Cancer: Extra- and Intracellular Determinants of Tumor-Associated Macrophages as Tumor Promoters. *Mediators Inflamm*, 2017. **2017**: p. 9294018.

Chapter 2:

Sample collection, management and processing within the ORCHESTRA consortium

Angelina Konnova participated in the preparation of the ORCHESTRA sample collection manual with the focus on the collection, storage and processing of blood samples (whole blood, serum, plasma, PBMCs). In this chapter, only collection of serum and plasma samples are discussed in detail due to their relevance for subsequent chapters. Additionally, Angelina Konnova established and optimised serology and ACE2 seroneutralization protocols. Cytokinome analysis was pre-established in the group and was optimised for COVID-19 studies by Angelina Konnova.

Objectives and brief description of sub-studies within ORCHESTRA

Several different sample types were analysed within the ORCHESTRA study for the purposes of identifying human and viral genetic markers indicative of disease severity as well as to study immune responses over time as a result of infection and immunization. Specifically, samples were collected from patients developing COVID-19 (including breakthrough and reinfection) in order to study both short- and long-term effects of infection on host immunity, respiratory and intestinal microbiome dynamics as well as host and viral genetic determinants underlying infection. Additionally, samples were collected from vaccinated fragile populations as well as vaccinated healthcare workers in order to study effects of vaccination on host immunity and respiratory and intestinal microbiome dynamics.

Samples collected within the framework of the ORCHESTRA study were in many cases subjected to more than one type of analysis. To provide an overview of research questions of interest within the project, a brief summary of each analysis can be found below.

Characterisation of SARS-CoV-2 viral variants (Task 6.2, *not part of this thesis*)

This task targeted two main points among selected patient populations: [i] to characterise the viral variants and to identify variants of concern (VOCs) by whole genome sequencing (WGS) in COVID-19 patients and in vaccinated individuals with breakthrough infections, and [ii] to study potential mutation selection in populations presenting with long viral replication or receiving immunoglobulin therapies, and [iii] to study the viral replication (viral load and excretion duration).

Characterisation of serological markers of SARS-CoV-2 infection (Task 6.3)

This task characterized the host antibody responses with quantitative serology (anti-S and anti-N) on Abbott, Roche, MesoScale Discovery (MSD), or similar platforms as well as (pseudo-) seroneutralisation assays. These assays were performed on populations with various degrees of COVID-19 severity and vaccinated individuals, also with breakthrough infections.

Characterisation of cellular immunity for SARS-CoV-2 infection (Task 6.4, *not part of this thesis*)

Vaccinated and non-vaccinated COVID-19 patients with varying degrees of disease severity and SARS-CoV-2-positive non-symptomatic individuals were studied for the balance and the phenotypes of T and B cells as a function of disease course and severity as well as response to vaccination. This task chiefly employed flow cytometric analyses with CD45, CD3, CD4, CD19, FOXP3, Ki-67, CD38 markers, viability and IFN γ release assays.

Cytokine analysis (Task 6.5)

Vaccinated and non-vaccinated COVID-19 patients with varying degrees of disease severity, SARS-CoV-2-positive non-symptomatic individuals and vaccinated individuals were studied on MSD panels, Luminex panels and on select ELISAs. As an outcome, panels of cytokine markers predicting disease severity, mortality, breakthrough infections, and long term sequelae were generated.

Next generation sequencing (NGS) of COVID-19 cohorts (Task 6.6, *not part of this thesis*)

In-depth human genetic analysis was conducted using WGS or whole exome sequencing (WES) to identify genetic factors causing or conferring susceptibility to severe manifestations of COVID-19 disease. Vaccinated subjects experiencing breakthrough infection were also studied through WGS or WES. The most promising variants were followed by functional analyses and correlated with markers of interest such as auto-antibodies against type I interferons (IFNs) detected in matched serum samples when available. Note that whole blood was only collected for this task within FrenchCovid and UNIBO cohorts.

Epigenome-wide analyses (Task 6.7, *not part of this thesis*)

Epigenome-wide methylation analyses of COVID-19-positive patients and matched control patients from population-based studies enabled the identification of differentially modified regions through COVID-19 infection, which result in severe disease or an efficient clearing of infection through immune responses. Likewise, the inclusion of baseline and follow-up samples from vaccination cohorts allowed the identification of longitudinal changes in DNAm patterns after immunization.

Intestinal Microbiome Profiling (Task 6.8, *not part of this thesis*)

This task profiled compositional and functional structures of the microbiome from faecal samples by NGS approaches, in order to elucidate the role of the intestinal microbiome in the susceptibility, progression and severity of COVID-19 infection.

Respiratory microbiome dynamics (Task 6.9, *not part of this thesis*)

We investigated differences in the respiratory microbiome composition by combining meta-transcriptomic and metagenomic sequencing to analyse both RNA and DNA viruses and the bacterial and fungal fractions. Firstly, this elucidated the role of commensal flora and of co-infecting respiratory pathogens in influencing COVID-19 disease severity. Secondly, long-term carriage and impact of SARS-CoV-2 on the respiratory microbiome was assessed on longitudinally collected prospective samples (6-12 months post-recovery and new infections).

Sampling timepoints

An overview of sample types collected at each time point can be found in Table 1 below. No collection material was provided within this study, but recommended materials to be used for each collection can be found in the section entitled “Detailed sample collection and storage instructions”.

Table 1. Overview of required biosamples associated analysis within WP6.

Sample type	Sample name	Task	Analysis
NP swab	NP swab	Task 6.2	Viral variant sequencing
		Task 6.9	Respiratory microbiome analysis
Serum (see Appendix 1)	Serum-1	Task 6.3	Serology
	Serum-2	Task 6.6	Assessment of autoantibodies against type I IFNs
EDTA plasma (see Appendix 2)	Plasma	Task 6.5	Cytokine analysis
Heparin (PBMCs)	blood PBMC-1 PBMC-2	Task 6.4	Cellular immunity characterization
EDTA whole blood	WB-1	Task 6.6	Human WGS or WES
	WB-2	Task 6.7	Epigenomics
Stool sample (faeces or rectal swab)	Stool Rectal swab	Task 6.8	Intestinal microbiome analysis

Sampling timepoints for COVID-19 patients (including re-infections and breakthrough infections in vaccinated individuals)

Sampling was required to be performed on the day of diagnosis and at following timepoints as shown in 2. Patient inclusion was primarily based on availability of informed consent for the outlined tasks as well as availability of multiple samples per patient. Informed consent forms should have clearly requested permission to perform human genetic and epigenetic analyses, without which these analyses cannot be undertaken. Only certain cohorts collected whole blood for human genetic analyses and epigenetic analyses required control patients within the same cohort.

Sampling timepoints for vaccinated individuals

Vaccinated individuals in WP4 and WP5 were sampled according to the time points outlined in **Table 3**. In case of breakthrough infections post vaccination, samples were collected as outlined in **Table 2**. Vaccination was (mostly) performed in two doses. Collection was performed prior to administration of dose 1 and dose 2, and 3, 6, and 12 months after the first dose (Table 3). In cases where patients received three vaccination doses, sampling timepoints in **Table 4** were followed.

Table 2. Overview sampling and data collection in ORCHESTRA cohorts in COVID-19 patients including long-term sequelae.

	D0 ¹	3 months ¹ ±1 month	6 months ¹ ±1 month	12 months ¹ ±1 month	18 months ¹ ±2 month	Objective
NP swab	x	x ^{2,3}	x ^{2,3}	x ^{2,3}	x ²	Viral variant and metagenomic sequencing
2 x 2 mL serum tube (serum)	2 x ⁹	x	x	x	2 x	Immune - serology and type I IFNs autoantibodies ⁶
4 mL EDTA blood tube (plasma)	x	x ⁴	x ⁴	x ⁴	x ²	Immune - cytokine and chemokine
2 x 9 mL heparin tube (PBMCs)	2 x	2 x ⁴	2 x ⁴	2 x ⁴	2 x ²	Immune - cellular
2 mL EDTA tube ⁷ (whole blood)	x ⁵					Genetic analyses
Stool sample (faeces or rectal swab)	x		x		x	Metagenomic sequencing

^{1.} Day 0: first positive SARS-CoV-2 PCR test. Follow-up of 3, 6, 12, and 18 months start from Day 0.

^{2.} Reassessed only if outside the normal ranges at the previous assessment or if clinically indicated.

^{3.} At least one of the three timepoints (month 3, month 6, month 12) is required to perform metagenomic analyses.

^{4.} At least one of the three timepoints (month 3, month 6, month 12) is required.

^{5.} Only one whole blood sample is required per patient for human genetic analyses, but the timepoint for collection is flexible.

^{6.} For type I IFN autoantibodies, the D0 time point is needed and ideally a second time point (month 12 or 18).

^{7.} Whole blood is only to be collected within FrenchCovid and UNIBO cohorts for human genetic analyses.

^{8.} “x” represents one sample; “2 x” represents two samples

Level I	Assessments of Level I are mandatory
Level II	Customized according to the feasibility of each cohort

Table 3. Overview sampling and data collection in ORCHESTRA cohorts for vaccinated individuals who receive 2 vaccine doses.

	1 st dose	2 nd dose ¹	3 months ² (± 1 month)	6 months ² (± 2 months)	12 months ² (± 3 months)	Objective
NP swab	x ³	x ³	x ⁴	x ⁴	x ⁴	Viral variant and metagenomic sequencing
2 x 2 mL serum tube (serum)	2 x ¹⁰	x	x	x	2 x	Immune - serology and type I IFNs auto-antibodies ⁷
4 mL EDTA blood tube (plasma)	x	x ⁵	x ⁵	x ⁵	x ⁵	Immune - cytokine and chemokine
2 x 9 mL heparin tube (PBMCs)	2 x	2 x ⁵	2 x ⁵	2 x ⁵	2 x ⁵	Immune - cellular
2 mL EDTA tube ⁸ (whole blood)	x ⁶					Genetic analyses
2 mL EDTA tube ⁹ (whole blood)	x	x	x			Epigenetic analyses
Stool sample (faeces or rectal swab)	x		x			Metagenomic sequencing

1. The assessment at 2nd dose is mandatory in patients who will receive such dose within 8-12 weeks after first dose.

2. 3, 6, and 12 months counted from 1st dose.

3. At least one timepoint at 1st or 2nd dose is required.

4. At least one of the three timepoints (month 3, month 6, month 12) is required.

5. At least one of the four timepoints (2nd dose, month 3, month 6, month 12) is required.

6. Only one whole blood sample is required per patient for human genetic analyses, but the timepoint for collection is flexible.

7. For type I autoantibodies, we need an early time point (1st or 2nd dose) and if possible the month 12 time point

8. Whole blood is only to be collected within FrenchCovid and UNIBO cohorts for human genetic analyses.

9. For epigenetic analyses, a baseline sample is required (1st or 2nd dose), as well as one follow-up timepoint (preferably month 3). If a baseline sample is not available, cohort is not eligible for inclusion in epigenetics task; collection of any additional samples and/or time-points is thus not required.

10. “x” represents one sample; “2 x” represents two samples

Level I	Assessments of Level I are mandatory
Level II	Customized according to the feasibility of each cohort

Table 4. Overview sampling and data collection in ORCHESTRA cohorts for vaccinated individuals who receive 3 vaccine doses.

	3 rd dose	1 month ² (\pm 1 month)	3 months ² (\pm 1 month)	6 months ² (\pm 2 months)	12 months ² (\pm 3 months)	Objective
NP swab	x ³	x ³	x ⁴	x ⁴	x ⁴	Viral variant and metagenomic sequencing
2 x 2 mL serum tube (serum)	x	x	x	x	x	Immune - serology and type I IFNs auto-antibodies ⁷
4 mL EDTA blood tube (plasma)	x	x ⁵	x ⁵	x ⁵	x ⁵	Immune - cytokine and chemokine
2 x 9 mL heparin tube (PBMCs)	2 x	2 x ⁵	2 x ⁵	2 x ⁵	2 x ⁵	Immune - cellular
2 mL EDTA tube ⁸ (whole blood)	x ⁶					Genetic analyses
Stool sample (faeces or rectal swab)	x		x			Metagenomic sequencing

1. The assessment at 2nd dose is mandatory in patients who will receive such dose within 8-12 weeks after first dose.
2. 1, 3, 6, and 12 months counted from 3rd dose.
3. At least one timepoint at 1st or 2nd dose is required.
4. At least one of the three timepoints (month 3, month 6, month 12) is required.
5. At least one of the four timepoints (2nd dose, month 3, month 6, month 12) is required.
6. Only one whole blood sample is required per patient for human genetic analyses, but the timepoint for collection is flexible.
7. For type I autoantibodies, we need an early time point (1st or 2nd dose) and if possible the month 12 time point
8. Whole blood is only to be collected within FrenchCovid and UNIBO cohorts for human genetic analyses.
9. “x” represents one sample; “2 x” represents two samples

Level I	Assessments of Level I are mandatory
Level II	Customized according to the feasibility of each cohort

Patient inclusion was primarily based on availability of informed consent for the outlined tasks as well as availability of multiple samples per patient. Informed consent forms should have clearly requested permission to perform human genetic and epigenetic analyses, without which these analyses cannot be undertaken. Only certain cohorts collected whole blood for genetic analyses and epigenetic analyses required control patients within the same cohort.

Storage instructions and destination sites

Table 5. Overview of samples to be shipped per time point per patient and their shipping conditions.

Sample type	Number of tubes/samples	Storage temp. (°C)	Shipping temp. (°C)	Destination site
Serum	2	Short-term at -20°C, long-term at -70°C or below	Dry ice	INSERM UANTWERPEN
EDTA plasma	1	Short-term at -20°C, long-term at -70°C or below	Dry ice	UANTWERPEN

Sample workflow, redcap instruments, and Labelling instructions

Patients enrolled in ORCHESTRA were assigned a unique ORCHESTRA-specific patient ID which identified the patient throughout the entire project using the ORCHESTRA Pseudonymization Tool (OPT). The OPT has been developed to support the pseudonymization of patients, data, and samples according to the workflows in ORCHESTRA. Several data quality checks and tests prevented multiple registrations of the same patient or sample at one site. Furthermore, the OPT offered the possibility to generate and print labels for collected samples in the study. This feature was implemented as a web-based application that ran directly in the local users' browsers (no sensitive data is leaving the sites when using this tool). The generated patient ID allowed to identify the patient in the RedCap CRF and was printed as a secondary identifier when sample labels were assigned to the vials in which they are stored. When using the OPT, each collected sample was assigned a unique ORCHESTRA-specific sample ID that was printed on the label attached to each sample vial. Each sample ID was visible in the corresponding WP6 RedCap instrument. When the results generated within WP6 were available, they were uploaded by CINECA in the corresponding RedCap instrument.

In the local lab in each cohort, collected samples were processed as described in this manual and, once ready, a label with the same sample ID assigned at the clinical site was reprinted and used to label the corresponding sample tube. The samples were stored according to the instructions in this manual and shipped to the respective WP6 lab. **Figure 3** outlines a pre-planned shipment agreement between the WP2 UNIVR cohort and WP6 laboratories.

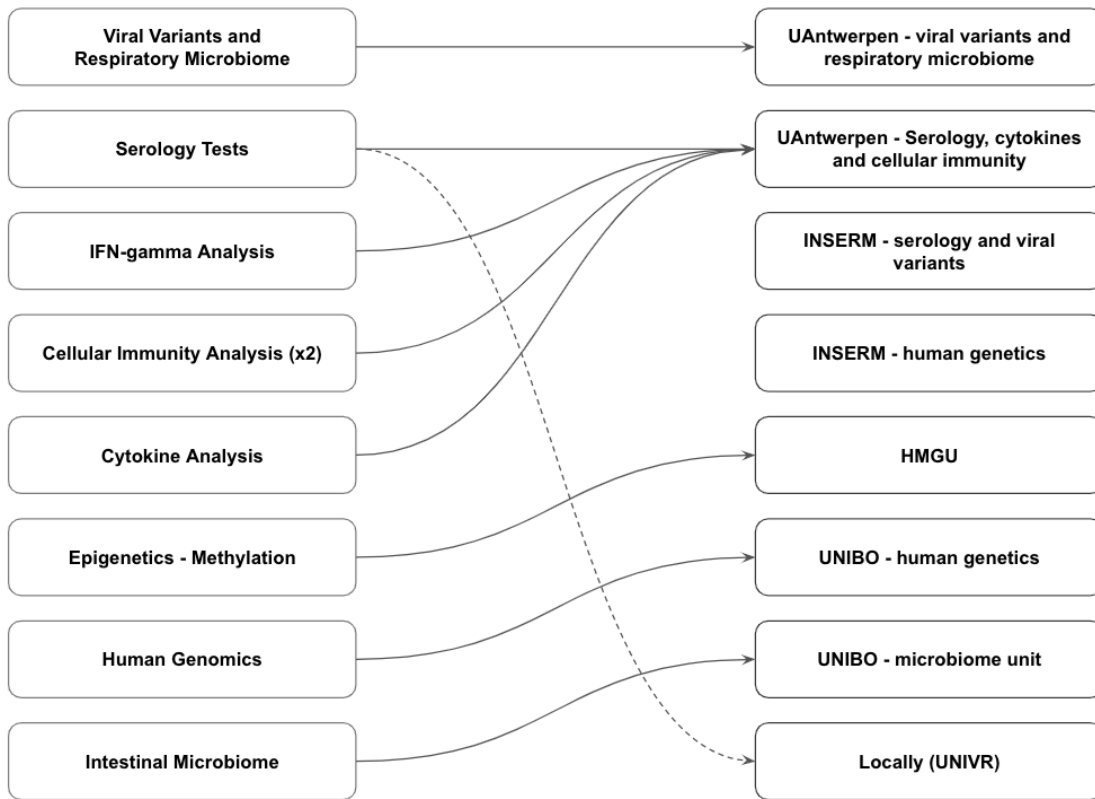


Figure 3. Pre-planned shipment agreement between the WP2 UNIVR cohort and WP6 laboratories.

For samples that were already collected but that do not have an assigned ORCHESTRA patient and sample ID generated by the OPT, new labels needed to be generated using this tool and the samples were re-labelled prior to shipment. For an overview of the re-labelling procedure, see **Figure 4**.

Each label (**Figure 5**) contained pre-printed information, including:

- a sample specific data matrix code
- a unique ORCHESTRA sample ID number (XXXSYYYYYYY where XXX represents a site- specific identifier, S = sample, and YYYYYYYY denotes a unique 7-digit number)
- a unique ORCHESTRA patient ID number (XXXPYYYYYYY where XXX represents a site-specific identifier, P = patient, and YYYYYYYY denotes a unique 7-digit number)
- the WP specific visit timepoint
- WP2: COVID19 INF, M3, M6, M12, M18
- WP4: 1st DOSE, 2nd DOSE, FU M3, FU M6, FU M12, T1 AFTER 3rd DOSE, T2 AFTER 3rd DOSE, T3 AFTER 3rd DOSE
- and the sample type (NP swab, Serum/Plasma, PBMC, EDTA whole blood, Stool/Rectal)

When labelling the sample tube to be shipped with the ORCHESTRA sample ID, the same sample ID was entered in the respective RedCap instrument linked to the patient. It was recommended to use the OPT for generation of labels and patient IDs, but if a cohort could not use this tool to print your own labels, labels were printed at the University of Antwerp, Belgium, and shipped to the site for re-labelling.

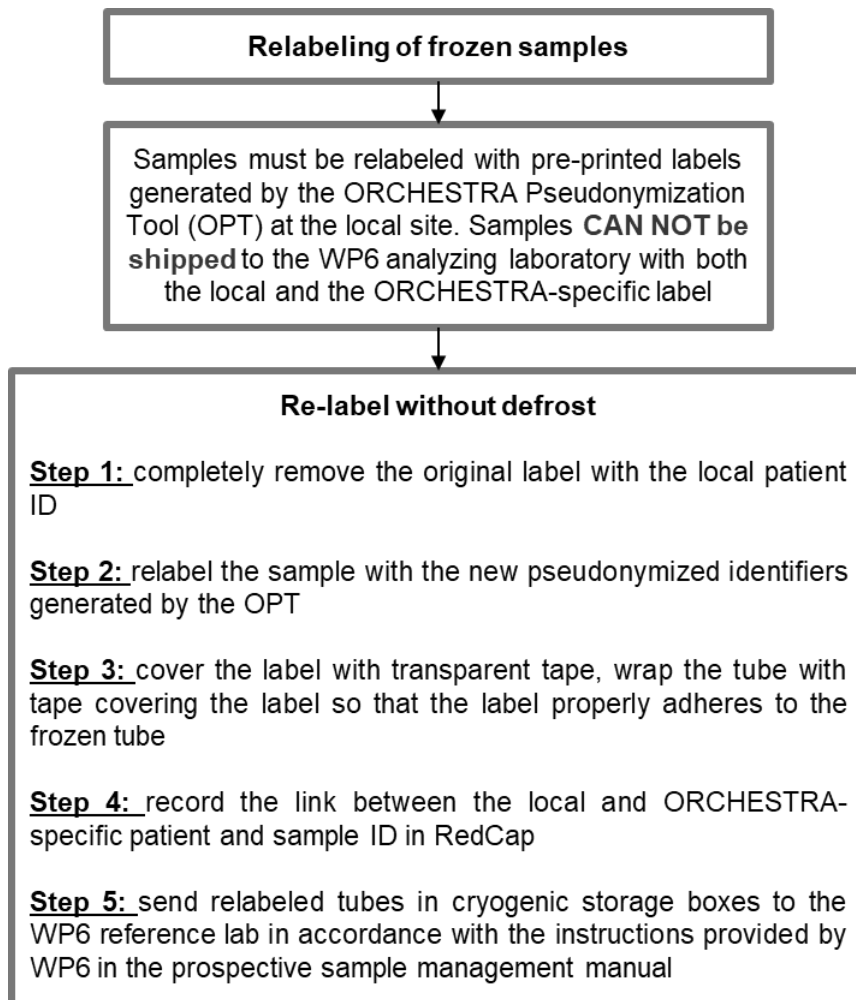


Figure 4. Overview of how frozen and stored samples are to be re-labelled prior to shipment within the ORCHESTRA study.

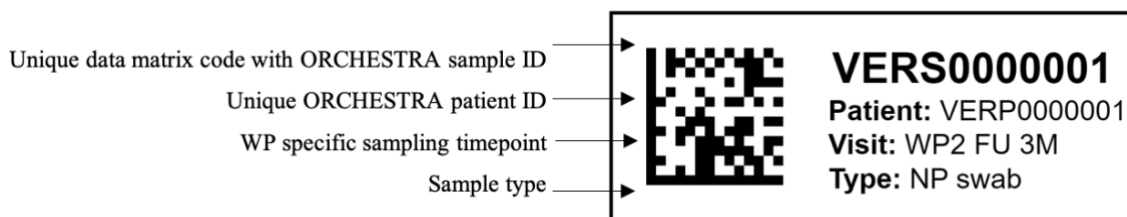


Figure 5. Example of labels to affix to tubes containing samples to be shipped in the ORCHESTRA study.

Study documentation

Prior to shipment, legal documentation was required to be shared with the destination site to comply with biobanking regulations. This documentation included:

- The document submitted for ethical approval along with the blank patient informed consent form
- The clearance by the ethical committee of the study
- A signed Transmission Sheet – Material and Data Transfer Agreement (**Appendix 5. Transmission Sheet – Material and Data Transfer Agreement**)

Shipment Manifest

Each sample shipped within ORCHESTRA needed to be registered locally in the study-specific RedCap database linking the local patient and sample ID with the ORCHESTRA-specific sample barcode number. The ORCHESTRA-specific information further had to be provided in a Shipment Manifest (**Appendix 3. Shipment Manifest**) to the University of Antwerp together with the Shipment Request Form (see **Appendix 4. Shipment Request Form**).

The Shipment Manifest contained the following pre-filled fields: the study name, sample barcode number, sampling timepoint, and sample type. The shipment-related fields, including subject identification number (ORCHESTRA sample ID generated by the ORCHESTRA pseudonymization tool) and shipment date, had to be completed by the local site. The completed manifest had to be sent to the University of Antwerp prior to shipment who provided it to the destination site, which completed the remaining fields linked to the delivery of the samples. In case if the destination site found any non-conformities, the local lab was requested to address these using the same Shipment Manifest and their fields: observation central lab, answer local lab, resolved.

Only samples indicated in the Shipment Manifest were shipped. The samples were kept frozen until shipment. The samples were shipped on dry ice.

Shipping instructions and sample reconciliation

Once samples have been selected by the responsible PI and the Shipment Manifest has been completed at the local site, shipments were prepared. In order to initiate the shipment process, each site needed to complete the Shipment Request Form (attached in Appendix 4. Shipment Request Form) for samples ready for transport and to send it to the University of Antwerp. Upon receiving this shipment request form, University of Antwerp sent out a confirmation e-mail to both the shipping and the receiving partner.

Provided that the Transmission Sheet and export license (if applicable) were in place, University of Antwerp contacted a courier. The courier provided the site with transport boxes, dry ice and transport documents to ensure the shipment arrived in good conditions at the destination site. Temperature trackers were shipped inside every shipment box to control shipment conditions and ensure sample quality. Further details of shipment arrangements, including details about the necessary documents and packaging instructions, were provided by the courier.

Upon arrival at the destination site, samples were reconciled, including verification of ORCHESTRA sample ID, ORCHESTRA patient ID, sample type and sampling timepoint. Samples were allocated a dedicated position within a freezer and biobanked using the BioSLIMS software provided by Antwerp University Hospital (UZA).

Anti-IgG measurements in serum samples

IgG titers were measured in serum samples using V-PLEX SARS-CoV-2 Panel 2 Kit (IgG; #K15359U-4), Panel 6 Kit (IgG; #K15433U-4), Panel 13 Kit (IgG; #K15463U-4), Panel 23 Kit (IgG; #K15567U-4), Panel 24 Kit (IgG; #K15575U-4), Panel 25 Kit (IgG; #K15583U-4), Panel 27 Kit (IgG; #K15606U-4), Panel 29 Kit (IgG; #K15624U-4), Panel 32 Kit (IgG; #K15668U-4), or Panel 34 Kit (IgG; #K156690U-4) on a QuickPlex SQ 120 instrument (Meso Scale Discovery (MSD)) according to the manufacturer's instructions. SARS-CoV-2 variants analysed on different panels are summarised in **Table 8**.

Serum samples were diluted with Diluent 100 (MSD) prior to analysis. The optimal dilution for serum and plasma samples was determined based on the test sample set with the goal of keeping negative or low samples in the measurable range, while preventing saturation of signal with strongly positive samples. Typically, post-vaccination or post-infection samples were measured at a 25,000-fold dilution. For the monoclonal antibody study, baseline samples were measured at 1,000-fold or 10,000-fold dilutions, while all other samples were measured at a final dilution of 10,000,000-fold or 100,000,000-fold dilutions.

For panels containing non-Omicron variants, calibrators were diluted according to manufacturer's instruction (**Figure 6A**). However, due to the low titres of Omicron-specific anti-IgG antibodies in the Reference Standard 1 (MSD), we modified the calibrator dilution scheme for panels containing Omicron variants (**Figure 6B**).

Table 8. SARS-CoV-2 variants analysed in MSD V-PLEX SARS-CoV-2 Panel Kits

	Panel 2	Panel 6	Panel 13	Panel 23	Panel 24	Panel 25	Panel 27	Panel 29	Panel 32	panel 34
Nucleocapsid (Wuhan)	X	X			X					X
RBD (Wuhan)	X	X			X					
Spike (Wuhan)	X	X	X	X	X	X	X	X	X	
Spike (D614G)		X								
Spike (B.1.1.7/Alpha)		X	X	X	X	X				
Spike (B.1.351/Beta)		X	X	X	X	X	X	X		
Spike (P.1/Gamma)		X	X	X	X					
Spike (P.2/Zeta)			X							
Spike (B.1.526.1/Iota)			X							
Spike (B.1.617)			X							
Spike (B.1.617.1/Kappa)			X							
Spike (B.1.617.2/Delta)			X							
Spike (B.1.617.2; AY.3; AY.5/Delta)				X						
Spike (B.1.617.2; AY.4/Delta)				X	X	X	X	X		
Spike (AY.4.2/Delta)				X						
Spike (B.1.617.3)			X							
Spike (B.1.640.2/IHU)						X				
Spike (BA.1/Omicron)				X	X	X			X	X
Spike (BA.1+L452R/Omicron)						X				
Spike (BA.1+R346K/Omicron)						X				
Spike (BA.2/Omicron)						X	X	X		
Spike (BA.2+L452M/Omicron)							X			
Spike (BA.2+L452R/Omicron)							X			
Spike (BA.2.12.1/Omicron)							X	X		
Spike (BA.2.75/Omicron)								X	X	X
Spike (BA.2.75.2/Omicron)									X	
Spike (BA.3/Omicron)						X	X			
Spike (BA.4/Omicron)							X	X		
Spike (BA.4.6/Omicron)									X	
Spike (BA.5/Omicron)							X	X	X	X
Spike (BF.7/Omicron)									X	X
Spike (BN.1/Omicron)										X
Spike (BQ.1/Omicron)									X	X
Spike (BQ.1.1/Omicron)									X	X
Spike (XBB.1/Omicron)									X	X
Spike (XBB.1.5/Omicron)										X

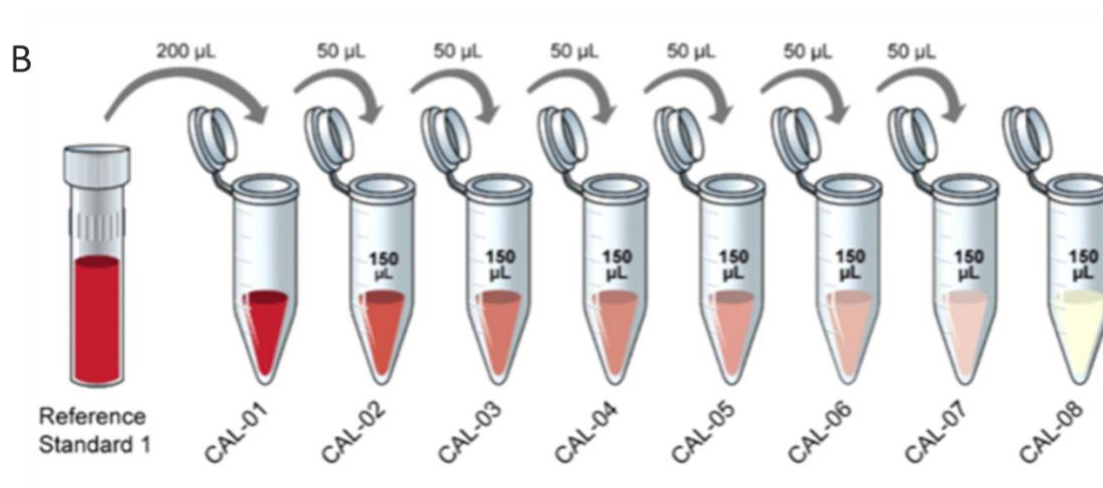
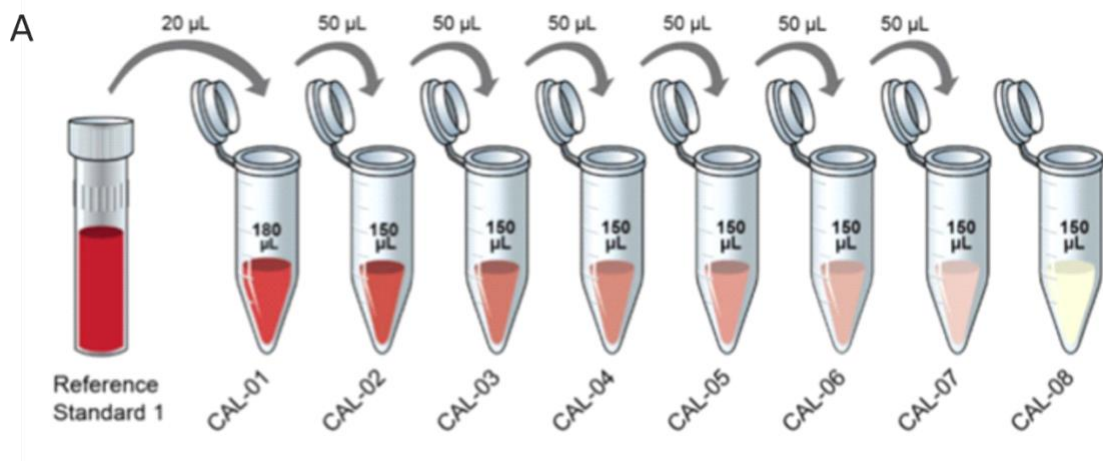


Figure 6. Dilution scheme of for the preparation of calibrator solutions. (A) Dilution scheme using 10-fold dilution of the Reference Standard 1 to generate CAL-01 on panels not containing Omicron variants. **(B)** Dilution scheme using undiluted Reference Standard 1 to generate CAL-01 on panels containing Omicron variants.

Quantitative IgG results were measured in Antibody Units (AU)/mL and converted to Binding Antibody Units (BAU)/mL using a conversion factor provided by the manufacturer and reported as such. Antibody responses were stratified into the groups based on the quantitative IgG measurements as described in **Table 9**. The upper limit for “Negative” was determined as the average plus one standard deviation of anti-Spike IgG measurements in 56 serum samples collected before 2019. The lower limits for “Low”, “Medium” and “High” were based on the BAU/mL concentrations of “Low” (NIBSC code 20/140), “Mid” (NIBSC code 20/148) and “High” (NIBSC code 20/150) WHO International Standards for anti-SARS-CoV-2 immunoglobulins.

Table 9. Stratification of quantitative IgG results

	Negative	Inconclusive	Low	Medium	High	Units
anti-Spike	<4.76	4.76 - <53	53 - <241	241 - <832	>832	BAU/mL
anti-RBD	<5.58	5.58 - <45	45 - <205	205 - <817	>817	BAU/mL
anti-N	<8.20	8.20 - <12	12 - <295	295 - <713	>713	BAU/mL

ACE2 neutralization measurements in serum samples

ACE2 neutralisation was measured in serum samples using V-PLEX SARS-CoV-2 Panel 2 Kit (IgG; #K15359U-4), Panel 6 Kit (IgG; #K15433U-4), Panel 13 Kit (IgG; #K15463U-4), Panel 23 Kit (IgG; #K15567U-4), Panel 24 Kit (IgG; #K15575U-4), Panel 25 Kit (IgG; #K15583U-4), Panel 27 Kit (IgG; #K15606U-4), Panel 29 Kit (IgG; #K15624U-4), Panel 32 Kit (IgG; #K15668U-4), or Panel 34 Kit (IgG; #K156690U-4) on a QuickPlex SQ 120 instrument (Meso Scale Discovery (MSD)) according to the manufacturer’s instructions. SARS-CoV-2 variants analysed on different panels are summarised in **Table 8**.

For ACE2 neutralisation analyses, serum samples were diluted with Diluent 100 (MSD) prior to analysis. The optimal dilution for serum and plasma samples was determined based on the test sample set with the goal of keeping negative or low samples in the measurable range, while preventing saturation of signal with strongly positive samples. Typically, post-vaccination or post-infection samples were measured at a 50-fold or 250-fold dilution. For the monoclonal antibody study, baseline samples were measured at 3,000-fold dilution. Calibrators were diluted according to manufacturer’s instruction with ACE2 Calibrator Reagent being used for non-Omicron panels and ACE2 Calibrator Reagent 2 (MSD) being used for Omicron-containing panels.

Due to the inability of ACE2 Calibrator Reagent and ACE2 Calibrator Reagent 2 to bind to some of the Omicron variants, results were reported as percent inhibition (% inhibition), calculated using the equation below:

$$\% \text{ Inhibition} = \left(1 - \frac{\text{Sample Signal}}{\text{Average Signal of the Blanc}} \right) \times 100\%$$

Additionally, for non-Omicron panels, the calibration curve was used to calculate neutralizing antibody concentrations in samples, by backfitting the measured signals for samples to the calibration curve. Neutralising antibody concentrations were measured in Units (U)/mL, which corresponds to neutralizing activity of 1 µg/mL monoclonal antibody to SARS CoV-2 Spike protein and reported as such.

Cytokine, chemokine and growth factor (CCG) measurements in plasma samples

CCGs were measured in plasma samples on a multiplex platform (Meso Scale Discovery (MSD), MD, USA) using off-the-shelf (V-plex) and customized (U-plex) panels, according to the manufacturer's instructions, following manufacturer instructions. Briefly, 96-well plates of the U-plex panels were coated with a capturing antibody coupled to a linker for one hour. The vascular injury panel (K15198D) was washed before use. The angiogenesis panel (K15190D) was first blocked with blocking buffer for one hour. Thereafter, all plates were washed three times with PBS-Tween (0.05%). Samples were incubated for one hour (except for the angiogenesis and the vascular injury panels, where two hours of incubation were performed), after which the plates were washed another three times. Detection antibody with a SULFO-TAG was added and after another one-hour incubation step (two hours for the angiogenesis panel), the plates were washed and read with MSD reading buffer on the QuickPlex SQ 120 (MSD).

In total, 36 CCGs relevant for SARS-CoV-2 infection or tumour growth and progression were measured in the study of patients with solid and haematological malignancies. These constituted brain-derived neurotrophic factor (BDNF), basic fibroblast growth factor (bFGF), C-reactive protein (CRP), cutaneous T-cell attracting chemokine (CTACK), vascular endothelial growth factor receptor 1 (Flt-1), interferon β (IFN- β), interferon γ (IFN- γ), IL-1 β , IL-1 receptor antagonist (IL-1Ra), IL-2, IL-4, IL-5, IL-6, IL-8, IL-10, IL-13, IL-15, IL-16, IL-17A, IL-18, IL-21, IL-33, IFN- γ induced protein 10 (IP-10; also called CXCL10), monocyte chemoattractant protein (MCP)-1, placental growth factor (PlGF), serum amyloid A (SAA), soluble intercellular adhesion molecule 1 (sICAM-1), soluble vascular cell adhesion molecule 1 (sVCAM-1), active and total (acid activated) tumor growth factor β (TGF- β), angiopoietin receptor 1 (Tie-2), tumor necrosis factor α (TNF- α), thymic stromal lymphopoietin (TSLP), vascular endothelial growth factor (VEGF)-A, VEGF-C and VEGF-D. An additional 5 CCGs were measured in a random subset of plasma samples from 100 cancer patients. These were granulocyte colony stimulating factor (G-CSF), granulocyte-macrophage colony-stimulating factor (GM-CSF), IL-7, IL-9, and macrophage inflammatory protein (MIP)-1 α .

In the monoclonal antibody study the following 40 CIBs were measured: bFGF, CRP, CTACK, eotaxin, erythropoietin (EPO), Flt-1, fractalkine, macrophage colony-stimulating factor (M-CSF), IFN- β , IFN- γ , IL-1 β , IL-1Ra, IL-2, IL-2 receptor α (IL-2R α), IL-4, IL-5, IL-6, IL-8, IL-10, IL-13, IL-15, IL-17A, IL-17F, IL-18, IL-22, IL-33, IP-10, MCP-1, MCP-2, MCP-3, macrophage inflammatory protein (MIP)-1 α , PlGF, SAA, sICAM-1, sVCAM-1, Tie-2, TNF- α , VEGF-A, VEGF-C, and VEGF-D. A small panel of 4 select CIBs, comprising, CRP, bFGF, Tie2, and M-CSF, was additionally utilized for validating CIB profile predictive of SARS-CoV-2 mutations.

Appendices

Appendix 1. Serum sample collection and storage instructions

Recommended materials

- 2 mL BD Vacutainer Serum tube (e.g., BD #368492)
- 2 mL Cryovial (e.g., Simport # T309-2A)
- Disposable plastic pipettes (2.5, 5 mL size)

Sample collection

5. Label the Serum tubes as instructed in the section entitled “Labelling instructions”.
6. Draw the patient’s blood into two Serum tubes (2 mL).
7. Slowly and gently invert the tubes 180° and back 5-6 times.
8. Transfer as soon as possible (within one hour) to the Local Laboratory.

Sample processing

5. Before centrifugation, allow blood to clot thoroughly for 60 minutes.
6. Label the tubes as instructed in the section entitled “Labelling instructions”.
7. Centrifuge the sample at 1300 g for 10 min at 20°C WITH THE BRAKE ON.
8. Transfer approx. 1 mL supernatant from each tube into separate cryovials using sterile disposable pipette taking care to not disturb the buffy coat.

Storage conditions

- After processing, store the cryovials as soon as possible in your freezer at -70°C or below until shipment.
- In case you do not have immediate access to a -70°C freezer, store them at -20°C and transfer them to a -70°C as soon as possible and within 2 days. Keep them at -70°C until shipment is arranged.

Appendix 2. EDTA plasma sample collection and storage instructions

In this section, two protocols for EDTA plasma isolation have been described. Depending on the laboratory protocol utilized, material required for isolation may vary.

Recommended materials

Common materials

- 4 mL BD Vacutainer K2E (EDTA) (e.g., BD Cat. No. 368861)
- 3 mL vial (e.g., Simport Cat. No. T309-3A)
- Disposable plastic pipettes (2.5, 5 mL size)

EDTA Plasma Protocol 1: Single-spin EDTA plasma isolation

- No additional material is required.

EDTA Plasma Protocol 2: Double-spin EDTA plasma isolation

- 3 mL BD Vacutainer EST Tubes (e.g., BD Cat. No. 362725)

Sample collection

1. Label the K2E (EDTA) tube as instructed in the section entitled “Labelling instructions”.
2. Draw the patient’s blood into the EDTA tube (4 mL).
3. Slowly and gently invert the tube 180° and back 8-10 times.
4. Transfer as soon as possible (within one hour) to the Local Laboratory.

Sample processing

EDTA Plasma Protocol 1: Single-spin EDTA plasma isolation

5. The samples should be processed within 120 minutes.
6. Label the 3 mL vial as instructed in the section entitled “Labelling instructions”.
7. Centrifuge the sample at 1300 g for 10 min at 20°C WITH THE BRAKE ON. This will give three layers: (from top to bottom) plasma, leucocytes (buffy coat), and erythrocytes.
8. Transfer approx. 2 mL of plasma into the 3 mL vial using sterile disposable pipette taking care to not disturb the buffy coat.

EDTA Plasma Protocol 2: Double-spin EDTA plasma isolation

5. The samples should be processed within 120 minutes.
6. Label the 3 mL vial as instructed in the section entitled “Labelling instructions”.
7. Centrifugation I: Centrifuge the sample at 1500 g for 15 min at 20°C WITH THE BRAKE ON. This will give three layers: (from top to bottom) plasma, leucocytes (buffy coat), and erythrocytes.

8. Collection of supernatant I: Transfer the plasma in a 3 mL centrifugation tube (e.g. 3 mL BD Vacutainer EST Tube) using sterile disposable pipette taking care to not disturb the buffy coat.
9. Centrifugation II: Centrifugation at 2000 g for 15 min at 20°C WITH THE BRAKE ON to remove all potentially remaining cells.
10. Collection of supernatant II: Transfer approx. 2 mL of plasma into the 3 mL vial using sterile disposable pipette taking care to not disturb the buffy coat.

Storage conditions

- After processing, store the cryovial as soon as possible in your freezer at -70°C or below until shipment.
- In case you do not have immediate access to a -70°C freezer, store it at -20°C and transfer it to a -70°C as soon as possible and within 2 days. Keep them at -70°C until shipment is arranged.

Appendix 3. Shipment Manifest

To be completed by local site							To be completed by Receiving Lab				To be completed by local site if requested	
Study	Subject identification number	Sample barcode number	Sample type	Sampling timepoint	Sample collection date	Shipment date	Arrived	Arrival date at receiving lab	Observation Receiving lab	Action Receiving lab	Resolved (Y/N/L/PALSD)	Answer local site
ORCHESTRA	VERP0000001	VER50000001	NP swab	WP2 FU 3M								

Example of the information that the receiving lab required when samples were shipped from sites to the receiving laboratory:

- Study “ORCHESTRA”: sample is from the ORCHESTRA study
- Patient ID: ORCHESTRA-specific pseudonymized patient ID generated by the ORCHESTRA pseudonymization tool (XXXPYYYYYYYY where XXX represents a site-specific identifier, P = patient, and YYYYYYYY denotes a unique 7-digit number)
- Sample ID: sample with unique ID number (XXXSYYYYYYYY where XXX represents a site-specific identifier, S = sample, and YYYYYYYY denotes a unique 7-digit number)
- Sample type “Serum-1”: sample is aliquot 1 of serum
- Sampling timepoint “1st dose”: sampling timepoint is at the day of COVID-19 diagnosis
- Shipment date: date of shipment
- Answer local site: only required in case there are discrepancies between the shipment manifest and the arriving shipment at the Receiving lab. The local lab will be contacted upon the arrival of the shipment in the Receiving lab with further details.

Blue fields are shipment-related questions and had to be completed by local site prior to shipment. The completed document had to be shared with the Receiving lab via University of Antwerp. Green fields were completed by the Receiving lab upon arrival of the shipment. If necessary, non-conformities were requested to be addressed at the local site in the purple fields. This was requested by the Receiving lab after the initial quality assessment of the shipment was completed.

Appendix 4. Shipment Request Form

ORCHESTRA	
SHIPMENT REQUEST FORM	
Date:	
Necessary information for the sample transport to the Laboratory:	
N° of tubes that will be shippednasopharyngeal swabs stored in tubes of mlserum aliquots stored in tubes of mlplasma samples stored in tubes of mlPBMC aliquots stored in tubes of mlwhole blood aliquots stored in tubes of mlstool samples stored in tubes of mlrectal swabs stored in tubes of ml
Number of boxes to be shipped
Box size:cm xcm xcm
Time during which the pickup is most convenienthrs tohrs andhrs tohrs
Days on which the shipment cannot take place in the coming period (holidays, closures, etc.)	
Pick-up address:	
Hospital Name:
Laboratory Name:
Address:
Contact Name:
Contact E-mail address:
Contact Tel:
Back-up contact Name:
Back-up E-mail address:
Back-up Tel:

Appendix 5. Transmission Sheet – Material and Data Transfer Agreement

ORCHESTRA Consortium Agreement

[Attachment 5: Transmission Sheet – Material and Data Transfer Agreement]

The Supplier (as defined below) agrees to the transfer of or access to the Material and/or Data (described below) to the Recipient (as defined below) for the conducting of the Project in accordance with the terms and conditions of the Consortium Agreement No..... signed between XXXX, and XXXX on .../.../.....

Materials	Designation: Quantities:
Data	Designation: Form:
Party supplying or giving access to the Material and/or Data (the "Supplier")
Name and address of the laboratory supplying or giving access to the Material and/or Data
Contact details of the scientist supplying or giving access to the Material and/or Data	Name: Email: Tel: Fax:
Recipient party for the Material and/or Data (the "Recipient")
Delivery address for the Material and/or Data	Address Name of recipient Email: Tel: Fax:

Signed in - original counterparts drafted in the English language, with one (1) for the Supplier and the other(s) for the Recipient

Witnessed, the Scientific Manager of the Laboratory
.....

Witnessed, the Scientific Manager of XXXX
.....

Chapter 3:

Predictive model for BNT162b2 vaccine response in cancer patients based on blood cytokines and growth factors

Angelina Konnova^{1,2†}, Fien HR De Winter^{1†}, Akshita Gupta^{1,2}, Lise Verbruggen³, An Hotterbeekx¹, Matilda Berkell^{1,2}, Laure-Anne Teuwen⁴, Greetje Vanhoutte^{3,4}, Bart Peeters⁵, Silke Raats³, Isolde Van der Massen³, Sven De Keersmaecker³, Yana Debie^{3,4}, Manon Huizing⁶, Pieter Pannus⁷, Kristof Y Neven^{7,8,9}, Kevin K Ariën^{10,11}, Geert A. Martens¹², Marc Van Den Bulcke⁷, Ella Roelant^{13,14}, Isabelle Desombere¹⁵, Sébastien Anguille⁴, Zwi Berneman^{3,4}, Maria E Goossens¹⁶, Herman Goossens², Surbhi Malhotra-Kumar², Evelina Tacconelli⁷, Timon Vandamme^{3,4}, Marc Peeters^{3,4††}, Peter van Dam^{3,4††}, Samir Kumar-Singh^{1,2*}

¹Molecular Pathology Group, Laboratory of Cell Biology & Histology, Faculty of Medicine and Health Sciences, University of Antwerp, Universiteitsplein 1, Wilrijk, B-2610, Belgium

²Laboratory of Medical Microbiology, Vaccine and Infectious disease Institute, University of Antwerp, Universiteitsplein 1, Wilrijk, B-2610, Belgium

³Multidisciplinary Oncological Center Antwerp (MOCA), Antwerp University Hospital, Drie Eikenstraat 655, 2650 Edegem, Belgium

⁴Center for Oncological Research (CORE), Integrated Personalized and Precision Oncology Network (IPPON), University of Antwerp, Universiteitsplein 1, 2610 Wilrijk, Belgium

⁵Department of Laboratory Medicine, Antwerp University Hospital, Drie Eikenstraat 655, 2650 Edegem, Belgium

⁶Biobank Antwerp, Drie Eikenstraat 655, 2650 Edegem, Belgium

⁷Scientific Directorate Epidemiology and Public Health, Sciensano, Rue Juliette Wytsmanstraat 14, 1050 Brussels, Belgium

⁸Centre for Environmental Sciences, Hasselt University, Hasselt, Belgium

⁹Federal Public Service (FPS) Health, Food Chain Safety and Environment, Brussels, Belgium

¹⁰Virology Unit, Institute of Tropical Medicine Antwerp, Nationalestraat 155, B-2000 Antwerp, Belgium

¹¹Department of Biomedical Sciences, University of Antwerp, Universiteitsplein 1, 2610 Edegem, Belgium

¹²Department of Laboratory Medicine, AZ Delta General Hospital, Roeselare, Belgium

¹³Clinical Trial Center (CTC), CRC Antwerp, Antwerp University Hospital, University of Antwerp, Drie Eikenstraat 655, 2650 Edegem, Belgium

¹⁴StatUa, Center for Statistics, University of Antwerp, Antwerp, Belgium

¹⁵Service Immune response, Scientific Directorate Infectious Diseases in Humans, Sciensano, Rue Juliette Wytsmanstraat 14, 1050 Brussels, Belgium

¹⁶Scientific Directorate Infectious Diseases in Humans, Sciensano, Rue Juliette Wytsmanstraat 14, 1050 Brussels, Belgium

¹⁷Division of Infectious Diseases, Department of Diagnostics and Public Health, University of Verona, P.le L.A. Scuro 10, 37134, Verona, Italy

†Shared first authors: *Angelina Konnova performed cytokine analysis and wrote the manuscript together with Fien De Winter. Fien De Winter was a post-doc, who supervised Angelina Konnova together with Prof. Samir Kumar-Singh.*

††Shared senior authors

*Correspondence: samir.kumarsingh@uantwerpen.be

Manuscript published in Frontiers in Immunology

2022 Dec 22;13:1062136. doi: 10.3389/fimmu.2022.1062136

Abstract

Background: Patients with cancer, especially hematological cancer, are at increased risk for breakthrough COVID-19 infection. So far, a predictive biomarker that can assess compromised vaccine-induced anti-SARS-CoV-2 immunity in cancer patients has not been proposed.

Methods: We employed machine learning approaches to identify a biomarker signature based on blood cytokines, chemokines, and immune- and non-immune-related growth factors linked to vaccine immunogenicity in 199 cancer patients receiving the BNT162b2 vaccine.

Results: C-reactive protein (general marker of inflammation), interleukin (IL)-15 (a pro-inflammatory cytokine), IL-18 (interferon-gamma inducing factor), and placental growth factor (an angiogenic cytokine) correctly classified patients with a diminished vaccine response assessed at day 49 with >80% accuracy. Amongst these, CRP showed the highest predictive value for poor response to vaccine administration. Importantly, this unique signature of vaccine response was present at different studied timepoints both before and after vaccination and was not majorly affected by different anti-cancer treatments.

Conclusion: We propose a blood-based signature of cytokines and growth factors that can be employed in identifying cancer patients at persistent high risk of COVID-19 despite vaccination with BNT162b2. Our data also suggest that such a signature may reflect the inherent immunological constitution of some cancer patients who are refractive to immunotherapy.

Introduction

The field of vaccination against infectious disease has witnessed rapid advances of technology throughout the COVID-19 pandemic, including the development of various anti-SARS-CoV-2 vaccines, such as mRNA and vector vaccines. The BNT162b2 mRNA COVID-19 vaccine elicits a range of immunological responses, especially a strong anti-SARS-CoV-2 IgG response in healthy individuals, which starts waning after approximately 3-6 months [1-3]. However, because the mechanisms determining the quality and quantity of immunological responses are not fully understood, this has led to concerns about the efficiency of these vaccines in immunosuppressed populations including patients with solid or hematological malignancies [4], especially when they are under active antineoplastic treatments. Several studies have shown that vaccine responses are compromised in patients with hematological malignancies under B cell depleting rituximab treatment, or with solid tumors receiving different chemotherapies [5-11].

Biomarkers of protection against SARS-CoV-2 infection generated by anti-SARS-CoV-2 vaccines have been studied for general population [12, 13]. For instance, a post-vaccine anti-SARS-CoV-2 response with BNT162b2 in healthy volunteers is shown to be accompanied by alterations in systemic cytokine, chemokine, and specific growth factors (CCGs), including increase in interleukin (IL)-15, interferon gamma (IFN- γ), and IFN- γ -induced protein 10 (IP-10/CXCL10) after the primer vaccination dose, and by tumor necrosis factor alpha (TNF- α) and IL-6 after the booster vaccination dose [12]. Importantly, transient increases in IL-15 and IFN- γ levels were also identified as biomarkers for anti-SARS-CoV-2 responses in a healthy population [12]. However, none of these biomarkers are currently available for cancer patients, where such a marker can distinguish subgroups of patients which are poorly protected by SARS-CoV-2 vaccination and remain in need of additional (preventive) options [14-16]. CCGs are not only important in the regulation of inflammation occurring in viral infections such as SARS-CoV-2 [12, 17-19] and influenza [20, 21], but also play an important role in the initiation and progression of cancers [22-25]. We recently demonstrated significant alterations in levels of several CCGs in blood of cancer patients including, but not limited to, CCGs that play an important role in the adaptive immune response in antigen presentation and/or T-helper and B cell functions [25]. In the present study, we propose a blood-based signature of cytokines/chemokines and growth factors that can be employed in identifying cancer patients at persistent high-risk of COVID-19 despite vaccination with BNT162b2.

Material and Methods

Patient Population and study design

A prospective, longitudinal, multi-cohort trial was initiated on February 15, 2021, in the Multidisciplinary Oncological Center Antwerp (MOCA), Antwerp University Hospital, Belgium, as described [5]. Briefly, study participants aged 18 years or older with a life expectancy of at least six months were recruited. Pregnant or breastfeeding women and patients with an immunodeficiency unrelated to cancer treatment were not included. All study participants provided written informed consent. A total of 200 cancer patients recruited in this study received at least one dose of the BNT162b2 vaccine. One patient withdrew after the primer dose and was excluded from the study. CCGs before and after the primer dose were measured for 199 patients, including 158 patients with

a solid tumor and 41 patients with a hematological malignancy (**Supplementary Table 1**). From these 199 patients, 187 patients received a booster dose 21 (± 2) days after the primer dose according to the study protocol. Nine patients received a delayed booster dose from 24 to 37 days due to an active SARS-CoV-2-CoV-2 infection or cancer treatment-related complications [5]. The study was approved by the local ethics committee and was executed in accordance with Good Clinical Practice and the Declaration of Helsinki (ICH GCP E6(R2)). The regulatory sponsor was the Antwerp University Hospital (EudraCT number 2021-000300-38).

The included population with solid tumors mainly consisted of patients with breast malignancies (52.8%), followed by patients with gastroenterological (10.1%) and gynecological malignancies (10.1%). Among patients with hematological malignancies, 75.6% of patients had chronic lymphocytic leukemia or lymphomas and 19.5% patients had myeloid malignancies. On the basis of cancer and treatment modalities, we defined 4 cohorts: (i) patients with solid tumors (ST) receiving only chemotherapy (n = 63); (ii) ST patients receiving immunotherapy with or without chemotherapy (n = 16); (iii) ST patients receiving targeted or hormonal therapy (n = 79); and (iv) a combined group of hematological malignancy patients (n = 41) receiving either rituximab (n = 29), targeted therapy (n = 1), or an allogenic hematopoietic stem cell transplantation more than one year ago (n = 11).

Sample collection and processing

Plasma samples were taken at the day of study inclusion (day 0, just before administration of the primer dose), day 1 (the day after the primer dose), day 21 (just before administration of the booster dose), and day 28 (7 days after the booster dose). Serum samples were collected at day 49 (**Figure 1**). For detailed methods, refer to **Supplementary Information**.

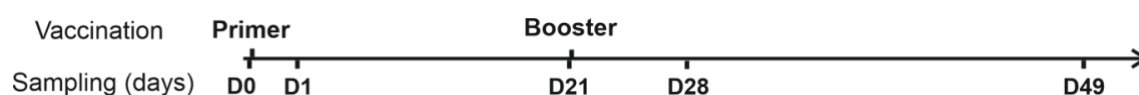


Figure 1. Timeline of the study. The BNT162b2 vaccine was administered on day 0 and 21. Heparin plasma samples for CCG analysis were collected on day 0 just prior to primer dose administration (D0), day 1 (D1), day 21 just prior to booster dose administration (D21), and day 28 (D28). For anti-RBD and anti-S1 serology, serum samples were collected on day 49 (D49) after the administration of the primer vaccine dose.

Cytokine, chemokine and growth factor (CCG) measurements in plasma

CCGs were measured in plasma samples on a multiplex platform (Meso Scale Discovery (MSD), MD, USA) using off-the-shelf (V-plex) and customized (U-plex) panels, according to the manufacturer's instructions, as previously described [25]. For detailed methods, refer to Supplementary Information.

In total, 36 CCGs relevant for SARS-CoV-2 infection or tumor growth and progression were measured. These constituted brain-derived neurotrophic factor (BDNF), basic fibroblast growth factor (bFGF), C-reactive protein (CRP), cutaneous T-cell attracting chemokine (CTACK), vascular endothelial growth factor receptor 1 (Flt-1), interferon β (IFN- β), interferon γ (IFN- γ), IL-1 β , IL-1 receptor antagonist (IL-1Ra), IL-2, IL-4, IL-5, IL-6, IL-8, IL-10, IL-13, IL-15, IL-16, IL-17A, IL-

18, IL-21, IL-33, IFN- γ induced protein 10 (IP-10; also called CXCL10), monocyte chemoattractant protein (MCP)-1, placental growth factor (PIGF), serum amyloid A (SAA), soluble intercellular adhesion molecule 1 (sICAM-1), soluble vascular cell adhesion molecule 1 (VCAM-1), active and total (acid activated) tumor growth factor β (TGF- β), angiopoietin receptor 1 (Tie-2), TNF- α , thymic stromal lymphopoietin (TSLP), vascular endothelial growth factor (VEGF)-A, VEGF-C and VEGF-D. An additional 5 CCGs were measured in a random subset of plasma samples from 100 cancer patients. These were granulocyte colony stimulating factor (G-CSF), granulocyte-macrophage colony-stimulating factor (GM-CSF), IL-7, IL-9, and macrophage inflammatory protein (MIP)-1 α .

Anti-RBD IgG measurements in serum

Anti-RBD immunoglobulin G (IgG) levels were measured in serum samples with an enzyme-linked immunosorbent assay (ELISA) as previously described [5]. A threshold for anti-RBD IgG of 200 IU/mL predicted a neutralization response required for 50% protection against symptomatic SARS-CoV-2 infection (99%-100% specificity at a sensitivity of 94.9%). As such, this threshold was used to differentiate high from low anti-SARS-CoV-2 serological responders, as described [5].

Statistics

Group differences in CCG profiles of patients belonging to different treatment cohorts were investigated by Partial Least-Squares Discriminant Analysis (PLS-DA) using MetaboAnalyst (version 5.0). For this, data was primarily normalized with autoscaling and log₁₀ transformation as described [25]. Different timepoints (before and after vaccination) were compared using a paired t-test on log-transformed data (SPSS v27). Good vs. poor anti-SARS-CoV-2 IgG responders and patients with vs. without severe adverse events were compared using a two-sample t-test on log-transformed data (SPSS v27). To evaluate correlation between quantitative IgG levels and CCG concentrations, a Spearman correlation coefficient was utilized (R, version 4.1.0, <http://www.rstudio.com/>). A *p*-value of < 0.05 (uncorrected) was considered statistically significant.

For the identification of the main predictors of qualitative response (good/poor responder), receiver operating characteristic (ROC) curves were constructed utilizing MetaboAnalyst. To further predict good/poor responder with a combined model of CCG levels, machine-learning-based Random Forest classifiers (RFC) were built (Python, package sklearn v2.0, <http://scikit-learn.sourceforge.net>). The main outcome variable was the development of an adequate immune response. To account for imbalanced groups, the Synthetic Minority Oversampling Technique (SMOTE, Python package imblearn 0.8.0) was utilized where 80% of the data was utilized as training set and the remaining 20% as test set. The models were bootstrapped 10 times and features for each model were selected based on 1) feature importance, 2) statistics from good vs. poor responder, 3) Individual ROC curve analysis, and, 4) a Pearson correlation matrix for independence of variables. Confusion matrices and ROC curves were drawn to calculate area under the curve (AUROC) value to verify reliability and to evaluate the performance of the constructed models.

Results

Activation of early immune responses by BNT162b2 in cancer patients

We observed a significant alteration of 23 CCGs after administration of the primer and/or the booster dose of the BNT162b2 vaccine in cancer patients under active treatment (Figure 1). Specifically, a day after the administration of the primer dose (day 1 vs. baseline day 0), anti-viral responses such as IFN- γ and IP-10 as well as T cell growth factor IL-9 were significantly upregulated (**Figure 2A, left panel**), suggesting, as expected, the importance of these immune mediators in the initial immune response to the vaccine.

On the other hand, we measured a downregulation of several CCGs after administration of the primer dose, such as IL-17A, IL-8, IL-4, TSLP, VCAM-1, ICAM-1, Tie-2, and VEGF-D. Most of these analytes are crucially involved in the adaptive immune response or in cancer progression [26, 27]. For example, downregulation of TSLP, that has an important role in the maturation of T cell populations and in enhancing Th2 responses [28], and of IL-4, a key Th2 cytokine with profound effects on B cell function, could be detrimental to the development of an adaptive immune response in the studied cancer patients (Figure 2A, left panel).

Seven days after booster dose administration, 14 CCGs were significantly elevated compared to the levels measured just before the booster dose administration. Interestingly, similar to alterations observed after administration of the primer dose, upregulated CCGs included molecules responsible for the anti-viral IFN responses (IP-10, IFN- γ , and IFN- γ -inducing IL-18), but also inflammatory marker CRP, Th1 cytokines (TNF- α , IL-1 β , IL-6, and IL-1Ra), MIP-1 α , and eosinophil and B-cell function promoting factor (IL-5) indicating activation of a wide range of immune markers despite the immunocompromised status of these patients (**Figure 2A, right panel**). Remarkably, after a non-significant drop one day after the primer dose administration, the levels of IL-5 gradually increased, especially after the administration of the booster dose at day 28. IL-5 is a major eosinophilic factor, but it was originally identified as a B cell growth and differentiation factor in inducing antibody secretion and class switching [29] and fits well with our data of highly upregulated IL-5 levels after the booster dose. Notably, within the power of our study, none of the studied immunomodulatory and Treg CCGs (i.e., IL-10, IL-2, and IL-2R α) were altered. Levels of vascular injury marker VCAM-1 and angiogenesis markers BDNF, bFGF and VEGF-A were also upregulated after booster dose administration (day 28), compared to the levels just before administration of the booster dose (day 21) (Figure 2A, right panel). Notably, angiogenic markers bFGF, BDNF and VEGF-A were significantly increased at both day 21 and day 28 compared to day 0 (**Figure 2B**). An independent regression analysis also showed that these angiogenic markers along with VEGF receptor (Flt-1) were significantly increasing over time after the primer dose administration (**Supplementary Figure 1**). However, in absence of a non-vaccinated cancer patient group it is difficult to ascertain whether this significant increase in angiogenic markers is the effect of vaccination or a part of natural progression of cancer in these patients.

We previously reported in this cohort that local or systemic adverse events (AEs) were mostly mild to moderate with only 3% (n = 5) and 6% (n = 12) patients experiencing severe local or systemic AEs after primer and booster dose, respectively [5]. Local reactogenicity was graded as mild, moderate, or severe. Systemic AEs were recorded according to the Common Terminology Criteria for Adverse Events version 5.0 (CTCAE v5.0; graded 0–5; grade 5 being death). Additionally, investigating

whether CCG responses are different in patients who developed severe AE, only PIGF was observed to be significantly downregulated after the primer dose in uncorrected paired t-test statistics ($p = 0.027$) and was not significant after post-hoc false discovery rate correction. These data fit well with studies suggesting that systemic adverse events noted after vaccination in cancer patients are not necessarily vaccine related [5, 16].

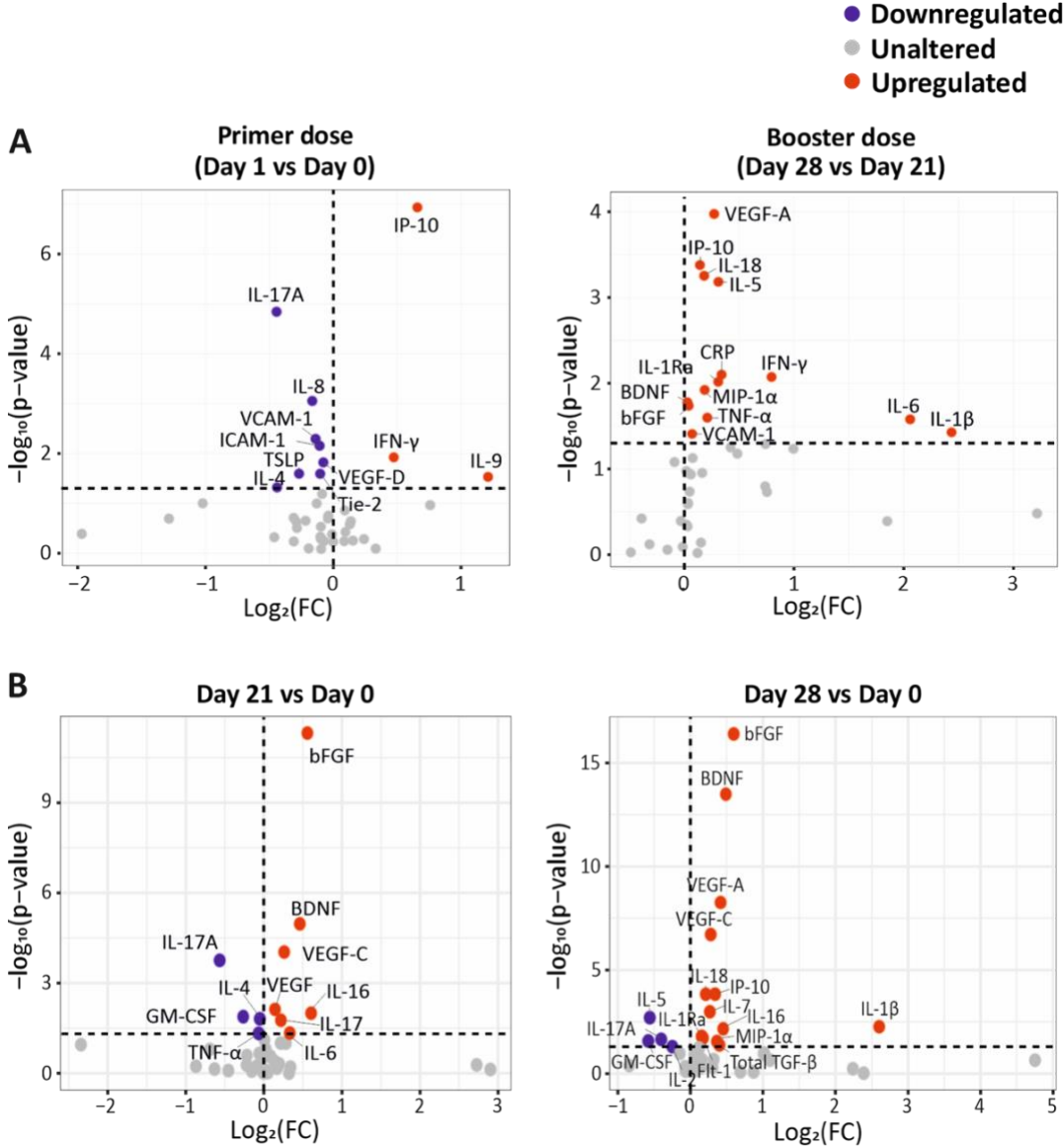


Figure 2. CCG alterations as a response to primer and booster dose vaccinations in cancer patients. (A) Differentially expressed CCGs after the administration of the primer and booster doses, compared to the CCG levels prior to vaccine administration. (B) Differentially expressed CCGs at day 21 and day 28, compared with baseline day 0. *P*-values were calculated using paired t-test. The vertical dotted line represents no change. The horizontal dotted line represents a *p*-value of 0.05.

Type of cancer therapy does not majorly alter the CCG profile induced by the BNT162b2 mRNA vaccine

An inadequate IgG immune response to the BNT162b2 mRNA vaccine was reported especially in hematological malignancy patients and notably in those receiving rituximab, an anti-CD20 B cell blocker [5]. We thus first questioned whether CCG profiles could discriminate hematological cancer patients receiving rituximab from those receiving stem cell transplantation, the other major treatment modality for hematological malignancy patients studied in this report, or from all other cancer and treatment groups combined. A significant discrimination was observed at day 1 for hematological cancer patients with or without rituximab (accuracy = 87%; $R^2 = 0.67$; $Q^2 = 0.30$), but was not observed at other timepoints, nor was observed at any timepoint when combining the groups of solid cancer and non-rituximab-treated hematological cancer patients (**Supplementary Figure 2**). As other treatment modalities, especially chemotherapy for patients with solid tumors, also showed a diminished immune response, we performed a similar discriminant analysis that showed no significant underlying difference in CCG profiles at any timepoint (**Figure 3**; **Supplementary Figure 3**).

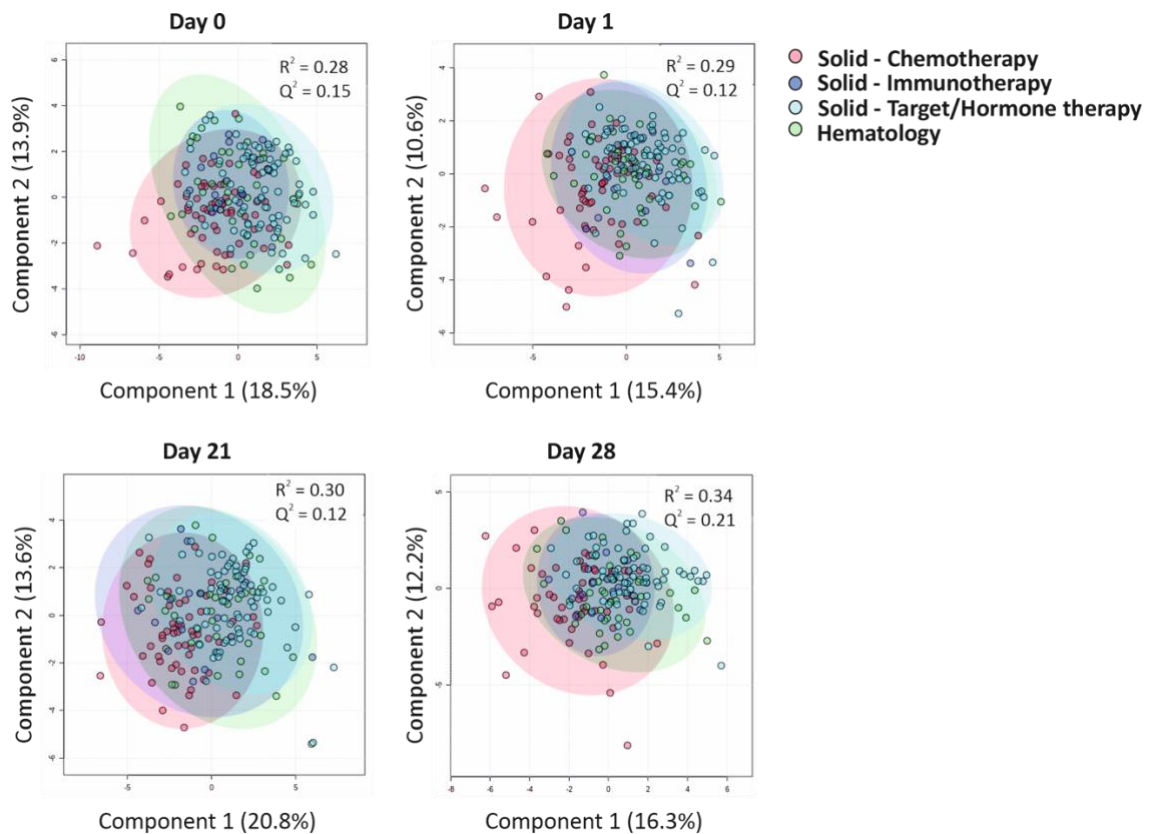


Figure 3. CCGs alterations as a response to primer and booster vaccinations in cancer patients undergoing different treatment regimens. Cluster analyses of CCGs at different timepoints with a Partial Least Squares-Discriminant Analysis (PLS-DA) reveal minor differences between patients undergoing distinct types of anti-cancer therapies. Hematological patients included patients receiving rituximab or patients who received an allogeneic hematopoietic stem cell transplantation at least one year before the primer dose vaccination.

Studying individual cytokines in a difference of mean analysis revealed that the only cytokine linked to vaccine administration and upregulated in all treatment groups was IP-10, which is indicative of an effective anti-viral immune response. Moreover, IP-10-regulator IFN- γ was also upregulated in patients with solid tumors treated with targeted or hormonal therapy (Supplementary Figure 3). Surprisingly, neutrophil chemoattractant IL-8 was downregulated in both hematological malignancy patients and patients with solid tumors treated with targeted/hormonal therapy. Moreover, all groups of patients with solid tumors demonstrated a significant downregulation of IL-17A, a pro-inflammatory cytokine involved mainly in the activation of neutrophils. Lastly, the solid tumor cohort treated with chemotherapy or targeted/hormone therapy showed a significant increase of VEGF-C, bFGF, and BDNF over 21 days (Supplementary Figure 3). These data indicate that except for rituximab-treated hematological malignancy groups that behave differently at day 1, type of cancer therapy is not a major driver for the observed CCG profiles induced by the BNT162b2 vaccination.

CRP, IL-15, IL-18, and PIGF predict a poor BNT162b2 immune response in cancer patients

Due to the limited ability of some patients with solid or hematological malignancies to develop a protective antibody response, we aimed to identify a unique CCG signature in cancer patients that could differentiate good from poor responders to BNT162b2 vaccination. For this, we examined the relationship between alterations in the studied CCGs at all sampling timepoints (day 0, day 1, day 21, and day 28) with levels of anti-RBD titers measured 28 days after the administration of the booster dose of the BNT162b2 vaccine (day 49) (Figure 1). This was done following several approaches. First, we utilized anti-RBD titers measured at day 49 as a continuous variable and correlated with CCGs at all studied timepoints. Amongst others, BDNF, VEGF-C, IFN- γ , IFN- β , and ICAM-1 were significantly positively associated with anti-RBD titers at one or several timepoints (**Figure 4A**). Additionally, bFGF, PIGF, IL-18, G-CSF, and pro-inflammatory cytokines IL-15 and IL-16 were significantly negatively associated with anti-RBD titers (Figure 4A). These data suggest that pre-existing and sustained CCG signatures in patients with solid and hematological malignancies can be predictive of the quantitative antibody response post-BNT162b2 vaccination.

Since the primary outcome of this study was the assessment of the level of protection conferred by vaccination, we further utilized a threshold of 200 IU/mL shown to predict a neutralization response conferring 50% protection against SARS-CoV-2 infection in our prior study [5]. Examining the ability of CCGs to predict poor responders (< 200 IU/mL) from good responders (\geq 200 IU/mL), 4 CCGs were identified to be significantly different at all studied timepoints that included CRP, IL-15, IL-18, and PIGF (**Figure 4B**).

Area under the curve receiver operating characteristic (AUROC) analysis was further performed to discriminate between good and poor responders. AUROC was constructed for each CCG and the top discriminant CCGs were utilized to build models. Performance was studied for each timepoint to assess the capability of the model to sustain at all studied timepoints. While inflammatory marker CRP on its own did not emerge as a good classifier (see **Supplementary Table 2** for more details) and did not correlate with anti-S or anti-RBD antibody titers measured as a continuous variable (Figure 4A), a highly significant difference was observed in CRP levels in good and poor responders at all studied timepoints (Figure 4B).

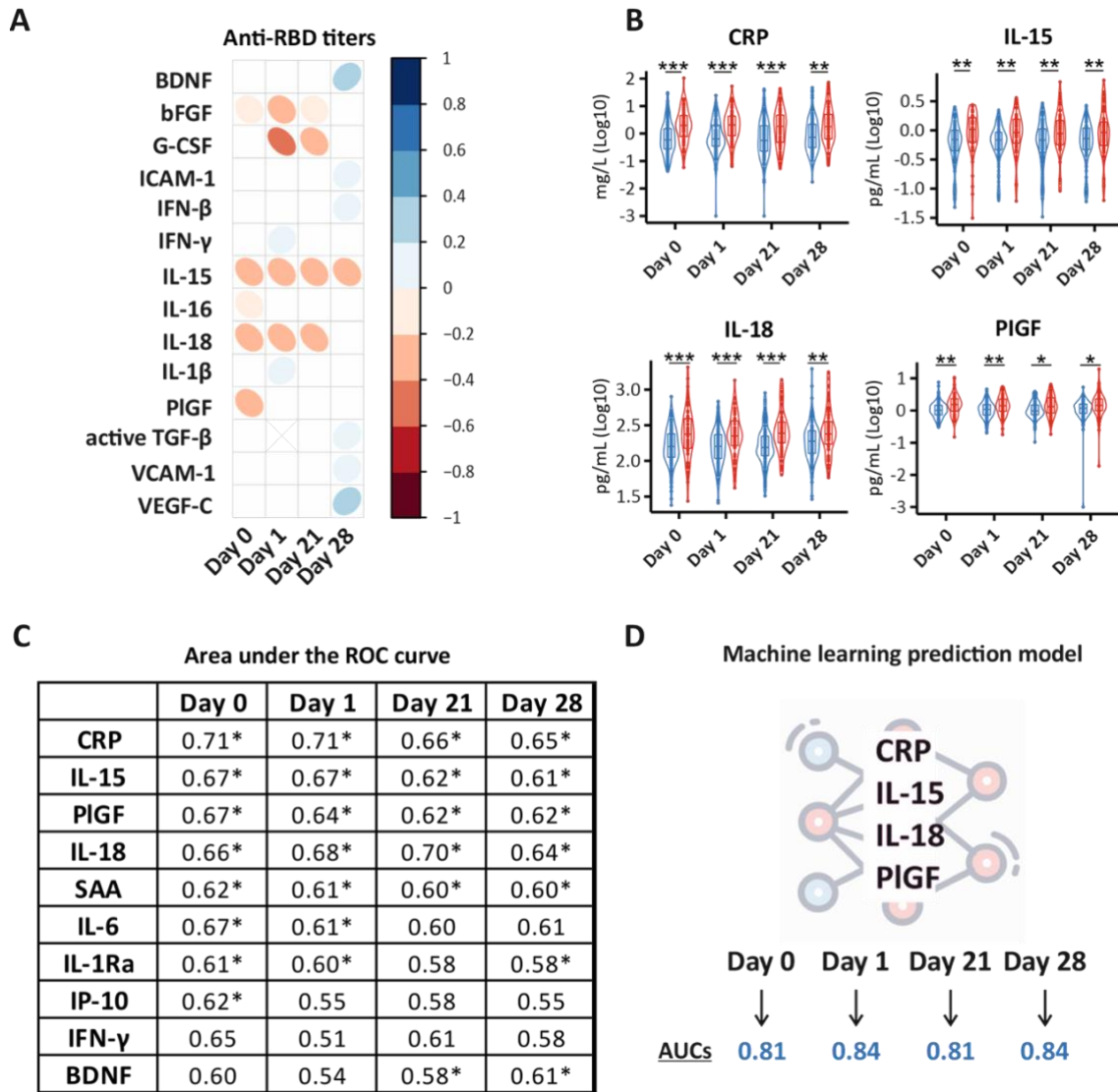


Figure 4. Prediction models for BNT162b2 immune response in cancer patients. (A) Correlation matrix depicting the correlation between CCG measurements (log₁₀ transformed) and quantitative anti-RBD IgG measurements at day 49. IgG antibody levels to SARS-CoV-2 RBD antigen were assessed with an enzyme-linked immunosorbent assay for quantitative detection of IgG antibody levels to SARS-CoV-2 RBD antigen. Only CCGs with significant correlations are shown. (B) Significantly different between good (≥ 200 IU/mL) (blue) and poor (< 200 IU/mL) (red) responders to the BNT162b2 vaccine. A good/poor responder threshold of anti-RBD IgG titer of 200 IU/mL used in this study predicts a neutralization response required for 50% protection against symptomatic SARS-CoV-2 infection (99%-100% specificity at a sensitivity of 95%). * $p < 0.05$, ** $p < 0.01$, *** $p < 0.001$. (C) Area Under the Receiver Operating Characteristic (AUROC) values for 10 predictors of the binary IgG response as good or poor responders at day 0, day 1, day 21, and day 28. * Denotes significant p-values of at least < 0.05 . (D) Random Forest Classifier predicted a model where a combination of CRP, IL-15, IL-18, and PIGF levels measured right before vaccine administration (day 0) and at day 1, day 21, and day 28 after the primer dose predicted good and poor responders with high accuracy (AUCs depicts averages of 10 individually constructed ROC curves).

Moreover, prior to vaccine administration, the upregulated inflammatory marker CRP showed the highest predictive value for vaccine response followed by NK-cell inducer IL-15, PIGF, IL-6, IL-18, and serum amyloid A (SAA). One day after administration of the primer dose, CRP, IL-18, IL-15, PIGF, IL6, and SAA remained in the signature predicting a worse qualitative antibody response. Similarly, prior to administration of the booster dose, the signature included CRP, IL-15, IL-18, PIGF, and SAA (**Figure 4C**).

Lastly, we performed Random Forest classification that validated the signature consisting of CRP, IL-15, IL-18, and PIGF, differentiating good from poor anti-SARS-CoV-2 BNT162b2 vaccine responders with more than 80% accuracy. Interestingly, this signature was maintained until day 28 after the administration of the primer dose (**Figure 4D, Supplementary Figure 4**).

Discussion

In this study, we show an alteration of a diverse group of inflammatory mediators and growth factors that includes interferons, Th1, Th2, and Th17 cytokines, as well as some markers of angiogenesis and vascular injury in a heterogeneous population of patients with solid or hematological malignancies vaccinated with BNT162b2. In a previous study, some of these CCGs including IFN- γ , IP-10, TNF- α , IL-6, IL-1Ra, CRP, MIP-1 α , and VEGF-A were shown to be upregulated upon BNT162b2 administration in healthy individuals [12]; however, the upregulation noted in healthy volunteers (up to 20-fold) is substantially higher than noted in our population of cancer patients (up to 2-fold). Additionally, an increase in IFN- γ and IP-10 levels was also observed in an elderly population upon administration of the BNT162b2 vaccine but at a larger magnitude than detected in our cohort [17]. These data suggest that BNT162b2 vaccine administration in cancer patients can generally elicit an anti-SARS-CoV-2-driven immune response that is similar in pattern, but not in magnitude, to healthy individuals. Even though our study is restricted to the BNT162b2 vaccine, we expect to observe similar alterations upon administration of other mRNA COVID-19 vaccines as well as non-mRNA vaccines, although they show a more pronounced upregulation of pro-inflammatory responses at least after the administration of the primer dose [30].

All cohorts of patients with solid and hematological malignancies undergoing different treatment regimens developed anti-viral interferon responses after vaccination with BNT162b2. However, with the exception of the rituximab treatment cohort, no major underlying differences in CCG profiles were identified between different cancer or treatment groups at any timepoint. These data suggest that despite having different tumor types and undergoing different therapies, patients respond similarly to vaccination with BNT162b2.

Previous studies have shown that antibody titers in patients with certain cancers, including but not limited to, advanced cancers and B cell hematological malignancies, are either absent or very low not only after SARS-CoV-2 infection, but also after SARS-CoV-2 vaccination [5, 7-11, 31-34]. In line with the major aim of this study, we identified a unique immune signature based on upregulated CRP, IL-15, IL-18, and PIGF that could be used to identify patients who did not sufficiently respond to vaccination with BNT162b2 vaccine. The signature was present at different studied timepoints before or after vaccination and was not majorly affected by different anti-cancer treatments. We believe that this unique biomarker signature would not only be useful for clinicians in identifying cancer patients at increased risk of developing SARS-CoV-2 for better patient care, but also be able

to guide health policies in categorizing cancer patients in need of enhancer vaccine doses or pre-exposure prophylaxis with synthetic monoclonal antibodies to protect potential non-responders to the BNT162b2 vaccine.

Lastly, our data also suggest that pro-inflammatory cytokines and growth factors interact to dictate an inherent immune response in cancer patients that could generally render them refractive to other immune interventions. Whether the identified signature or similar immune-based CCG profiles can be predictive of primary resistance to immunotherapy, observed in approximately 12% of the patients [35], remains open to future investigations.

Declaration of Interest

The authors declare that the research was conducted in the absence of any commercial or financial relationships that could be construed as a potential conflict of interest.

Author contributions

Conceptualization: SK-S, PvD, MP; Funding acquisition: SK-S, PvD, MP, ET; Overall study supervision: SK-S; Clinical data and sample collection: LV, LAT, GV, SR, IVdM, SDK, YD, GM, BP; Biobanking: MH; CCG analysis: AK, FDW, AG, AH; Serology and seroneutralization analyses: PP, KN, KA, MVDB, ID, MG; Statistical analysis: AK, FDW, AG, AH; Data curation: AK, AG, ER; Data interpretation: SK-S, PvD, MP, TV, SMK, AK, FDW, AG, AH, MB; Manuscript writing: SK-S, AK, FDW, AG, PvD, AH, MB; All authors read, gave input, and approved the final manuscript.

Funding

This work was supported by the Belgian Government through Sciensano [grant numbers COVID-19_SC004, COVID-19_SC059, COVID-19_SC061], ORCHESTRA project, which has received funding from the European Union's Horizon 2020 research and innovation program [grant agreement number 101016167] and University of Antwerp-GOA grant [s30729].

Supplementary Methods

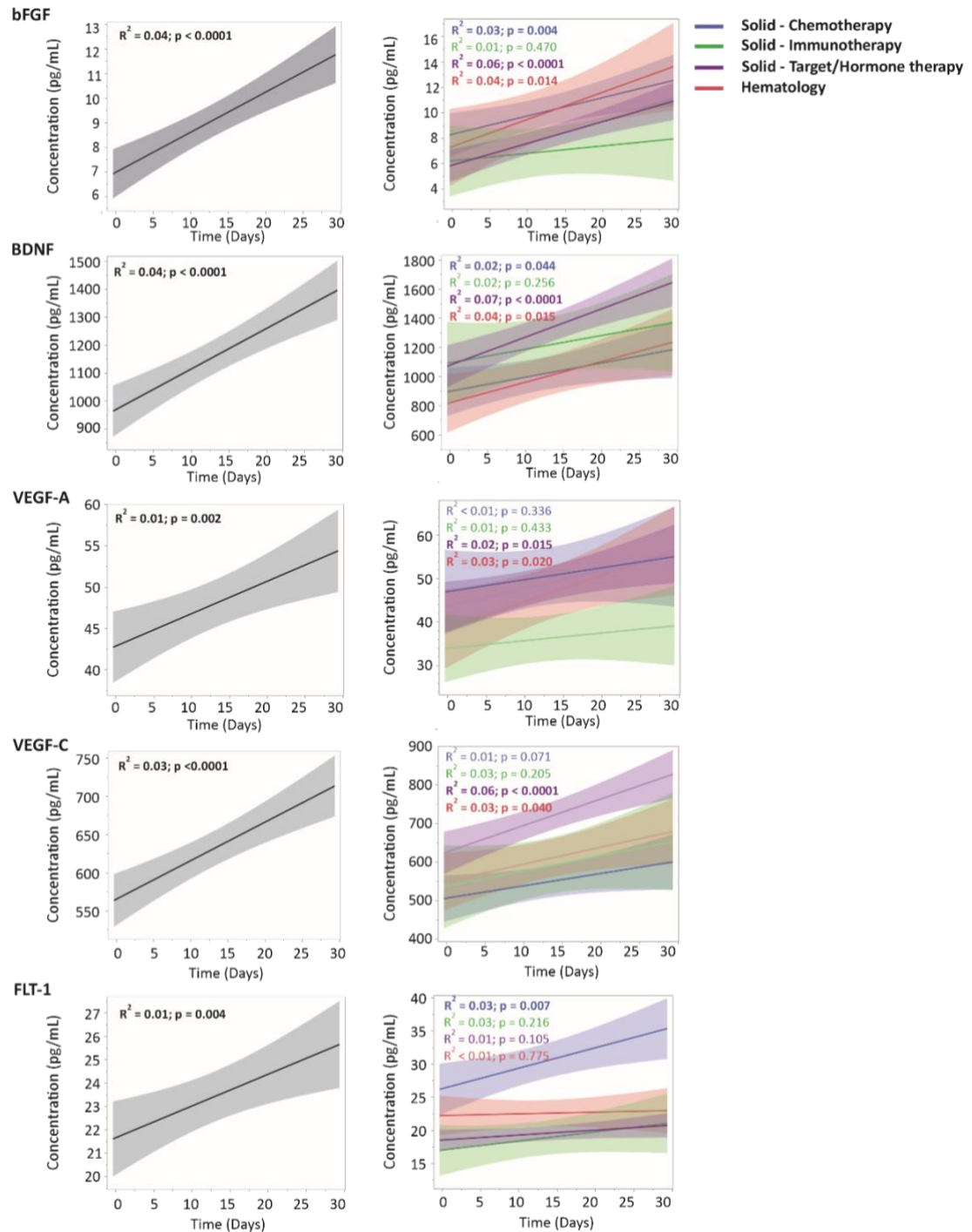
Sample collection and processing

Whole blood was prospectively collected in heparin blood and serum collection tubes. Within 3 hours of blood collection, plasma was prepared by centrifuging twice at $1900 \times g$ for 10 minutes without brakes. Blood in the serum collection tubes was allowed to clot thoroughly for 60 minutes and serum was prepared by centrifuging at $1300 \times g$ for 10 minutes without brakes. Aliquots were flash frozen in liquid nitrogen and stored in the Biobank of Antwerp University Hospital at -80°C until further analysis.

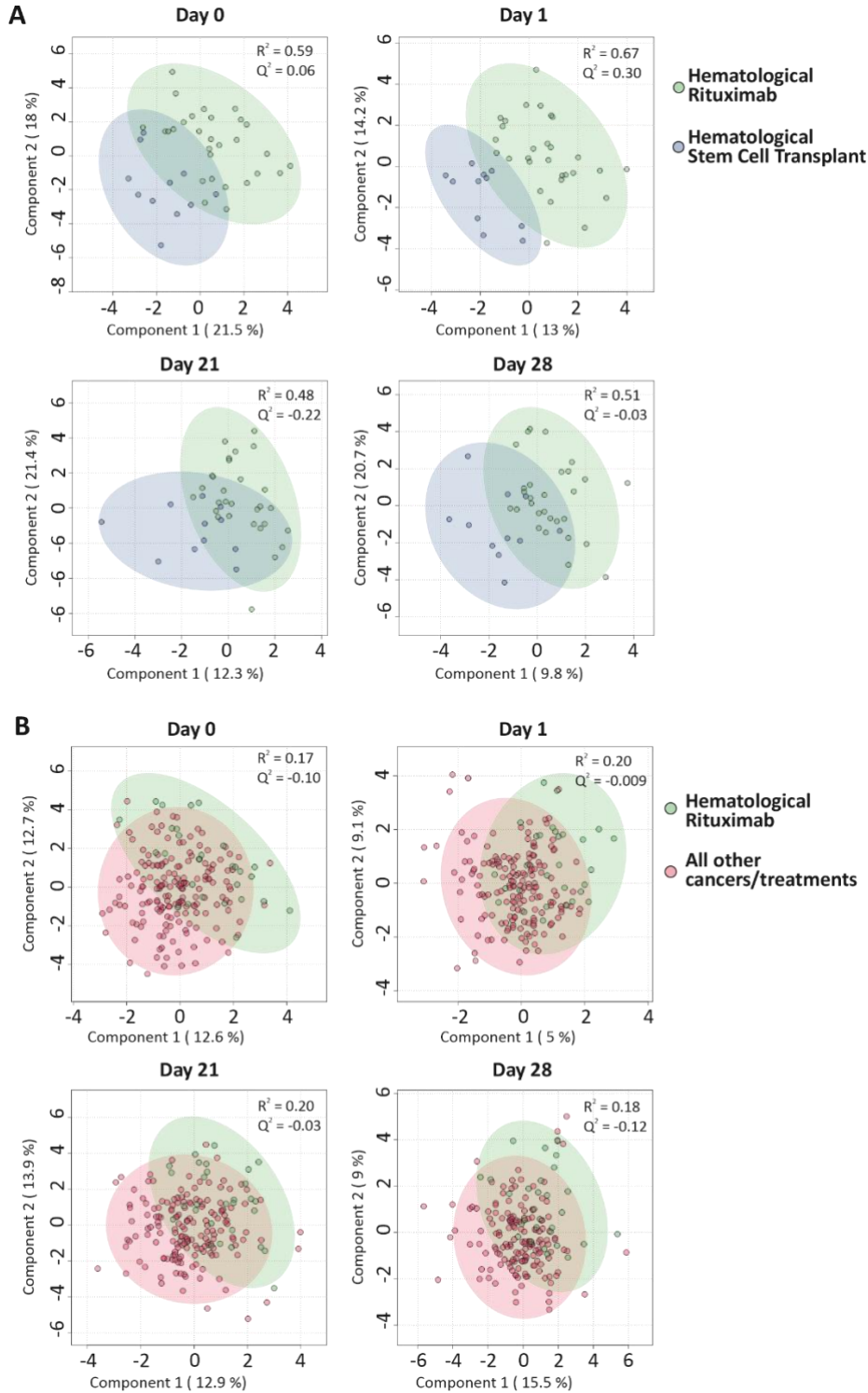
Cytokine, chemokine and growth factor (CCG) measurements in plasma

CCGs were measured in plasma samples on a multiplex platform (Meso Scale Discovery (MSD), MD, USA) using off-the-shelf (V-plex) and customized (U-plex) panels, following manufacturer instructions. Briefly, 96-well plates of the U-plex panels were coated with a capturing antibody coupled to a linker for one hour. The vascular injury panel (K15198D) was washed before use. The angiogenesis panel (K15190D) was first blocked with blocking buffer for one hour. Thereafter, all plates were washed three times with PBS-Tween (0.05%). Samples were incubated for one hour (except for the angiogenesis and the vascular injury panels, where two hours of incubation were performed), after which the plates were washed another three times. Detection antibody with a SULFO-TAG was added and after another one-hour incubation step (two hours for the angiogenesis panel), the plates were washed and read with MSD reading buffer on the QuickPlex SQ 120 (MSD).

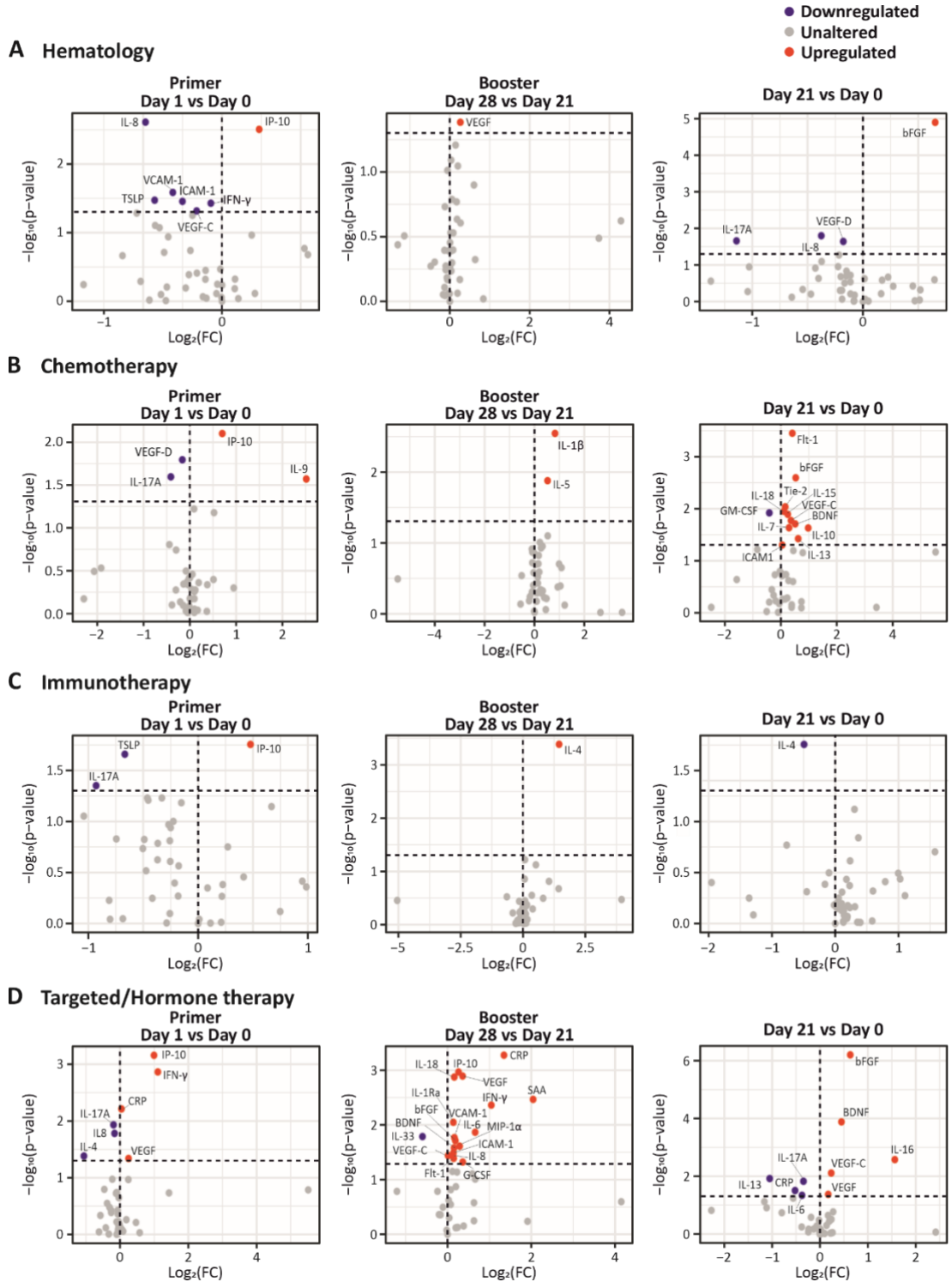
Supplementary Figures and Tables



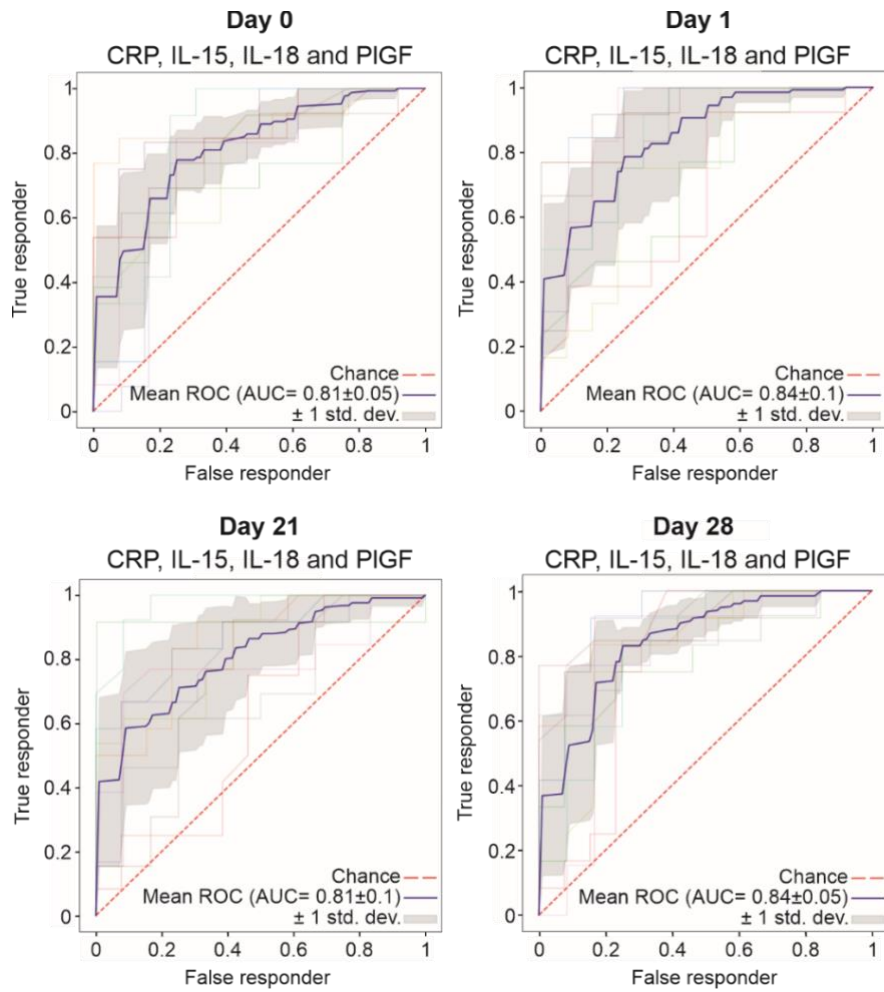
Supplementary Figure 1. Temporal alterations in cytokines, chemokines and growth factors (CCGs) levels in vaccinated cancer patients. Time is represented as days since primer dose vaccination. *P*-values in the graph refer to significance of the slope of the regression lines.



Supplementary Figure 2. CCG analysis in patients with and without hematological malignancies. Cluster analyses of CCGs at different timepoints with partial least squares-discriminant analysis (PLS-DA) reveal (A) differences between patients with hematological malignancies treated with rituximab and patients that received a stem cell transplantation, or (B) between patients with hematological malignancies treated with rituximab versus all other cancers/treatments group



Supplementary Figure 3. Volcano plots depicting differentially expressed CCGs after the administration of the primer and booster doses compared to the CCG levels prior to vaccine administration (**A**) in cancer with hematological malignancies, (**B**) patients with solid cancers treated with chemotherapy, (**C**) immunotherapy and (**D**) targeted or hormonal therapy. *P*-values were calculated using paired *t*-test. The vertical dotted line represents no change. The horizontal dotted line represents a *p*-value of 0.05.



Supplementary Figure 4. ROC curves for the combination of CRP, IL-15, IL-18 and PIGF in a random forest classifier model with Synthetic Minority Oversampling Technique (SMOTE) for the prediction of the qualitative IgG response (good versus poor responder) are depicted for day 0, day 1, day 21 and day 28.

Supplementary Table 1. Patient characteristics *Percentage of total patients with solid tumors.

Demographics	Target/hormone therapy (<i>n</i> = 79)	Immuno-therapy (<i>n</i> = 16)	Chemo-therapy (<i>n</i> = 63)	Hema-tological (<i>n</i> = 41)	Overall (<i>n</i> = 199)
Sex, <i>n</i> (%)					
Female	70 (88.6)	4 (25.0)	43 (68.3)	17 (41.5)	134 (67.3)
Male	9 (11.4)	12 (75.0)	20 (31.7)	24 (58.5)	65 (32.7)
Age, years					
Mean (SD)	59.5 (12.1)	68.3 (8.09)	60.0 (13.2)	61.2 (11.5)	60.7 (12.2)
Median (range)	60.0 (31.0-86.0)	69.5 (56.0-84.0)	61.0 (26.0-88.0)	63.0 (25.0-79.0)	62.0 (25.0-88.0)
BMI					
Mean (SD)	25.7 (4.74)	27.0 (4.13)	25.5 (5.19)	25.2 (3.88)	25.6 (4.67)
Median (range)	25.5 (17.8-40.0)	26.9 (19.7-34.5)	24 (18.9-44.8)	24.4 (17.1-35.5)	25.1 (17.1-44.8)
Missing, <i>n</i> (%)	0 (0)	0 (0)	3 (4.8)	2 (4.9)	5 (2.5)
ECOG score, <i>n</i> (%)					
0	73 (92.4)	11 (68.8)	48 (76.2)	38 (92.7)	170 (85.4)
1	6 (7.6)	5 (31.2)	13 (20.6)	3 (7.3)	27 (13.6)
2	0 (0)	0 (0)	1 (1.6)	0 (0)	1 (0.5)
Missing	0 (0)	0 (0)	1 (1.6)	0 (0)	1 (0.5)
Autoimmune disease, <i>n</i> (%)	4 (5.1)	0 (0)	1 (1.6)	3 (7.3)	8 (4.0)
Kidney disease, <i>n</i> (%)	1 (1.3)	1 (6.2)	5 (7.9)	1 (2.4)	8 (4.0)
Hypertension, <i>n</i> (%)	20 (25.3)	4 (25.0)	22 (34.9)	8 (19.5)	54 (27.1)
Diabetes, <i>n</i> (%)	3 (3.8)	2 (12.5)	10 (15.9)	5 (12.2)	20 (10.1)
Coronary disease, <i>n</i> (%)	4 (5.1)	2 (12.5)	10 (15.9)	7 (17.1)	23 (11.6)
Smoking status, <i>n</i> (%)					
Current smoker	5 (6.3)	1 (6.2)	5 (7.9)	2 (4.9)	13 (6.5)
Former smoker	21 (26.6)	11 (68.8)	21 (33.3)	18 (43.9)	71 (35.7)
Non-smoker	51 (64.6)	3 (18.8)	29 (46.0)	21 (51.2)	104 (52.3)
Missing	3 (2.5)	1 (6.2)	8 (12.7)	0 (0)	11 (5.5)
Stage, <i>n</i> (%)					
I	20 (25.3)	0 (0)	6 (9.5)	NA	26 (16.5)*
II	19 (24.1)	2 (12.5)	6 (9.5)	NA	27 (17.1)*
III	6 (6.3)	2 (12.5)	6 (9.5)	NA	14 (8.2)*
IV	33 (41.8)	12 (75.0)	42 (66.7)	NA	87 (55.1)*
Missing	2 (2.5)	0 (0)	3 (4.8)	NA	46 (29.1)*

Supplementary Table 2. Predictive value of CRP with outcome good responder versus poor responder. Although CRP had an AUC of 0.71, at the clinical cut-off of 4 mg/L it had only a sensitivity of 30% and a specificity of 88% at baseline day 0. If used to identify patients that would benefit from adjuvant therapy, too many patients would be missed. An optimal cut-off of CRP to differentiate poor from good responders was 1 mg/L that provided a sensitivity and specificity of 72% and 61%, respectively.

Cut-Off	Sensitivity	Specificity	Positive likelihood ratio	Negative Likelihood ratio
1 mg/L	72%	61%	1.85	0.46
2 mg/L	49%	81%	2.59	0.63
4 mg/L	30%	88%	2.48	0.80
10 mg/L	13%	96%	3.28	0.91

References

1. Goldberg Y, Mandel M, Bar-On YM, Bodenheimer O, Freedman L, Haas EJ, et al. Waning Immunity after the BNT162b2 Vaccine in Israel. *New England Journal of Medicine*. 2021;385(24):e85. <https://doi.org:10.1056/NEJMoa2114228>
2. Polack FP, Thomas SJ, Kitchin N, Absalon J, Gurtman A, Lockhart S, et al. Safety and Efficacy of the BNT162b2 mRNA Covid-19 Vaccine. *N Engl J Med*. 2020;383(27):2603-15. <https://doi.org:10.1056/NEJMoa2034577>
3. Thomas SJ, Moreira ED, Jr., Kitchin N, Absalon J, Gurtman A, Lockhart S, et al. Safety and Efficacy of the BNT162b2 mRNA Covid-19 Vaccine through 6 Months. *N Engl J Med*. 2021;385(19):1761-73. <https://doi.org:10.1056/NEJMoa2110345>
4. Teijaro JR, Farber DL. COVID-19 vaccines: modes of immune activation and future challenges. *Nat Rev Immunol*. 2021;21(4):195-7. <https://doi.org:10.1038/s41577-021-00526-x>
5. Peeters M, Verbruggen L, Teuwen L, Vanhoutte G, Vande Kerckhove S, Peeters B, et al. Reduced humoral immune response after BNT162b2 coronavirus disease 2019 messenger RNA vaccination in cancer patients under antineoplastic treatment. *ESMO Open*. 2021;6(5):100274. <https://doi.org:10.1016/j.esmoop.2021.100274>
6. Cortés A, Casado JL, Longo F, Serrano JJ, Saavedra C, Velasco H, et al. Limited T cell response to SARS-CoV-2 mRNA vaccine among patients with cancer receiving different cancer treatments. *Eur J Cancer*. 2022;166:229-39. <https://doi.org:10.1016/j.ejca.2022.02.017>
7. Massarweh A, Eliakim-Raz N, Stemmer A, Levy-Barda A, Yust-Katz S, Zer A, et al. Evaluation of Seropositivity Following BNT162b2 Messenger RNA Vaccination for SARS-CoV-2 in Patients Undergoing Treatment for Cancer. *JAMA Oncol*. 2021;7(8):1133-40. <https://doi.org:10.1001/jamaoncol.2021.2155>

8. Maneikis K, Šablauskas K, Ringelevičiūtė U, Vaitekėnaitė V, Čekauskienė R, Kryžauskaitė L, et al. Immunogenicity of the BNT162b2 COVID-19 mRNA vaccine and early clinical outcomes in patients with haematological malignancies in Lithuania: a national prospective cohort study. *The Lancet Haematology*. 2021;8(8):e583-e92. [https://doi.org:10.1016/s2352-3026\(21\)00169-1](https://doi.org:10.1016/s2352-3026(21)00169-1)
9. Fendler A, Shepherd STC, Au L, Wilkinson KA, Wu M, Byrne F, et al. Adaptive immunity and neutralizing antibodies against SARS-CoV-2 variants of concern following vaccination in patients with cancer: the CAPTURE study. *Nature Cancer*. 2021;2(12):1305-20. <https://doi.org:10.1038/s43018-021-00274-w>
10. Linardou H, Spanakis N, Koliou GA, Christopoulou A, Karageorgopoulou S, Alevra N, et al. Responses to SARS-CoV-2 Vaccination in Patients with Cancer (ReCOVer Study): A Prospective Cohort Study of the Hellenic Cooperative Oncology Group. *Cancers (Basel)*. 2021;13(18). <https://doi.org:10.3390/cancers13184621>
11. Chung DJ, Shah GL, Devlin SM, Ramanathan LV, Doddi S, Pessin MS, et al. Disease- and Therapy-Specific Impact on Humoral Immune Responses to COVID-19 Vaccination in Hematologic Malignancies. *Blood Cancer Discov*. 2021;2(6):568-76. <https://doi.org:10.1158/2643-3230.Bcd-21-0139>
12. Bergamaschi C, Terpos E, Rosati M, Angel M, Bear J, Stellas D, et al. Systemic IL-15, IFN-gamma, and IP-10/CXCL10 signature associated with effective immune response to SARS-CoV-2 in BNT162b2 mRNA vaccine recipients. *Cell Rep*. 2021;36(6):109504. <https://doi.org:10.1016/j.celrep.2021.109504>
13. Miyashita Y, Yoshida T, Takagi Y, Tsukamoto H, Takashima K, Kouwaki T, et al. Circulating extracellular vesicle microRNAs associated with adverse reactions, proinflammatory cytokine, and antibody production after COVID-19 vaccination. *NPJ Vaccines*. 2022;7(1):16. <https://doi.org:10.1038/s41541-022-00439-3>
14. Monin MB, Marx B, Meffert L, Boesecke C, Rockstroh JK, Strassburg CP, et al. SARS-CoV-2 PrEP complicates antibody testing after vaccination: a call for awareness. *Ann Hematol*. 2022;101(9):2089-90. <https://doi.org:10.1007/s00277-022-04859-y>
15. Pagano L, Salmanton-García J, Marchesi F, Blennow O, Gomes da Silva M, Glenthøj A, et al. Breakthrough COVID-19 in vaccinated patients with hematologic malignancies: results from EPICOVIDEHA survey. *Blood*. 2022. <https://doi.org:10.1182/blood.2022017257>
16. Walle T, Bajaj S, Kraske JA, Rösner T, Cussigh CS, Kälber KA, et al. Cytokine release syndrome-like serum responses after COVID-19 vaccination are frequent and clinically inapparent under cancer immunotherapy. *Nat Cancer*. 2022. <https://doi.org:10.1038/s43018-022-00398-7>
17. Lee HK, Knabl L, Knabl L, Kapferer S, Pateter B, Walter M, et al. Robust immune response to the BNT162b mRNA vaccine in an elderly population vaccinated 15 months after recovery from COVID-19. *medRxiv*. 2021. <https://doi.org:10.1101/2021.09.08.21263284>

18. Tahtinen S, Tong AJ, Himmels P, Oh J, Paler-Martinez A, Kim L, et al. IL-1 and IL-1ra are key regulators of the inflammatory response to RNA vaccines. *Nat Immunol.* 2022;23(4):532-42. <https://doi.org:10.1038/s41590-022-01160-y>
19. Funakoshi Y, Yakushijin K, Ohji G, Hojo W, Sakai H, Takai R, et al. Safety and immunogenicity of the COVID-19 vaccine BNT162b2 in patients undergoing chemotherapy for solid cancer. *J Infect Chemother.* 2022;28(4):516-20. <https://doi.org:10.1016/j.jiac.2021.12.021>
20. Skibinski DAG, Jones LA, Zhu YO, Xue LW, Au B, Lee B, et al. Induction of Human T-cell and Cytokine Responses Following Vaccination with a Novel Influenza Vaccine. *Sci Rep.* 2018;8(1):18007. <https://doi.org:10.1038/s41598-018-36703-7>
21. Williams CM, Roy S, Califano D, McKenzie ANJ, Metzger DW, Furuya Y. The Interleukin-33-Group 2 Innate Lymphoid Cell Axis Represents a Potential Adjuvant Target To Increase the Cross-Protective Efficacy of Influenza Vaccine. *J Virol.* 2021;95(22):e0059821. <https://doi.org:10.1128/jvi.00598-21>
22. Mantovani A, Allavena P, Sica A, Balkwill F. Cancer-related inflammation. *Nature.* 2008;454(7203):436-44. <https://doi.org:10.1038/nature07205>
23. Grivennikov SI, Greten FR, Karin M. Immunity, Inflammation, and Cancer. *Cell.* 2010;140(6):883-99. <https://doi.org:https://doi.org/10.1016/j.cell.2010.01.025>
24. Lan T, Chen L, Wei X. Inflammatory Cytokines in Cancer: Comprehensive Understanding and Clinical Progress in Gene Therapy. *Cells.* 2021;10(1). <https://doi.org:10.3390/cells10010100>
25. De Winter FHR, Hotterbeekx A, Huizing MT, Konnova A, Fransen E, Jongers B, et al. Blood Cytokine Analysis Suggests That SARS-CoV-2 Infection Results in a Sustained Tumour Promoting Environment in Cancer Patients. *Cancers (Basel).* 2021;13(22). <https://doi.org:10.3390/cancers13225718>
26. Landskron G, De la Fuente M, Thuwajit P, Thuwajit C, Hermoso MA. Chronic Inflammation and Cytokines in the Tumor Microenvironment. *Journal of Immunology Research.* 2014;2014:149185. <https://doi.org:10.1155/2014/149185>
27. Kong J, Hao Y, Wan S, Li Z, Zou D, Zhang L, et al. Comparative study of hematological and radiological feature of severe/critically ill patients with COVID-19, influenza A H7N9, and H1N1 pneumonia. *J Clin Lab Anal.* 2021;35(12):e24100. <https://doi.org:10.1002/jcla.24100>
28. Kitajima M, Lee HC, Nakayama T, Ziegler SF. TSLP enhances the function of helper type 2 cells. *Eur J Immunol.* 2011;41(7):1862-71. <https://doi.org:10.1002/eji.201041195>
29. Kinashi T, Harada N, Severinson E, Tanabe T, Sideras P, Konishi M, et al. Cloning of complementary DNA encoding T-cell replacing factor and identity with B-cell growth factor II. *Nature.* 1986;324(6092):70-3. <https://doi.org:10.1038/324070a0>
30. Heo JY, Seo YB, Kim EJ, Lee J, Kim YR, Yoon JG, et al. COVID-19 vaccine type-dependent differences in immunogenicity and inflammatory response: BNT162b2 and ChAdOx1 nCoV-19. *Front Immunol.* 2022;13:975363. <https://doi.org:10.3389/fimmu.2022.975363>

31. van Dam PA, Huizing M, Papadimitriou K, Prenen H, Peeters M. High mortality of cancer patients in times of SARS-CoV-2: Do not generalize! *Eur J Cancer*. 2020;138:225-7. <https://doi.org:10.1016/j.ejca.2020.07.021>
32. van Dam P, Huizing M, Roelant E, Hotterbeekx A, De Winter FHR, Kumar-Singh S, et al. Immunoglobulin G/total antibody testing for SARS-CoV-2: A prospective cohort study of ambulatory patients and health care workers in two Belgian oncology units comparing three commercial tests. *European Journal of Cancer*. 2021;148:328-39. <https://doi.org:10.1016/j.ejca.2021.02.024>
33. Fendler A, Au L, Shepherd STC, Byrne F, Cerrone M, Boos LA, et al. Functional antibody and T cell immunity following SARS-CoV-2 infection, including by variants of concern, in patients with cancer: the CAPTURE study. *Nat Cancer*. 2021;2(12):1321-37. <https://doi.org:10.1038/s43018-021-00275-9>
34. Overheu O, Quast DR, Schmidt WE, Sakiñ-Güler T, Reinacher-Schick A. Low Serological Prevalence of SARS-CoV-2 Antibodies in Cancer Patients at a German University Oncology Center. *Oncol Res Treat*. 2022;45(3):112-7. <https://doi.org:10.1159/000520572>
35. Haslam A, Prasad V. Estimation of the Percentage of US Patients With Cancer Who Are Eligible for and Respond to Checkpoint Inhibitor Immunotherapy Drugs. *JAMA Netw Open*. 2019;2(5):e192535. <https://doi.org:10.1001/jamanetworkopen.2019.2535>

Chapter 4:

Using machine learning to predict antibody response to SARS-CoV-2 vaccination in Solid Organ Transplant Recipients: the multicentre ORCHESTRA cohort

Prof. Maddalena Giannella^{1,2}, Prof. Manuel Huth^{3,4}, Prof. Elda Righi⁵, Prof. Jan Hasenauer^{3,4}, Prof. Lorenzo Marconi², **Angelina Konnova**^{6,7}, Akshita Gupta^{6,7}, Dr. An Hotterbeekx^{6,7}, Dr. Matilda Berkell^{6,7}, Prof. Zaira R. Palacios-Baena^{8,9}, Maria Cristina Morelli¹⁰, Mariarosa Tamè¹¹, Marco Busutti¹², Luciano Potena¹³, Elena Salvaterra¹⁴, Work Package 4. ORCHESTRA study group, Giuseppe Feltrin¹⁵, Gino Gerosa¹⁶, Lucrezia Furian¹⁷, Patrizia Burra¹⁸, Salvatore Piano¹⁹, Umberto Cillo²⁰, Mara Cananzi²¹, Monica Loy²², Gianluigi Zaza²³, Francesco Onorati²⁴, Amedeo Carraro²⁵, Fiorella Gastaldon²⁶, Maurizio Nordio²⁷, Prof. Samir Kumar-Singh^{6,7}, Prof. Jesús Rodríguez Baño^{8,9}, Prof. Tiziana Lazzarotto^{28,29}, Prof. Pierluigi Viale^{1,2}, Prof. Evelina Tacconelli⁵

¹Department of Medical and Surgical Sciences, University of Bologna, Bologna, Italy

²Infectious Diseases Unit, Department of Integrated Management of Infectious Risk, IRCCS Azienda Ospedaliero-Universitaria di Bologna, Policlinico Sant'Orsola, Bologna, Italy

³Faculty of Mathematics and Natural Sciences, University of Bonn, Bonn, Germany

⁴Institute of Computational Biology, Helmholtz Zentrum München - German Research Center for Environmental Health, Neuherberg, Germany

⁵Division of Infectious Diseases, Department of Diagnostics and Public Health, University of Verona, Verona, Italy

⁶Molecular Pathology Group, Cell Biology & Histology, Faculty of Medicine and Health Sciences, University of Antwerp, Antwerp, Belgium

⁷Laboratory of Medical Microbiology, Vaccine & Infectious Disease Institute, University of Antwerp, Antwerp, Belgium

⁸Infectious Diseases and Microbiology Clinical Unit, University Hospital Virgen Macarena; Department of Medicine, School of Medicine, University of Seville; and Biomedicine Institute of Seville (IBiS)/CSIC, Seville, Spain

⁹Centro de Investigación Biomédica en Red en Enfermedades Infecciosas (CIBERINFEC), Instituto de Salud Carlos III, Madrid, Spain

¹⁰Internal Medicine Unit for the Treatment of Severe Organ Failure, IRCCS Azienda Ospedaliero-Universitaria di Bologna, Policlinico Sant'Orsola, Bologna, Italy

¹¹Gastroenterology Unit, Department of Digestive, Hepatic and Endocrine-metabolic Diseases, IRCCS Azienda Ospedaliero-Universitaria di Bologna, Policlinico Sant'Orsola, Bologna, Italy

¹²Nephrology, Dialysis and Renal Transplantation Unit, IRCCS Azienda Ospedaliero-Universitaria di Bologna, Policlinico Sant'Orsola, Bologna, Italy

¹³Division of Cardiology, IRCCS Azienda Ospedaliero-Universitaria di Bologna, Policlinico Sant'Orsola, Bologna, Italy

¹⁴Division of Interventional Pulmonology Unit, IRCCS Azienda Ospedaliero-Universitaria di Bologna, Policlinico Sant'Orsola, Bologna, Italy

¹⁵Regional Center for Transplant Coordination, Padua, Italy

¹⁶Cardiac Surgery Unit, Department of Cardio-Thoracic, Vascular Sciences and Public Health, University of Padua, Padua, Italy

¹⁷Kidney and Pancreas Transplantation Unit, Department of Surgical, Oncological and Gastroenterological Sciences, University of Padua, Padua, Italy

¹⁸Unit of Gastroenterology and Multivisceral Transplant, Department of Surgery, Oncology and Gastroenterology, University Hospital of Padua, Padua, Italy

¹⁹Unit of Internal Medicine and Hepatology (UIMH), Department of Medicine - DIMED, University of Padua, Padua, Italy

²⁰Department of Surgery, Oncology and Gastroenterology, Hepatobiliary Surgery and Liver Transplantation Unit, Padua University Hospital, Padua, Italy

²¹Unit of Pediatric Gastroenterology, Digestive Endoscopy, Hepatology and Care of the Child with Liver Transplantation, Department of Women's and Children's Health, University Hospital of Padua, Padua, Italy

²²Thoracic Surgery and Lung Transplant Center, Department of Cardio-Thoracic, Vascular Sciences and Public Health, University of Padua, Padua, Italy

²³Renal Unit, Department of Medicine, University Hospital of Verona, Verona, Italy

²⁴Division of Cardiac Surgery, University of Verona, Verona, Italy

²⁵Liver Transplant Unit, Department of Surgery and Dentistry, University and Hospital Trust of Verona, Verona, Italy

²⁶Department of Nephrology, Dialysis and Transplantation, San Bortolo Hospital, Vicenza, Italy

²⁷Nephrology, Dialysis and Transplantation Unit, Treviso Hospital, Treviso, Italy

²⁸Section of Microbiology, Department of Experimental, Diagnostic and Specialty Medicine, University of Bologna, Bologna, Italy

²⁹Microbiology Unit, Department of Integrated Management of Infectious Risk, IRCCS Azienda Ospedaliero-Universitaria di Bologna, Policlinico Sant'Orsola, Bologna, Italy

Angelina Konnova performed serology analysis for this manuscript.

Published in Clinical Microbiology and Infection

2023 Aug;29(8):1084.e1-1084.e7. doi: 10.1016/j.cmi.2023.04.027

Abstract

Objectives: The study aim was to assess predictors of negative antibody response (AbR) in solid organ transplant (SOT) recipients after the first booster of SARS-CoV-2 vaccination.

Methods: Solid organ transplant recipients receiving SARS-CoV-2 vaccination were prospectively enrolled (March 2021–January 2022) at six hospitals in Italy and Spain. AbR was assessed at first dose (t0), second dose (t1), 3 ± 1 month (t2), and 1 month after third dose (t3). Negative AbR at t3 was defined as an anti-receptor binding domain titre <45 BAU/mL. Machine learning models were developed to predict the individual risk of negative (vs. positive) AbR using age, type of transplant, time between transplant and vaccination, immunosuppressive drugs, type of vaccine, and graft function as covariates, subsequently assessed using a validation cohort.

Results: Overall, 1615 SOT recipients (1072 [66.3%] males; mean age±standard deviation [SD], 57.85 ± 13.77) were enrolled, and 1211 received three vaccination doses. Negative AbR rate decreased from 93.66% (886/946) to 21.90% (202/923) from t0 to t3. Univariate analysis showed that older patients (mean age, 60.21 ± 11.51 vs. 58.11 ± 13.08), anti-metabolites (57.9% vs. 35.1%), steroids (52.9% vs. 38.5%), recent transplantation (<3 years) (17.8% vs. 2.3%), and kidney, heart, or lung compared with liver transplantation (25%, 31.8%, 30.4% vs. 5.5%) had a higher likelihood of negative AbR. Machine learning (ML) algorithms showing best prediction performance were logistic regression (precision-recall curve-PRAUC mean 0.37 [95%CI 0.36–0.39]) and k-Nearest Neighbours (PRAUC 0.36 [0.35–0.37]).

Conclusions: Almost a quarter of SOT recipients showed negative AbR after first booster dosage. Unfortunately, clinical information cannot efficiently predict negative AbR even with ML algorithms.

Note: The AbR was studied at UAntwerp as a central laboratory of ORCHESTRA. The samples and clinical data were collected by the clinical partners of ORCHESTRA.

Introduction

Solid organ transplant (SOT) recipients are at higher risk for a complicated course of COVID-19 [1,2] and considered a priority setting for vaccination in several countries [3]. When testing was performed for research purposes, the immune response to vaccination in SOT recipients, in particular antibody response (AbR), was lower than that observed in immunocompetent patients [4]. We previously showed that post-vaccine antibody levels in SOT recipients were lower than in the healthcare workers (HCWs) (Fig. 1) [3]. Also among vaccinated individuals, SOT recipients are likely to have a higher risk for hospitalization and death compared with immunocompetent individuals [5,6]. Based on this evidence, booster dosages in SOT recipients have been recommended. However, studies have shown that although an increase in AbR could be observed after the third, fourth, or even fifth dosage, a negative or low-level AbR may still persist in a percentage of patients, ranging from 10% to 30%, and that the impact of further booster doses after the first one is limited [[7], [8], [9], [10]].

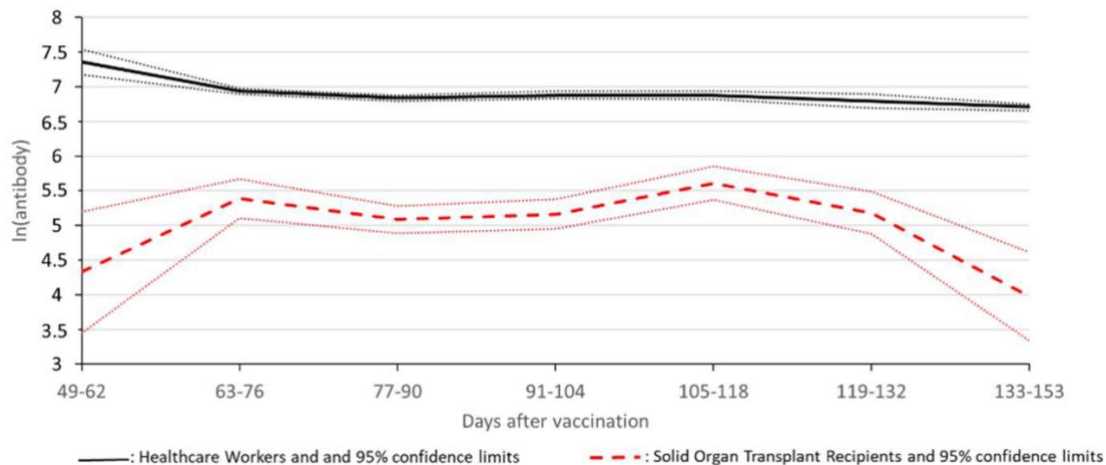


Figure 1. Mean ln (RBD) and 95% confidence limits in HCWs (continuous line) and SOT recipients (broken line) between 49 and 153 days after vaccination, adjusted for sex and age. The mean ln (AbR) in the two populations for the periods between 49 and 153 days after vaccination in individuals with positive AbR. The ratio of ln (AbR) between HCWs and SOT recipients ranged between 1.2 and 1.7, i.e., between 3.3 and 5.5 on arithmetic scale; SOT recipients showed a significant increase up to 76 days ($p < 0.001$), then a non-significant decrease in ln (AbR) after 118 days ($p = 0.1$); conversely, HCWs experienced a strong decrease in ln (AbR) up to 76 days ($p = 0.02$), and a less pronounced decrease between 76 and 118 days ($p = 0.04$). The work presented in this graph was performed by the candidate, Angelina Konnova, who was in the working group of the published published [3].

To increase protection against COVID-19 in this population, additional strategies have been proposed, such as the modulation of immunosuppressive therapy near the administration of booster doses [11], and/or the pre-exposure treatment with monoclonal antibodies [12]. Although the implementation of these strategies usually has been subordinated to the assessment of AbR, international transplant societies have discouraged the routine use of such practices

(<https://tts.org/tid-about/tid-officers-and-council?id=749>, accessed in August 2022). Hesitance to use anti-spike antibody levels as a marker for either vulnerability to or protection from SARS-CoV-2 infection is due to several reasons, including variability in antibody assays, lack of an antibody threshold associated with protection in immunocompromised patients, potential for protective cellular responses, logistic issues, and costs [13]. However, recent data have shown that there is a relationship between non-high level AbR and increased risk of breakthrough infection (BI) after three mRNA SARS-CoV-2 vaccine doses in SOT recipients; as well as that the probability of reaching immunization is inversely related to that of developing BI, mainly for some type of grafts as heart transplant recipients [14].

On this background, we deemed that a tool able to predict a negative AbR after at least a booster dose of mRNA SARS-CoV-2 vaccine in SOT recipients could be useful to stratify patients in order to personalize antibody testing in this setting. In this regard, machine learning (ML) methodology has recently been reported as a very useful tool to predict AbR after two doses of SARS-CoV-2 vaccine in SOT recipients [15]. Thus, we have used ML models, including traditional logistic regression analysis, to build a predictive binary-response model to identify SOT recipients at higher risk of a negative AbR after the first booster of SARS-CoV-2 vaccination (Fig. S1).

Methods

We used the multicentre prospective longitudinal cohort of SOT recipients within the Horizon 2020 ORCHESTRA project-work package 4 (<https://orchestra-cohort.eu/>), which aims to create a new pan-European cohort to rapidly advance the knowledge on the COVID-19 infection. The study was approved by the Agenzia Italiana del Farmaco (AIFA) and the Ethics Committee of Istituto Nazionale per le Malattie Infettive (INMI) Lazzaro Spallanzani (document n. 359 of Study's Registry 2020/2021) and registered at ClinicalTrials.gov with the number NCT05222139. Informed consent was obtained from all the enrolled patients.

The cohort runs at six hospitals (five in Italy — Bologna, Verona, Padova, Vicenza, and Treviso — and one in Seville, Spain). Participants were enrolled from 1 March, 2021 to 31 December, 2021 and followed up until 31 January, 2022. The database was locked on 1 March, 2022 after careful revision for incongruent or missing data. Data sources were clinical charts and hospital electronic records. All data were gathered anonymously and managed using the REDCap electronic data capture tools hosted at the Interuniversity Consortium CINECA (<https://redcap-dev.orchestra.cineca.it/>) [16]. SOT recipients undergoing SARS-CoV-2 vaccination during the enrolment period and who accepted to participate into the ORCHESTRA project were prospectively enrolled. As previously described [17], patients were assessed for AbR to SARS-CoV-2 vaccination at pre-defined timepoints: first dose (t0), second dose (t1), 3 ± 1 month after the first dose (t2), and at 1 month after the third dose (t3). All patients had a minimum follow-up of one month after the third dosage.

Variables

The primary endpoint was AbR at t3. The response was stratified into non-reactive (<5.58 BAU/mL), inconclusive (5.58 – <45 BAU/mL), positive-low (45 – <205 BAU/mL), positive-mild (205 – <817 BAU/mL), and positive-high (>817 BAU/mL) according to WHO International SARS-CoV-2 Antibody Standards criteria. For the purpose of the study, a negative AbR was defined as an anti-receptor binding domain (RBD) titre <45 BAU/mL (including non-reactive and inconclusive results).

Exposure variables collected at t0 included age, sex, comorbidities other than the cause of transplant according to the Charlson index, and type and date of transplant. Data on immunosuppressive regimen, receipt of induction regimen in the past 6 months, and graft function defined as good, impaired, or failure according to the judgement of attending physicians were collected at each timepoint.

Laboratory assays

The Elecsys® Anti-SARS-CoV-2 ECLIA assay and V-PLEX SARS-CoV-2 Panel 6 Kit (IgG) from Meso Scale Discovery (MSD, MD, USA) were used to detect AbR according to the manufacturer instructions and as previously described [17].

Statistical analysis

The distribution of age is reported by mean and standard deviation (SD). Due to the censored structure caused by the detection thresholds of the serology tests, we refrain from reporting AbR titres by means (SD) or median and interquartile ranges. Patients with a previous history of documented SARS-CoV-2 infection or with positive anti-N antibodies before or between doses were excluded from the analysis. The dataset used in the statistical analysis consisted of 14 binary covariates encoded with 0 and 1, and age as the only non-binary variable, reported as integers. These variables were chosen based on univariate statistical analysis ($p < 0.1$) (age, type of transplant, time between transplant and vaccination, and immunosuppressive drugs), and on clinical relevance (type of vaccine and graft function) (see Table S1). An ordinal logistic regression analysis was performed to identify risk factors, utilizing the five ordinal antibody levels (non-reactive, inconclusive, positive-low, positive-mild, and positive-high) as the outcome variable. The objective of this model was to determine the magnitude and direction of the covariates' effect.

The analysis was executed using R version 4.1.3, and the MASS package was used to train the ordinal logistic regression.

The ML model training and validation methods are described in Supplementary Text and Tables S1–S3.

Results

Characteristics of study cohort

The study cohort consisted of 1615 SOT recipients of kidney ($n = 886$), liver ($n = 350$), heart ($n = 340$), and lung ($n = 56$) transplants, with 17 patients having multiple organ transplantation (liver-kidney, $n = 10$; liver-heart, $n = 2$; kidney-heart, $n = 2$; kidney-lung, $n = 2$; and lung-heart, $n = 1$). The type and number of SOT recipients enrolled by each centre are detailed in Table S4. The majority of the study population consisted of males ($n = 1072$), and the mean (SD) age was 57.85 (13.77) y. Time from transplant to vaccination onset was less than 1 year, between 1 and 3 years, and more than 3 years in 6, 47, and 870 individuals, respectively. Graft failure occurred in 35 patients.

During the study period, 1211 patients received three doses of SARS-CoV-2 vaccine. This was mRNA based in all but 11 patients, who received a viral vector vaccine either as the first, second, or third dose (see Table S5). In 318 out of 1211 patients (26.2%), a change in the types of vaccine received between the initial vaccination schedule (first two dosages) and the booster dosage was

reported. In the majority of cases (n = 301), it consisted of shifting from BNT162b2 (Pfizer) to mRNA-1273 (Moderna). The mean (SD) time between the second and the third dose was 190.35 (34.26) days.

Serological assessment

Overall, 946 participants were assessed for AbR at first dose, 975 at second dose, 1363 at 3 ± 1 month after the first dosage, and 923 at one month after the third dosage. The rate of patients with anti-RBD levels ≥ 45 BAU/mL progressively increased from 6.34% (60/946), 14.05% (137/975), 50.92% (694/1363) to 78.11% (721/923) at each timepoint. The rate of individuals with a high AbR (>817 BAU/mL) increased from 1.80% (17/946), 5.95% (58/975), 20.00% (273/1363), to 63.20% (583/923), whereas the number of negative responses (<45 BAU/mL) decreased from 93.80% (886/946), 85.90% (889/975), 49.20% (669/1363), to 21.90% (202/923). For patients with multiple consecutive assessments, transition of the AbR from t0 to t3 is shown in Fig. 2.

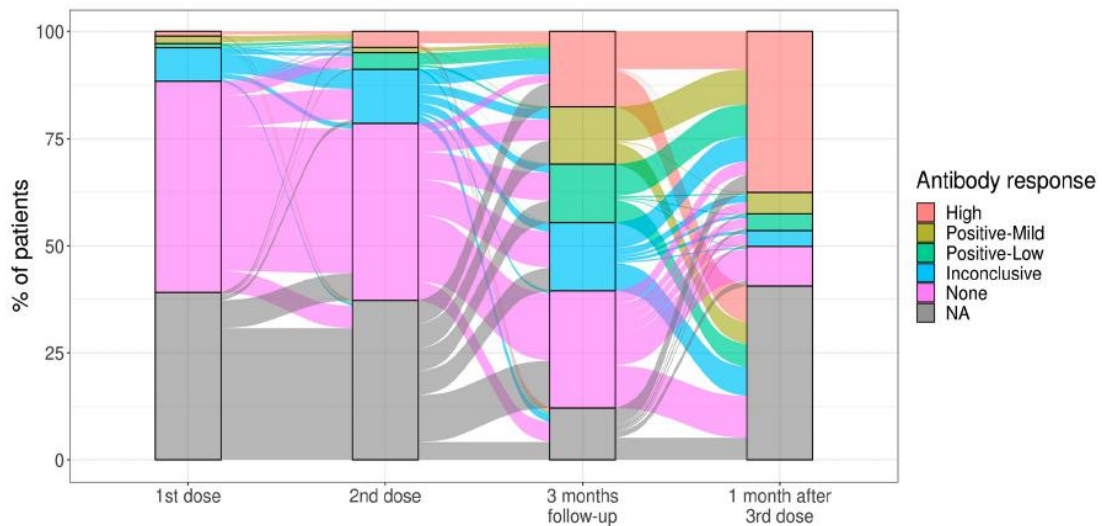


Figure 2. Distribution of antibody response. Individuals are classified as having a no antibody response if their antibody level is between 0 and 5.58 BAU/ml, Inconclusive if the level is between 5.58 and 45, positive-low the level is between 45 and 205, positive-mild if the level is between 205 and 817 BAU/ml, and classified as having a high antibody response if their antibody level is above 817 BAU/ml. Transitions between bars show the transition fractions of individuals across time points (part of this thesis).

Predictors of negative antibody response

Univariate analysis showed that kidney, heart, or lung transplant recipients had a higher likelihood of a negative AbR compared with liver transplant recipients. Furthermore, older patients, those taking anti-metabolites and/or steroids, and patients with recent transplant (<3 years) appeared to have an increased probability of a negative AbR (Table 1).

The ordinal logistic regression (see Table S6) showed a significant negative influence of age (log odds ratio, -0.03) and anti-metabolites (-1.10) on the AbR. In addition, the analysis showed that

patients with heart (-1.72), kidney (-1.59), or lung (-2.25) transplants were more likely to have a lower AbR than patients with a liver transplant. The type of vaccine, the time from transplant to the vaccination, and a graft failure did not seem to influence AbR after the booster dose. Parameter estimates and 95% confidence intervals are reported in Fig. 3.

Table 1. Comparison of patients with positive and negative antibody responses

Empty Cell	Total N = 923 (%)	Positive antibody response N = 721 (%)	Negative antibody response N = 202 (%)	<i>p</i>
Demographic data				
Age (mean ± SD) (y)	58.57 ± 12.78	58.11 ± 13.08	60.21 ± 11.51	0.027
Age group				0.063
<39 y	77 (8.34%)	63 (81.82%)	14 (18.18%)	
40–49 y	125 (13.54%)	109 (87.20%)	16 (12.80%)	
50–59 y	235 (25.46%)	181 (77.02%)	54 (22.98%)	
60–69 y	288 (31.20%)	214 (74.31%)	74 (25.69%)	
≥70 y	198 (21.45%)	154 (77.78%)	44 (22.22%)	
Sex				0.140
Male	615 (67.73%)	492 (80.00%)	123 (20.00%)	
Female	303 (33.37%)	235 (74.26%)	78 (25.74%)	
Comorbidities				0.188
No	134 (14.52%)	111 (82.84%)	23 (17.16%)	
Yes	789 (85.48%)	610 (77.31%)	179 (22.69%)	
Type of graft^a				
Kidney	515 (55.26%)	386 (74.95%)	129 (25.05%)	0.011
Heart	176 (18.88%)	120 (68.18%)	56 (31.82%)	<0.001
Liver	218 (23.39%)	206 (94.50%)	12 (5.50%)	<0.001
Lung	23 (2.47%)	16 (69.57%)	7 (30.43%)	0.4539
Type of vaccine^b				
BNT162b2 (Pfizer)	476 (57.91%)	372 (78.15%)	104 (21.85%)	
mRNA-1273 (Moderna)	346 (42.09%)	275 (79.48%)	71 (20.52%)	

Empty Cell	Total N = 923 (%)	Positive antibody response N = 721 (%)	Negative antibody response N = 202 (%)	<i>p</i>
Time from transplant to vaccination				0.091
Less than 1 year	6 (0.65%)	4 (66.67%)	2 (33.33%)	
1 to 3 years	47 (5.09%)	32 (68.09%)	15 (31.91%)	
More than 3 years	870 (94.26%)	685 (78.74%)	185 (21.26%)	
Induction regimen in the last 6 months				
No	923 (100%)	721 (78.11%)	202 (21.89%)	
Any	0 (0%)	0 (0.00%)	0 (0.00%)	
Immunosuppressive drugs at the time of vaccination				
Calcineurin inhibitors	641 (42.48%)	500 (78.00%)	141 (22.00%)	0.447
Tacrolimus	483 (75.35%)	372 (77.02%)	111 (22.98%)	0.445
Cyclosporine	157 (24.49%)	127 (80.89%)	30 (19.11%)	0.414
Anti-metabolites	377 (25.05%)	260 (69.05%)	117 (30.95%)	<0.001
Mycophenolate mofetil	370 (98.14%)	253 (68.38%)	117 (31.54%)	<0.001
Azathioprine	7 (1.86%)	7 (100.00%)	0 (0.00%)	0.343
mTOR	105 (6.96%)	88 (83.81%)	17 (16.19%)	0.594
Everolimus	89 (84.76%)	72 (80.90%)	17 (19.10%)	0.594
Sirolimus	16 (15.24%)	16 (100.00%)	0 (0.00%)	0.067
Steroids	385 (25.51%)	278 (72.21%)	107 (27.79%)	<0.001
Impaired graft function				0.354
Good	888 (96.21%)	696 (78.38%)	192 (21.62%)	
Impaired or Failure	35 (3.79%)	25 (71.43%)	10 (28.57%)	

a: Multiple grafts are possible.

b: Only third-dose vaccines.

The predictive power of the ML models in the validation cohort was assessed using the balanced accuracy (BA) (Fig. S2) and the area under the precision-recall curve (PRAUC) (Fig. S3) as decision criteria. Further evaluation measures, such as accuracy, sensitivity, and specificity, are depicted in Figs. S4–S7. The results showed that relative performance of different models is almost independent

of the AbR threshold. At an AbR level of 45, the top three performers were logistic regression (LR) (BA, 0.66 [0.65, 0.67]; PRAUC, 0.37 [0.36, 0.39]), k-Nearest Neighbours (KNN) (BA, 0.65 [0.64, 0.66]; PRAUC, 0.36 [0.35, 0.37]), and ordinal logistic regression (OLR) (BA, 0.63 [0.62, 0.64]; PRAUC, 0.34 [0.33, 0.35]). However, when examining the average specificities (Fig. S4) and sensitivities (Fig. S5) at this threshold, it was found that LR and the OLR performed well in predicting SOT recipients with negative AbR (OLR, 0.71 [0.68, 0.73]; LR, 0.70 [0.68, 0.72]), but performed worse in predicting those with positive AbR (OLR, 0.56 [0.54, 0.58]; LR, 0.62 [0.61, 0.64]). Tree-based methods, such as the Bagged tree and the Gradient Boosting Machine (GBM), performed well in predicting patients with a positive AbR (BT, 0.83 [0.82, 0.84]; GBM, 0.78 [0.77, 0.8]), but poorly in predicting those with negative AbR (BT, 0.30 [0.28, 0.32]%; GBM, 0.35 [0.33, 0.37]).

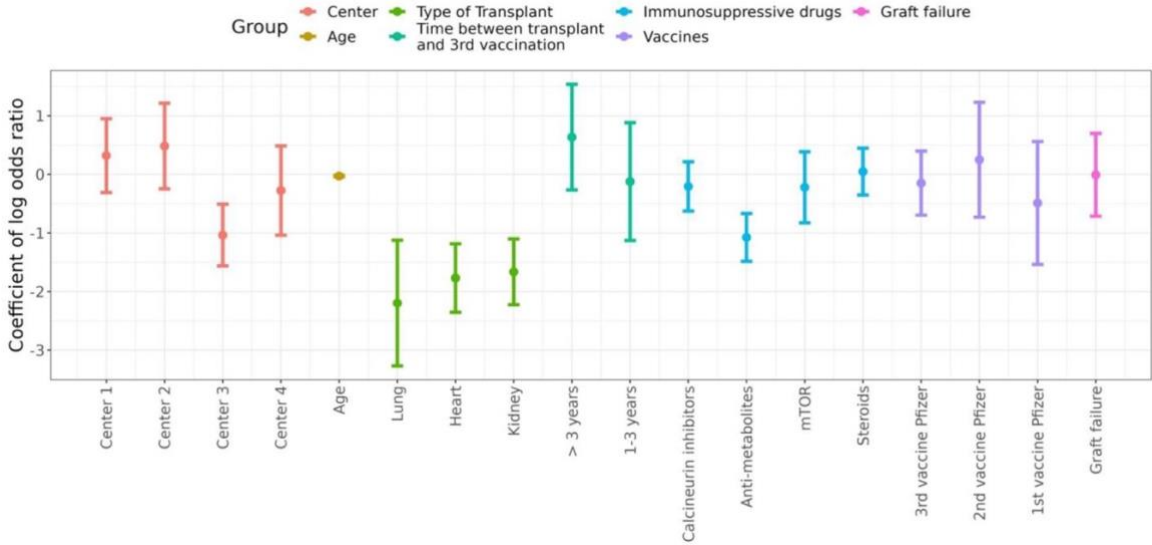


Figure 3. Parameter estimates ordinal logistic regression. Results of the ordinal logistic regression model using the depicted covariates and the 5 categories “None”, “Inconclusive”, “Positive-low”, “Positive-mild”, and “High” with None being encoded as the state with the lowest antibody response and High being the state with the highest antibody response. Hence, negative coefficients indicate a more negative antibody response. Confidence intervals are at the 95% level. The coefficients can be interpreted as an increase in the log odds ratio, if the respective control variable increases by one. There are only four out of the six centers included in the graph since one center had only observations with missing data at the 3rd vaccination and one center has no parameter since it is the reference group. The confidence intervals for age are due to their size not properly depicted in the graph. However, its 95% confidence interval does not cover zero. Exact values and p-values are given in Supplemental Table 6. The transplant results are in comparison to liver transplants, the timing of vaccination in comparison to less than one year and the Pfizer vaccine parameters in comparison to Moderna.

The tree-based methods, such as the GBM, appear to have overfitted the training data, as demonstrated by an average BA of 0.94 [0.94, 0.95] and an average PRAUC of 0.94 [0.93, 0.95] (Figs. S8 and S9). On the other hand, other methods, such as LR, did not exhibit such overfitting in the training set (BA, 0.70 [0.70, 0.71]; PRAUC, 0.44 [0.44, 0.45]). For the area under the receiver operating characteristic curve (AUROC) — a metric which we report for comparison with prior

research — we found that the LR model achieved an average AUROC of 0.72 [0.71–0.73], the k-nearest neighbour algorithm had an average AUROC of 0.73 [0.72–0.74], and the OLR model had an average AUROC of 0.68 [0.67–0.69] (Fig. S6).

Discussion

Our data confirm the persistence of lack of response in almost one fourth of the patients after booster dose. Using this data, we aimed to develop a prediction models based on easy-to-obtain clinical covariates, such as age, type of transplant, time from transplant to first dosage, types of immunosuppressive drugs, type of mRNA vaccine received, and graft failure. Unfortunately, the best ML model we found only reached a moderate prediction accuracy. This suggests that the clinical covariates provide only limited information.

Our results are consistent with those obtained by Alejo et al. [15], who developed and validated a ML model to predict AbR to two doses of SARS-CoV-2 mRNA vaccines using a nationwide cohort of 1031 SOT recipients, and an external single-centre cohort of 512 SOT recipients in the United States. The authors used 19 clinical factors very similar to those used in our models. Indeed, Alejo et al. found that mycophenolate mofetil use, a shorter time since transplant, and older age were the strongest predictors of a negative AbR. The performance of the model was good in the training set (AUROC, 0.79) and moderate in the external test set (AUROC, 0.67). The main difference between the U.S. cohort and our cohort is the definition of negative AbR (which is < 0.8 U/mL if assessed by Roche and ≤ 1.1 AU if assessed by EUROIMMUN) used in the U.S. cohort [15]. Alejo et al. used a GBM to predict antibody responses. We found that LR analysis was most accurate in predicting a negative AbR, while tree-based ML models performed worse. A possible explanation for this is that the tree-based methods might have overfitted the training data, as indicated by the Figs. S8–S13, despite being optimized through cross-validation of the hyperparameters (Table S1). This overfitting results in poor generalization performance when applied to the unseen validation cohort in contrast to the not overfitting other models.

Our study has limitations. First, due to the censored structure caused by the detection thresholds of the serology tests, we refrained from reporting and assessing quantitative antibody levels. Second, regarding the type of SARS-CoV2 vaccines (BNT162b2, mRNA-1273, and ChAdOx1), the predictive power of ChAdOx1 could not be assessed due to limited number of subjects exposed. Third, we did not analyse cellular immune response that is an essential component in the clinical protection of SOT recipients from clinically relevant SARS-CoV2 infections. Finally, we developed the model with AbR assessed one month after the first booster dosage, while currently most fragile patients should have received several booster dosages. However, it has been shown that the impact of further booster dosages on AbR may be limited, with lower than 50% of seronegative patients achieving a positive AbR or showing a significant increase in antibody levels [18,19]. Thus, we deem that our model could be valid also in patients exposed to more than one booster dosage.

Although booster dosage in SOT recipients is associated with a progressive increase in AbR, one fourth of this population remains negative or with suboptimal antibody levels. Unfortunately, clinical characteristics are of limited values in developing high performing predictive models of negative AbR.

ORCHESTRA-WP4 study group

Natascia Carocchia, Beatrice Tazza, Cecilia Bonazzetti, Francesca Fani, Michela Di Chiara, Maria Eugenia Giacomini, Oana Vatamanu, Zeno Pasquini, Renato Pascale, Matteo Rinaldi, Clara Solera Horna, Caterina Campoli, Giacomo Fornaro, Fabio Trapani, Luciano Attard, Antonio Gramegna, Valeria Cesari, Simona Varani, Elena Rosselli Del Turco, Sara Tedeschi, Kristian Scolz, Gaetano La Manna, Valeria Grandinetti, Marcello Demetri, Simona Barbuto, Chiara Abenavoli, Giovanni Vitale, Laura Turco, Matteo Ravaioli, Matteo Cescon, Valentina Bertuzzo, Angela Lombardi, Alessandra Trombi, Marco Masetti, Paola Prestinenzi, Mario Sabatino, Laura Giovannini, Aloisio Alessio, Antonio Russo, Maria Francesca Scuppa, Laura Borgese, Giampiero Dolci, Gianmaria Paganelli, Giorgia Comai, Liliana Gabrielli, Chiara Gamberini, and Marta Leone. IRCCS Policlinico Sant'Orsola, University of Bologna, Bologna, Italy. Simona Granata, Alberto Verlatto, and Rossella Elia. Renal Unit, Department of Medicine, University Hospital of Verona, Verona, Italy. Alex Borin. Liver Transplant Unit, Department of Surgery and Dentistry, University and Hospital Trust of Verona, Verona, Italy. Livio San Biagio, Alessandra Francica, and Ilaria Tropea. Division of Cardiac Surgery, University of Verona, Verona, Italy. Maria Mongardi, Mariana Nunes Pinho Guedes, Gaia Maccarone, Concetta Sciammarella, Massimo Mirandola, Lorenzo Maria Canziani, Chiara Konishi, Chiara Perlini, and Giulia Rosini. Division of Infectious Diseases, Department of Diagnostics and Public Health, University of Verona, Verona, Italy. Francesca Russo and Michele Mongillo. Direzione Prevenzione sicurezza alimentare veterinaria, Regione Veneto, Italy. Maria Giulia Caponcello, Natalia Maldonado, Paula Olivares, David Gutiérrez-Campos, Ana Belén Martín-Gutiérrez, Ana Silva, Virginia Palomo, Almudena Serna, and Marta Fernández-Regaña. Infectious Diseases and Microbiology Unit, Hospital Universitario Virgen Macarena, and Department of Medicine, University of Sevilla/Biomedicines Institute of Sevilla, Sevilla, Spain. Ana Belén Hidalgo, Ioana Hrom, Myriam Adorna, Rubén Murillo, and Ma Isabel García-Sánchez. Biobank Nodo Hospital Virgen Macarena (Biobanco del Sistema Sanitario Público de Andalucía) integrated in the Spanish National biobanks Network (PT20/00069). Paolo Angeli, Alessandra Brocca, Nicola Zeni, Roberta Gagliardi, and Simone Incicco. Unit of Internal Medicine and Hepatology (UIMH), Department of Medicine - DIMED, University of Padua, Padua, Italy. Andrea Carraro, Josè Igeno San Miguel, Emanuele Vianello, and Susanna Negrisolo. Paediatric Nephrology, Dialysis and Transplant Unit, Department of Women's and Children's Health, Padua University Hospital, Padua, Italy. Enrico Gringeri, Patrizia Boccagni, Francesco Enrico D'amico, Riccardo Boetto, and Lara Borsetto. Department of Surgery, Oncology and Gastroenterology, Hepatobiliary Surgery and Liver Transplantation Unit, Padua University Hospital, Padua, Italy. Erica Nuzzolese, Marianna Di Bello, and Caterina Di Bella. Kidney and Pancreas Transplantation Unit, Department of Surgical, Oncological and Gastroenterological Sciences, University of Padua, Padua, Italy. Paola Gaio. Unit of Paediatric Gastroenterology, Digestive Endoscopy, Hepatology and Care of the Child with Liver Transplantation, Department of Women's and Children's Health, University Hospital of Padua, Padua, Italy. Luigi Garufi and Chiara Tessari, SaimaImran. Cardiac Surgery Unit, Department of Cardiac, Thoracic, Vascular Sciences and Public Health, University of Padua, Padua, Italy. Debora Bizzarro and Francesco Paolo Russo. Unit of Gastroenterology and Multivisceral Transplant, Department of Surgery, Oncology and Gastroenterology, University Hospital of Padua, Padua, Italy. Lorena Brunello, Marta Tenan, and Monica Rizzolo. Nephrology Unit, Treviso Hospital, Treviso,

Italy. Carlotta Caprara, Grazia Maria Virzì, and Matteo Marcello. Department of Nephrology, Dialysis and Transplantation, San Bortolo Hospital, Vicenza, Italy.

Transparency declaration

Salvatore Piano reports consulting fees from Plasma Protein Therapeutics Association (PPTA) and Resolution Therapeutics and participation in Advisory board for Mallinckrodt Inc. Pierluigi Viale reports consulting fees from bioMérieux, Mundipharma, AstraZeneca, Tillots Pharma, Gilead, Shionogi, Sobi, Advanzpharma, MSD, Angelini and Pfizer. All other authors report no potential conflicts of interest.

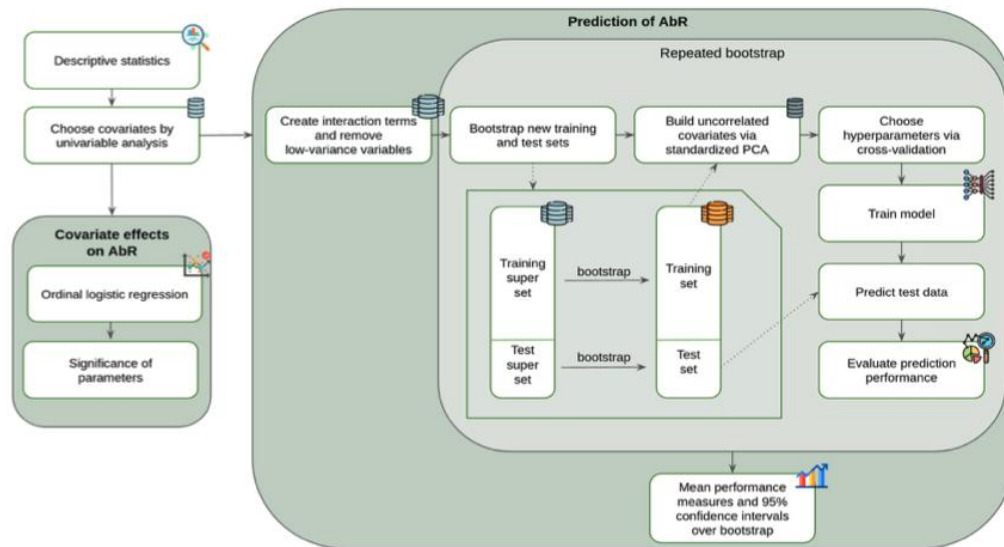
Financial support

This work was supported by the European Union's Horizon 2020 Research and Innovation Program, grant agreement 101016167, within the ORCHESTRA project (EU H2020 ORCHESTRA).

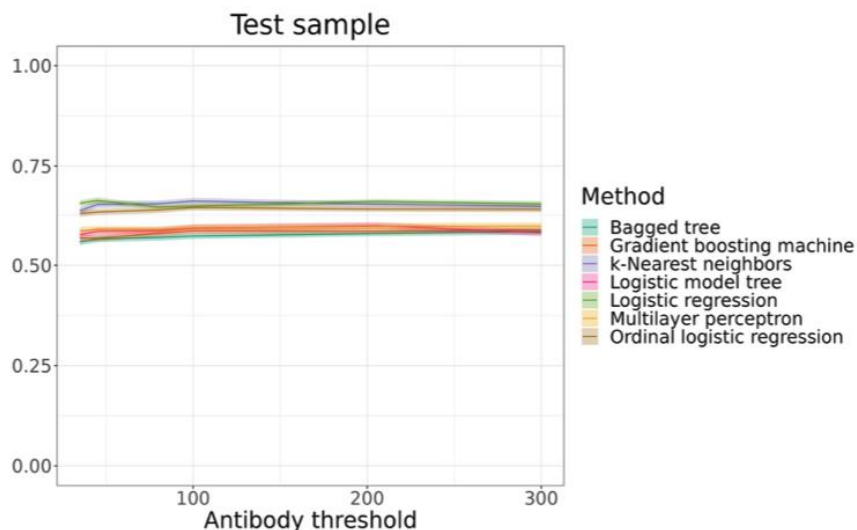
Author contributions

The authors confirm contribution to the paper as follows: study conception and design: Giannella M, Tacconelli E, Huth M, Hasenauer J; clinical data collection: Marconi L, Palacios-Baena ZR, Morelli MC, Tamè M, Busutti M, Potena L, Salvaterra E, Feltrin G, Gerosa G, Furian L, Burra P, Piano S, Cillo U, Cananzi M, Loy M, Zaza G, Onorati F, Carraro A, Righi E, Gastaldon F, Nordio M; immunological analysis and interpretation of results: Konnova A, Gupta A, Hotterbeekx A, Berkell M, Lazzarotto T, Kumar-Singh S; statistical analysis and interpretation of results: Huth M, Hasenauer J, Giannella M, Tacconelli E; draft manuscript preparation: Giannella M, Tacconelli E, Huth M, Hasenauer J; draft manuscript revision: Righi E, Rodríguez Baño J, Viale P. All authors reviewed the results and approved the final version of the manuscript.

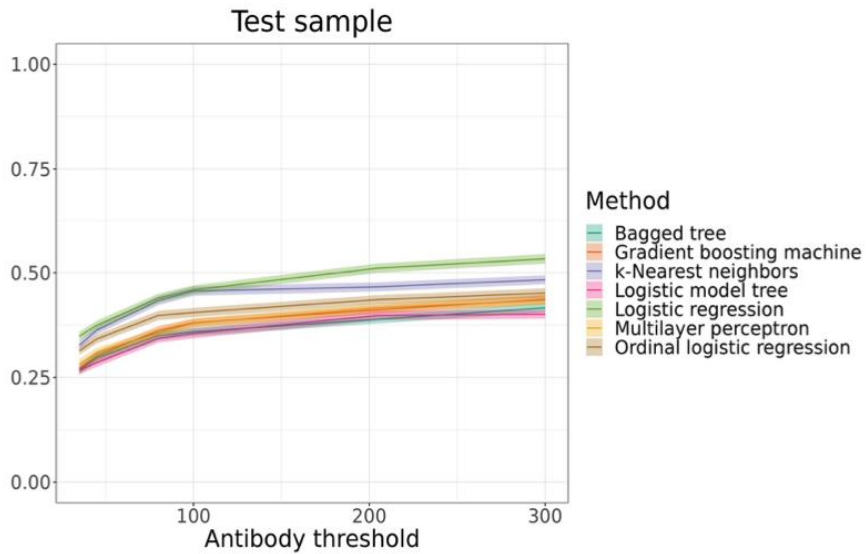
Supplementary Figures and Tables



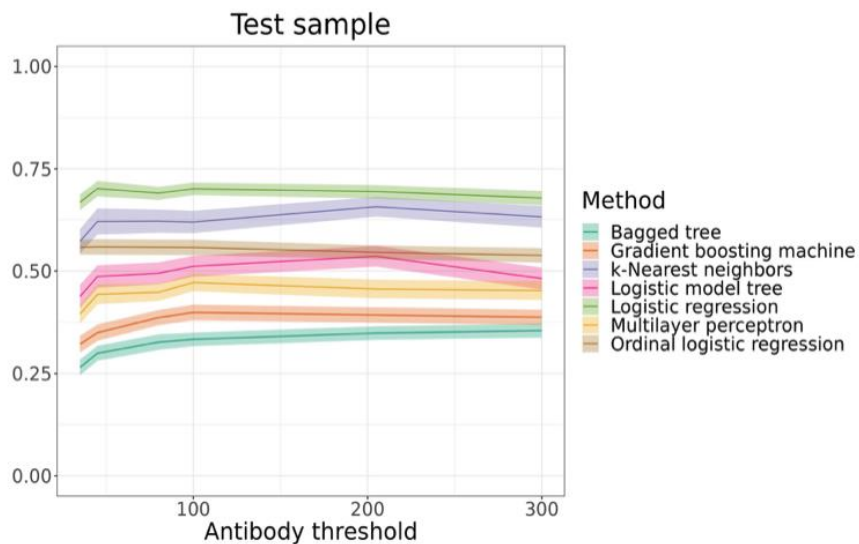
Supplementary Figure 1. Data analysis workflow. Overview of our data analysis workflow. We first built descriptive statistics which we used to determine the covariate structure for the prediction of the antibody response and the examination of the effects of the covariates on the antibody response. In order to assess the effects of the covariates on the antibody response, we ran an ordinal logistic regression. In order to predict the antibody response, we extend the covariates by their pair-wise interaction terms. We trained the model with 4 centers and tested it on an unseen validation test center. We ran 200 bootstrap samples of different machine learning algorithms in order to obtain means and confidence intervals for the key prediction performance measures.



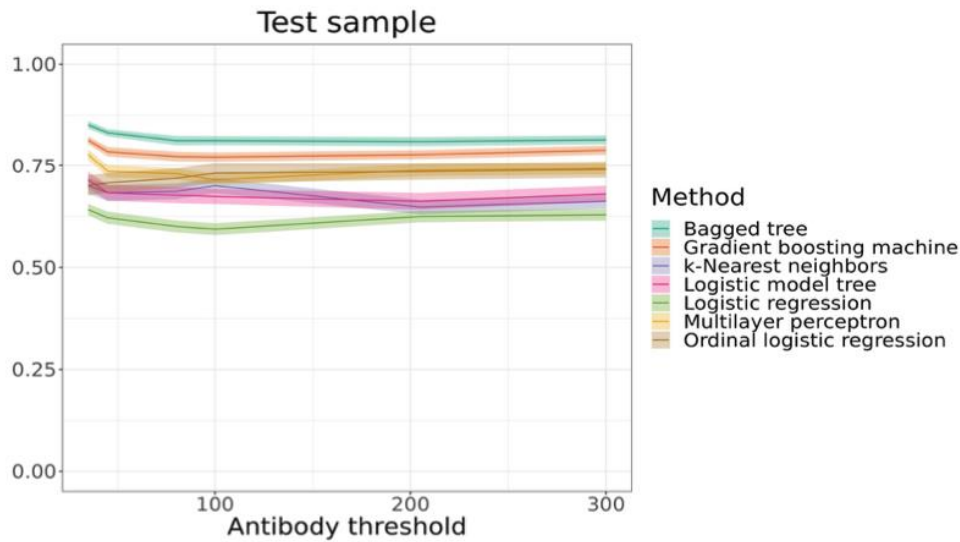
Supplementary Figure 2. Balanced accuracy. The figure shows the balanced accuracy for out-of-sample predictions of different machine learning algorithms, averaged over 200 runs. The 95% confidence intervals are also reported. The x-axis represents the antibody level threshold at which individuals are classified as having a positive antibody response, and the y-axis represents the balanced accuracy, which is computed as the mean of sensitivity and specificity.



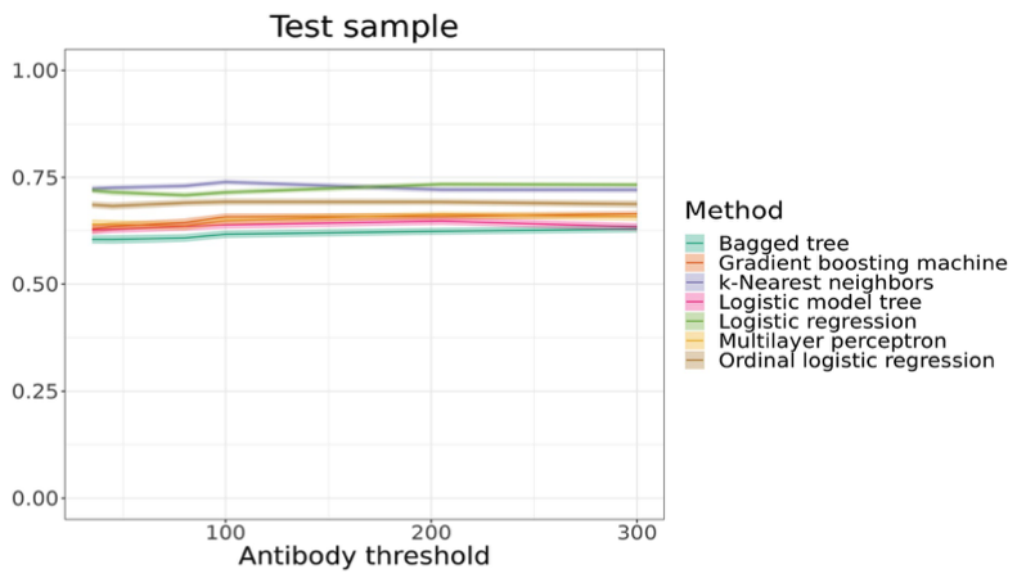
Supplementary Figure 3. Area under the precision recall curve (PRAUC). The figure shows the area under the precision recall curve for out-of-sample predictions of different machine learning algorithms, averaged over 200 runs. The 95% confidence intervals are also reported. The x-axis represents the antibody level threshold at which individuals are classified as having a positive antibody response, and the y-axis represents the area under the precision recall curve. The area under the precision recall curve can be computed by first calculating the precision and recall values for different thresholds of the classifier, then plotting these values on a precision-recall curve, and computing the area under the curve.



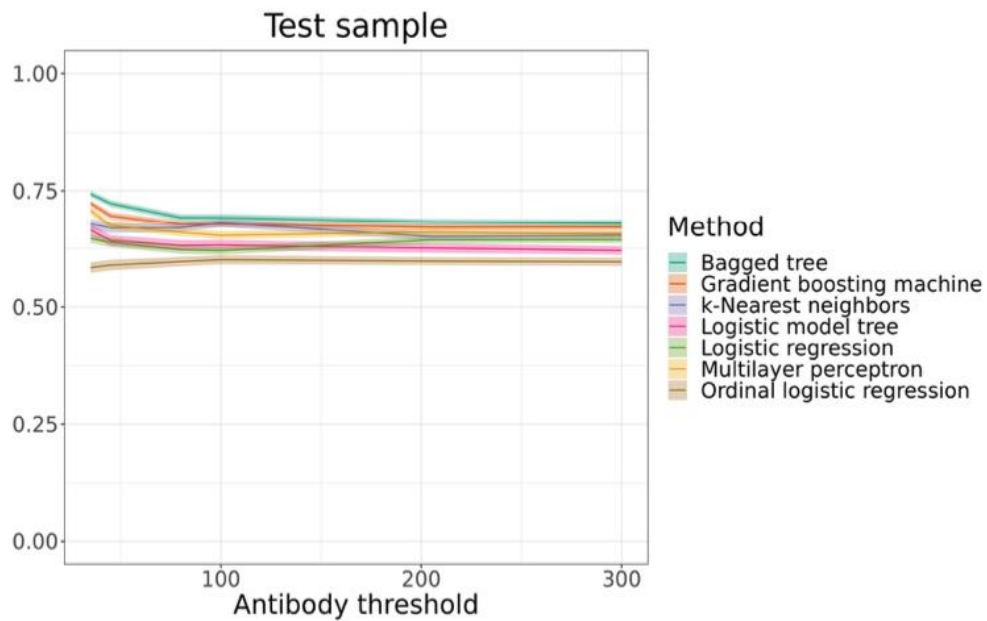
Supplementary Figure 4. Specificity. The figure shows the specificity for out-of-sample predictions of different machine learning algorithms, averaged over 200 runs. The 95% confidence intervals are also reported. The x-axis represents the antibody level threshold at which individuals are classified as having a positive antibody response, and the y-axis represents the specificity, which is computed as the true negative rate.



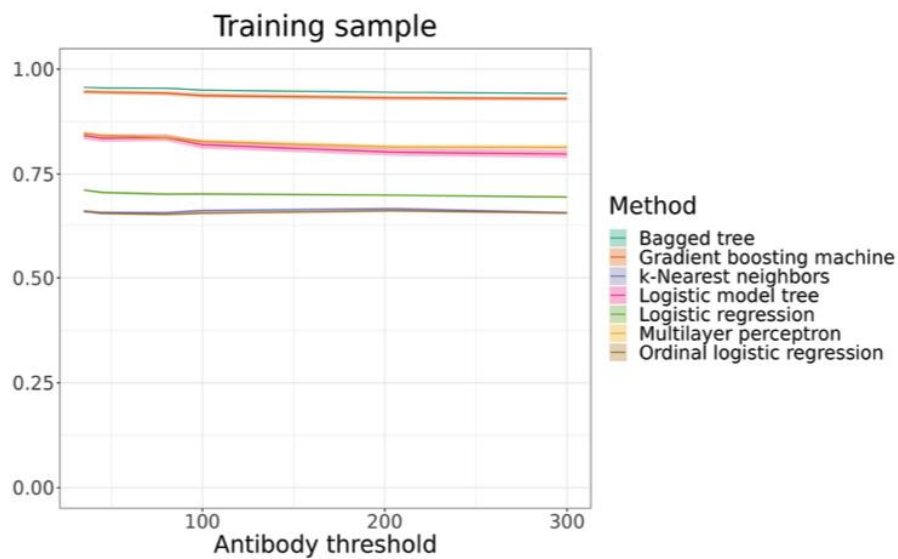
Supplementary Figure 5. Sensitivity. The figure shows the sensitivity for out-of-sample predictions of different machine learning algorithms, averaged over 200 runs. The 95% confidence intervals are also reported. The x-axis represents the antibody level threshold at which individuals are classified as having a positive antibody response, and the y-axis represents the sensitivity, which is computed as the true positive rate.



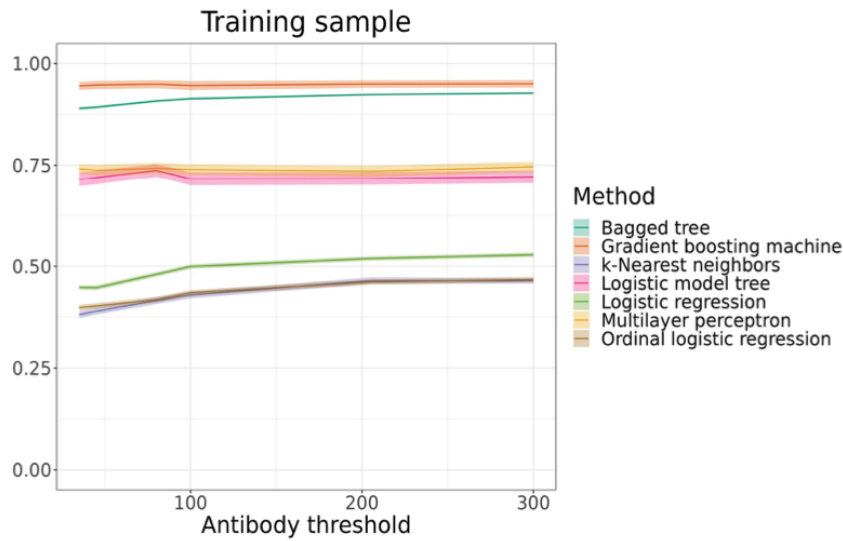
Supplementary Figure 6. AUROC. The figure shows the area under the receiver operator curve (AUROC) for out-of-sample predictions of different machine learning algorithms, averaged over 200 runs. The 95% confidence intervals are also reported. The x-axis represents the antibody level threshold at which individuals are classified as having a positive antibody response, and the y-axis represents the AUROC, which is computed as the area under the receiver operator curve.



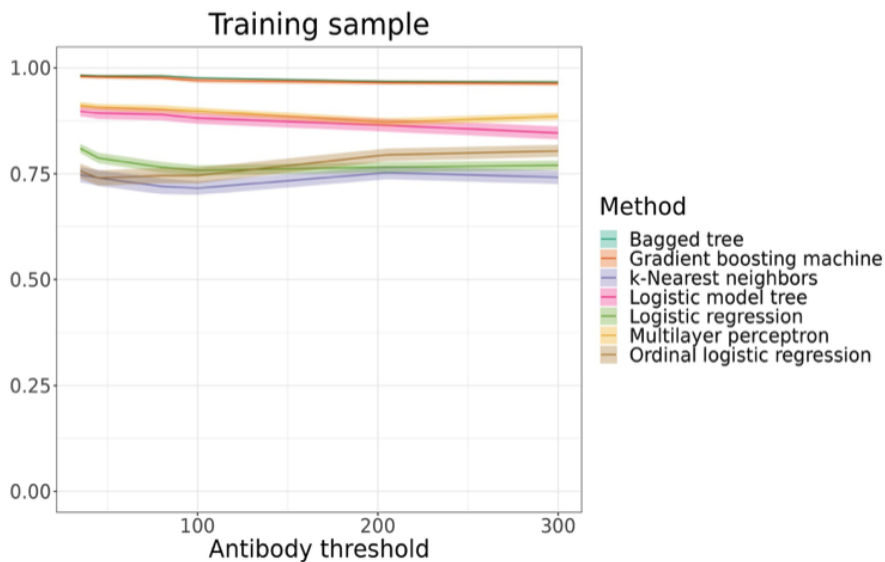
Supplementary Figure 7. Accuracy. The figure shows the accuracy for out-of-sample predictions of different machine learning algorithms, averaged over 200 runs. The 95% confidence intervals are also reported. The x-axis represents the antibody level threshold at which individuals are classified as having a positive antibody response, and the y-axis represents the accuracy, which is computed as the true negative rate.



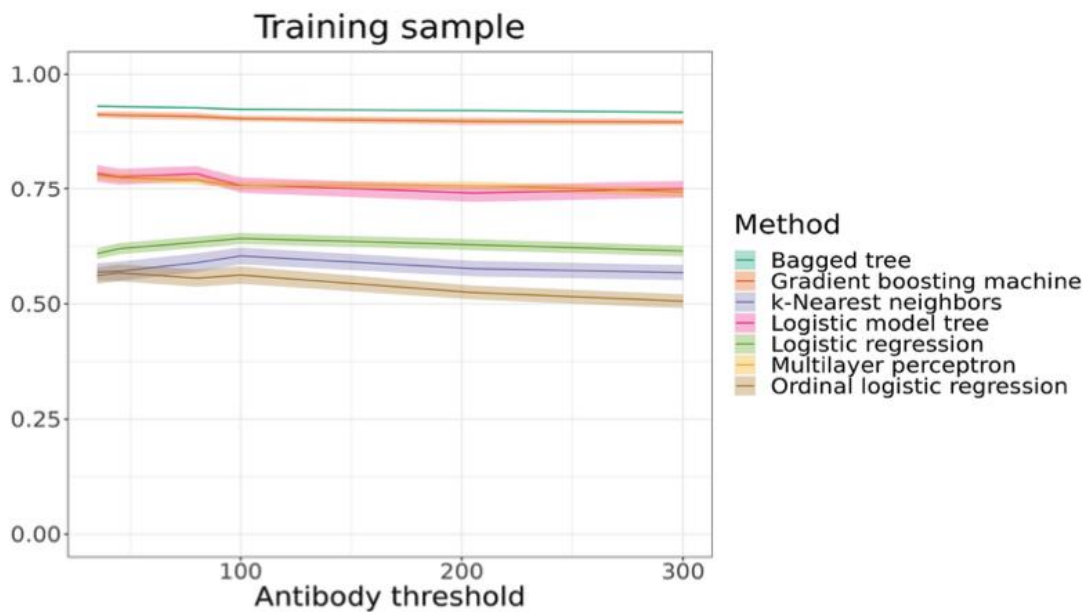
Supplementary Figure 8. In-sample balanced accuracy. The figure shows the balanced accuracy for in-sample predictions of different machine learning algorithms, averaged over 200 runs. The 95% confidence intervals are also reported. The x-axis represents the antibody level threshold at which individuals are classified as having a positive antibody response, and the y-axis represents the balanced accuracy, which is computed as the mean of sensitivity and specificity.



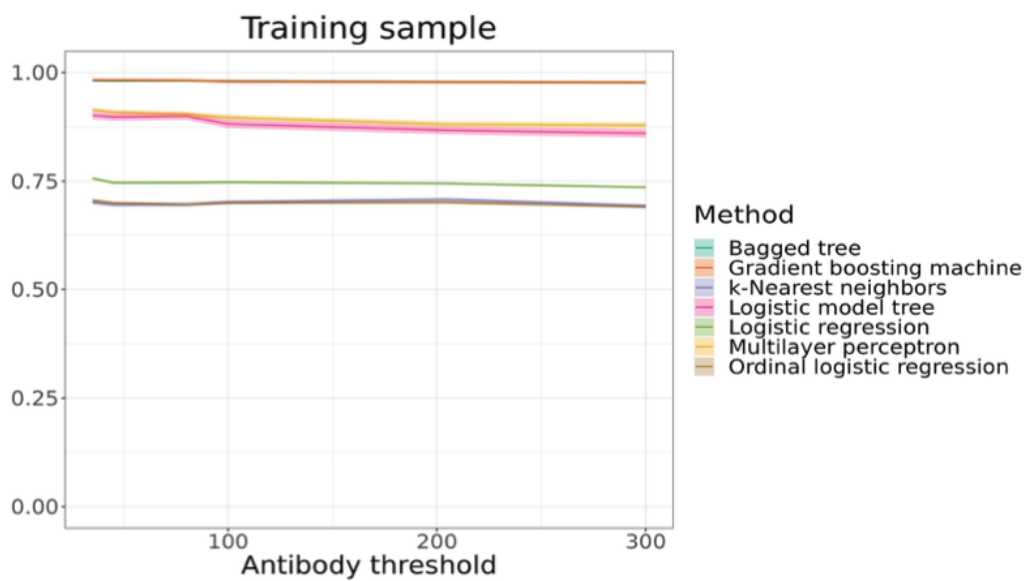
Supplementary Figure 9. In-sample area under the precision recall curve (PRAUC). The figure shows the area under the precision recall curve for in-sample predictions of different machine learning algorithms, averaged over 200 runs. The 95% confidence intervals are also reported. The x-axis represents the antibody level threshold at which individuals are classified as having a positive antibody response, and the y-axis represents the area under the precision recall curve. The area under the precision recall curve can be computed by first calculating the precision and recall values for different thresholds of the classifier, then plotting these values on a precision-recall curve, and computing the area under the curve.



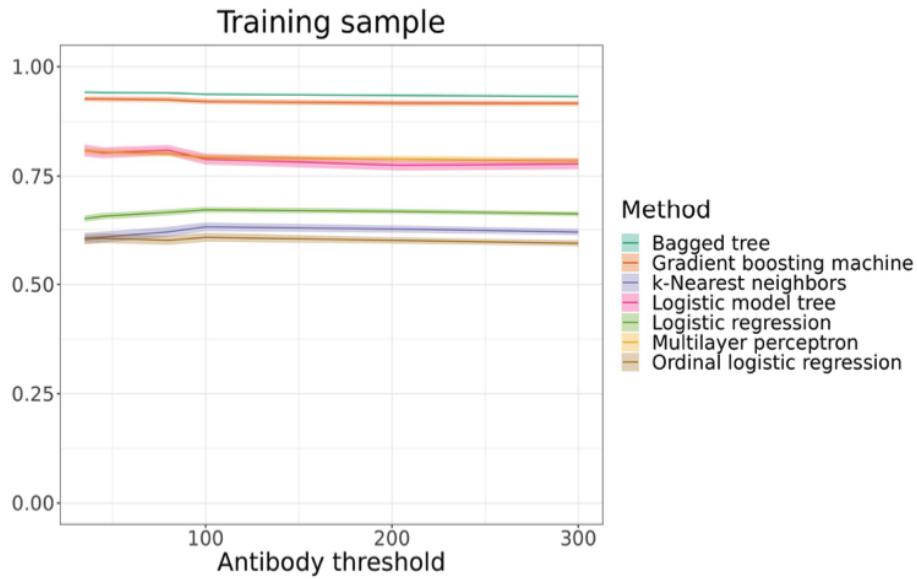
Supplementary Figure 10. In-sample specificity. The figure shows the specificity for in-sample predictions of different machine learning algorithms, averaged over 200 runs. The 95% confidence intervals are also reported. The x-axis represents the antibody level threshold at which individuals are classified as having a positive antibody response, and the y-axis represents the specificity, which is computed as the true negative rate.



Supplementary Figure 11. In-sample sensitivity. The figure shows the sensitivity for in-sample predictions of different machine learning algorithms, averaged over 200 runs. The 95% confidence intervals are also reported. The x-axis represents the antibody level threshold at which individuals are classified as having a positive antibody response, and the y-axis represents the sensitivity, which is computed as the true positive rate.



Supplementary Figure 12. In-sample AUROC. The figure shows the area under the receiver operator curve (AUROC) for in-sample predictions of different machine learning algorithms, averaged over 200 runs. The 95% confidence intervals are also reported. The x-axis represents the antibody level threshold at which individuals are classified as having a positive antibody response, and the y-axis represents the AUROC, which is computed as the area under the receiver operator curve.



Supplementary Figure 13. In-sample accuracy. The figure shows the accuracy for in-sample predictions of different machine learning algorithms, averaged over 200 runs. The 95% confidence intervals are also reported. The x-axis represents the antibody level threshold at which individuals are classified as having a positive antibody response, and the y-axis represents the accuracy, which is computed as the true negative rate.

Supplementary Table 1. Machine Learning Methods

Method	Caret method	Hyperparameters	Description
Logistic regression	glm	-	Yields linear decision boundaries.
Boosted logistic regression	LogitBoost	Number of boosting iterations	Aggregates one node logistic model trees using boosting to decrease variance of the estimate.
Bagged tree	treebag	-	Aggregates decision trees using bagging to decrease variance of the estimate.
Gradient boosting machine	gbm	Number of boosting iterations, Maximal tree depth, Minimal terminal node size, Shrinkage parameter	Iteratively adds new models to the ensemble, where each new model attempts to correct the mistakes of the previous models.
K-Nearest Neighbors	knn	Number of neighbors	Classifies an individual based on a majority vote of its k-nearest neighbors
Multilayer perceptron	mlp	Number of hidden units	Fully connected neural network with 1 hidden layer.
Ordinal logistic regression	polr	Link function (Logistic, Cauchy, Probit)	Linear decision boundaries for multiple ordinal classes. To achieve a binary classification, the ordinal classes can be aggregated in the end to 2 classes. The advantage is that during the training phase more knowledge about the outcome variable is known but as a disadvantage, a further hyperparameter (how to binarize the ordinal classes) needs to be estimated.

* All models include the number of principal components as additional hyperparameter

Supplementary Table 2: Comparison of patients with positive and negative antibody responses – Training super set

	Total N=697(%)	Positive antibody response N=545 (%)	Negative antibody response N=152 (%)	<i>p</i>
Demographic data				
Age (mean±SD) (years)	58.91±12.21	58.46±12.48	60.54±11.07	0.046
Age group				0.028
< 39 y	51 (7.32 %)	42 (82.35 %)	9 (17.65 %)	
40-49 y	101 (14.49 %)	89 (88.12 %)	12 (11.88 %)	
50-59 y	181 (25.97 %)	141 (77.90%)	40 (22.10 %)	
60-69 y	210 (30.13 %)	151 (71.90 %)	59 (28.10 %)	
>= 70 y	154 (22.09 %)	122 (79.2 %)	32 (20.78 %)	
Sex				0.041
Male	453 (65.27 %)	366 (80.79 %)	87 (19.21 %)	
Female	241 (34.73 %)	176 (73.03 %)	65 (26.97 %)	
Comorbidities				0.436
Yes	638 (91.54 %)	496 (77.74 %)	142 (22.26 %)	
No	59 (8.46 %)	49 (83.05 %)	10 (16.95 %)	
Type of graft¹				
Kidney	434 (62.27 %)	330 (76.04 %)	104 (23.96 %)	0.009
Heart	103 (14.78 %)	67 (65.05 %)	36 (34.95 %)	< 0.001
Liver	147 (21.09 %)	139 (94.56 %)	8 (5.44 %)	< 0.001
Lung	22 (3.16 %)	16 (72.73 %)	6 (27.27 %)	0.713
Type of vaccine²				
BNT162b2 (Pfizer)	285 (47.11 %)	221 (77.54 %)	64 (22.46 %)	
mRNA-1273 (Moderna)	320 (52.89 %)	257 (80.31 %)	63 (19.69 %)	

1 Multiple grafts are possible.

2 Only third dose vaccines.

Time from transplant to vaccination				0.003
Less than 1 year	5 (0.72 %)	5 (100 %)	0 (0.00 %)	
1 to 3 years	14 (2.01 %)	6 (68.09 %)	8 (31.91 %)	
More than 3 years	678 (97.27 %)	534 (78.74 %)	144 (21.26 %)	
Induction regimen in the last 6 months				
No	697 (100 %)	545 (78.11%)	152 (21.89 %)	
Any	0 (0 %)	0 (0.00 %)	0 (0.00 %)	
Immunosuppressive drugs at the time of vaccination				
Calcineurin inhibitors	426 (61.11 %)	333 (76.27 %)	120 (23.73 %)	0.248
Tacrolimus	354 (83.10 %)	270 (76.27 %)	111 (23.73 %)	0.248
Cyclosporine	72 (16.90 %)	63 (87.50 %)	9 (12.50 %)	0.062
Anti-metabolites	374 (53.66 %)	243 (69.05 %)	76 (30.95 %)	<0.001
Mycophenolate mofetil	370 (98.93 %)	239 (68.20 %)	76 (31.80 %)	< 0.001
Azathioprine	4 (1.07 %)	4 (100.00 %)	0 (0.00 %)	0.651
mTOR	53 (7.60 %)	41 (83.81 %)	12 (16.19 %)	0.418
Everolimus	43 (81.13 %)	31 (72.09 %)	12 (27.91 %)	0.418
Sirolimus	10 (18.78 %)	10 (100.00 %)	0 (0.00 %)	0.195
Steroids	304 (43.62 %)	226 (74.34 %)	78 (25.66 %)	0.038
Impaired graft function				0.574
Good	664 (95.27 %)	521 (78.46 %)	143 (21.54 %)	
Impaired or Failure	33 (4.73 %)	24 (72.73 %)	9 (27.27 %)	

Supplementary Table 3: Comparison of patients with positive and negative antibody responses – Test super set

	Total N=198(%)	Positive antibody response N=157 (%)	Negative antibody response N=41 (%)	<i>p</i>
Demographic data				
Age (mean±SD) (years)	57.70±14.53	57.25±15.01	59.44±12.56	0.344
Age group				0.837
< 39 y	24 (12.12 %)	20 (82.35 %)	4 (17.65 %)	
40-49 y	21 (10.61 %)	18 (83.33 %)	3 (16.67 %)	
50-59 y	47 (23.74 %)	35 (74.47%)	12 (25.53 %)	
60-69 y	69 (34.85 %)	56 (81.16 %)	13 (18.84 %)	
>= 70 y	40 (20.20 %)	31 (77.50 %)	9 (22.50 %)	
Sex				0.590
Male	142 (71.72 %)	113 (79.58 %)	29 (20.42 %)	
Female	54 (28.28 %)	43 (79.63 %)	11 (20.37 %)	
Comorbidities				0.189
Yes	125 (63.13 %)	95 (76.00 %)	30 (24.00 %)	
No	73 (37.87 %)	62 (84.93 %)	11 (15.07 %)	
Type of graft³				
Kidney	63 (31.82 %)	44 (76.04 %)	19 (23.96 %)	0.040
Heart	69 (34.85 %)	50 (72.46 %)	19 (27.54 %)	0.121
Liver	66 (33.33 %)	63 (95.45 %)	3 (4.55 %)	< 0.001
Lung	0	0	0	0.713
Type of vaccine⁴				
BNT162b2 (Pfizer)	189 (47.11 %)	150 (79.37 %)	39 (20.63 %)	
mRNA-1273 (Moderna)	0	0	0	
Time from transplant to vaccination				0.364
Less than 1 year	14	9	5	

3 Multiple grafts are possible.

4 Only third dose vaccines.

	(0.71 %)	(64.28 %)	(35.72 %)	
1 to 3 years	37 (18.69 %)	26 (70.27 %)	9 (29.73 %)	
More than 3 years	149 (75.25 %)	122 (81.88 %)	27 (18.12 %)	
Induction regimen in the last 6 months				
No	198 (100 %)	157 (79.29 %)	41 (20.71 %)	
Any	0 (0 %)	0 (0.00 %)	0 (0.00 %)	
Immunosuppressive drugs at the time of vaccination				
Calcineurin inhibitors	185 (93.43 %)	146 (76.27 %)	39 (23.73 %)	0.431
Tacrolimus	105 (56.76 %)	86 (81.90 %)	19 (18.10 %)	0.431
Cyclosporine	80 (43.24 %)	60 (75.00 %)	20 (25.00 %)	0.294
Anti-metabolites	115 (58.08 %)	81 (69.05 %)	34 (30.95 %)	<0.001
Mycophenolate mofetil	113 (98.26 %)	79 (69.91 %)	34 (30.09 %)	< 0.001
Azathioprine	2 (1.74 %)	2 (100.00 %)	0 (0.00 %)	
mTOR	47 (23.74 %)	43 (83.81 %)	4 (16.19 %)	0.084
Everolimus	41 (87.23 %)	37 (90.24 %)	4 (9.76 %)	0.084
Sirolimus	6 (12.77 %)	6 (100.00 %)	0 (0.00 %)	
Steroids	59 (29.80 %)	39 (66.10 %)	20 (33.90 %)	0.005
Impaired graft function				0.880
Good	196 (98.99 %)	156 (79.59 %)	40 (20.41 %)	
Impaired or Failure	2 (1.01 %)	1 (50.00 %)	1 (50.00 %)	

Supplementary Table 4: Type and number of SOT recipients enrolled by each center

	Overall SOT enrolled ⁵ (N)	Kidney N = 886 (% per organ) [% per centre]	Liver N = 350 (% per organ) [% per centre]	Heart N = 340 (% per organ) [% per centre]	Lung N = 56 (% per organ) [% per centre]
Bologna	633	279 (31.49 %) [44.08 %]	179 (51.14 %) [28.27 %]	146 (42.94 %) [23.06 %]	36 (64.29 %) [5.69 %]
Padova	338	91 (10.27 %) [26.92 %]	120 (34.29 %) [35.50 %]	111 (32.65 %) [32.84 %]	17 (30.36 %) [5.03 %]
Vicenza	249	247 (27.88 %) [99.20 %]	3 (0.86 %) [1.20 %]	2 (0.59 %) [0.80 %]	2 (3.57 %) [0.80 %]
Verona	203	80 (9.03 %) [39.41 %]	44 (12.57 %) [21.67 %]	81 (23.82 %) [39.90 %]	0 (0.00 %) [0.00 %]
Treviso	169	167 (18.85 %) [98.82 %]	3 (0.86 %) [1.78 %]	0 (0.00 %) [0.00 %]	0 (0.00 %) [0.00 %]
Seville	23	22 (2.48 %) [95.65 %]	1 (0.29 %) [4.35 %]	0 (0.00 %) [0.00 %]	1 (1.79 %) [4.35 %]

Individuals can have multiple transplants such that numbers do not add up to the overall SOT enrolled column.

Supplementary Table 5: Type of COVID-19 vaccine received at each dose

	I dose	II dose	III dose
BNT162b2	1396	1374	633
mRNA-1273	185	191	471
ChAdOx1	3	8	3

Supplemental Table 6: Estimates of ordinal logistic regression

	Parameter	SE	95% CI	Pr(> t)
Age	-0.0274	0.0059	[-0.0390, -0.0158]	<0.01***
Type of transplant				
Kidney	-1.5949	0.2798	[-2.1432, -1.0465]	<0.01***
Heart	-1.7190	0.2914	[-2.2901, -1.1479]	<0.01***
Lung	-2.2476	0.5297	[-3.2859, -1.2094]	<0.01***
Time from transplant to 3rd vaccination				
More than 3 years	0.6183	0.4594	[-0.2821, 1.5186]	0.18
1 to 3 years	-0.1284	0.5120	[-1.1319, 0.8751]	0.80
Immunosuppressive drugs at the time of vaccination				
Calcineurin inhibitors	-0.1622	0.2092	[-0.5722, 0.2478]	0.44
Anti-metabolites	-1.0990	0.2052	[-1.5012, -0.6968]	<0.01***
mTOR	-0.2828	0.2996	[-0.8699, 0.3044]	0.35
Steroids	-0.0393	0.1993	[-0.4300, 0.3513]	0.84
Vaccines				
1st Pfizer	-0.5251	0.5321	[-1.5680, 0.5179]	0.32
2nd Pfizer	0.2457	0.4997	[-0.7337, 1.2252]	0.62
3rd Pfizer	-0.1163	0.2736	[-0.6526, 0.4199]	0.67
Center				
Padova	0.3517	0.3171	[-0.2698, 0.9731]	0.27
Treviso	0.5092	0.3659	[-0.2080, 1.2265]	0.16
Verona	-1.0108	0.2654	[-1.5309, -0.4906]	<0.01***
Vicenza	-0.2696	0.3827	[-1.0197, 0.4805]	0.48
Graft failure	0.0132	0.3592	[-0.6908, 0.7173]	0.97
Intercepts				
None Inconclusive	-5.2032	0.6940	[-6.5634, -3.8429]	<0.01***
Inconclusive Positive-Low	-4.7511	0.6904	[-5.0025, -4.5000]	<0.01***
Positive-Low Positive-Mild	-4.3521	0.6878	[-4.5945, -4.1100]	<0.01***
Positive-Mild High	-3.9099	0.6850	[-4.1243, -3.6954]	<0.01***
AIC			1987.02	
Residual Deviance			1943.02	

*** significant at the 99% confidence level

** significant at the 95% confidence level

* significant at the 90% confidence level

References

1. Gatti M, Rinaldi M, Bussini L, Bonazzetti C, Pascale R, Pasquini Z, et al. Clinical outcome in solid organ transplant recipients affected by COVID-19 compared to general population: a systematic review and meta-analysis. *Clin Microbiol Infect* 2022;28:1057e65. <https://doi.org/10.1016/j.cmi.2022.02.039>.
2. Bartelt L, van Duin D. An overview of COVID-19 in solid organ transplantation. *Clin Microbiol Infect* 2022;28:779e84. <https://doi.org/10.1016/j.cmi.2022.02.005>. 1084.e7 M. Giannella et al. / *Clinical Microbiology and Infection* 29 (2023) 1084.e1e1084.e7
3. Giannella M, Pierrotti LC, Helantera I, Manuel O. SARS-CoV-2 vaccination in solid-organ transplant recipients: what the clinician needs to know. *Transpl Int* 2021;34:1776e88. <https://doi.org/10.1111/tri.14029>.
4. Lee ARYB, Wong SY, Chai LYA, Lee SC, Lee MX, Muthiah MD, et al. Efficacy of covid-19 vaccines in immunocompromised patients: systematic review and meta-analysis. *BMJ* 2022;376:e068632. <https://doi.org/10.1136/bmj-2021-068632>.
5. Kwon JH, Tenforde MW, Gaglani M, Talbot HK, Ginde AA, McNeal T, et al. mRNA vaccine effectiveness against coronavirus disease 2019 hospitalization among solid organ transplant recipients. *J Infect Dis* 2022;226:797e807. <https://doi.org/10.1093/infdis/jiac118>.
6. Hippisley-Cox J, Coupland CA, Mehta N, Keogh RH, Diaz-Ordaz K, Khunti K, et al. Risk prediction of COVID-19 related death and hospital admission in adults after COVID-19 vaccination: national prospective cohort study. *BMJ* 2021;374:n2244. <https://doi.org/10.1136/bmj.n2244>.
7. Karaba AH, Zhu X, Liang T, Wang KH, Rittenhouse AG, Akinde O, et al. A third dose of SARS-CoV-2 vaccine increases neutralizing antibodies against variants of concern in solid organ transplant recipients. *Am J Transplant* 2022;22: 1253e60. <https://doi.org/10.1111/ajt.16933>.
8. Karaba AH, Johnston TS, Aytenfisu TY, Akinde O, Eby Y, Ruff JE, et al. A fourth dose of COVID-19 vaccine does not induce neutralization of the omicron variant among solid organ transplant recipients with suboptimal vaccine response. *Transplantation* 2022;106:1440e4. <https://doi.org/10.1097/TP.0000000000004140>.
9. Mitchell J, Alejo JL, Chiang TPY, Kim J, Chang A, Abedon AT, et al. Antibody response to a fourth dose of SARS-CoV-2 vaccine in solid organ transplant recipients: an update. *Transplantation* 2022;106:e338e40. <https://doi.org/10.1097/TP.0000000000004137>.
10. Abedon AT, Teles MS, Alejo JL, Kim JD, Mitchell J, Chiang TPY, et al. Improved antibody response after a fifth dose of a SARS-CoV-2 vaccine in solid organ transplant recipients: a

case series. Transplantation 2022;106:e262e3.
<https://doi.org/10.1097/TP.0000000000004092>.

11. Yahav D, Rozen-Zvi B, Mashraki T, Atamna A, Ben-Zvi H, Bar-Haim E, et al. Immunosuppression reduction when administering a booster dose of the BNT162b2 mRNA SARS-CoV-2 vaccine in kidney transplant recipients without adequate humoral response following two vaccine doses: protocol for a randomised controlled trial (BECAME study). *BMJ Open* 2021;11:e055611. <https://doi.org/10.1136/bmjopen-2021-055611>.
12. Dhand A, Razonable RR. COVID-19 and solid organ transplantation: role of anti-SARS-CoV-2 monoclonal antibodies. *Curr Transplant Rep* 2022;9:26e34. <https://doi.org/10.1007/s40472-022-00357-2>.
13. Werbel WA, Segev DL. SARS-CoV-2 antibody testing for transplant recipients: a tool to personalize protection versus COVID-19. *Am J Transplant* 2022;22: 1316e20. <https://doi.org/10.1111/ajt.16993>.
14. Bonazzetti C, Tazza B, Gibertoni D, Pasquini Z, Caroccia N, Fani F, et al. Relationship between immune response to SARS-CoV2 vaccines and development of breakthrough infection in solid organ transplant recipients: the CONTRAST cohort. *Clin Infect Dis* 2023:ciad016. <https://doi.org/10.1093/cid/ciad016>.
15. Alejo JL, Mitchell J, Chiang TP, Chang A, Abedon AT, Werbel WA, et al. Predicting a positive antibody response after 2 SARS-CoV-2 mRNA vaccines in transplant recipients: a machine learning approach with external validation. *Transplantation* 2022;106(10):e452e60. <https://doi.org/10.1097/TP.0000000000004259>.
16. Harris PA, Taylor R, Minor BL, Elliott V, Fernandez M, O'Neal L, et al. The REDCap consortium: building an international community of software platform partners. *J Biomed Inform* 2019;95:103208. <https://doi.org/10.1016/j.jbi.2019.103208>.
17. Giannella M, Righi E, Pascale R, Rinaldi M, Caroccia N, Gamberini C, et al. Evaluation of the kinetics of antibody response to COVID-19 vaccine in solid organ transplant recipients: the prospective multicenter ORCHESTRA cohort. *Microorganisms* 2022;10:1021. <https://doi.org/10.3390/microorganisms10051021>.
18. Kamar N, Abravanel F, Marion O, Romieu-Mourez R, Couat C, Del Bello A, et al. Assessment of 4 doses of SARS-CoV-2 messenger RNA based vaccine in recipients of a solid organ transplant. *JAMA Netw Open* 2021;4:e2136030. <https://doi.org/10.1001/jamanetworkopen.2021.36030>.
19. Caillard S, Thauinat O, Benotmane I, Masset C, Blancho G. Antibody response to a fourth messenger RNA COVID-19 vaccine Dose in kidney transplant recipients: a case series. *Ann Intern Med* 2022;175:455e6. <https://doi.org/10.7326/L21-0598>.

Chapter 5:

Host immunological responses facilitate development of SARS-CoV-2 mutations in patients receiving antibody treatments

Akshita Gupta^{1,2*}, **Angelina Konnova**^{1,2*}, Mathias Smet^{1,2*}, Matilda Berkell^{1,2*}, Alessia Savoldi³, Matteo Morra³, Vincent Van averbeke¹, Fien De Winter¹, Denise Peserico⁴, Elisa Danese⁴, An Hotterbeekx¹, Elda Righi³, mAb ORCHESTRA working group, Pasquale De Nardo³, Evelina Tacconelli³, Surbhi Malhotra-Kumar^{2#}, Samir Kumar-Singh^{1,2#†}

mAb ORCHESTRA working group: Basil Britto Xavier², Christine Lammens², Shahla Mahmoudi¹, Nour Chebly², Anna Gorska³, Chiara Zanchi³, Giulia Rosini³, Rebecca Scardellato³, Laura Rovigo³, Francesco Luca³, Lorenzo Tavernaro³, Salvatore Hermes Dall'O³, Chiara Konishi De Toffoli³, Massimo Mirandola^{3,5}, Concetta Sciammarella³, Riccardo Cecchetto⁶, Davide Gibellini⁶, Giuseppe Lippi⁴, Matteo Gelati⁴, Michela Conti³

¹Molecular Pathology Group, Cell Biology & Histology, Faculty of Medicine and Health Sciences, University of Antwerp, Antwerp, Belgium

²Laboratory of Medical Microbiology, Vaccine & Infectious Disease Institute, University of Antwerp, Antwerp, Belgium

³Division of Infectious Diseases, Department of Diagnostics and Public Health, University of Verona, Verona, Italy

⁴Section of Clinical Biochemistry, University of Verona, Verona, Italy

⁵School of Health Sciences, University of Brighton, Brighton, United Kingdom

⁶Section of Microbiology, Department of Diagnostics and Public Health, University of Verona, Verona, Italy

** Shared first authors: Angelina Konnova performed serology, sernoneutralization, and the analyses of cytokine, chemokine and growth factors, which are part of this thesis. T cell immunity was performed by Akshita Gupta (not a part of this thesis) and viral variant sequencing and viral loads were performed by Mathias Smet (also not a part of this thesis). Matilda Berkell is a post-doc, who supervised Mathias Smet along with Prof. Malhotra-Kumar.*

Shared senior authors † Correspondence: samir.kumarsingh@uantwerpen.be

Published in The Journal of Clinical Investigation

2023 Mar 15;133(6):e166032. doi: 10.1172/JCI166032.

Abstract

Background: The role of host immunity in emergence of evasive SARS-CoV-2 Spike mutations under therapeutic monoclonal antibody (mAb) pressure remains to be explored.

Methods: In a prospective, observational, monocentric ORCHESTRA cohort study, conducted between March 2021 and November 2022, mild-to-moderately ill COVID-19 patients (n=204) receiving bamlanivimab, bamlanivimab/etesevimab, casirivimab/imdevimab, or sotrovimab were longitudinally studied over 28 days for viral loads, de novo Spike mutations, mAb kinetics, seroneutralization against infecting variants of concern, and T-cell immunity. Additionally, a machine learning-based circulating immune-related (CIB) biomarker profile predictive of evasive Spike mutations was constructed and confirmed in an independent dataset (n=19) that included patients receiving sotrovimab or tixagevimab/cilgavimab.

Results: Patients treated with various mAbs developed evasive Spike mutations with remarkable speed and high specificity to the targeted mAb-binding sites. Immunocompromised patients receiving mAb therapy not only continued to display significantly higher viral loads, but also showed higher likelihood of developing de novo Spike mutations. Development of escape mutants also strongly correlated with neutralizing capacity of the therapeutic mAbs and T-cell immunity, suggesting immune pressure as an important driver of escape mutations. Lastly, we showed that an anti-inflammatory and healing-promoting host milieu facilitates Spike mutations, where 4 CIBs identified patients at high risk of developing escape mutations against therapeutic mAbs with high accuracy.

Conclusions: Our data demonstrate that host-driven immune and non-immune responses are essential for development of mutant SARS-CoV-2. These data also support point-of-care decision-making in reducing the risk of mAb treatment failure and improving mitigation strategies for possible dissemination of escape SARS-CoV-2 mutants.

Introduction

The coronavirus replication machinery encodes proofreading functions resulting in fewer errors compared to other RNA viruses, however, multiple SARS-CoV-2 variants of concern (VOCs) have emerged throughout the pandemic carrying VOC-defining mutations. For example, Alpha (B.1.1.7), Beta (B.1.351), Gamma (P.1), Delta, Zeta, Eta, Theta, Iota, and Omicron variants have been shown to carry distinct sets of mutations, which evade existing natural neutralizing antibody responses (1-4).

SARS-CoV-2 mutation rates are higher in immunocompromised or severely ill patients who show prolonged SARS-CoV-2 infections or carriage (5-12). Immunocompromised individuals are also unable to develop sufficient antibody titers after administration of COVID-19 vaccines. To tackle this, synthetic neutralizing monoclonal antibodies to SARS-CoV-2 (mAbs) targeting the Spike protein have been developed that demonstrate clinical benefit for mild-to-moderately ill COVID-19 patients at high risk of developing severe disease (13-20). For example, the first widely available mAb, bamlanivimab, that targets an epitope on the receptor-binding domain (RBD), led to a reduced rate of hospitalization, ICU admission, and mortality compared with usual care (21). The addition of etesevimab to bamlanivimab resulted in improved clinical outcomes due to overlapping binding epitopes within Spike RBD, concomitant to the emergence of SARS-CoV-2 VOCs, mainly B.1.351 and P.1 (22). The success of combination mAb therapy and decreasing efficacies to emerging variants led to use of casirivimab/imdevimab, with distinct binding sites in Spike RBD, in at-risk populations, resulting in decreased rates of hospitalization (23). As the pandemic evolved and new VOCs were identified, sotrovimab was developed with a modified Fc domain along with an increased half-life (13, 14). Recently, an intramuscularly administered combination of non-competing antibodies tixagevimab and cilgavimab, again with distinct binding sites, has also been introduced in patient care (16). These modifications target highly conserved Spike epitopes, causing conformational transitions necessary for association with the ACE2 receptor (15, 16), resulting in reduced risk of disease progression and death (13, 24).

Several reports have also identified *de novo* mutations under therapeutic mAb pressure, including E484Q/K and Q493K/R under bamlanivimab/etesevimab pressure (25-27) and P337R/S, E340D/K/V, and G446S/V under casirivimab/imdevimab and/or sotrovimab pressure (28-31). However, despite the widespread use of mAbs, these studies are rather few and were conducted in limited patient numbers. Moreover, the role of host immune pressure in selection of mAb-driven *de novo* SARS-CoV-2 Spike RBD mutations has not been explored so far.

Here, we characterize the development of SARS-CoV-2 Spike RBD mutations in patients treated with bamlanivimab, bamlanivimab/etesevimab, casirivimab/imdevimab, or sotrovimab in relation to their neutralization potential against SARS-CoV-2 VOCs. We focus on natural humoral and cellular host immunity, including responses mediated by cytokines and other correlates of adaptive evolution.

Results

Immunocompromised COVID-19 patients receiving early mAb therapy continue to display significantly higher viral loads compared to non-immunocompromised patients (*not part of this thesis*)

The H2020-funded ORCHESTRA project (Connecting European Cohorts to Increase Common and Effective Response to SARS-CoV-2 Pandemic) includes work package 2 (WP2), prospectively enrolling high-risk patients receiving early treatment for symptomatic COVID-19. Clinical efficacies of bamlanivimab, bamlanivimab/etesevimab, casirivimab/imdevimab, or sotrovimab in 740 mild-to-moderate non-hospitalized COVID-19 patients have been described (19, 20) (for eligibility criteria, see **Supplemental Table 1**). From this WP2 cohort, patients were prospectively invited to a sub-study assessing immunological and virological responses to mAbs studied by WP6 of the ORCHESTRA project.

Overall, 204 patients were enrolled receiving bamlanivimab (n = 45), bamlanivimab/etesevimab (n = 108), casirivimab/imdevimab (n = 17), or sotrovimab (n = 34) (**Table 1**). Patients were assessed and sampled before mAb infusion (D0) and after treatment at day (D)2, D7, and in 98 patients at D28. The maximum study length of 28 days was chosen as the mean duration of SARS-CoV-2 RNA shedding from the upper respiratory tract has been estimated as not more than 17 days (32, 33). Patient groups did not differ significantly in WHO progressive severity score (34). The median age of the total study cohort was 64 years (inter-quartile range (IQR): 62-74) and 53.9% of the enrolled patients were males. During the 28-day follow-up, 28 patients (28/204; 13.7%) were hospitalized for severe COVID-19 (bamlanivimab: 8/45 (17.7%); bamlanivimab/etesevimab: 20/108 (18.5%)) and 3/204 patients died (1.5%). For patient characteristics, see Table 1.

SARS-CoV-2 whole-genome sequencing revealed variants belonging to five distinct clades, of which the most frequent were 20I/Alpha (n = 161), 21K/Omicron (n = 27), and 21L/Omicron (n = 7). Patients receiving bamlanivimab, bamlanivimab/etesevimab, or casirivimab/imdevimab mostly carried Alpha sub-variants (B.1.1.7, 146/170; Q.4, 15/170) at baseline except for 3 patients who carried 20A/B.1.462 or 20D/C.36.3 (Table 1). All patients treated with sotrovimab carried Omicron sub-variants, the most common being 21K/BA.1 with the S:R346K substitution (n = 14; BA.1.1, BA.1.1.1), followed by 21K/BA.1 (n = 13; BA.1, BA.1.17, BA.1.17.2), and 21L/BA.2 (n = 7; BA.2, BA.2.9).

Differences in viral loads in patients undergoing different mAb treatments were longitudinally studied by comparing cyclic threshold (Ct) values for open reading-frame (ORF1)ab-, N protein-, and S protein-encoding genes by RT-qPCR. A gradual, significant increase in Ct values was observed for all gene targets indicating a decreasing viral load (**Figure 1A, Supplemental Table 2 and 3**). Due to the S:Δ69/70 deletion in Alpha (B.1.1.7, Q.4) and BA.1(+R346K)/Omicron sub-variants, most samples were qPCR-negative for the S gene. Compared to patients infected with Alpha sub-variants, patients carrying Omicron sub-variants showed significantly higher viral loads before mAb infusion (D0) that stayed significantly higher till 48h after mAb infusion (D2 timepoint; **Figure 1B**).

Table 1. Patient characteristics of enrolled patients treated with bamlanivimab, bamlanivimab/etesevimab, casirivimab/imdevimab, or sotrovimab in the study. Statistical assessments of categorical and continuous variables were assessed across monoclonal antibody therapy groups using chi-square test of independence and analysis of variance (ANOVA), respectively. IQR: inter quartile range. mo: months. NS: non-significant.

Patient characteristics	Bamlanivimab (N=45)	Bamlanivimab/ etesevimab (N=108)	Casirivimab/ imdevimab (N=17)	Sotrovimab (N=34)	P-value
Male (%)	30 (66.7)	59 (54.6)	9 (52.9)	12 (35.2)	NS
Age (median, IQR)	63 (58-78)	65 (58-75)	53 (47-63)	69 (61-75)	0.03
< 65 years	58 (52-61)	58 (51-62)	52 (47-62)	58 (50-63)	NS
≥ 65 years	78 (72-83)	75 (70-78)	76 (74-77)	75 (70-79)	NS
BMI (median, IQR)	28 (24-31)	29 (25-35)	29 (26-36)	28 (24-30)	NS
Hospital admission (%)	8 (17.8)	20 (18.5)	0 (0.0)	0 (0.0)	0.012
Death (%)	2 (4.4)	1 (0.9)	0 (0.0)	0 (0.0)	NS
At enrolment WHO progression severity score (median, IQR)	Mild/2 (2-2)	Mild/2 (2-2)	Mild/2 (2-2)	Mild/3 (3-3)	NS
Worst WHO severity score during disease (median, IQR)	6 (4.75-7)	4 (4-5.25)	2 (2-2)	3 (3-3)	< 0.001
Days from symptoms onset to mAb infusion (median, IQR)	6 (4-7)	5 (4-6)	6 (5-7)	3 (2-4)	< 0.001
sO ₂ % (median, IQR)	95 (94-97)	97 (95-98)	97 (97-98)	97 (96-98)	< 0.001
Anti-SARS-CoV-2 vaccination (>2 weeks post-dose, ≥ 2 doses, %)	0 (0.0)	0 (0.0)	1 (5.8)	25 (73.5)	< 0.001
Ongoing COVID-related therapy					
Prednisone (%)	5 (11.1)	19 (17.6)	3 (17.6)	0 (0.0)	< 0.001
Azithromycin (%)	3 (6.7)	10 (9.3)	1 (5.9)	0 (0.0)	< 0.001
Amoxicillin/clavulanate (%)	1 (2.2)	6 (5.6)	2 (11.8)	0 (0.0)	NS
Immunocompromising condition (%)	3 (6.7)	12 (11.1)	2 (11.8)	17 (50.0)	< 0.001

Solid organ cancer (with ongoing therapy/ongoing stopped < 6 mo) (%)	0 (0.0)	0 (0.0)	0 (0.0)	4 (11.8)	< 0.001
Hematologic cancer (with ongoing CHT/ongoing stopped < 6 mo) (%)	0 (0.0)	1 (0.9)	0 (0.0)	8 (23.5)	< 0.001
Solid organ transplant recipients (%)	0 (0.0)	0 (0.0)	1 (5.9)	5 (14.7)	< 0.001
Immunological diseases requiring immunosuppressive agents (%)	3 (6.7)	11 (10.2)	1 (5.9)	5 (14.7)	NS
Other comorbidities					
Diabetes (with or without damage) (%)	8 (17.8)	20 (18.5)	2 (11.8)	5 (14.7)	NS
Cardiovascular disease (ischemic/arrhythmia/hypertension) (%)	12 (26.7)	45 (41.7)	6 (35.3)	14 (41.2)	0.012
Chronic renal failure (with or without need of dialysis) (%)	2 (4.4)	5 (4.6)	1 (5.9)	3 (8.8)	NS
Chronic pulmonary diseases (%)	10 (22.2)	18 (16.7)	4 (23.5)	7 (20.6)	NS
Any neurological/vascular disease (%)	3 (6.7)	9 (8.3)	0 (0.0)	1 (2.9)	NS
Symptoms					
Anosmia (%)	3 (6.7)	2 (1.9)	3 (17.6)	0 (0.0)	0.007
Ageusia (%)	5 (11.1)	7 (6.5)	2 (11.8)	0 (0.0)	NS
Cough (%)	33 (73.3)	59 (54.6)	6 (35.3)	14 (41.2)	0.001
Fever (%)	33 (73.3)	78 (72.2)	12 (70.6)	16 (47.0)	0.039
Sore throat (%)	5 (11.1)	18 (16.7)	4 (23.5)	9 (26.5)	NS
Asthenia (%)	28 (62.2)	41 (38.0)	6 (35.3)	11 (32.4)	0.020
Headache (%)	9 (20.0)	19 (17.6)	3 (17.6)	7 (20.6)	NS
GI symptoms (%)	9 (20.0)	15 (13.9)	4 (23.5)	1 (2.9)	NS
Dyspnea (%)	1 (2.2)	5 (4.6)	0 (0.0)	1 (2.9)	NS
Myalgia (%)	14 (31.1)	36 (33.3)	9 (52.9)	6 (17.6)	NS
Number of symptoms per patient (median, IQR)	3 (2-4)	2 (1-3)	2 (2-4)	2 (1-3)	0.001
Viral variant					
B.1.1.7/Alpha (%)	40 (88.8)	91 (84.3)	15 (88.2)	0 (0.0)	< 0.001
Q.4/Alpha (%)	3 (6.6)	12 (11.1)	0 (0.0)	0 (0.0)	
BA.1/Omicron (%)	0 (0.0)	0 (0.0)	0 (0.0)	13 (38.2)	
BA.1+R346K/Omicron (%)	0 (0.0)	0 (0.0)	0 (0.0)	14 (41.2)	
BA.2/Omicron (%)	0 (0.0)	0 (0.0)	0 (0.0)	7 (20.6)	
B.1.462 (%)	1 (2.2)	1 (0.9)	0 (0.0)	0 (0.0)	
C.36.3 (%)	0 (0.0)	0 (0.0)	1 (5.9)	0 (0.0)	

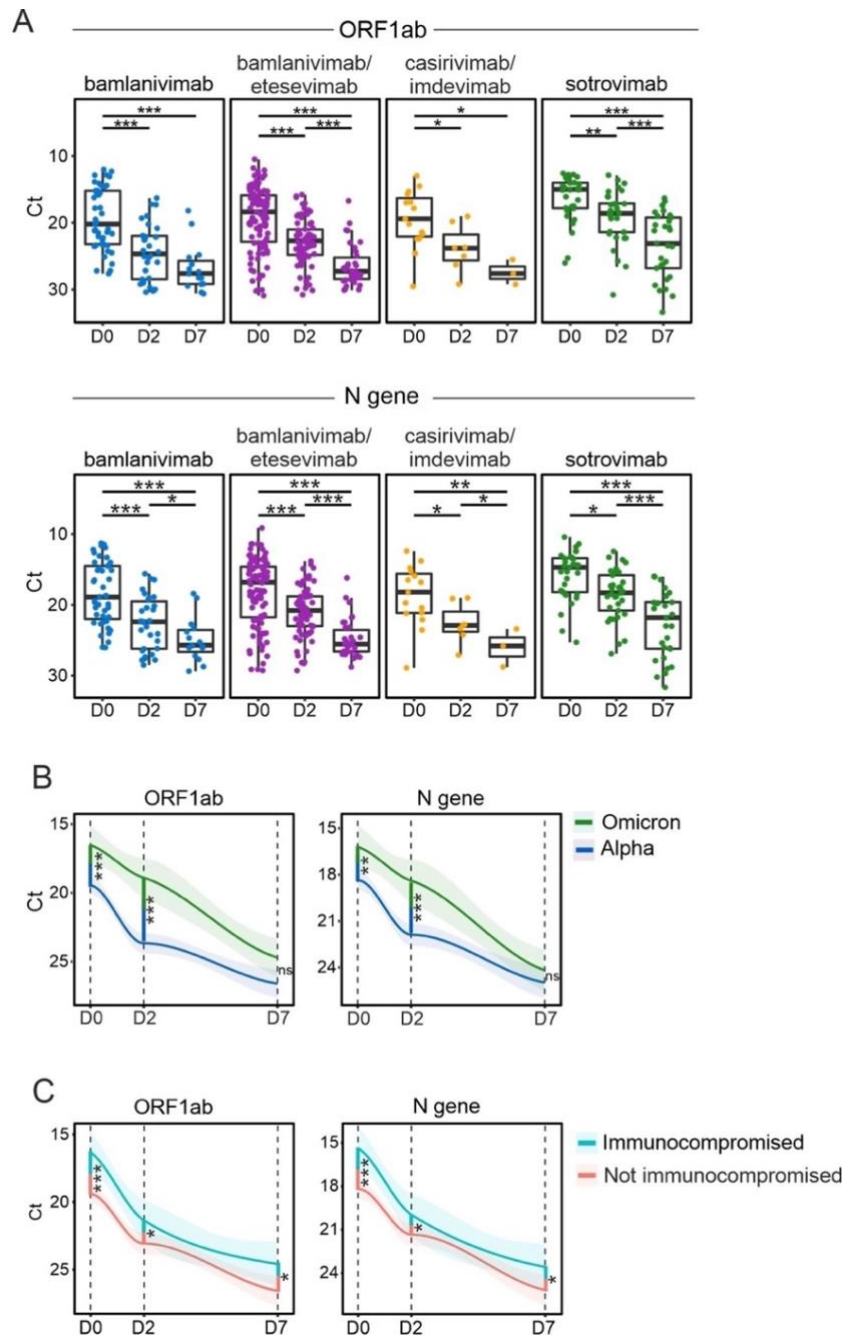


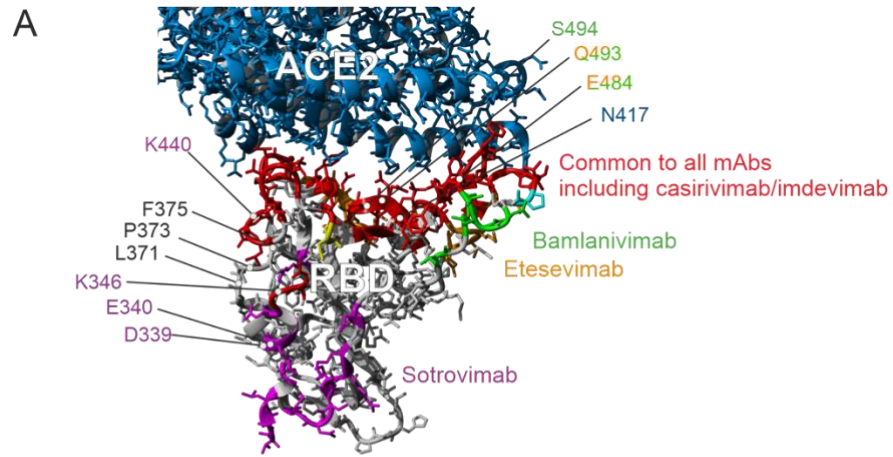
Figure 1. Immunocompromised and Omicron-infected COVID-19 patients display higher viral loads after mAb administration. Quantitative real-time reverse transcription (RT-q)PCR detection of SARS-CoV-2 was performed on nasopharyngeal swab samples collected at D0, D2, and D7 from patients treated with different therapeutic mAbs. **(A)** A steady increase in Cyclic threshold (Ct) values was observed over 7 days for all mAb-treated groups. Box plots indicate median (middle line), 25th, 75th percentile (box), and 5th and 95th percentile (whiskers). All data points, including outliers, are displayed. **(B)** Overall, patients carrying Omicron (BA.1, BA1+R346K, or BA.2) displayed higher viral loads than patients carrying Alpha sub-variants

(B.1.1.7 or Q4). (C) Immunocompromised patients carried higher viral loads, irrespective of the infecting SARS-CoV-2 variant and mAb treatment. Line graphs in B and C represent smoothed conditional means with shaded areas displaying 95% confidence intervals for all measured timepoints. Cross-sectional and longitudinal statistical comparisons were performed using Mann-Whitney followed by Bonferroni post-hoc correction. *: $p < 0.05$. **: $p < 0.01$. ***: $p < 0.001$. ns: non-significant. mAb: monoclonal antibody. D0: sample collected prior to mAb infusion. D2: 2 ± 1 days after mAb infusion. D7: 7 ± 2 days after mAb infusion. A limited number of NPS samples were collected at day 28 ($n = 9$) across all 4 mAb therapy groups and were therefore excluded from this analysis. See Supplemental Table 2 and 3 for details on Ct values at each timepoint. (Results presented in this Figure are not a part of this thesis, but are necessary to understand the relevance of further work that is part of my thesis)

As several studies have shown that immunocompromised individuals show a prolonged carriage of SARS-CoV-2 (5, 7), we investigated whether these patients receiving mAb therapy also carried higher viral loads. Immunocompromised status was defined clinically on the basis of patients on active immunosuppressive treatment for cancer, organ transplants, and/or immunological diseases, as described (19, 20) (Table 1, Supplemental Table 1). We show that immunocompromised patients have higher viral loads at the time of enrolment irrespective of the mAb treatment (ΔCt 3.03 and 2.76 for ORF1ab and N, respectively; $p \leq 0.001$). Remarkably, significantly higher viral loads persisted in immunocompromised patients at both D2 and D7 timepoints (ΔCt at D7, 1.89 and 1.79 for ORF1ab and N, respectively; $p \leq 0.03$) (Figure 1C). These data suggest that prolonged viral shedding occurs in immunocompromised COVID-19 patients with mild-to-moderate disease despite receiving mAb therapies.

Immunocompromised patients display higher rates of SARS-CoV-2 Spike RBD mutations (*not part of this thesis*)

To study the emergence of amino acid-substituting SARS-CoV-2 mutants in response to mAb treatment, 204 patients were studied longitudinally for mutations occurring at D2 or D7, compared to pre-therapy (D0) timepoint. Overall, 35 patients (17.2%) developed non-synonymous mutations at 43 unique positions in the SARS-CoV-2 genome, which resulted in 48 unique amino acid substitutions. Seventeen patients developed mutations across 26 unique positions randomly distributed across the SARS-CoV-2 genome (ORFs 1ab, 3a, and 7ab, or the M and N genes), and each position was only found to be mutated in one patient each (**Supplemental Figure 1, Supplemental Table 4**). The remaining 22/48 non-synonymous mutations occurred within the S gene in 22 patients overall. In total, 16 unique amino acid substitutions occurred in Spike RBD (residues 319-541) in a total of 17 patients. All mutations identified in patients receiving bamlanivimab with or without etesevimab have been previously reported whereas most emerging Spike RBD mutants in the sotrovimab-treated group were novel and occurred in clusters (see later). As (RT-q)PCR errors have been suggested to be amplified to high allele frequencies resulting in sequencing errors, especially under low viral load conditions (8, 11), all non-synonymous Spike RBD mutations in sotrovimab patients were re-confirmed by either Sanger or repeated NextSeq sequencing on independently extracted RNA.



B

	bamlanivimab					bamlani- etesevimab			sotrovimab								
	Pt 1	Pt 2	Pt 3	Pt 4	Pt 5	Pt 6	Pt 7	Pt 8	Pt 9	Pt 10	Pt 11	Pt 12	Pt 13	Pt 14	Pt 15	Pt 16	Pt 17
D339												G					G
E340									K			D	D	K	V	D	
K346									R	R							
L371									S	S							
P373									S	S							S
F375									S	S							S
N417																	K
K440																	N
E484	A			K	K			D									
Q493		R						K	R								
S494			P														

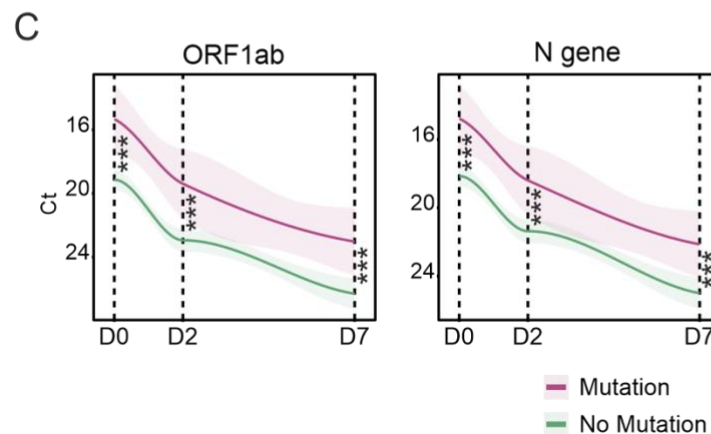


Figure 2. De novo SARS-CoV-2 Spike RBD mutations evolving under mAb pressure. (A) Schematic quaternary structure of the SARS-CoV-2 Spike RBD protein when bound to the human (h)ACE2 receptor (PDB: 6M0J). Key RBD-binding sites of bamlanivimab, etesevimab, and sotrovimab are highlighted in the protein structure with corresponding colours. Binding sites common to all mAbs, including casirivimab and imdevimab, are indicated in red whereas hACE2 is highlighted in blue. **(B)** SARS-CoV-2 genomes longitudinally isolated from patients receiving mAb therapy were screened for the emergence of de novo mutations resulting in amino acid substitutions in the Spike RBD region. Most commonly, escape mutants occurred in residues

harbored within the respective mAb binding site. Pt: patient. **(C)** Patients developing Spike RBD mutations were found to harbor significantly higher viral loads at all timepoints. Cross-sectional statistical comparisons were performed using Mann-Whitney test. Lines represent smoothed conditional means and shaded areas display 95% confidence intervals for all measured timepoints. ***: $p < 0.005$. For more details on non-synonymous de novo changes and sample numbers, see **Supplemental Figure 1 and 7**, and **Supplemental Table 4**. (Results presented in this Figure are not a part of this thesis, but are necessary to understand the relevance of further work that is part of my thesis)

A remarkable mutational homogeneity was identified wherein the same mutations developed independently in SARS-CoV-2 Spike RBD in different patients under mAb pressure. For instance, all eight patients developing Spike RBD mutations receiving bamlanivimab or bamlanivimab/etesevimab involved only 3 residues (E484, Q493, S494, **Figure 2, A and B; Supplemental Figure 2**). Amongst these, Q493R/K was present in 3 patients and involved a residue common to both bamlanivimab and etesevimab binding sites suggesting a potential loss-of-function of binding of both mAbs to the mutated SARS-CoV-2 Spike protein. Similarly, mutations identified in sotrovimab-treated patients were present in either ACE2 (N417) or sotrovimab binding sites (D339, E340, R346, K440), except for three mutations involving residues L371, P373, and F375 identified in three patients (Figure 2B). These mutations involved alternate residues of SARS-CoV-2 Spike RBD and were notably substituted to serine, consistent with the Wuhan protein sequence. Two additional reversions (D339G and K346R) were identified in the sotrovimab-treated group, the latter mutation reversing the BA.1.1-defining R346K substitution (35).

Notably, a highly diverse S gene mutation rate was also observed under the different mAb treatment:variant combinations. For example, 9/34 (26.5%) patients carrying Omicron and receiving sotrovimab developed Spike RBD mutations, which was significantly higher compared to patients receiving other mAb treatments and carrying Alpha or other variants, i.e., 5/45 (11.1%) patients receiving bamlanivimab, 3/108 (2.8%) receiving bamlanivimab/etesevimab, and none (0/17) in the casirivimab/imdevimab group (Pearson $\chi^2 = 21.005$; $n = 204$; $df = 3$; $p < 0.001$).

Interestingly, patients with de novo Spike RBD mutations had approximately 10-fold increased burden of viral genetic material at D0 compared to patients without SARS-CoV-2 mutations across all mAb treatment groups (average ΔCt for ORF1ab and N = 3.37, range 2.9–3.8, $p \leq 0.001$), and remained elevated at both D2 and D7 timepoints ($p < 0.005$ for both time points; **Figure 2C**). These data suggest that higher viral loads predispose to development of SARS-CoV-2 mutations. As immunocompromised individuals carried higher viral loads, we further assessed whether these individuals are more likely to develop Spike RBD mutations. Out of 17 patients who developed SARS-CoV-2 Spike RBD mutations, six were immunocompromised (35.3%), while only 11 patients of 170 non-immunocompromised patients developed mutations (6.5%). Using Chi-square and odds ratio (OR) as a test and measure of association, respectively, we showed that immunocompromised individuals treated with mAbs had significant 3-fold greater odds of developing Spike RBD mutations compared to non-immunocompromised patients (Pearson $\chi^2 = 4.633$; $n = 204$; $df = 1$; $p = 0.031$; OR=3.097, 95% CI [1.060, 9.050]). Together, these data suggest that COVID-19 patients receiving mAb therapy develop Spike RBD mutations that are not only mAb-therapy- or variant-dependent, but the rate of intra-host Spike mutations are also substantially increased in patients who are immunocompromised.

Therapeutic mAb titers are not directly associated with development of Spike RBD mutations

We investigated anti-S and anti-RBD titers for different mAb treatment groups along with naturally developing anti-N titers at all timepoints. As sotrovimab was given to patients who were vaccinated (73.5%; 14 days post dose, ≥ 2 doses; $n = 25$; see Table 1), we first showed that, as expected, vaccine-related anti-S and anti-RBD titers, but not anti-N titers, were significantly elevated in the sotrovimab group at time of enrolment (D0) (**Supplemental Figure 3**). To address whether intervention with mAbs targeting SARS-CoV-2 could dampen the development of natural immunity, we studied anti-N titers that are not expected to be affected by therapeutic mAbs. A significant rise in anti-N titers was observed for all treatment groups, although the increase from pre-infusion titers (D0) to titers at D7 and D28 was smaller for the casirivimab/imdevimab and sotrovimab therapy groups compared to all others (**Figure 3A, Supplemental Table 5**). No significant difference in anti-S and anti-RBD titers was identified between patients infected with dominant circulating SARS-CoV-2 variants, including Omicron sub-variants (**Figure 3B**).

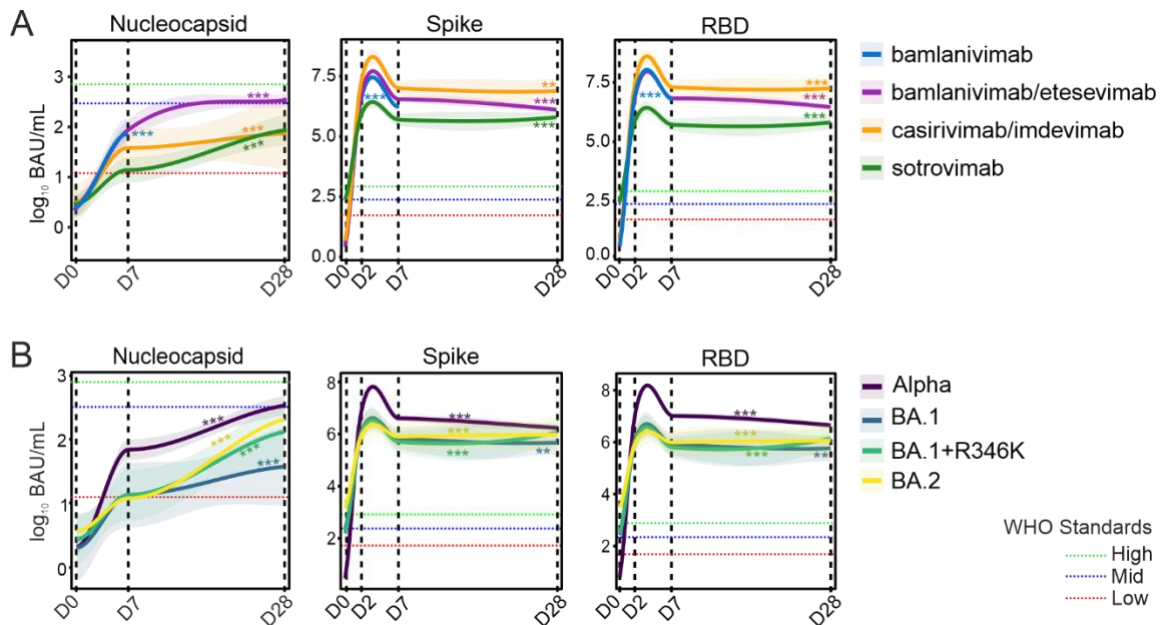


Figure 3. Temporal evolution of anti-N, anti-S, and anti-RBD serology titers in patients receiving mAb therapies. (A) Natural immunity was assessed based on anti-N titers, revealing a gradual increase through D28. High anti-S and anti-RBD titers due to therapeutic mAb administration persisted from D2 to D28 in patients in all treatment groups. (B) Similarly, high anti-S and anti-RBD titers were observed in patients receiving sotrovimab monotherapy carrying Omicron sub-variants (BA.1, BA1+R346K, or BA.2). Red, green, and blue dotted lines indicate SARS-CoV-2 WHO reference standard values for low, medium, and high antibody titers, respectively. Line graphs in A and B represent conditional means and shaded areas displaying 95% confidence intervals for all measured timepoints. Linear mixed models were utilized to investigate evolution of antibody titers over time for different mAbs with asterisks indicating significance of the slopes of the curves. **: $p < 0.01$. ***: $p < 0.001$. For more details on serology in patients with or without vaccination and sample numbers, see **Supplemental Table 5** and **Supplemental Figure 7**.

To study whether therapeutic antibodies could be linked to development of SARS-CoV-2 Spike RBD mutations, we first showed that pre-therapy (D0), anti-S or anti-RBD titers were not significantly different in Spike RBD mutation carriers ($n = 204$; anti-S, $F = 0.032$, $p = 0.859$; anti-RBD, $F = 0.140$, $p = 0.708$). Similarly, we studied whether levels of therapeutic mAbs in blood could be associated with Spike RBD mutations in our cohort. At the first post-therapy timepoint (D2), the average titers for anti-RBD and anti-S were 11.5 and 6.4 million BAU/mL, respectively. By comparison, the WHO International SARS-CoV-2 Antibody Standards for “High blood immunoglobulin” corresponds to the anti-RBD titer of 817 BAU/mL and anti-S titers of 832 BAU/mL. Both anti-S and anti-RBD titers dropped at D7 and further at D28 for the majority of the mAb treatment groups, but average anti-RBD and anti-S titers at D28 remained at 5.8 and 2.9 million BAU/mL, respectively. The bioavailability of IgGs at the mucosal barrier, where the mAb-selection pressure likely exists, is not known; however, with more than 10,000 times ‘free’ therapeutic mAb titers measured in blood than those required for effective virus neutralization, expectedly, we did not find any direct selective pressure of therapeutic mAbs in the development of SARS-CoV-2 Spike RBD mutations.

Neutralizing capacities of mAbs are (co-)drivers of development of escape mutants

We further investigated whether development of Spike RBD mutations is linked to the neutralization potential of different mAbs. Studying neutralizing capacities of the four mAb regimens in an ACE2 neutralization assay, we first showed a highly significant difference by which these mAbs neutralize five past or currently circulating SARS-CoV-2 variants (**Figure 4; Supplemental Figure 4**). Casirivimab/imdevimab appeared to have the highest neutralizing activity against most variants, including Wuhan, Alpha, and Omicron/BA.2 variants. Sotrovimab monotherapy showed best neutralization results against Omicron BA.1 (including BA.1+R346K sub-lineages), however, neutralizing activity of sotrovimab against BA.2 was lower compared to BA.1 and BA.1+R346K ($p < 0.05$), as shown previously where sotrovimab retained activity against both BA.1 and BA.1+R346K, but its activity against BA.2 dropped 27-fold (35).

Remarkably, in the sotrovimab-treated group, both BA.1 and BA.2 infections were observed allowing us to assess whether neutralizing potential of mAbs could increase the likelihood of development of Spike RBD mutations. We show that for BA.1 and BA.1+R346K groups against which sotrovimab shows good neutralizing capacity, 9/27 (33.3%) of patients developed mutations. On the other hand, none of the patients in the BA.2 group (0/7) developed Spike RBD mutations against which sotrovimab shows poor neutralization capacity, data were also statistically significant (likelihood ratio = 4.97, $n = 34$; $df = 1$, $p = 0.026$). Importantly, a higher proportion of immunocompromised patients (4/7, 57.1%) were present in the BA.2 group that did not develop mutations compared to the BA.1 group (13/27, 48.1%) (Spearman correlation, co-variance = 0.201, $p = 0.708$). These data strongly suggest that seroneutralization capacities of therapeutic mAbs are independently linked with development of SARS-CoV-2 escape mutants.

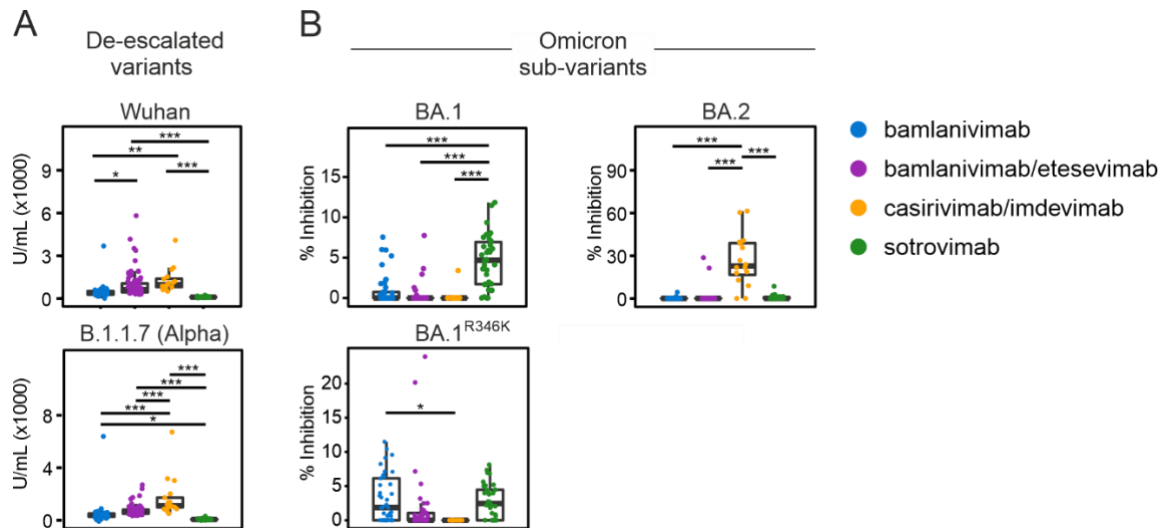


Figure 4. Anti-S neutralization capacity of bamlanivimab, bamlanivimab/etesevimab, casirivimab/imdevimab, and sotrovimab. Neutralization capacity was measured against (A) de-escalated variants and (B) Omicron sub-variants at D2. Sotrovimab monotherapy proved most effective in neutralizing BA.1. Bamlanivimab showed increased neutralizing activity against BA.1. Casirivimab/imdevimab combination therapy proved highly effective in neutralization of BA.2. Box plots indicate median (middle line), 25th, 75th percentile (box), and 5th and 95th percentile (whiskers). All data points, including outliers, are displayed. Statistical assessments were performed using pairwise t-tests with Bonferroni post-hoc correction. *: $p < 0.05$. **: $p < 0.01$. ***: $p < 0.001$. For details on tested variants of concern and sample numbers, see **Supplemental Table 6** and **Supplemental Figure 7**.

Natural adaptive T-cell immunity is associated with development of SARS-CoV-2 escape mutants (*not part of this thesis*)

Existing immunity against SARS-CoV-2 infections as a result of current or past exposure, vaccination against SARS-CoV-2, or human immune system variations could strongly influence the disease outcome in patients receiving different mAb regimens. To address the impact of mAb therapies on T helper (Th) cell immunity, lymphocytes collected at D0 and D28 were stimulated by either a SARS-CoV-2 Nucleocapsid or a complete Spike protein peptide pool (see Supplemental Methods). CD4⁺ Th cell-activation was subsequently studied by both a general marker, CD154 (CD40L), and by IFN- γ , a cytokine-associated marker of antigen-reactive Th cells.

At D0, the number of both S- and N-activated Th cells was significantly higher in the sotrovimab-treated group ($n = 25$) compared to bamlanivimab/etesevimab ($n = 42$) and casirivimab/imdevimab ($n = 5$) groups ($p < 0.01$, **Figure 5A**). While the higher number of S-activated Th cells in sotrovimab patients could be explained by vaccination, with most of the patients in this group being fully vaccinated, a concurrently higher number of N-activated Th cells in sotrovimab patients suggests a likely higher rate of prior SARS-CoV-2 exposure, as vaccination was administered to patients in this group later in the pandemic. Furthermore, over 28 days, the sotrovimab-treated group also showed a significantly higher increase in N-activated CD4⁺IFN- γ ⁺ cells compared to bamlanivimab/etesevimab and casirivimab/imdevimab groups ($p < 0.001$). These data suggest that

sotrovimab does not majorly curb development of natural immunity and fits well with the higher viral clearance observed in the sotrovimab-treated group carrying Omicron sub-variants compared to bamlanivimab/etesevimab and casirivimab/imdevimab groups carrying Alpha sub-variants (Figure 5A, Figure 1B).

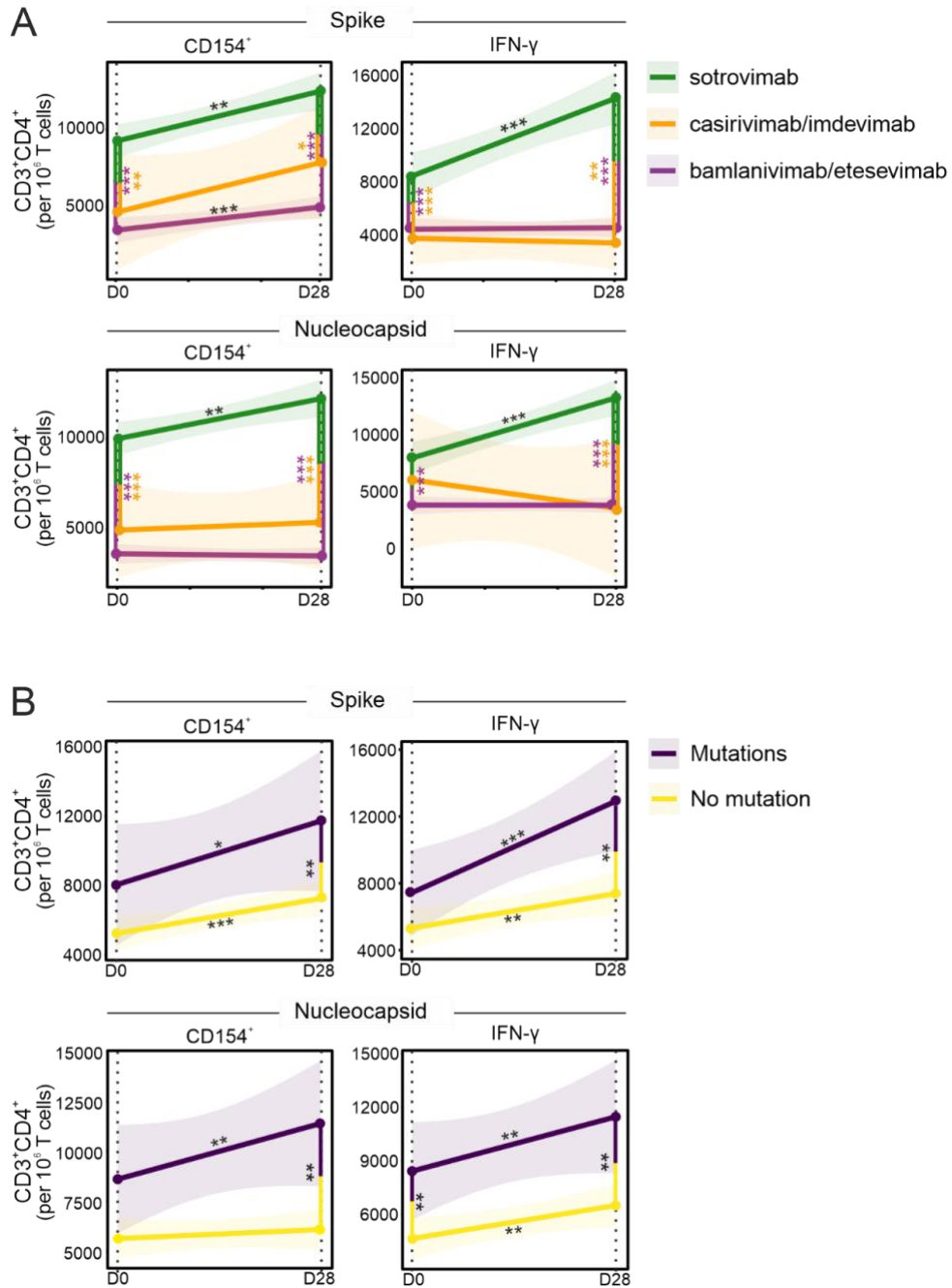


Figure 5. Longitudinal T cell responses in patients receiving mAb therapy. Evolution of IFN- γ and CD154 expression in SARS-CoV-2 Spike- and Nucleocapsid-stimulated CD4⁺ T cells in patients was studied over 28 days after receiving bamlanivimab/etesevimab, casirivimab/imdevimab, or sotrovimab. (A) Patients receiving sotrovimab therapy show a consistent significant increase in T cell expression during the first 28 days post mAb

administration. For the utilized gating strategy, refer to **Supplemental Figure 8. (B)** Patients with de novo mutations in the SARS-CoV-2 Spike RBD region show an increased T cell expression compared to those without. Linear mixed models were utilized to investigate evolution of Th cell immunity over time between the different mAb groups. Regression curves represent smoothed conditional means and shaded areas display 95% confidence intervals for all measured timepoints with asterisks on lines representing the significance of the slopes. Vertical lines with asterisks represent the significance of pairwise comparisons between patients with or without de novo mutations before mAb treatment (D0) and after 28 days of treatment (D28). *: $p < 0.05$, **: $p < 0.01$. ***: $p < 0.001$. (Results presented in this Figure are not a part of this thesis, but are necessary to understand the relevance of further work that is part of my thesis)

Addressing whether mAb-induced Spike RBD mutations were associated with Th cell immunity, we further showed that patients developing mutations had slightly higher proportions of N-activated CD4+CD154+ and CD4+IFN- γ + cells before mAb treatment, which was statistically significant for CD4+IFN- γ + cells ($p < 0.05$; **Figure 5B**). However, strikingly, patients exhibiting de novo mutations also developed stronger Th cell immunity over 28 days with significantly increased S- and N-activated CD4+CD154+ and CD4+IFN- γ + cells at 28 days ($p < 0.01$). Although whether activated CD4+ Th cells could stimulate naïve B cells to produce specific antibodies against the mutant virus, or whether pre-existing high-affinity antibodies induced by previous vaccinations in sotrovimab-treated patients bias memory B cell selection in contributing to the increased frequency of SARS-CoV-2 mutants (36, 37) is not known, our data strongly support the premise that the identified de novo mutations in the SARS-CoV-2 Spike protein are indeed escape mutations that evade therapeutic mAb neutralization, thereby facilitating a more natural progression of disease and resulting in more robust SARS-CoV-2-specific Th cell immunity.

Host immune profile as a predictor of Spike RBD escape mutants

Studies have shown that pro-inflammatory cytokines when uncontrolled and exaggerated can lead to immunopathogenesis such as cytokine release syndrome disorder; however, under homeostatic conditions they are believed to play a major role in the control and resolution of SARS-CoV-2 infection (38, 39). Moreover, cytokines along with growth factors are critical to fundamental homeostatic processes such as wound healing and tissue repair (40). We hypothesized that a host environment that is, one, less hostile to the virus and, two, facilitates tissue repair, would together allow boosted cell infection cycles for rapid viral evolution under mAb pressure. To address this hypothesis, we studied 40 blood cytokines, chemokines, and growth factors as part of circulating immune-related biomarkers (CIB) involved in either COVID-19 pathogenesis and/or wound healing.

Significant alterations occurred in levels of 34/40 (85.0%) cytokines between different treatment groups (**Supplemental Figure 5**), which are also linked to infection with different SARS-CoV-2 variants. We further utilized area under the curve receiver operating characteristic (AUROC) analysis to discriminate between patients developing de novo Spike RBD mutations from those who did not or those who rapidly cleared the virus. AUROC for CIBs just before mAb administration identified 11 biomarkers to be significantly altered. Amongst these, 8 biomarkers were significantly increased in patients developing mutations at D2, and included angiogenic growth factors (bFGF, PlGF, and VEGF-D), angiogenic factors' receptors (Tie-2 and Flt-1), and drivers of healing responses through macrophages (MCP-2 and MCP-3)(41) (**Figure 6A**).

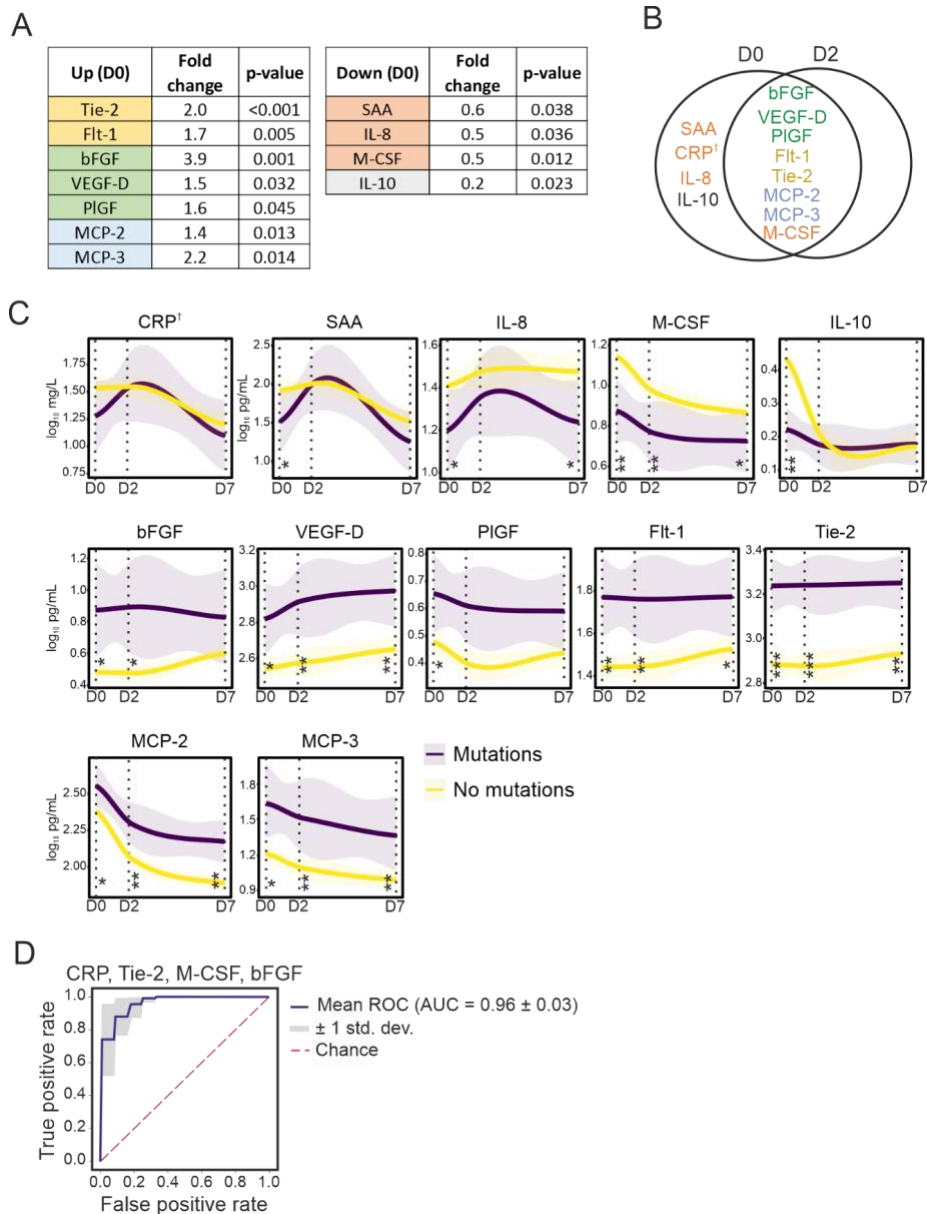


Figure 6. Circulating immune-related biomarkers (CIB) in COVID-19 patients receiving mAb therapy. (A) Several CIBs are significantly up- or downregulated at D0 in COVID-19 patients that developed SARS-CoV-2 Spike RBD mutations after administration of mAb treatments, compared to who did not. (B) Eleven CIBs were significantly altered at D0 in patients with de novo Spike RBD mutations, for which the majority ($n = 8$) were also altered at D2. (C) Temporal evolution of CIBs altered in patients with or without de novo mutations, receiving mAb therapy through day 7 after treatment. Lines represent smoothed conditional means and shaded areas display 95% confidence intervals for all measured timepoints. P-values refer to significance of the slope of the regression lines. Vertical lines with asterisks represent the significant difference between CIB levels at the specified timepoints. (D) Receiver operator characteristic (ROC) curve in a random forest classifier model with Synthetic Minority Oversampling Technique (SMOTE) for the prediction of mutation versus no-mutation are depicted for D0. *: $p < 0.05$. **: $p < 0.01$. ***: $p < 0.001$. †: not significant. For details on the progression of CIBs from D0 to D7 and sample numbers, see **Supplemental Figure 5 and 7**.

The four biomarkers that were significantly downregulated were acute phase inflammatory marker SAA, neutrophil chemokine IL-8, immunomodulatory marker IL-10, as well as M-CSF, a key cytokine involved in macrophage differentiation that enhances the inflammatory response of primed macrophages (42). Interestingly, after 48h of mAb infusion, the only cytokines observed to be significantly altered (n = 8) were those that were also significantly altered at D0 (**Figure 6B**). By day 7, several of these mutation-associated cytokines stayed altered (**Figure 6C**). These data suggest that, firstly, therapeutic mAbs do not majorly alter cytokine profiles in mildly ill COVID-19 patients, and secondly, cytokines identified to be linked to de novo Spike RBD mutation development are quite robust.

AUROC data were further validated with Random Forest classification, which identified a signature consisting of SAA, Tie-2, bFGF, and M-CSF that correctly identified patients with de novo Spike RBD mutations with high predictability (mean ROC of 96%). While CRP on its own missed statistical significance with AUROC analysis, replacing CRP with SAA did not change the accuracy of the model, likely because of high degree of co-linearity identified between CRP and SAA (Pearson's R = 0.937, p < 0.001; **Figure 6D**).

This signature was further independently tested on 19 patients comprising 8 patients receiving sotrovimab and 11 patients receiving tixagevimab/cilgavimab. Patient characteristics are described in **Supplemental Figure 6A**. One patient each receiving sotrovimab or tixagevimab/cilgavimab developed Spike RBD mutations within seven days of receiving mAb therapy. All 19 samples were correctly classified utilizing the CIB-based signature, both by Random Forest classification (AUCROC = 1) or a binomial logistic regression model ($\chi^2 = 12.787$; n = 19; df = 4; p < 0.012, **Supplemental Figure 6, B and C**). Remarkably, bFGF levels alone led to a 100% correct classification with mutation carriers having bFGF levels of ≥ 23.7 pg/mL (n = 2, range 23.7–34.4 pg/mL) and non-mutation carriers with levels ≤ 19 pg/mL (n = 17; Av 5.5 pg/mL, range 0.5-19 pg/mL). These data not only suggest that a diminished pro-inflammatory and homeostatic cytokine immune milieu could facilitate development of de novo Spike RBD mutations, but also describe a CIB profile present before mAb administration that predicts development of escape mutations against therapeutic mAbs for SARS-CoV-2 in high-risk patients with high accuracy.

Discussion

Absence of virus from respiratory tract samples is suggested to occur once serum neutralizing antibody titers of 1:80 or 2,000 BAU/mL are achieved (33, 43). Considering that the average serum antibody titers in mAb-treated patients are more than a million BAU/mL, or 1,000-fold higher than “high seropositivity” as defined by the WHO International SARS-CoV-2 Antibody Standards, our data suggest that therapeutic mAbs are unable to readily cross the respiratory mucosal barrier and neutralize SARS-CoV-2. All therapeutic mAbs investigated in this study are IgG subtypes, and while special mechanisms such as receptor-mediated IgG transport exist, most of the mucosal humoral immunity is either mediated by IgA or extravasated plasma cells that then locally secrete immunoglobins, including IgG (44-46). These data suggest that while therapeutic neutralizing mAbs efficiently clear SARS-CoV-2 from systemic tissue and reduce the risk of severe disease, the virus continues to thrive in the epithelial cells and mucosal barrier of the respiratory tract. With immunocompromised individuals exhibiting 4-fold higher viral loads compared to

immunocompetent COVID-19 patients, these data not only support the evidence that immunocompromised patients have prolonged SARS-CoV-2 shedding (5, 7), but also suggest that innate cellular immunity is decisively involved in SARS-CoV-2 clearance from the respiratory tract. Our study design where patients received exogenous immunoglobins without affecting host plasma cells, also offers novel insights into the relatively higher importance of local secretion of immunoglobins by mucosal plasma cells, as opposed to transepithelial transport of immunoglobins, in conferring mucosal immunity. These data can also be extrapolated to humoral mucosal immunity against other respiratory viral and bacterial pathogens.

Not only do we show that respiratory viral carriage is more abundant in immunocompromised patients, we also show that occurrence of de novo mutations is significantly higher in these patients, as shown for severely or chronically ill immunocompromised COVID-19 patients previously (8-12). Most mutations in SARS-CoV-2 are either deleterious or relatively neutral and only a small proportion impact viral characteristics like transmissibility, virulence, and/or resistance to existing host immunity (1, 47). Concerns have also been raised that mutation rates could be overestimated due to reverse transcriptase or sequencing errors (11, 48). However, for the following reasons we believe that the identified mutations in Spike RBD are existent and non-neutral. First, novel and unusually clustered mutations were reconfirmed by performing sequencing on independently extracted RNA making it a high-fidelity observation. Second, Spike RBD mutations were identified 2-7 days after mAb treatment in contrast to studies where mutations were observed before treatment, for example, case studies where mutations in Spike were fixed before casirivimab/imdevimab treatment (8, 49). Third, observed de novo mutations are highly specific to cognate mAb or ACE2 binding sites or its immediate proximity. For example, Spike RBD mutations developing in bamlanivimab- or bamlanivimab/etesevimab-treated patients had no overlap with mutated sites observed in sotrovimab-treated patients. Fourth, the de novo mutations are also highly evasive to therapeutic antibodies. For example, sotrovimab given empirically to BA.2-infected patients, against which sotrovimab shows little neutralization, did not lead to development of escape mutations, while it did for BA.1-infected patients against which sotrovimab is highly active. Fifth, sotrovimab-receiving BA.1-infected patients had more robust SARS-CoV-2-specific Th cell immunity, likely due to lack of SARS-CoV-2 neutralization. And, lastly, possible non-neutrality of some mutations described in the study are supported by prior reports on identical or similar mutations (25-31) (see Supplemental Table 4). Amino acid residues typically observed in Omicron sub-variants reverting back to those of the original Wuhan sequence (D339G, L371S, P373S, F375S, N417K, and K440N) are equally interesting, some of which have also been observed previously (17), supporting our seroneutralization data showing that sotrovimab is not active against Wuhan and some of the other de-escalated variants.

While we show that the de novo Spike RBD mutations are unequivocally mAb-specific, we also show that mutations accumulate in acutely infected patients and occur rather rapidly, within 7 days of treatment. Prior studies have proposed that selection pressure created during chronic or severe infections drives the emergence of SARS-CoV-2 mutations (8-12). Our data suggest that neither the chronic nature of the disease, nor its severity are necessary for occurrence of mutations if immune pressure is profound and rapid, as that induced by synthetic neutralizing mAb therapy. Both RNA and DNA viruses are capable of generating de novo diversity in a short period of time while adapting to new hosts and environments (50). One thing common to both our and previous studies is that the

mutation rate is significantly higher in immunocompromised patients (8-12), however, we also show that higher viral loads, regardless of the cause, are directly linked to Spike RBD mutation development.

We identify two specific components of host immunity that are associated with these mutations. Firstly, we demonstrate that downregulated pro-inflammatory cytokines are linked with higher rates of mutation, likely due to decreased viral clearance and more replication cycles giving the virus a higher chance to adapt evolutionarily. Cytokine immunity is an important component of innate and adaptive host immunity, and while examples exist where pro-inflammatory cytokines could be suppressed by viruses (51), the cytokine alterations associated with *de novo* mutations are likely driven by host-genetic susceptibilities to SARS-CoV-2 (52). Secondly, in a mutually non-exclusive independent mechanism, we also show that patients developing *de novo* mutations had stronger Th cell immunity following mAb treatment, suggesting strong immune pressure on the virus to adapt (6). Additionally, we describe an upregulation of key host growth factors, such as angiogenic growth factors and their receptors, that could be a consequence of SARS-CoV-2-induced lung damage. However, because patients only had mild disease, we propose that a reparative milieu, likely also genetically driven, while facilitating a rapid recovery of patients, could also allow boosted cell infection cycles enabling the virus to adapt. Our pharmacokinetic studies further showed that levels of all mAbs were retained at more than one million BAU/mL over 4 weeks, suggesting a sustained longstanding environment wherein mutant SARS-CoV-2 could be sheltered and mutate further, posing threats for viral rebound infections and dissemination of novel mutants. It is hypothesized that almost all SARS-CoV-2 variants originated in immunocompromised chronic carriers (53). Our data therefore emphasize the need of optimized mitigation strategies in immunocompromised patients receiving mAb treatment to reduce the risk of SARS-CoV-2 spreading to other high-risk patients in both a hospital and community setting.

Lastly, we suggest that assessment of CRP or SAA (general marker of inflammation), bFGF (angiogenic ligand), Tie-2 (angiogenic growth factor receptor), and M-CSF (pro-inflammatory and immune regulatory mediator) in high-risk patients with SARS-CoV-2 infection under evaluation for mAbs therapy could identify patients, with high predictability, who are also at risk of developing escape mutations against therapeutic mAbs. This or similar biomarker-based stratification could also benefit decision making. For example, identification of immunocompromised patients who are also at high risk of developing *de novo* mutations could benefit from alternative strategies such as anti-viral treatments or convalescent plasma containing high titers of polyclonal antibodies (54-56).

As limitations, samples analyzed in this study were collected during an extended time-period, resulting in underlying differences in the patient population, such as rate of vaccination and circulating SARS-CoV-2 variants. At the same time, the heterogeneity of infecting VOCs and inclusion of vaccinated individuals among high-risk groups could be considered a strength of the study, as this enables representation of real-world data and rapid changes in epidemiological scenarios typical of the SARS-CoV-2 pandemic. Being a prospective monocentric cohort within a European project, this study had the advantage of homogenous sampling and enrolment protocols, but lacks external validity. Finally, a very limited number of nasopharyngeal swab samples were collected at D28, thereby not allowing us to study the impact of mutation on prolonged carriage.

Despite these limitations, we show in a comprehensive analysis of patients with diverse mAb treatments, development of adaptive mutations that highly correlate with neutralizing capacities of

therapeutic mAbs and provide direct evidence that anti-SARS-CoV-2 host-driven responses are necessary and essential for development of mutant SARS-CoV-2. While these data, on one hand, suggest a critical balance between successful viral killing and development of VOC-like mutations in niched environments such as respiratory mucosa; on the other hand, our data also prompt close and extensive monitoring, and isolation of patients and contacts to limit the spread of potential VOC-like mutants, especially in high-risk populations.

Material and Methods

Study design

Samples were collected as part of the prospective, observational, monocentric ORCHESTRA cohort study conducted from 9 March 2021 to 30 November 2022 in the early COVID-19 treatment Outpatient Clinic, Infectious Diseases Section of the University Hospital of Verona, Italy. All outpatients aged ≥ 18 years, presenting with mild-to-moderate COVID-19 (confirmed by quantitative real-time Reverse Transcription (RT-q)PCR or a positive antigenic 3rd generation test) at high risk for clinical worsening in accordance with Italian Medicine Agency indications (for definition see ref. (19, 20)) were offered monoclonal antibody therapy and enrolled in this study. All enrolled patients received treatment with either bamlanivimab, bamlanivimab/etesevimab, casirivimab/imdevimab, or sotrovimab. In addition, a limited number of patients receiving tixagevimab/cilgavimab ($n = 11$) were also enrolled for assessment of the CIB profile predictive of development of SARS-CoV-2 mutations. Inclusion/exclusion criteria for patient enrolment have been published (19, 20).

Samples were collected from enrolled patients to study the effect of mAb therapy on SARS-CoV-2 viral load, mutations induced by different mAbs, mAb kinetics, neutralization capacity of mAb, cellular immunity, and CIB responses, which were analyzed within ORCHESTRA WP6. For each enrolled patient, 4 timepoints were analyzed: (i) D0: just prior to mAb infusion, (ii) D2: 2 ± 1 days after mAb infusion at D0, (iii) D7: 7 ± 2 days after mAb infusion at D0, and (iv) D28: 28 ± 4 days after mAb infusion. Nasopharyngeal swab, serum, and peripheral blood mononuclear cells (PBMCs) samples were collected along with clinical data. An overview of sample numbers included for each analysis is available in **Supplemental Figure 7**.

SARS-CoV-2 viral load and variant sequencing

RNA was extracted using the MagMAX Viral/Pathogen II Nucleic acid kit on a KingFisher Flex Purification System (ThermoFisher). Real-Time RT-qPCR was performed using the TaqPath™ COVID-19 CE-IVD RT-PCR Kit (ThermoFisher) on a QuantStudio™ 5 Real Time PCR instrument (384-well block, 5 colors, ThermoFisher). Extracted RNA was subjected to automated cDNA conversion and multiplexed library preparation using the Illumina COVIDSeq Test kit on a Zephyr G3 NGS (PerkinElmer) and sequenced using the High Output Kit v2 on a NextSeq 500/550 instrument (Illumina Inc.). Identified single nucleotide polymorphisms (SNPs) were verified by Sanger sequencing. For detailed methods, refer to Supplemental Information.

Serology

Blood was collected in 10 mL serum tubes (BD vacutainer K2E, BD biosciences) and serum samples were prepared within 3h of blood collection. Anti-N, anti-S, and anti-RBD SARS-CoV-2 IgG titers

were measured in serum samples using a multiplexed panel (Meso Scale Discovery (MSD)) and data provided in WHO-recommended BAU units. For detailed methods, refer to Supplemental Information.

ACE2 neutralization measurements in serum

ACE2 neutralization was measured in serum samples against Wuhan, Alpha/B.1.1.7, Omicron/BA.1, Omicron/BA.1+R346K, and Omicron/BA.2 using V-PLEX SARS-CoV-2 Panel 6, 13, 23, and 25 (ACE2) on the QuickPlex SQ 120 system (MSD) according to the manufacturer instructions. Further details regarding the Spike variants, against which the neutralizing antibody titers were measured, are displayed in Supplemental Table 6. For detailed methods, refer to Supplemental Information.

Measurements of circulating immune-related biomarkers (CIB) in serum

CIBs were measured in serum samples using U-plex and V-plex panels (#K15198D, #K15190D) on the QuickPlex SQ 120 system (MSD), according to the manufacturer instructions. The following 40 CIBs were measured for D0, D2, and D7 timepoints: basic fibroblast growth factor (bFGF), C-reactive protein (CRP), cutaneous T-cell attracting chemokine (CTACK), eotaxin, erythropoietin (EPO), vascular endothelial growth factor receptor 1 (Flt-1), fractalkine, macrophage colony-stimulating factor (M-CSF), interferon β (IFN- β), interferon γ (IFN- γ), interleukin (IL)-1 β , IL-1 receptor antagonist (IL-1Ra), IL-2, IL-2 receptor α (IL-2R α), IL-4, IL-5, IL-6, IL-8, IL-10, IL-13, IL-15, IL-17A, IL-17F, IL-18, IL-22, IL-33, IFN- γ induced protein 10 (IP-10), monocyte chemoattractant protein (MCP)-1, MCP-2, MCP-3, macrophage inflammatory protein (MIP)-1 α , placental growth factor (PIGF), serum amyloid A (SAA), soluble intercellular adhesion molecule 1 (sICAM-1), soluble vascular cell adhesion molecule 1 (sVCAM-1), angiopoietin receptor 1 (Tie-2), tumor necrosis factor α (TNF- α), vascular endothelial growth factor (VEGF)-A, VEGF-C, and VEGF-D. A small panel of 4 select CIBs, comprising, CRP, bFGF, Tie2, and M-CSF, was additionally utilized for validating CIB profile predictive of SARS-CoV-2 mutations. For detailed methods, refer to Supplemental Information.

SARS-CoV-2 specific cellular responses

PBMCs were isolated using cellular preparation tubes (BD Biosciences) according to the manufacturer's instructions and stored in fetal bovine serum (FBS) with 10% DMSO at -80°C until further use. Stimulation and staining were performed using the SARS-CoV-2 T Cell Analysis Kit (PBMC), human (Miltenyi Biotech). PBMCs were stimulated with a pool of lyophilized peptides, consisting of 15-mer sequences covering the complete protein-encoding sequence of the SARS-CoV-2 surface or Spike glycoprotein (GenBank MN908947.3, Protein QHD43416.1) and the complete sequence of the nucleocapsid phosphoprotein (GenBank MN908947.3, Protein QHD43423.2) from Miltenyi Biotech. For detailed methods, refer to Supplemental Information.

Flow cytometry

After stimulation, staining of surface and intracellular antigens was carried out with the following fluorochrome-conjugated recombinant human IgG1 isotype antibodies (Miltenyi Biotech): CD3-APC REAfinity (clone REA613), CD4-Vio Bright-B515 REAfinity (clone REA623), CD8-VioGreen REAfinity (clone REA734), CD14-CD20-VioBlue REAfinity (clone REA599, clone REA780), IFN- γ -PE REAfinity (clone REA600), TNF- α -PE-Vio 770 REAfinity (clone REA656),

CD154-APCVio 770 REAfinity (clone REA238). Samples were captured on a NovoCyte Quanteon 4025 flow cytometer (Agilent) and analyzed using FlowJo v10.8.1 (BD) (Supplemental Figure 8). For detailed methods, refer to Supplemental Information.

Statistical analysis

All data were statistically analyzed and visualized in Rstudio v.1.3.1073 using R v.4.0.4. One-way analysis of variance (ANOVA) was utilized for longitudinal and cross-sectional comparisons of IgG titers, titers of neutralizing antibodies, and CIB concentrations across treatment groups followed by pairwise two-tailed t-tests. Cyclic threshold (Ct) values were compared using non-parametric Kruskal-Wallis followed by pairwise testing using Mann-Whitney. Post hoc p-value correction was conducted using Bonferroni's multiple-comparison correction method for all analyses. Throughout the statistical analyses, values below the detection range were recorded as 1/10th the lower limit of quantitation (LLQ) and values above the detection range were recorded as upper limit of quantitation (ULQ). A (corrected) p-value < 0.05 was considered statistically significant. For the identification of the main predictors of qualitative responses (mutation/no mutation in the Spike RBD region [residues 319-541]), receiver operating characteristic (ROC) curves were constructed utilizing MetaboAnalyst. Machine-learning-based Random Forest classifiers (RFC) were further built by the Python package sklearn v2.0 to independently predict development of de novo Spike RBD mutations in patients receiving mAb regimens. Each model was built with a training set of values consisting of 70% of the data and a test set of 30% (57). To account for imbalanced groups, the Synthetic Minority Oversampling Technique (SMOTE, Python package imblearn 0.8.0) was utilized in combination with the RCF method. The models were bootstrapped 100 times and features for each model were selected based on i) feature importance, ii) statistics from mutation vs. non-mutation, iii) individual ROC curve analysis, and iv) a Pearson correlation matrix for independence of variables. Confusion matrices and ROC curves were drawn to calculate area under the curve (AUROC) values to verify reliability and to evaluate the performance of the constructed models. The CIB model built to predict emergence of evasive SARS-CoV-2 Spike RBD mutations in patients treated with mAbs in the main study population, was validated both by RFC and binomial logistic regression in a patient cohort on independently generated dataset. Linear mixed models were utilized to investigate evolution of antibody titers and Th cell immunity over time between the different mAb groups.

Study approval

Participants were recruited from the Infectious Diseases Section of the University Hospital of Verona from 9 March 2021 to 30 November 2022. All volunteers provided informed, written consent before study participation. This study was approved by the University Hospital Verona Ethics Board (protocol number: 19293) and conducted in accordance with the Declaration of Helsinki.

Data availability

Data supporting the findings of this study are available within Supplemental Information files. SARS-CoV-2 genome sequences obtained in the project were submitted to GISAID. Trimmed read data generated and used for identification of emerging de novo Spike RBD mutants in this study have been submitted to the European Nucleotide Archive (ENA) under the project accession PRJEB55794. All other data generated in this study are available from the corresponding author upon request.

Author Contribution

Conceptualization: SKS, ET, SMK, PDN; Overall study supervision: SKS; Clinical data and sample collection: AS, PDN, MM, DP, ED, ER, ET; RT-qPCR and viral variant sequencing: MS, MB, SMK; Bioinformatic analysis: MB, MS; Serological analysis: AK, AG, FDW; Circulating immune-related biomarker (CIB) analysis: AK, AG, FDW, AH; PBMC isolations: DP, PD, ER; PBMC analysis: AG, VVA, AK, FDW; Statistical analysis: MB, AG, AK, SKS; Data interpretation: SKS, SMK, ET, AG, AK, MB, MS; Manuscript writing: SKS, MB, AG, AK, MS, SMK, ET; All authors read, gave input, and approved the final manuscript. The first co-authorship and their order was determined by their contributors to the findings described in this manuscript.

Supplementary Methods

RNA extraction, cDNA conversion, library preparation, and SARS-CoV-2 genome sequencing

RNA was extracted using the MagMAX Viral/Pathogen II Nucleic acid kit on a KingFisher Flex Purification System (ThermoFisher). Each batch of samples taken forward for extraction was processed together with a Twist synthetic SARS-CoV-2 RNA positive Ctrl. 18 (Cat. No: 104338, Twist Bioscience). Extracted RNA was subjected to automated cDNA conversion and multiplexed library preparation using the Illumina COVIDSeq Test kit (Illumina Inc.) on a Zephyr G3 NGS system (PerkinElmer, MA, USA). DNA concentrations were quantified using the Qubit dsDNA HS Assay Kit (Invitrogen, Cat. No. Q33231) using a Qubit Fluorometer 3.0 (ThermoFisher). Pooled libraries were sequenced utilizing the High Output Kit v2 with a 1.4 nM PhiX Library positive control v3 using a 1% spike-in on a NextSeq 500/550 instrument (Illumina Inc.). All steps were performed according to manufacturer's instructions.

SARS-CoV-2 RT-qPCR

Real-Time RT-qPCR was performed using the TaqPath™ COVID-19 CE-IVD RT-PCR Kit (ThermoFisher) on a QuantStudio™ 5 Real Time PCR instrument (384-well block, 5 colors, ThermoFisher), which detects three genes in the SARS-CoV-2-viral genome: the S protein, N protein, and ORF1ab. MS2 (phage control) was added to each sample prior to RNA extraction to serve as internal control. RT-qPCR analysis was performed using FastFinder (UgenTec). Samples were considered positive if both the MS2 phage control (Ct < 32) and at least two gene targets were detected (Ct < 37).

SARS-CoV-2 variant detection

Raw sequencing data quality for each sample was assessed using FastQC (<https://www.bioinformatics.babraham.ac.uk/projects/fastqc/>) followed by quality trimming using a Phred score cut-off of 25 with TrimGalore v. 0.6.7 (<https://github.com/FelixKrueger/TrimGalore>). Read mapping was performed against the SARS-CoV-2 genome (GenBank: NC_045512.2) using the CLC Genomics Workbench v.9.5.3 (Qiagen) with a length and a similarity fraction of 0.5 and 0.8, respectively. Consensus sequences were extracted, and clade and lineage assignment performed using Nextstrain (<https://clades.nextstrain.org/>) and Pangolin (<https://pangolin.cog-uk.io/>), respectively. SARS-CoV-2 genome sequencing was considered successful if: i) was successfully

classified by both Pangolin and NextClade, and ii) the resulting genome sequence harbored < 15% ambiguous base calls (Ns) in the consensus sequence.

For detection of single nucleotide variations (SNPs) acquired during monoclonal antibody treatment in patients who provided samples at D0, as well as D2 and/or D7, trimmed reads were mapped against the SARS-CoV-2 genome (GenBank: NC_045512.2) using the CLC Genomics Workbench v.9.5.3 (Qiagen) with a length and a similarity fraction of 0.7 and 0.99, respectively. SNPs resulting in amino acid substitutions were of particular interest and analyzed further in this study.

SNP validation using Sanger sequencing

Patients harboring non-synonymous mutations in the Spike RBD region (residues 319 – 541) were subjected to Sanger sequencing. For this purpose, RNA extraction and cDNA conversion was repeated and used for the validation.

Primers binding in the region of interest were selected from the Artic primer pool v3 (nCoV-2019 sequencing protocol v3 (LoCost) by performing in silico PCR using the CLC Genomics Workbench v.9.5.3 (Qiagen) or designed using NCBI PrimerBlast with standard parameters (National Center for Biotechnology Information) utilizing the Wuhan (GenBank: NC_045512.2) and Omicron/BA1.1 (GenBank: OM664849) genomes as templates with the following criteria: i) optimal primer length = 25 bp, ii) >5 bp difference in length between forward and reverse primers, and iii) $\Delta T_m < 5^\circ\text{C}$. Designed primer pairs were validated in silico using FastPCR (<https://primerdigital.com/>) using standard parameters.

PCR amplification was performed using 50 ng cDNA, Q5 Hot start 2x MM (New England Biolabs), forward and reverse primers at a final concentration of 0.5 μM each, and Nuclease-free water (Ambion, ThermoFisher) in a total volume of 45 μL with the following temperature profile: 98°C for 15s followed by 35 cycles of denaturation at 96°C for 30 s and annealing at 63°C for 5 min. Successful amplification was confirmed with 1.5% agarose gel electrophoresis (150 V, 200 mA, 1h) using a 100 bp DNA ladder (ThermoFisher).

Obtained PCR products were then subjected to automatic template clean-up and sample preparation using Illustra™ ExoProStar™ (Merck) and ABI PRISM® BigDye™ Terminator cycle sequencing kits (ThermoFisher) with Biomek® FX and NX liquid handlers (Tecan), followed by sequencing on an Applied Biosystems 3730XL DNA Analyzer (ThermoFisher). Sequence analysis was performed using the CLC Genomics Workbench v.9.5.3 (Qiagen).

Serology

Blood was collected in 10 mL serum tubes (BD vacutainer K2E, BD Biosciences) and serum samples were prepared within 3h of blood collection. Serum was allowed to clot thoroughly for 60 min before separation by centrifuging for 10 min at 1300 g. Aliquots were flash frozen in liquid nitrogen, shipped to the University of Antwerp for further processing and stored at -80°C until analysis.

IgG titers were measured in serum samples using the V-PLEX SARS-CoV-2 Panel 6 Kit (IgG; #K15433U-4) on a QuickPlex SQ 120 instrument (Meso Scale Discovery (MSD)) according to the manufacturer's instructions. IgG titers to the following antigens were measured: SARS-CoV-2 Nucleocapsid, SARS-CoV-2 S1 RBD, SARS-CoV-2 Spike, SARS-CoV-2 Spike (D614G), SARS-CoV-2 Spike (B.1.1.7/Alpha), SARS-CoV-2 Spike (B.1.351/Beta), SARS-CoV-2 Spike

(P.1/Gamma). Baseline samples were measured at 1:1,000 or 1:10,000, while all other samples were measured at a final dilution of 1:10,000,000 or 1:100,000,000 in Diluent 100 (MSD). Quantitative IgG results were measured in Antibody Units (AU)/mL converted to Binding Antibody Units (BAU)/mL using a conversion factor provided by the manufacturer and reported as such. Patients were considered negative if their levels were under 4.76 BAU/mL for anti-spike, under 5.58 BAU/mL for anti-RBD, and under 8.20 BAU/mL for anti-nucleocapsid, these limits were determined by calculating the average plus one standard deviation of IgG measurements in 56 serum samples collected before 2019.

ACE2 neutralization measurements in serum

ACE2 neutralization measured in diluted serum samples (1:3,000) using V-PLEX SARS-CoV-2 Panel 6, 13, 23 and 25 (ACE2) and measured on the QuickPlex SQ 120 instrument (MSD) according to the manufacturer's instructions. Details regarding the Spike variants, against which the neutralizing antibody titers were measured, are displayed in **Supplemental Table 6**. Quantitative ACE2 neutralization results were measured in Units (U)/mL for all variants except Omicron sub-variants, which corresponds to neutralizing activity of 1 µg/mL monoclonal antibody to SARS CoV-2 Spike protein (upper limit of quantitation: 63,000 U/mL; lower limit of quantitation: 15 U/mL). Omicron sub-variants were measured as percent inhibition (% inhibition) calculated as $100 \times [1 - (\text{Sample signal}/\text{Average signal of the blanks})]$.

SARS-CoV-2 specific cellular responses

Peripheral blood mononuclear cells (PBMCs) were isolated using cellular preparation tubes (BD Biosciences, Germany) according to the manufacturer's instructions and frozen in fetal bovine serum (FBS) with 10% DMSO until further use. Stimulation and staining were performed using the SARS-CoV-2 T Cell Analysis Kit (PBMC) human (Miltenyi Biotech). Briefly, PBMCs were thawed and rested overnight in RPMI 1640 medium (Gibco, ThermoFisher, the Netherlands) supplemented with 5% heat-inactivated AB serum (Sigma-Aldrich, Merck), 100 U/ml penicillin (Biochrom), and 0.1 mg/ml streptomycin (Biochrom). 1×10^6 PBMCs were stimulated with a pool of lyophilized peptides, consisting mainly of 15-mer sequences with 11 amino acids overlap, covering the complete protein coding sequence (residues 5–1273) of the SARS-CoV-2 surface or Spike glycoprotein of SARS-CoV-2 (GenBank MN908947.3, Protein QHD43416.1) and the complete sequence of the nucleocapsid phosphoprotein (GenBank MN908947.3, Protein QHD43423.2) from Miltenyi Biotech. Both peptide pools were used at 1 µg/mL per peptide. Stimulation controls were performed with equal concentrations of sterile water/10% DMSO (unstimulated) as negative control and Cytostim (Miltenyi Biotech) as positive control. Incubation was performed at 37 °C, 5% CO₂ for 6h with 2 µg/mL brefeldin A (Sigma-Aldrich, Merck) added after 2 h.

Flow cytometry

After stimulation, staining of surface and intracellular antigens was carried out with the following fluorochrome-conjugated recombinant human IgG1 isotype antibodies (Miltenyi Biotech) at 0.25x recommended volume: CD3-APC REAfinity (clone REA613), CD4-Vio Bright-B515 REAfinity (clone REA623), CD8-VioGreen REAfinity (clone REA734), CD14-CD20-VioBlue REAfinity (clone REA599, clone REA780), IFN-γ-PE REAfinity (clone REA600), TNF-α-PE-Vio 770 REAfinity (clone REA656), CD154-APCVio 770 REAfinity (clone REA238). Cells were washed

with cell staining buffer (PBS 1% bovine serum albumin, 2mM EDTA) unless stated otherwise. Briefly, dead cells were stained for 10 min with Viability 405/452 Fixable Dye (1:200) with subsequent fixation and permeabilization for 20min (Inside stain kit, Miltenyi Biotech). Cells were washed with permeabilization buffer and surface marker, and intracellular staining was carried out for 15 min. Cells were washed in permeabilization buffer and resuspended in cell staining buffer. Samples were captured on a NovoCyte Quanteon 4025 flow cytometer (Agilent) and analyzed using FlowJo v10.8.1 (BD) (**Supplemental Figure 8**)

Supplemental Tables

Supplemental Table 1. Eligibility criteria. Italian Medicines Agency Emergency Use Authorization eligibility criteria for bamlanivimab, bamlanivimab/etesevimab, casirivimab/imdevimab, and sotrovimab therapy in adult patients as described by Savoldi et al.(2, 3).

Patients enrolled during March 2021 – 15 June 2021:

All the following criteria should be met:

Confirmed diagnosis of SARS-CoV-2 infection either by polymerase chain reaction or 3rd generation antigenic test on nasopharyngeal swab

Onset of at least one of the COVID-19 related symptoms among fever, cough, dyspnea, headache, myalgia, gastrointestinal symptoms, asthenia ≤ 10 days

Age ≥ 18 years

Body weight ≥ 40 kg

No need for oxygen therapy

No need for hospitalization

Presence of at least one of the following medical conditions:

BMI ≥ 35 Kg/m²

Subject chronically undergoing peritoneal dialysis or hemodialysis

Uncontrolled diabetes mellitus (HbA1c $\geq 9\%$ or 75 mmol/L) or with chronic complications

Primary immunodeficiency

Secondary immunodeficiency (e.g., hematologic cancer patient in ongoing myeloid/immunosuppressive therapy or suspension for <6 months)

Cardio-cerebrovascular disease (including arterial hypertension with documented organ damage) in subjects aged ≥ 55 years

Chronic Obstructive Pulmonary Disease and/or other chronic respiratory disease in subjects ≥ 55 years

Patients enrolled during 16 June – ongoing:

All the following criteria should be met:

Confirmed diagnosis of SARS-CoV-2 infection either by polymerase chain reaction or 3rd generation antigenic test on nasopharyngeal swab

Onset of at least one of the COVID-19 related symptoms among fever, cough, dyspnea, headache, myalgia, gastrointestinal symptoms, asthenia ≤ 7 days

Age ≥ 18 years

Body weight ≥ 40 kg

No need for oxygen therapy

No need for hospitalization

Presence of at least one of the following medical conditions:

Age > 65 years

BMI ≥ 30 Kg/m²

Chronic kidney disease (including dialysis)

Uncontrolled diabetes mellitus (HbA1c $\geq 9\%$ or 75 mmol/L) or with chronic complications

Primary immunodeficiency

Secondary immunodeficiency (e.g., hematologic cancer patient in ongoing myeloid/immunosuppressive therapy or suspension for <6 months)

Cardio-cerebrovascular disease (including arterial hypertension with documented organ damage)

Chronic Obstructive Pulmonary Disease and/or other chronic respiratory disease

Chronic liver disease

Hemoglobinopathies

Neurodevelopmental diseases and neurodegenerative diseases

Supplemental Table 2. Results of real-time reverse transcriptase quantitative (RT-)qPCR detection of the *ORF1ab*, *N*, and *S* protein genes in nasopharyngeal swab samples collected from patients treated with bamlanivimab, bamlanivimab/etesevimab, casirivimab/imdevimab, or sotrovimab. Statistical comparisons between treatment groups at each timepoint were performed using Kruskal-Wallis. Ct: cyclic threshold. CI: confidence interval. Only Ct values for variants of concern were considered. Positive samples collected at day 28 post mAb infusion were limited (2/14) and were therefore excluded from this analysis. D0: sample collected prior to mAb infusion. D2: 2 ± 1 days after mAb infusion. D7: 7 ± 2 days after mAb infusion.

Treatment	D0			D2			D7		
	n	Ct average (95% CI)	p-value	n	Ct average (95% CI)	p-value	n	Ct average (95% CI)	p-value
ORF1ab									
Bamlanivimab	44	19.25 (17.8 - 20.7)	0.008	33	24.33 (22.8 - 25.8)	2.20E-07	16	26.14 (23.9 - 28.4)	0.335
Bamlanivimab/etesevimab	107	19.31 (18.4 - 20.2)		80	23.21 (22.4 - 24.0)		43	26.62 (25.7 - 27.5)	
Casirivimab/imdevimab	17	19.29 (17.2 - 21.4)		15	24.11 (21.9 - 26.3)		5	27.84 (26.1 - 29.6)	
Sotrovimab	34	16.35 (15.2 - 17.5)		33	19.02 (17.7 - 20.4)		34	24.49 (22.6 - 26.4)	
S protein									
Bamlanivimab	0	-	-	0	-	-	0	-	-
Bamlanivimab/etesevimab	0	-		0	-		0	-	
Casirivimab/imdevimab	0	-		0	-		0	-	
Sotrovimab	7	14.94 (12.7 - 17.2)		7	17.09 (13.6 - 20.6)		6	23.40 (19.8 - 27.0)	
N protein									
Bamlanivimab	44	18.18 (16.8 - 19.5)	0.108	33	22.58 (21.2 - 24.0)	2.70E-05	16	24.28 (22.1 - 26.4)	0.686
Bamlanivimab/etesevimab	107	18.18 (17.3 - 19.1)		80	21.38 (20.5 - 22.2)		43	25.08 (24.3 - 25.9)	
Casirivimab/imdevimab	17	18.66 (16.6 - 20.8)		15	22.82 (20.7 - 25.0)		5	26.38 (23.8 - 29.0)	
Sotrovimab	34	16.06 (14.9 - 17.2)		33	18.51 (17.3 - 19.7)		34	23.96 (22.1 - 25.8)	

Supplemental Table 3. Results of real-time reverse transcriptase quantitative (RT-)qPCR detection of the *ORF1ab*, *N*, and *S* protein genes in nasopharyngeal swab samples collected from patients with different variants – Alpha and Omicron sub-variants. Statistical comparisons between treatment groups at each timepoint were performed using Kruskal-Wallis. Ct: cyclic threshold. CI: confidence interval. Positive samples collected at day 28 post mAb infusion were limited (2/14) and were therefore excluded from this analysis. D0: sample collected prior to mAb infusion. D2: 2 ± 1 days after mAb infusion. D7: 7 ± 2 days after mAb infusion.

	D0			D2			D7		
	n	Ct average (95% CI)	p-value	n	Ct average (95% CI)	p-value	n	Ct average (95% CI)	p-value
ORF1ab									
Alpha	161	19.3 (18.6 – 20.0)	2.10E-04	123	23.5 (22.8 – 24.2)	1.20E-08	62	26.5 (25.7 – 27.3)	0.057
Omicron	34	15.1 (14.0 – 17.9)		33	18.6 (16.4 – 21.4)		34	23.6 (19.5 – 29.0)	
B.1.1.7	146	19.4 (18.6 – 20.2)	9.60E-04	110	23.5 (22.8 – 24.3)	4.80E-07	56	26.9 (26.1 – 27.6)	0.096
Q.4	15	18.5 (16.2 – 20.9)		13	23.4 (20.2 – 26.7)		6	22.8 (17.8 – 27.9)	
BA.1	13	18.2 (15.8 – 20.6)		13	20.1 (17.3 – 22.9)		13	25.0 (21.9 – 28.1)	
BA.1+R346K	14	15.3 (14.0 – 16.7)		13	18.9 (17.2 – 20.6)		14	23.9 (20.4 – 27.4)	
BA.2	7	14.8 (14.1 – 15.1)		7	16.1 (15.1 – 19.7)		7	23.4 (21.7 – 27.3)	
N gene									
Alpha	161	18.2 (17.5 – 18.9)	0.008	123	21.7 (21.1 – 22.4)	5.40E-06	62	24.9 (24.1 – 25.6)	0.375
Omicron	34	15.3 (13.5 – 18.3)		33	18.2 (16.0 – 20.7)		34	23.0 (19.7 – 28.4)	
B.1.1.7	146	18.3 (17.5 – 19.1)	0.023	110	21.8 (21.1 – 22.5)	1.20E-04	56	25.3 (24.6 – 25.9)	0.248
Q.4	15	17.4 (15.1 – 19.7)		13	21.7 (18.7 – 24.6)		6	21.2 (16.5 – 25.9)	
BA.1	13	17.7 (15.3 – 20.2)		13	19.3 (17.0 – 21.7)		13	24.4 (21.3 – 27.5)	
BA.1+R346K	14	15.3 (13.8 – 16.8)		13	18.6 (17.0 – 20.2)		14	23.5 (20.0 – 27.0)	
BA.2	7	14.4 (13.5 – 14.6)		7	15.4 (14.4 – 19.4)		7	23.0 (20.8 – 26.8)	

Supplemental Table 4. De novo SARS-CoV-2 variants emerging during the first seven days of monoclonal antibody treatment. Only non-synonymous mutations detected at D2 or D7 compared to D0 are reported. All reference positions refer to the Wuhan variant (GenBank: NC_045512.2). *: deletion. †: variant of concern mutation emerging irrespective of mAb therapy. Fs: frameshift. D0: sample collected prior to mAb infusion. D2: 2 ± 1 days after mAb infusion. D7: 7 ± 2 days after mAb infusion.

Reference position	ORF/gene	Amino acid substitution	Previously reported mutations in the same codon	References
701	ORF1ab	G146S	—	—
1478	ORF1ab	A405S	—	—
2841	ORF1ab	V859A	—	—
2864	ORF1ab	E867*	—	—
4592	ORF1ab	E1443*	—	—
6456	ORF1ab	C2064Y	—	—
6615	ORF1ab	L2117S	—	—
6843	ORF1ab	S2193F	—	—
7860	ORF1ab	T2532I	—	—
7987	ORF1ab	Q2574H	—	—
8505	ORF1ab	T2747I	—	—
11490	ORF1ab	S3742F	—	—
12067	ORF1ab	M3934I	—	—
13065	ORF1ab	L4267S	—	—
14503	ORF1ab	H4747Y	—	—
16795	ORF1ab	V5511L	—	—
18551	ORF1ab	S6096T	—	—
21458	ORF1ab	I7065T	—	—
22484	S	V308L	—	—
22578	S	D339G	G339D †	(4)
22580	S	E340K	E340K/A/D/G/Q	(5-7)
22581	S	E340V	E340K/A/D/G/Q	(5-7)
22582	S	E340D	E340K/A/D/G/Q	(5-7)
22599	S	K346R	R346K/T/S/M	(8)
22673	S	L371S	S371L, L371S †	(4, 9)
22679	S	P373S	S373P, P373S †	(4, 9)
22686	S	F375S	F375S †	(9)
22813	S	N417K	K417N/T †	(4, 5, 10, 11)
22882	S	K440N	N440K	(8)
23012	S	E484K	E484K/Q	(8, 12-15)
23013	S	E484A	—	—
23014	S	E484D	—	—
23039	S	Q493K	Q493K	(8, 10, 11, 15)
23040	S	Q493R	Q493R	(8, 10, 11, 15)

23042	S	S494P	S494P	(12, 14)
23401	S	Q613H	—	—
23709	S	I716T	—	—
24029	S	F823I	—	—
24939	S	C1126F	—	—
25024	S	Y1155fs	—	—
25407	ORF3a	M5I	—	—
25784	ORF3a	W131L	—	—
25811	ORF3a	L140P	—	—
27145	M	T208I	—	—
27462	ORF7a	C23W	—	—
27610	ORF7a	H73Y	—	—
27874	ORF7b	T40I	—	—
28987	N	Q239fs	—	—

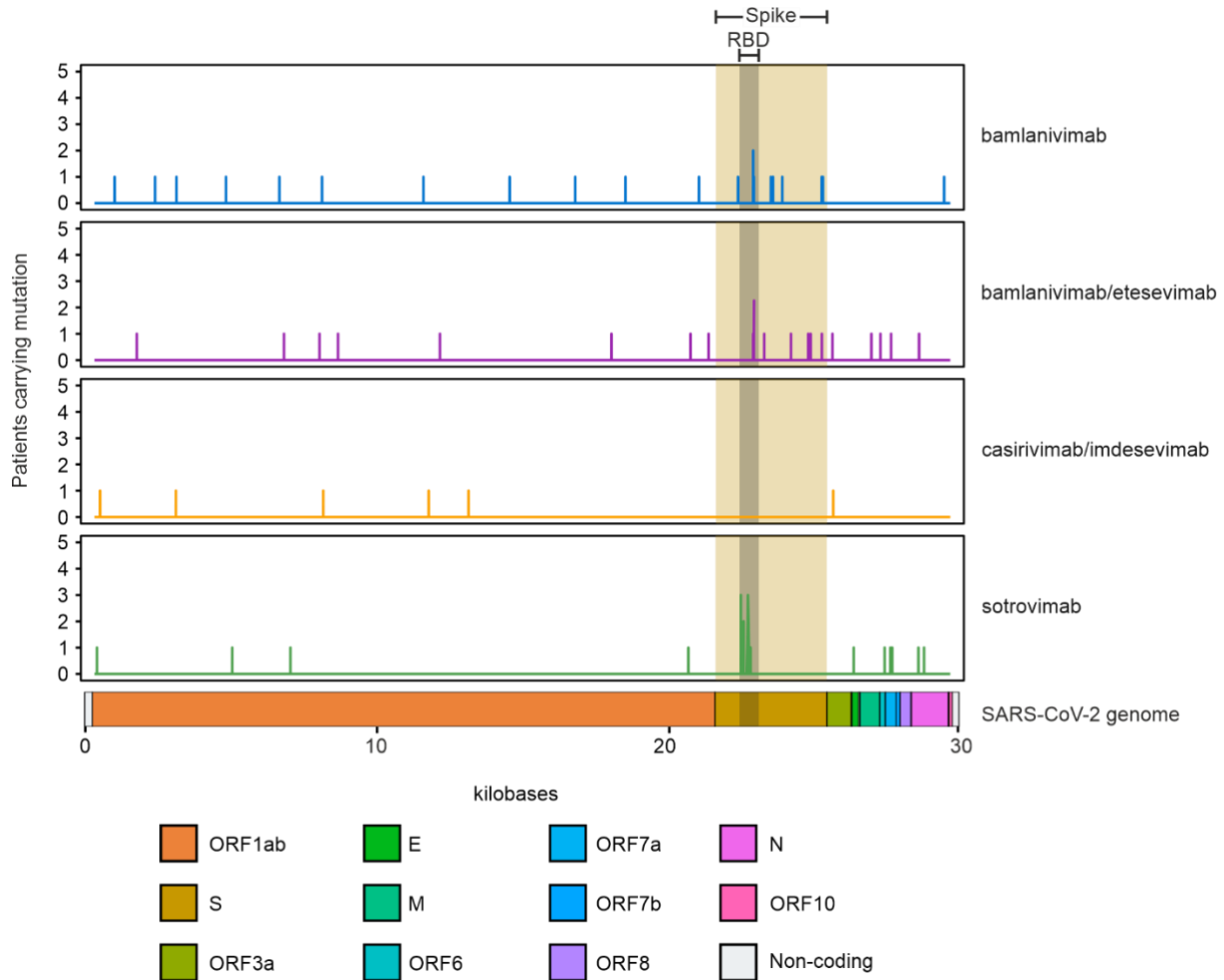
Supplemental Table 5. Distribution of patients tested for serological analysis among different treatment groups. Number and percentage of patients receiving bamlanivimab, bamlanivimab/etesevimab, casirivimab/imdevimab, or sotrovimab therapy that were fully vaccinated (14 days after second vaccination dose) or unvaccinated.

Therapy	Bamlanivimab			Bamlanivimab/etesevimab			Casirivimab/imdevimab			Sotrovimab		
Unvaccinated	n = 45			n = 108			n = 16			n = 10		
	Spike	RBD	Nucleocaps id	Spike	RBD	Nucleocaps id	Spike	RBD	Nucleocaps id	Spike	RBD	Nucleocaps id
Negative	30 (66.6%)	34 (75.5%)	36 (80.0%)	88 (81.5%)	90 (83.3%)	98 (90.7%)	12 (75%)	11 (68.8%)	13 (81.3%)	1 (10%)	3 (30%)	7 (70%)
Inconclusive	9 (9.2%)	7 (15.5%)	3 (6.6%)	18 (16.7%)	15 (13.9%)	2 (1.9%)	2 (12.5%)	2 (12.5%)	0 (0%)	6 (60%)	3 (30%)	0 (0%)
Positive – Low	2 (4.4%)	3 (6.6%)	4 (8.8%)	2 (1.9%)	2 (1.9%)	8 (7.4%)	0 (0%)	2 (12.5%)	3 (18.6%)	2 (20%)	3 (30%)	3 (30%)
Positive – Medium	1 (4.4%)	0 (0%)	0 (0%)	0 (0%)	1 (0.9%)	0 (0%)	2 (12.5%)	1 (6.2%)	0 (0%)	0 (0%)	1 (10%)	0 (0%)
Positive – High	0 (0%)	0 (0%)	0 (0%)	0 (0%)	0 (0%)	0 (0%)	0 (0%)	0 (0%)	0 (0%)	1 (10%)	1 (10%)	0 (0%)
Vaccinated	n = 0			n = 0			n = 1			n=25		
	Spike	RBD	Nucleocaps id	Spike	RBD	Nucleocaps id	Spike	RBD	Nucleocaps id	Spike	RBD	Nucleocaps id
Negative	0 (0%)	0 (0%)	0 (0%)	0 (0%)	0 (0%)	0 (0%)	0 (0%)	0 (0%)	1 (100%)	3 (12%)	2 (8%)	22 (88%)
Inconclusive	0 (0%)	0 (0%)	0 (0%)	0 (0%)	0 (0%)	0 (0%)	0 (0%)	0 (0%)	0 (0%)	3 (12%)	4 (16%)	1 (4%)
Positive – Low	0 (0%)	0 (0%)	0 (0%)	0 (0%)	0 (0%)	0 (0%)	1 (100%)	1 (100%)	0 (0%)	1 (4%)	1 (4%)	2 (8%)
Positive – Medium	0 (0%)	0 (0%)	0 (0%)	0 (0%)	0 (0%)	0 (0%)	0 (0%)	0 (0%)	0 (0%)	0 (0%)	0 (0%)	0 (0%)
Positive – High	0 (0%)	0 (0%)	0 (0%)	0 (0%)	0 (0%)	0 (0%)	0 (0%)	0 (0%)	0 (0%)	18 (72%)	18 (72%)	0 (0%)

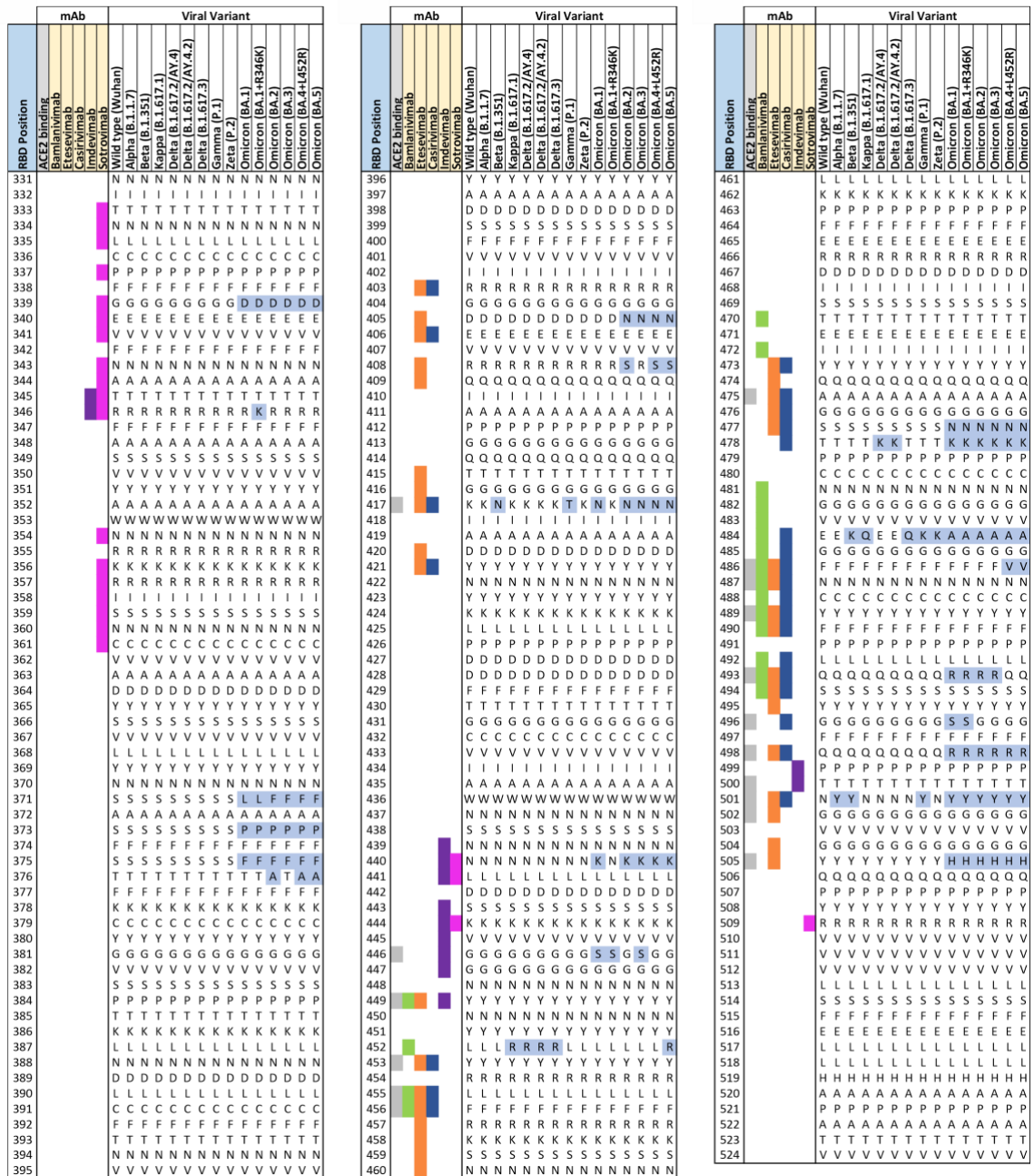
Supplemental Table 6. SARS-CoV-2 Spike antigens of variants of concern (VOCs) tested by ACE2 seroneutralization in relation to the wild-type (Wuhan) SARS-CoV-2 variant. Amino acid modification and commonly used variant of concern (VOC) designations are summarized as described for the utilized V-PLEX Serology Panel (Meso Scale Discovery (MSD)) for VOCs and variants of interest used in this study.

Lineages	Amino Acid Modifications	Common Designation
B.1.1.7	Δ H69-V70, Δ Y144, N501Y, A570D, D614G, P681H, T716I, S982A, D1118H	Alpha
B.1.1.529; BA.1; BA.1.15	A67V, Δ H69-V70, T95I, G142D, Δ 143-145, Δ 211/L212I, ins214EPE, G339D, S371L, S373P, S375F, K417N, N440K, G446S, S477N, T478K, E484A, Q493R, G496S, Q498R, N501Y, Y505H, T547K, D614G, H655Y, N679K, P681H, N764K, D796Y, N856K, Q954H, N969K, L981F	Omicron sub-lineage
B.1.1.529; BA.1+R346K; BA.1.1; BA.1.1.15	A67V, Δ 69-70, T95I, G142D/ Δ 143-145, Δ 211/L212I, ins214EPE, G339D, R346K, S371L, S373P, S375F, K417N, N440K, G446S, S477N, T478K, E484A, Q493R, G496S, Q498R, N501Y, Y505H, T547K, D614G, H655Y, N679K, P681H, N764K, D796Y, N856K, Q954H, N969K, L981F	Omicron sub-lineage
B.1.1.529; BA.2; BA.2.1; BA.2.2; BA.2.3; BA.2.5; BA.2.6; BA.2.7; BA.2.8; BA.2.10; BA.2.12	T19I, (L24-A27)toS, G142D, V213G, G339D, S371F, S373P, S375F, T376A, D405N, R408S, K417N, N440K, S477N, T478K, E484A, Q493R, Q498R, N501Y, Y505H, D614G, H655Y, N679K, P681H, N764K, D796Y, Q954H, N969K	Omicron sub-lineage

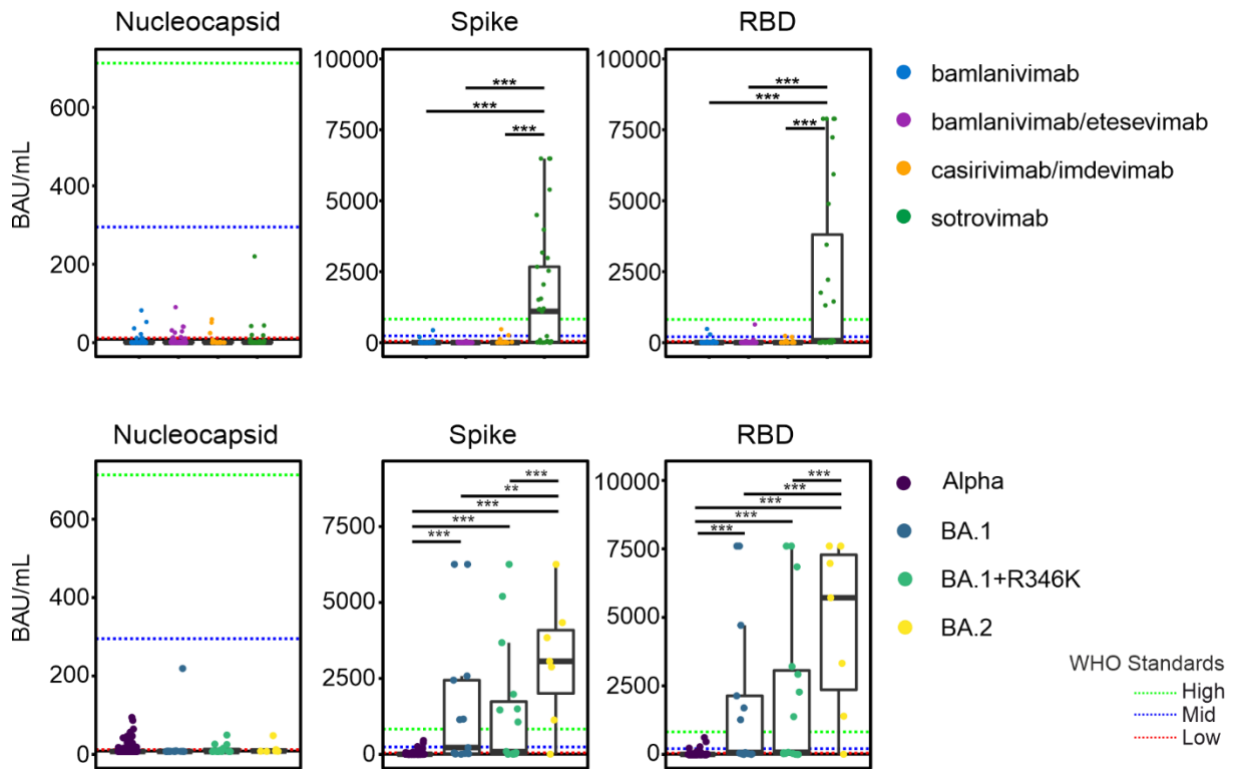
Supplemental Figures



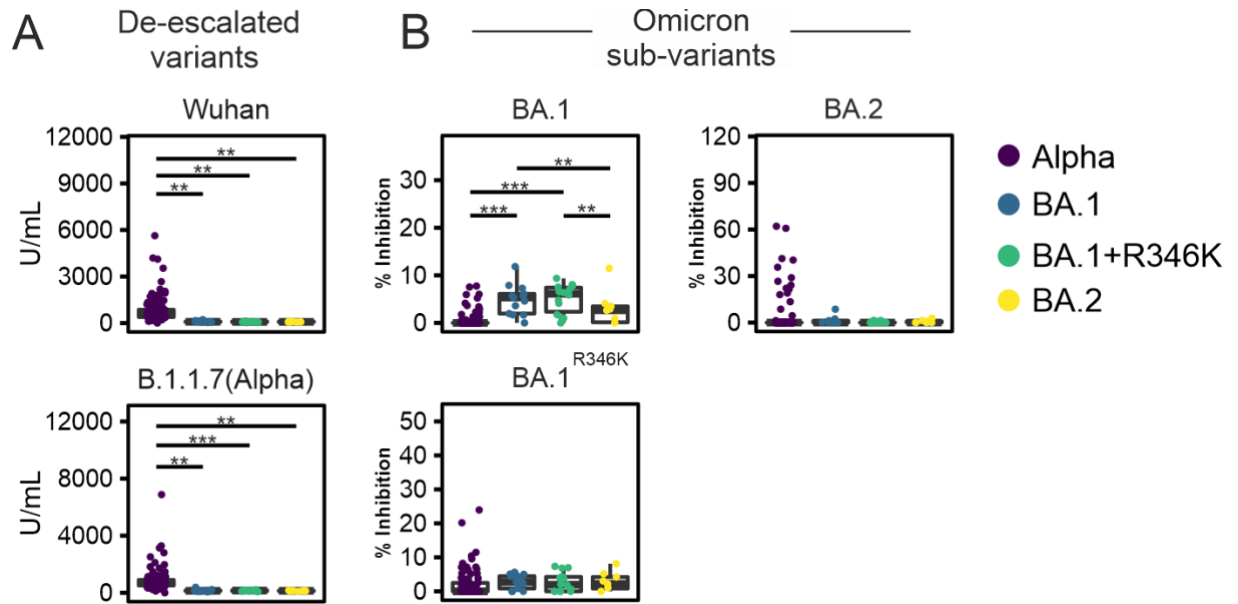
Supplemental Figure 1. Patients receiving mAb treatment develop non-synonymous de novo mutations in the SARS-CoV-2 genome two (D2) to seven days (D7) after mAb infusion. Number of events of unique de novo mutations identified at D2 or D7 compared to D0 (baseline) are plotted across the positions in the SARS-CoV-2 genome. The number of patients developing mutations at specific positions in the SARS-CoV-2 genome are displayed for patients receiving bamlanivimab, bamlanivimab/etesevimab, casirivimab/imdevimab, or sotrovimab in the study. Only non-synonymous mutations are indicated in the figure. The Spike gene is highlighted in yellow, whereas Spike RBD is indicated in gray. D0: sample collected prior to mAb infusion. D2: 2 ± 1 days after mAb infusion. D7: 7 ± 2 days after mAb infusion. For more details, see Supplemental Table 4.



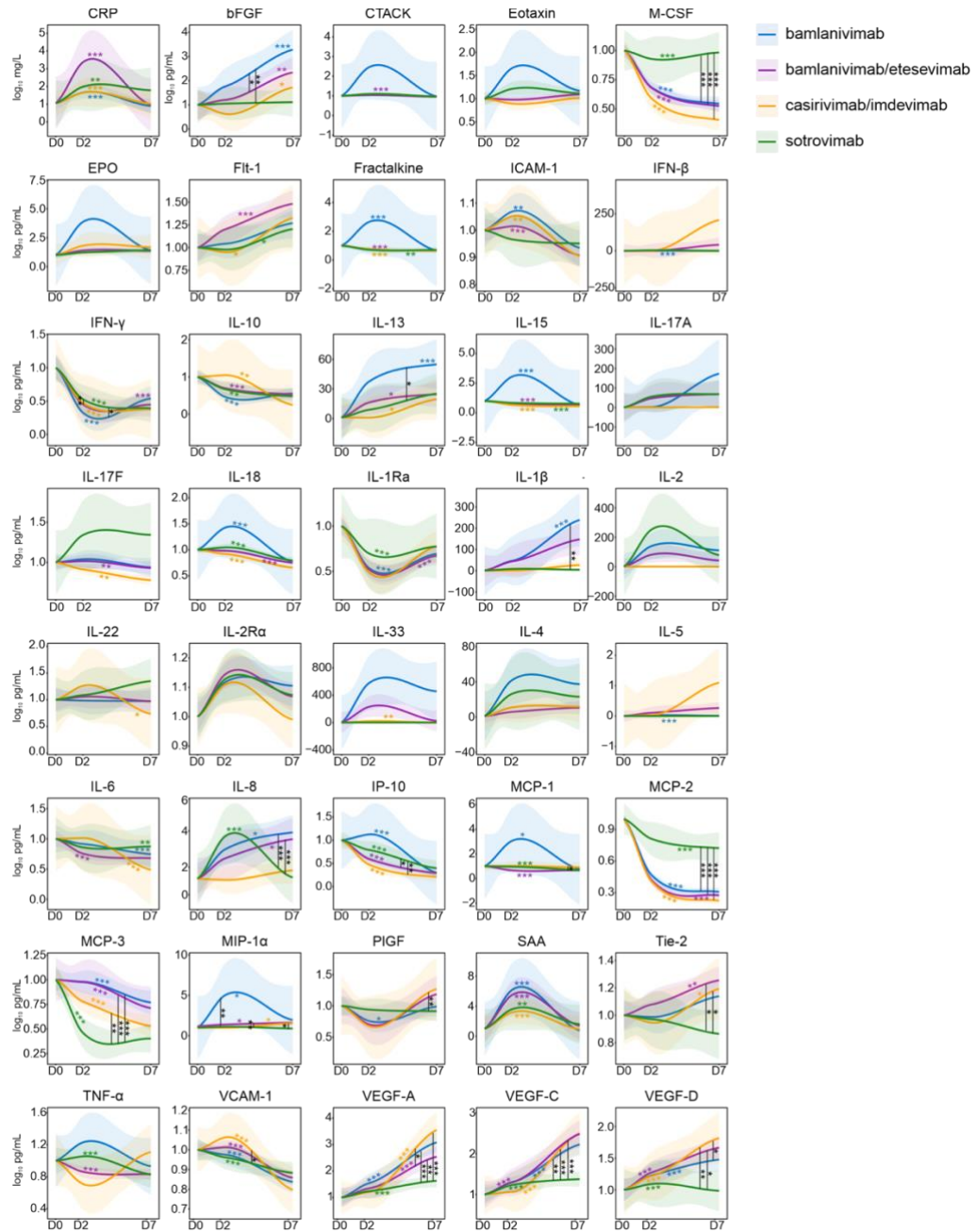
Supplemental Figure 2. Multiple-sequence alignment of Spike RBD protein sequences of different SARS-CoV-2 variants and binding sites for human ACE2 (grey), bamlanivimab (green), etesevimab (orange), casirivimab (blue), imdevimab (purple), and sotrovimab (magenta). Spike RBD sequences from Wuhan (NC_045512), Alpha (B.1.1.7: EPI_ISL_674612), Beta (B.1.351: EPI_ISL_940877), Kappa (B.1.617.1: EPI_ISL_1384866), Delta (B.1.617.2/AY.4: EPI_ISL_1758376, B.1.617.2/AY.4.2: OX014422; B.1.617.3: MZ359842), Gamma (P.1: EPI_ISL_2777382), Zeta (P.2: EPI_ISL_717936), and Omicron (BA.1: EPI_ISL_6795848, BA.1+R346K: EPI_ISL_8724963, BA.2: EPI_ISL_8135710, BA.3: OM508650, BA.4+L452R: EPI_ISL_11542550, BA.5: EPI_ISL_11542604) are displayed. Non-synonymous amino acid residues compared to the Wuhan reference are highlighted in blue. Adapted from ref. (1).



Supplemental Figure 3. Anti-N, anti-S, and anti-RBD serology titers of patients receiving mAb therapy at D0 stratified by therapy and variant. Red, green, and blue dotted lines indicate SARS-CoV-2 WHO reference standard values for low, medium, and high antibody titers, respectively. Longitudinal statistical comparisons were performed using Mann-Whitney followed by Bonferroni post-hoc correction. Box plots indicate median (middle line), 25th, 75th percentile (box), and 5th and 95th percentile (whiskers). All data points, including outliers, are displayed. **: $p < 0.01$. ***: $p < 0.001$. D0: sample collected prior to mAb infusion. BAU: Binding antibody units.



Supplemental Figure 4. Anti-S neutralization capacity of Alpha (B.1.1.7/Q4), BA.1, BA.1+R346K, and BA.2 was measured against (A) de-escalated variants, as well as (B) Omicron sub-variants at D2. Anti-S neutralizing antibody measurements against 5 different SARS-CoV-2 variants of concern in patients infected with Alpha, BA.1, BA.1+R346K, and BA.2 variants. Statistical assessments were performed using pairwise t-tests with Bonferroni post-hoc correction. Box plots indicate median (middle line), 25th, 75th percentile (box), and 5th and 95th percentile (whiskers). All data points, including outliers, are displayed. **: $p < 0.01$. ***: $p < 0.001$.



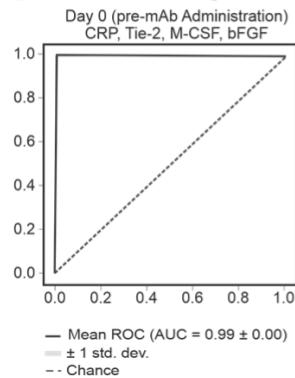
Supplemental Figure 5. Temporal evolution of circulating immune-related biomarkers (CIBs) in patients receiving bamlanivimab, bamlanivimab/etesevimab, casirivimab/imdevimab, or sotrovimab therapy. Time is represented as days after mAb therapy (D0, D2, and D7). Cross-sectional and longitudinal statistical comparisons were performed using Mann-Whitney followed by Bonferroni post-hoc correction. Lines represent smoothed conditional means for studied timepoints and shaded area display 95% confidence intervals for all measured timepoints. Colored asterisks in the graph refer to the significance of the slope from the 4 separate regression lines. Vertical lines with asterisks represent the significance of the pairwise comparison between the slopes in bamlanivimab, bamlanivimab/etesevimab, casirivimab/imdevimab, and sotrovimab therapy groups. D0: sample collected prior to mAb infusion. D2: 2 ± 1 days after mAb infusion. D7: 7 ± 2 days after mAb infusion. D28: 28 ± 4 days after mAb infusion. *: $p < 0.05$. **: $p < 0.01$. ***: $p < 0.001$.

A

Patient characteristics	Non mutation (n=17)	Mutation carriers (n=2)	P-value
Sotrovimab therapy (Spike RBD amino acid substitution)	7 (41.2)	1 (K346R, L371S, P373S, F375S)	NA
Tixagevimab/cilgavimab therapy (Spike RBD amino acid substitution)	10 (58.8)	1 (R408S)	NA
Male (%)	9 (52.9)	1 (50.0)	NS
Age (mean, IQR or range)*	66 (62-75)	62 (51-72)	NS
< 65 years	57 (52-64)	51 (51-51)	NS
≥ 65 years	76 (72-79)	72 (72-72)	NS
BMI (median, IQR or range)	28 (25-31)	22 (21-24)	NS
WHO progression severity scale – At enrolment (mean, IQR or range)*	2 (2-3)	3 (2-3)	NS
WHO progression severity scale – Worst (mean, IQR or range)*	2 (2-3)	3 (2-3)	NS
Days from symptoms onset to mAb infusion (mean, IQR or range)*	2 (1-3)	3 (2-3)	NS
sO2 % (mean, IQR or range)*	97 (96-98)	96 (94-97)	NS
Anti-SARS-CoV-2 vaccination (>2 weeks post-dose, ≥2 doses, %)	16 (94.1)	2 (100)	NS
Ongoing COVID-related therapy (prednisone, azithromycin, amoxicillin/clavulanate)	0 (0.0)	0 (0.0)	NS
Immunocompromising condition (%)	7 (41.2)	2 (100)	NS
Solid organ cancer (with ongoing therapy/ongoing stopped < 6 mo) (%)	1 (5.9)	0 (0.0)	NS
Hematologic cancer (with ongoing CHT/ongoing stopped < 6 mo) (%)	3 (17.6)	1 (50.0)	NS
Solid organ transplant recipients (%)	0 (0.0)	0 (0.0)	NS
Immunological diseases requiring immunosuppressive agents (%)	4 (23.5)	1 (50.0)	NS
Other comorbidities			
Diabetes (with or without damage) (%)	2 (11.8)	0 (0.0)	NS
Cardiovascular disease (ischemic/arrhythmia/hypertension) (%)	9 (52.9)	0 (0.0)	NS
Chronic renal failure (with or without need of dialysis) (%)	0 (0.0)	0 (0.0)	NS
Chronic pulmonary diseases (%)	5 (29.4)	1 (50.0)	NS
Any neurological/vascular disease (%)	1 (5.9)	0 (0.0)	NS
Viral variant			
BA.1/Omicron (%)	3 (17.6)	0 (0.0)	NS
BA.1+R346K/Omicron (%)	1 (5.9)	1 (50.0)	
BA.2/Omicron (%)	7 (41.2)	0 (0.0)	
BA.4/Omicron (%)	1 (5.9)	0 (0.0)	
BA.5/Omicron (%)	2 (11.8)	0 (0.0)	
BE.1/Omicron (%)	1 (5.9)	1 (50.0)	

*: where n=2, ranges are displayed; NA: not applicable; NS: non-significant,

B Machine Learning Classifier

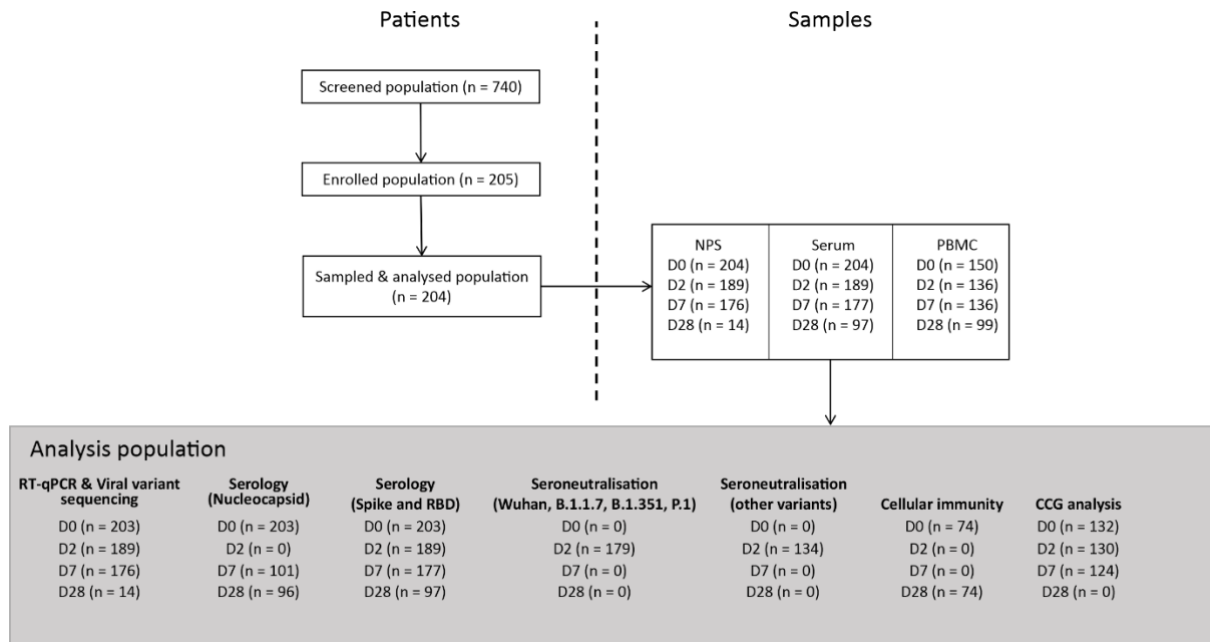


C

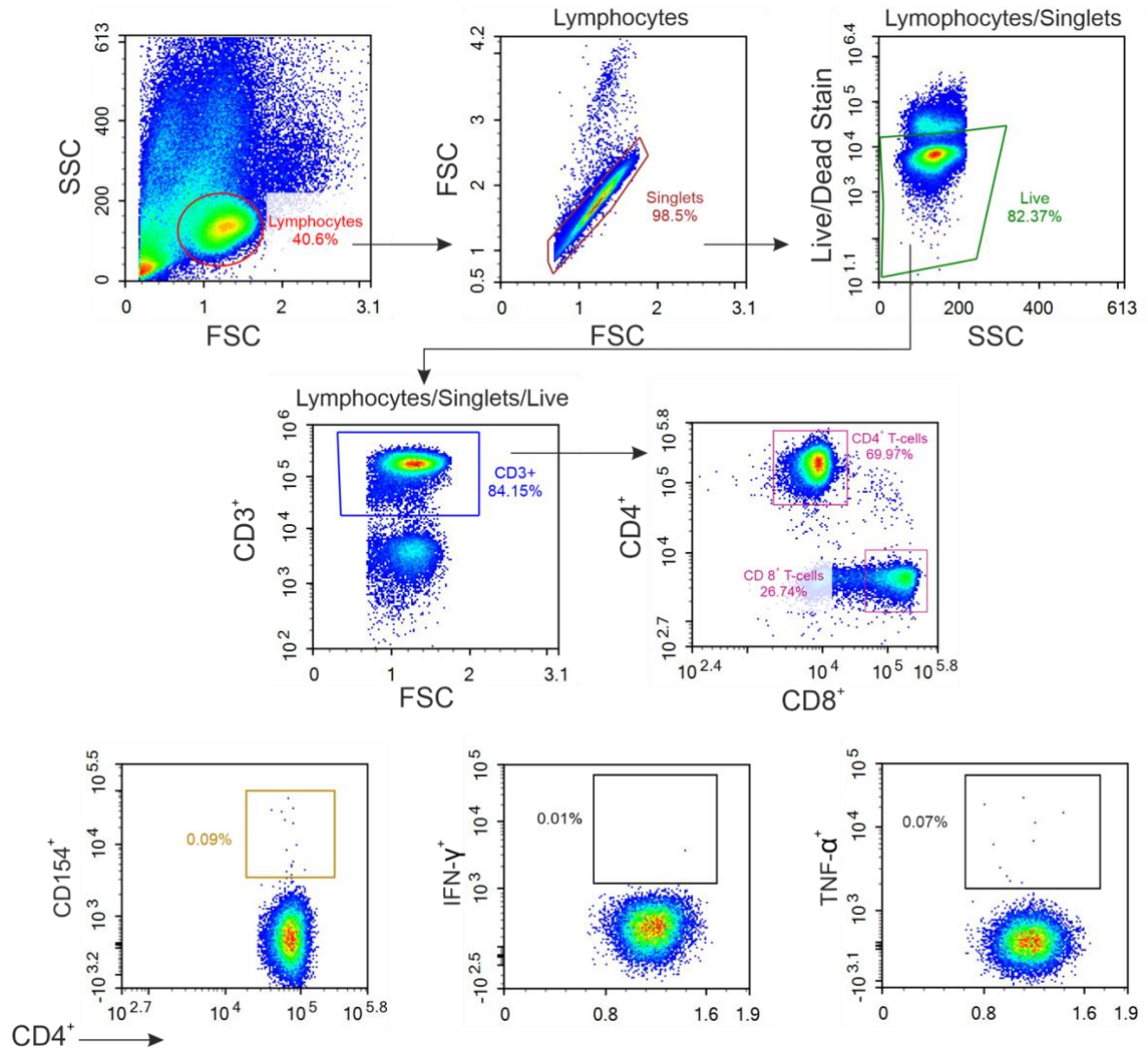
Regression classification

		Mutations		Percentage Correct
		No	Yes	
Mutations	No	17	0	100
	Yes	0	2	100
Overall Percentage				100

Supplementary Figure 6. Out-of-sample performance of circulating immune-related biomarkers (CIBs) predicting *de novo* SARS-CoV-2 Spike RBD mutations in COVID-19 patients receiving mAb therapy. (A) Clinical characteristics of the enrolled patients for CIB validation. Statistical assessments of categorical and continuous variables were assessed across mAb therapy groups using chi-square tests of independence and analysis of variance (ANOVA), respectively. IQR: interquartile range. mo: months. (B) Utilizing random forest classification with SMOTE analysis based on a CIB panel comprising 4 biomarkers (CRP, Tie-2, M-CSF, and bFGF) before mAb treatment predicted *de novo* Spike RBD mutation development with AUROC of 0.99 within seven days of treatment. (C) Binomial logistic regression also predicted patients with or without *de novo* Spike RBD mutations with 100% accuracy.



Supplemental Figure 7. Overview of patient and sample inclusion in the study. D0: sample collected prior to mAb infusion. D2: 2 ± 1 days after mAb infusion. D7: 7 ± 2 days after mAb infusion. D28: 28 ± 4 days after mAb infusion.



Supplemental Figure 8. Representative flow cytometry plots for analysis of activated CD4⁺ T helper (Th) cells and their expression of effector cytokines. Gating strategy after specific stimulation with either a SARS-CoV-2 Nucleocapsid or a complete Spike peptide pool. PBMCs were gated on lymphocytes. Singlets were gated with dead cells excluded. Live CD3⁺ T cells were identified. Within the CD4⁺ Th cell populations activated CD154⁺ Th cells were gated, and the expression of IFN- γ and TNF- α analyzed. PBMC: Peripheral blood mononuclear cells

References

1. Harvey WT, Carabelli AM, Jackson B, Gupta RK, Thomson EC, Harrison EM, et al. SARS-CoV-2 variants, spike mutations and immune escape. *Nat Rev Microbiol.* 2021;19(7):409-24.
2. Liu Z, VanBlargan LA, Bloyet LM, Rothlauf PW, Chen RE, Stumpf S, et al. Identification of SARS-CoV-2 spike mutations that attenuate monoclonal and serum antibody neutralization. *Cell host & microbe.* 2021;29(3):477-88.e4.

3. Ai J, Wang X, He X, Zhao X, Zhang Y, Jiang Y, et al. Antibody evasion of SARS-CoV-2 Omicron BA.1, BA.1.1, BA.2, and BA.3 sub-lineages. *Cell Host Microbe*. 2022;30(8):1077-83.e4.
4. Huang M, Wu L, Zheng A, Xie Y, He Q, Rong X, et al. Atlas of currently available human neutralizing antibodies against SARS-CoV-2 and escape by Omicron sub-variants BA.1/BA.1.1/BA.2/BA.3. *Immunity*. 2022;55(8):1501-14.e3.
5. Andreano E, Piccini G, Licastro D, Casalino L, Johnson NV, Paciello I, et al. SARS-CoV-2 escape from a highly neutralizing COVID-19 convalescent plasma. *Proc Natl Acad Sci U S A*. 2021;118(36).
6. Andreano E, and Rappuoli R. SARS-CoV-2 escaped natural immunity, raising questions about vaccines and therapies. *Nat Med*. 2021;27(5):759-61.
7. Lee JS, Yun KW, Jeong H, Kim B, Kim MJ, Park JH, et al. SARS-CoV-2 shedding dynamics and transmission in immunosuppressed patients. *Virulence*. 2022;13(1):1242-51.
8. Harari S, Tahor M, Rutsinsky N, Meijer S, Miller D, Henig O, et al. Drivers of adaptive evolution during chronic SARS-CoV-2 infections. *Nat Med*. 2022;28(7):1501-8.
9. Lythgoe KA, Hall M, Ferretti L, de Cesare M, MacIntyre-Cockett G, Trebes A, et al. SARS-CoV-2 within-host diversity and transmission. *Science*. 2021;372(6539).
10. Braun KM, Moreno GK, Wagner C, Accola MA, Rehrauer WM, Baker DA, et al. Acute SARS-CoV-2 infections harbor limited within-host diversity and transmit via tight transmission bottlenecks. *PLoS Pathog*. 2021;17(8):e1009849.
11. Tonkin-Hill G, Martincorena I, Amato R, Lawson ARJ, Gerstung M, Johnston I, et al. Patterns of within-host genetic diversity in SARS-CoV-2. *Elife*. 2021;10.
12. Valesano AL, Rumpfelt KE, Dimcheff DE, Blair CN, Fitzsimmons WJ, Petrie JG, et al. Temporal dynamics of SARS-CoV-2 mutation accumulation within and across infected hosts. *PLoS Pathog*. 2021;17(4):e1009499.
13. Gupta A, Gonzalez-Rojas Y, Juarez E, Crespo Casal M, Moya J, Falci DR, et al. Early Treatment for Covid-19 with SARS-CoV-2 Neutralizing Antibody Sotrovimab. *N Engl J Med*. 2021;385(21):1941-50.
14. Planas D, Saunders N, Maes P, Guivel-Benhassine F, Planchais C, Buchrieser J, et al. Considerable escape of SARS-CoV-2 Omicron to antibody neutralization. *Nature*. 2022;602(7898):671-5.
15. Pinto D, Park YJ, Beltramello M, Walls AC, Tortorici MA, Bianchi S, et al. Cross-neutralization of SARS-CoV-2 by a human monoclonal SARS-CoV antibody. *Nature*. 2020;583(7815):290-5.
16. Dong J, Zost SJ, Greaney AJ, Starr TN, Dingens AS, Chen EC, et al. Genetic and structural basis for SARS-CoV-2 variant neutralization by a two-antibody cocktail. *Nat Microbiol*. 2021;6(10):1233-44.

17. Javanmardi K, Segall-Shapiro TH, Chou CW, Boutz DR, Olsen RJ, Xie X, et al. Antibody escape and cryptic cross-domain stabilization in the SARS-CoV-2 Omicron spike protein. *Cell host & microbe*. 2022;30(9):1242-54.e6.
18. Taylor PC, Adams AC, Hufford MM, de la Torre I, Winthrop K, and Gottlieb RL. Neutralizing monoclonal antibodies for treatment of COVID-19. *Nat Rev Immunol*. 2021;21(6):382-93.
19. Savoldi A, Morra M, De Nardo P, Cattelan AM, Mirandola M, Manfrin V, et al. Clinical efficacy of different monoclonal antibody regimens among non-hospitalised patients with mild to moderate COVID-19 at high risk for disease progression: a prospective cohort study. *Eur J Clin Microbiol Infect Dis*. 2022;41(7):1065-76.
20. Savoldi A, Morra M, Castelli A, Mirandola M, Berkell M, Smet M, et al. Clinical Impact of Monoclonal Antibodies in the Treatment of High-Risk Patients with SARS-CoV-2 Breakthrough Infections: The ORCHESTRA Prospective Cohort Study. *Biomedicines*. 2022;10(9):2063.
21. Ganesh R, Pawlowski CF, O'Horo JC, Arndt LL, Arndt RF, Bell SJ, et al. Intravenous bamlanivimab use associates with reduced hospitalization in high-risk patients with mild to moderate COVID-19. *The Journal of Clinical Investigation*. 2021;131(19).
22. Gottlieb RL, Nirula A, Chen P, Boscia J, Heller B, Morris J, et al. Effect of Bamlanivimab as Monotherapy or in Combination With Etesevimab on Viral Load in Patients With Mild to Moderate COVID-19: A Randomized Clinical Trial. *Jama*. 2021;325(7):632-44.
23. Razonable RR, Pawlowski C, O'Horo JC, Arndt LL, Arndt R, Bierle DM, et al. Casirivimab-Imdevimab treatment is associated with reduced rates of hospitalization among high-risk patients with mild to moderate coronavirus disease-19. *EClinicalMedicine*. 2021;40:101102.
24. Montgomery H, Hobbs FDR, Padilla F, Arbetter D, Templeton A, Seegobin S, et al. Efficacy and safety of intramuscular administration of tixagevimab-cilgavimab for early outpatient treatment of COVID-19 (TACKLE): a phase 3, randomised, double-blind, placebo-controlled trial. *Lancet Respir Med*. 2022.
25. Simons LM, Ozer EA, Gambut S, Dean TJ, Zhang L, Bhimalli P, et al. De novo emergence of SARS-CoV-2 spike mutations in immunosuppressed patients. *Transpl Infect Dis*. 2022:e13914.
26. Jensen B, Luebke N, Feldt T, Keitel V, Brandenburger T, Kindgen-Milles D, et al. Emergence of the E484K mutation in SARS-COV-2-infected immunocompromised patients treated with bamlanivimab in Germany. *Lancet Reg Health Eur*. 2021;8:100164.
27. Guigon A, Faure E, Lemaire C, Chopin MC, Tinez C, Assaf A, et al. Emergence of Q493R mutation in SARS-CoV-2 spike protein during bamlanivimab/etesevimab treatment and resistance to viral clearance. *J Infect*. 2022;84(2):248-88.
28. Destras G, Bal A, Simon B, Lina B, and Josset L. Sotrovimab drives SARS-CoV-2 omicron variant evolution in immunocompromised patients. *Lancet Microbe*. 2022;3(8):e559.

29. Birnie E, Biemond JJ, Appelman B, de Bree GJ, Jonges M, Welkers MRA, et al. Development of Resistance-Associated Mutations After Sotrovimab Administration in High-risk Individuals Infected With the SARS-CoV-2 Omicron Variant. *JAMA*. 2022.
30. Rockett R, Basile K, Maddocks S, Fong W, Agius JE, Johnson-Mackinnon J, et al. Resistance Mutations in SARS-CoV-2 Delta Variant after Sotrovimab Use. *N Engl J Med*. 2022;386(15):1477-9.
31. Ragonnet-Cronin M, Nutalai R, Huo J, Dijokaite-Guraliuc A, Das R, Tuekprakhon A, et al. Genome-first detection of emerging resistance to novel therapeutic agents for SARS-CoV-2. *bioRxiv*. 2022:2022.07.14.500063.
32. Cevik M, Tate M, Lloyd O, Maraolo AE, Schafers J, and Ho A. SARS-CoV-2, SARS-CoV, and MERS-CoV viral load dynamics, duration of viral shedding, and infectiousness: a systematic review and meta-analysis. *Lancet Microbe*. 2021;2(1):e13-e22.
33. van Kampen JJA, van de Vijver D, Fraaij PLA, Haagmans BL, Lamers MM, Okba N, et al. Duration and key determinants of infectious virus shedding in hospitalized patients with coronavirus disease-2019 (COVID-19). *Nat Commun*. 2021;12(1):267.
34. WHO Working Group on the Clinical Characterisation Management of C-i. A minimal common outcome measure set for COVID-19 clinical research. *Lancet Infect Dis*. 2020;20(8):e192-e7.
35. Iketani S, Liu L, Guo Y, Liu L, Chan JF, Huang Y, et al. Antibody evasion properties of SARS-CoV-2 Omicron sublineages. *Nature*. 2022;604(7906):553-6.
36. Tas JMJ, Koo JH, Lin YC, Xie Z, Steichen JM, Jackson AM, et al. Antibodies from primary humoral responses modulate the recruitment of naive B cells during secondary responses. *Immunity*. 2022;55(10):1856-71.e6.
37. Schaefer-Babajew D, Wang Z, Muecksch F, Cho A, Raspe R, Johnson B, et al. Antibody feedback regulation of memory B cell development in SARS-CoV-2 mRNA vaccination. *medRxiv*. 2022.
38. Darif D, Hammi I, Kihel A, El Idrissi Saik I, Guessous F, and Akarid K. The pro-inflammatory cytokines in COVID-19 pathogenesis: What goes wrong? *Microb Pathog*. 2021;153:104799.
39. Fajgenbaum DC, and June CH. Cytokine Storm. *N Engl J Med*. 2020;383(23):2255-73.
40. Behm B, Babilas P, Landthaler M, and Schreml S. Cytokines, chemokines and growth factors in wound healing. *J Eur Acad Dermatol Venereol*. 2012;26(7):812-20.
41. Boddaert J, Bielen K, s Jongers B, Manocha E, Yperzeele L, Cras P, et al. CD8 signaling in microglia/macrophage M1 polarization in a rat model of cerebral ischemia. *PLoS One*. 2018;13(1):e0186937.
42. Kremlev SG, Chapoval AI, and Evans R. CSF-1 (M-CSF) enhances the inflammatory response of fibronectin-primed macrophages: pathways involved in activation of the cytokine network. *Nat Immun*. 1998;16(5-6):228-43.

43. Meschi S, Matusali G, Colavita F, Lapa D, Bordi L, Puro V, et al. Predicting the protective humoral response to a SARS-CoV-2 mRNA vaccine. *Clin Chem Lab Med.* 2021;59(12):2010-8.
44. Spiekermann GM, Finn PW, Ward ES, Dumont J, Dickinson BL, Blumberg RS, et al. Receptor-mediated immunoglobulin G transport across mucosal barriers in adult life: functional expression of FcRn in the mammalian lung. *J Exp Med.* 2002;196(3):303-10.
45. Cerutti A. The regulation of IgA class switching. *Nat Rev Immunol.* 2008;8(6):421-34.
46. Pabst O. New concepts in the generation and functions of IgA. *Nat Rev Immunol.* 2012;12(12):821-32.
47. Gussow AB, Auslander N, Faure G, Wolf YI, Zhang F, and Koonin EV. Genomic determinants of pathogenicity in SARS-CoV-2 and other human coronaviruses. *Proceedings of the National Academy of Sciences.* 2020;117(26):15193-9.
48. Gelbart M, Harari S, Ben-Ari Y, Kustin T, Wolf D, Mandelboim M, et al. Drivers of within-host genetic diversity in acute infections of viruses. *PLoS Pathog.* 2020;16(11):e1009029.
49. Choi B, Choudhary MC, Regan J, Sparks JA, Padera RF, Qiu X, et al. Persistence and Evolution of SARS-CoV-2 in an Immunocompromised Host. *N Engl J Med.* 2020;383(23):2291-3.
50. Sanjuán R, and Domingo-Calap P. Mechanisms of viral mutation. *Cell Mol Life Sci.* 2016;73(23):4433-48.
51. Mogensen TH, Melchjorsen J, Malmgaard L, Casola A, and Paludan SR. Suppression of proinflammatory cytokine expression by herpes simplex virus type 1. *J Virol.* 2004;78(11):5883-90.
52. Ellinghaus D, Degenhardt F, Bujanda L, Buti M, Albillos A, Invernizzi P, et al. Genomewide Association Study of Severe Covid-19 with Respiratory Failure. *N Engl J Med.* 2020;383(16):1522-34.
53. Corey L, Beyrer C, Cohen MS, Michael NL, Bedford T, and Rolland M. SARS-CoV-2 Variants in Patients with Immunosuppression. *N Engl J Med.* 2021;385(6):562-6.
54. Ripoll JG, Gorman EK, Juskewitch JE, Razonable RR, Ganesh R, Hurt RT, et al. Vaccine-boosted convalescent plasma therapy for patients with immunosuppression and COVID-19. *Blood Adv.* 2022;6(23):5951-5.
55. Estcourt LJ, Cohn CS, Pagano MB, Iannizzi C, Kreuzberger N, Skoetz N, et al. Clinical Practice Guidelines From the Association for the Advancement of Blood and Biotherapies (AABB): COVID-19 Convalescent Plasma. *Ann Intern Med.* 2022;175(9):1310-21.
56. Agarwal A, Rochwerg B, Lamontagne F, Siemieniuk RA, Agoritsas T, Askie L, et al. A living WHO guideline on drugs for covid-19. *Bmj.* 2020;370:m3379.
57. Breiman L. Random Forests. *Machine Learning.* 2001;45(1):5-32.

Supplementary References

1. Arora P, Zhang L, Krüger N, Rocha C, Sidarovich A, Schulz S, et al. SARS-CoV-2 Omicron sublineages show comparable cell entry but differential neutralization by therapeutic antibodies. *Cell host & microbe*. 2022;30(8):1103-11.e6.
2. Savoldi A, Morra M, De Nardo P, Cattelan AM, Mirandola M, Manfrin V, et al. Clinical efficacy of different monoclonal antibody regimens among non-hospitalised patients with mild to moderate COVID-19 at high risk for disease progression: a prospective cohort study. *European journal of clinical microbiology & infectious diseases : official publication of the European Society of Clinical Microbiology*. 2022;41(7):1065-76.
3. Savoldi A, Morra M, Castelli A, Mirandola M, Berkell M, Smet M, et al. Clinical Impact of Monoclonal Antibodies in the Treatment of High-Risk Patients with SARS-CoV-2 Breakthrough Infections: The ORCHESTRA Prospective Cohort Study. *Biomedicines*. 2022;10(9):2063.
4. Shrestha LB, Foster C, Rawlinson W, Tedla N, and Bull RA. Evolution of the SARS-CoV-2 omicron variants BA.1 to BA.5: Implications for immune escape and transmission. *Rev Med Virol*. 2022:e2381.
5. Rockett R, Basile K, Maddocks S, Fong W, Agius JE, Johnson-Mackinnon J, et al. Resistance Mutations in SARS-CoV-2 Delta Variant after Sotrovimab Use. *N Engl J Med*. 2022;386(15):1477-9.
6. Birnie E, Biemond JJ, Appelman B, de Bree GJ, Jonges M, Welkers MRA, et al. Development of Resistance-Associated Mutations After Sotrovimab Administration in High-risk Individuals Infected With the SARS-CoV-2 Omicron Variant. *JAMA*. 2022.
7. Ragonnet-Cronin M, Nutalai R, Huo J, Dijokaite-Guraliuc A, Das R, Tuekprakhon A, et al. Genome-first detection of emerging resistance to novel therapeutic agents for SARS-CoV-2. *bioRxiv : the preprint server for biology*. 2022:2022.07.14.500063.
8. Weisblum Y, Schmidt F, Zhang F, DaSilva J, Poston D, Lorenzi JC, et al. Escape from neutralizing antibodies by SARS-CoV-2 spike protein variants. *eLife*. 2020;9.
9. Zhao Z, Zhou J, Tian M, Huang M, Liu S, Xie Y, et al. Omicron SARS-CoV-2 mutations stabilize spike up-RBD conformation and lead to a non-RBM-binding monoclonal antibody escape. *Nature communications*. 2022;13(1):4958.
10. Guigon A, Faure E, Lemaire C, Chopin MC, Tinez C, Assaf A, et al. Emergence of Q493R mutation in SARS-CoV-2 spike protein during bamlanivimab/etesevimab treatment and resistance to viral clearance. *The Journal of infection*. 2022;84(2):248-88.
11. Jary A, Marot S, Faycal A, Leon S, Sayon S, Zafilaza K, et al. Spike Gene Evolution and Immune Escape Mutations in Patients with Mild or Moderate Forms of COVID-19 and Treated with Monoclonal Antibodies Therapies. *Viruses*. 2022;14(2).
12. Jensen B, Luebke N, Feldt T, Keitel V, Brandenburger T, Kindgen-Milles D, et al. Emergence of the E484K mutation in SARS-COV-2-infected immunocompromised patients treated with bamlanivimab in Germany. *Lancet Reg Health Eur*. 2021;8:100164.

13. Simons LM, Ozer EA, Gambut S, Dean TJ, Zhang L, Bhimalli P, et al. De novo emergence of SARS-CoV-2 spike mutations in immunosuppressed patients. *Transpl Infect Dis.* 2022:e13914.
14. Choi B, Choudhary MC, Regan J, Sparks JA, Padera RF, Qiu X, et al. Persistence and Evolution of SARS-CoV-2 in an Immunocompromised Host. *N Engl J Med.* 2020;383(23):2291-3.
15. Scherer EM, Babiker A, Adelman MW, Allman B, Key A, Kleinhenz JM, et al. SARS-CoV-2 Evolution and Immune Escape in Immunocompromised Patients. *N Engl J Med.* 2022;386(25):2436-8.

Chapter 6: Neutralization capacity of bamlanivimab with or without etesevimab, casirivimab/imdevimab, sotrovimab and tixagevimab/cilgavimab monoclonal antibodies against currently circulating SARS-CoV-2 Omicron variants

Angelina Konnova^{1,2*}, Alessia Savoldi^{3*}, Akshita Gupta^{1,2*}, Matteo Morra³, Matilda Berkell^{1,2}, Mathias Smet^{1,2}, An Hotterbeekx¹, Elda Righi³, mAb ORCHESTRA working group, Surbhi Malhotra-Kumar², Pasquale De Nardo³, Evelina Tacconelli³, Samir Kumar-Singh^{1,2}

mAb ORCHESTRA working group: Vincent Van averbeke¹, Fien De Winter¹, Shahla Mahmoudi¹, Nour Chebly², Basil Britto Xavier², Chiara Zanchi³, Giulia Rosini³, Rebecca Scardellato³, Laura Rovigo³, Francesco Luca³, Lorenzo Tavernaro³, Salvatore Hermes Dall'O³, Chiara Konishi De Toffoli³, Concetta Sciammarella³, Michela Conti³, Massimo Mirandola^{3,5}, Denise Peserico⁴, Elisa Danese⁴, Giuseppe Lippi⁴, Matteo Gelati⁴, Riccardo Cecchetto⁶, Davide Gibellini⁶

¹Molecular Pathology Group, Cell Biology & Histology, Faculty of Medicine and Health Sciences, University of Antwerp, Antwerp, Belgium

²Laboratory of Medical Microbiology, Vaccine & Infectious Disease Institute, University of Antwerp, Antwerp, Belgium

³Division of Infectious Diseases, Department of Diagnostics and Public Health, University of Verona, Verona, Italy

⁴Section of Clinical Biochemistry, University of Verona, Verona, Italy

⁵School of Health Sciences, University of Brighton, Brighton, United Kingdom

⁶Section of Microbiology, Department of Diagnostics and Public Health, University of Verona, Verona, Italy

** Shared first authors: Angelina Konnova performed serology, seroneutralization, and the analyses of cytokine, chemokine and growth factors, which are part of this thesis. Clinical data was collected by Alessia Savoldi. T cell immunity was performed by Akshita Gupta (not a part of this thesis)*

Correspondence: samir.kumarsingh@uantwerpen.be

Manuscript ready for submission

Abstract

Background: Monoclonal antibodies (mAbs) provide a new line of pre-exposure prophylaxis and/or post-exposure treatment for vulnerable patients at high risk of developing severe COVID-19. A varying ability of different mAbs to neutralize SARS-CoV-2 variants has recently been observed in in vitro studies, where a majority of mAbs exhibited a significantly lowered or completely compromised ability to neutralize Omicron variants. However, the varying ability of patients to metabolize different mAbs, different doses, and different modes of administration require careful clinical assessment.

Methods: Within H2020 ORCHESTRA project, mild-to-moderately ill COVID-19 patients receiving bamlanivimab, bamlanivimab/etesevimab, casirivimab/imdevimab, sotrovimab or tixagevimab/cilgavimab (n = 223) were studied for their neutralizing capacities against 32 SARS-CoV-2-CoV-2 variants of concern (VOCs) by an ACE2 neutralization assay. Since tixagevimab/cilgavimab got approval for prophylaxis, but was used in patients exposed to SARS-CoV-2, we also studied the kinetics and neutralization capacities of tixagevimab/cilgavimab for up to 28 days after administration and compared with the kinetics and neutralization capacities of other therapeutic mAbs.

Results: For intramuscularly (i.m.) administered tixagevimab/cilgavimab, anti-Spike and anti-RBD titres as well as seroneutralization against Wuhan wild-type peaked at Day 28, compared to all other mAbs that peaked immediately after administration (assessed at Day 2). Studying seroneutralization response against 32 VOCs at Day 2, casirivimab/imdevimab combination was the most effective therapy against the majority of SARS-CoV-2 variants, including de-escalated, Delta and Omicron variants and subvariants (BA.2, BA.2L452M, BA.2.12, BA.2.75, BA.4.,6 and BF.7). However, for other Omicron sub-variants (BA.1, BA.1L452R, BA.1R346K, BA.2L452R, BA.2.75.2, BA.3, BQ.1, BQ.1.1, and XBB.1), sotrovimab demonstrated a superior neutralization capacity. Additionally, casirivimab/imdevimab, sotrovimab, and tixagevimab/cilgavimab demonstrated comparable neutralization against BA.4 and BA.5. Specific mutations, such as L452R, drove mAb resistance. Lastly, we report here a high inter-patient variability in the titres and neutralization capacities of the studied mAbs suggesting that host-derived factors influence the pharmacokinetics (PK) characteristics of anti-SARS-CoV-2 mAbs.

Conclusions: Here we show comparative data of at least three commonly used mAbs in the treatment of mild-to-moderately ill COVID-19 patients. Our data suggest that clinicians should take the circulating variant into consideration while prescribing different mAbs. Lastly, our data do not support the use of i.m.-administered tixagevimab/cilgavimab over other mAb, if equally effective in neutralizing the relevant VOC.

Introduction

The COVID-19 pandemic has underscored the urgent need for effective therapeutics to combat the SARS-CoV-2 infections. Monoclonal antibodies (mAbs) have emerged as a promising class of therapeutics for the treatment of COVID-19 due to their ability to target specific viral proteins and neutralize the virus, potentially preventing disease progression. In this study, we compared the efficacy of five different mAbs, bamlanivimab, bamlanivimab/etesevimab, casirivimab/imdevimab, sotrovimab, and tixagevimab/cilgavimab, in the treatment of COVID-19 patients.

While vaccines remain the best strategy to prevent COVID-19, mAbs benefits certain vulnerable populations before or after exposure to SARS-CoV-2, such as the unvaccinated or recently vaccinated high-risk patients, when other COVID-19 treatments cannot be instituted. Thus, in 2021–2022, bamlanivimab, bamlanivimab/etesevimab, casirivimab/imdevimab, and sotrovimab got Emergency Use Authorization (EUA) for treatment of mild-to-moderate COVID-19, or post-exposure prophylaxis for COVID-19¹⁻⁵. Tixagevimab/cilgavimab on the other hand got approval for pre-exposure prophylaxis (see **Introduction (Part B), Table 2**).

However, as SARS-CoV-2 evolved, a varying ability to neutralize different SARS-CoV-2 variants was observed in *in vitro* studies, with a majority of mAbs exhibiting a significantly lowered or completely compromised ability to neutralize Omicron variants⁶⁻⁸. Moreover, *in vitro* studies have demonstrated that mAbs were largely inactive against successive sub-lineages of Omicron, such as BQ.1, BQ.1.1, XBB and XBB.1^{9,10}. This loss of effectiveness against currently circulating SARS-CoV-2 variant has led to the withdrawal of EUA for all anti-Spike mAb therapies by US Food and Drug Administration (FDA), while authorisation by European Medical Agency (EMA) exists for casirivimab/imdevimab, sotrovimab, and tixagevimab/cilgavimab. This is specifically to tackle management of severe COVID-19 in immunocompromised populations or pre-exposure prophylaxis, especially in conjunction with the rapid emergence of treatment resistance⁵.

Mutation-prone nature of SARS-CoV-2 has highlighted the need for more polyclonal antibody preparations, however, the success of polyclonal preparations is dependent on their pharmacokinetic properties, as they markedly differ from those of non-mAb drugs¹¹. For example, distribution of antibodies, such as IgGs, into tissue is slow because of the molecular size of mAbs, and volumes of distribution are generally low. The mode of administration is also critical for the pharmacokinetics of mAbs with low to intermediate bioavailability upon intramuscular or subcutaneous administration, compared to intravenous administration. Additionally, despite the fact that pharmacokinetic interactions are generally not to be expected with mAb co-treatment, other patient characteristics, such as altered function of phagocytic cells of the immune system, might affect mAb metabolism in certain patient populations. To the best of our knowledge, while extensive studies have been performed *in vitro*, clinical studies comparing neutralizing capacity of anti-SARS-CoV-2 mAbs are as yet limited^{12,13}. This is important as relative efficacy of different combinations of mAbs has yet to be fully investigated for potential future reuse of existing therapies.

Here, we compare the neutralizing capacities of five different mAbs or their combinations, specifically bamlanivimab, bamlanivimab/etesevimab, casirivimab/imdevimab, sotrovimab, and tixagevimab/cilgavimab, in the treatment of COVID-19 patients against 23 SARS-CoV-2 variants of concern (VOCs). We also provide important insights into the relative efficacy of different mAbs

regimens and their interplay with key phagocytic cytokines during the management of COVID-19 and guide the clinical use of these mAbs.

Material and Methods

Trial design and sample collection

This is a prospective, observational, monocentric ORCHESTRA cohort study to evaluate SARS-CoV-2 mAbs for the treatment of mild-to-moderately ill COVID-19 patients in the Outpatient Clinic, Infectious Diseases Section of the University Hospital of Verona, Italy⁵. Eligible population constituted non-hospitalized adults (≥ 18 years) with symptomatic SARS-CoV-2 infection.

Between 9 March 2021 to 30 November 2022, a total of 223 outpatients ($n=223$) aged ≥ 18 years, presenting with mild-to-moderate COVID-19 (confirmed by quantitative real-time Reverse Transcription (RT-q)PCR or a positive antigenic 3rd generation test) and at high risk for clinical worsening in accordance with Italian Medicine Agency indications (for definition see ref. ⁴) were enrolled and received bamlanivimab ($n = 45$), bamlanivimab/etesevimab ($n = 108$), casirivimab/imdevimab ($n = 17$), sotrovimab ($n = 34$), or tixagevimab/cilgavimab ($n = 18$). Inclusion/exclusion criteria for patient enrolment have been published ^{3,4}.

Samples were collected from enrolled patients to study the effect of mAb therapy on mAb kinetics and neutralization capacity of mAb and were analyzed within ORCHESTRA WP6. For each enrolled patient, 4 timepoints were analysed: (i) D0: just prior to mAb infusion, (ii) D2: 2 ± 1 days after mAb infusion at D0, (iii) D7: 7 ± 2 days after mAb infusion at D0, and (iv) D28: 28 ± 4 days after mAb infusion. Serum samples were collected along with clinical data.

SARS-CoV-2 viral load and confirmation

RNA was extracted using the MagMAX Viral/Pathogen II Nucleic acid kit on a KingFisher Flex Purification System (ThermoFisher). Real-Time RT-qPCR was performed using the TaqPath™ COVID-19 CE-IVD RT-PCR Kit (ThermoFisher) on a QuantStudio™ 5 Real Time PCR instrument (384-well block, 5 colors, ThermoFisher).

Serology

Blood was collected in 10 mL serum tubes (BD biosciences) and serum samples were prepared within 3h of blood collection. Anti-N, anti-S, and anti-RBD SARS-CoV-2 IgG titres were measured in serum samples using a multiplexed panel (Meso Scale Discovery (MSD)) and data provided in WHO-recommended BAU units.

ACE2 neutralization measurements in serum

ACE2 neutralization was measured in serum samples against Wuhan, B.1.1.7, B.1.351, P.1, P.2, B.1.526.1, B.1.617, B.1.617.1, B.1.617.2 (AY.3); B.1.617.2 (AY 4), B.1.617.2 (AY 4.2) 2, B.1.617.3, BA.1, BA.1^{L452R}, BA.1^{R346K}, BA.2, BA.2^{L452M}, BA.2^{L452R}, BA.2.12.1, BA.2.75, BA.2.75.2, BA.3, BA.4, BA.4.6, BA.5, BF.7, BN.1, BQ.1, BQ.1.1, XBB.1, and XBB.1.5 using V-PLEX SARS-CoV-2 Panels 6, 13, 23, 25, 27, 29 and 32 (ACE2) on the QuickPlex SQ 120 system (MSD) according to the manufacturer instructions. Measurements for all variant, except B.1.617.2 (AY 4.2), BA.1^{L452R}, and BA.1^{R346K}, were performed in duplicates.

Measurements of circulating immune-related biomarkers (CIB) in serum

CIBs were measured in serum samples using U-plex and V-plex panels (#K15198D, #K15190D) on the QuickPlex SQ 120 system (MSD), according to the manufacturer instructions. The following 40 CIBs were measured for D0, D2, and D7 timepoints: basic fibroblast growth factor (bFGF), C-reactive protein (CRP), cutaneous T-cell attracting chemokine (CTACK), eotaxin, erythropoietin (EPO), vascular endothelial growth factor receptor 1 (Flt-1), fractalkine, macrophage colony-stimulating factor (M-CSF), interferon β (IFN- β), interferon γ (IFN- γ), interleukin (IL)-1 β , IL-1 receptor antagonist (IL-1Ra), IL-2, IL-2 receptor α (IL-2R α), IL-4, IL-5, IL-6, IL-8, IL-10, IL-13, IL-15, IL-17A, IL-17F, IL-18, IL-22, IL-33, IFN- γ induced protein 10 (IP-10), monocyte chemoattractant protein (MCP)-1, MCP-2, MCP-3, macrophage inflammatory protein (MIP)-1 α , placental growth factor (PIGF), serum amyloid A (SAA), soluble intercellular adhesion molecule 1 (sICAM-1), soluble vascular cell adhesion molecule 1 (sVCAM-1), angiotensin receptor 1 (Tie-2), tumor necrosis factor α (TNF- α), vascular endothelial growth factor (VEGF)-A, VEGF-C, and VEGF-D

Statistics

All data were statistically analyzed and visualized in Rstudio v.1.3.1073 using R v.4.0.4. One-way analysis of variance (ANOVA) was utilized for longitudinal and cross-sectional comparisons of IgG titres and titres of neutralizing antibodies. Pearson correlation coefficient was used to assess correlations between Ct values, cytokine concentrations and neutralizing antibody titres. Throughout the statistical analyses, values below the detection range were recorded as 1/10th the lower limit of quantitation (LLQ) and values above the detection range were recorded as upper limit of quantitation (ULQ). A (corrected) p-value < 0.05 was considered statistically significant.

Results

Tixagevimab/cilgavimab should not be recommended for the treatment of acute COVID-19

We first demonstrated that bamlanivimab, bamlanivimab/etesevimab, casirivimab/imdevimab and sotrovimab, administered intravenously, indeed reached the highest anti-Spike and anti-RBD IgG titres at the first studied timepoint after mAb administration (individual trends published in⁵) (**Figure 1**). Despite the fact that anti-Spike and anti-RBD titres remained significantly higher throughout the whole study than the titres achieved naturally post vaccination or infection, we observed a significant reduction by Day 7 and further reduction at Day 28.

However, a different kinetics trend was observed for tixagevimab/cilgavimab, a combination of intramuscularly administered mAbs, for which the titres continued to increase throughout the study period, reaching the highest concentration at Day 28 (Figure 1). Similar trend was observed in terms of seroneutralisation, suggesting that tixagevimab/cilgavimab requires a longer period of time to reach high titres.

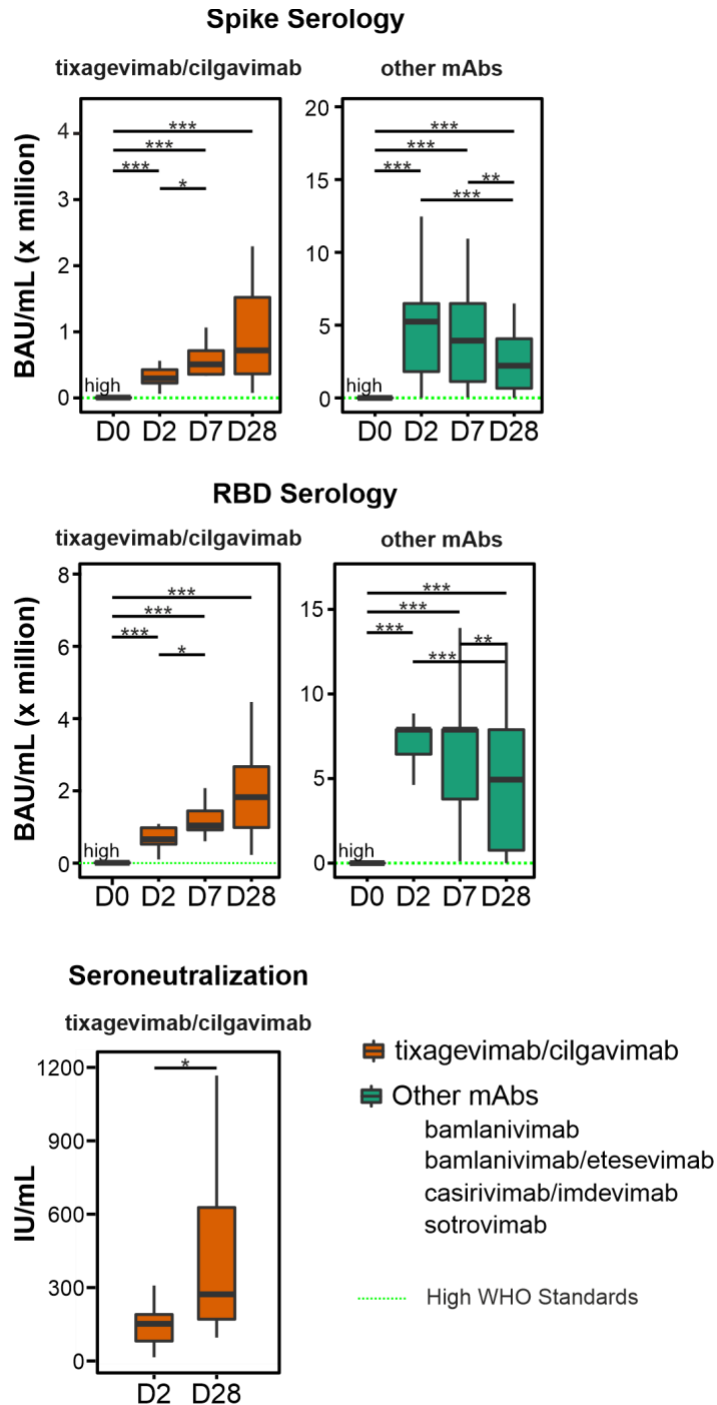


Figure 1. Longitudinal serological and seroneutralisation analysis of mAb titres. Anti-Spike and anti-RBD serology and seroneutralisation titre evolution was measured for tixagevimab/cilgavimab and other relevant mAbs (bamlanivimab, bamlanivimab/etesevimab, casirivimab/imdevimab, sotrovimab) at Day 0 (D0, prior mAb administration) and at Day 2 (D2), Day 7 (D7), and Day 28 (D28) after mAb administration. Additionally, anti-Spike seroneutralisation against the Wuhan variant evolution was measured for tixagevimab/cilgavimab. Box plots indicate median (middle line), 25th, 75th percentile (box), and the 5th and 95th percentile (whiskers). All data points, including outliers, are displayed. *: $p < 0.05$. **: $p < 0.01$. ***: $p < 0.001$

Casirivimab/imdevimab and sotrovimab show non-overlapping superior neutralisation of the majority of Omicron sub-variants

We further evaluated the efficacies or their neutralization potential of studied mAbs against previously and currently circulating SARS-CoV-2 variants using ACE2 neutralization assays (**Figure 2**). We show that casirivimab/imdevimab combination was the most effective therapy against the majority of variants, including de-escalated, Delta and Omicron sub-variants (BA.2, BA.2^{L452M}, BA.2.12, BA.2.75, BA.4.6, BN.1 and BF.7) (**Figure 3**). However, for other sub-variants (BA.1, BA.1^{L452R}, BA.1^{R346K}, BA.2^{L452R}, BA.2.75.2, BA.3, BQ.1, BQ.1.1, XBB.1, and XBB.1.5), sotrovimab demonstrated a significantly superior neutralization capacity. Additionally, for BA.4 and BA.5, casirivimab/imdevimab, sotrovimab, and tixagevimab/cilgavimab demonstrated comparable neutralization. Due to the delayed kinetics response of tixagevimab/cilgavimab, we also compared tixagevimab/cilgavimab neutralisation at Day 28 with neutralisation achieved by other mAbs at Day 2, but did not observe superiority of tixagevimab/cilgavimab over other mAbs in neutralizing different SARS-CoV-2 variants, except BA.2^{L452R}, BA.4, and BA.5 variants (**Supplementary Figure 1**).

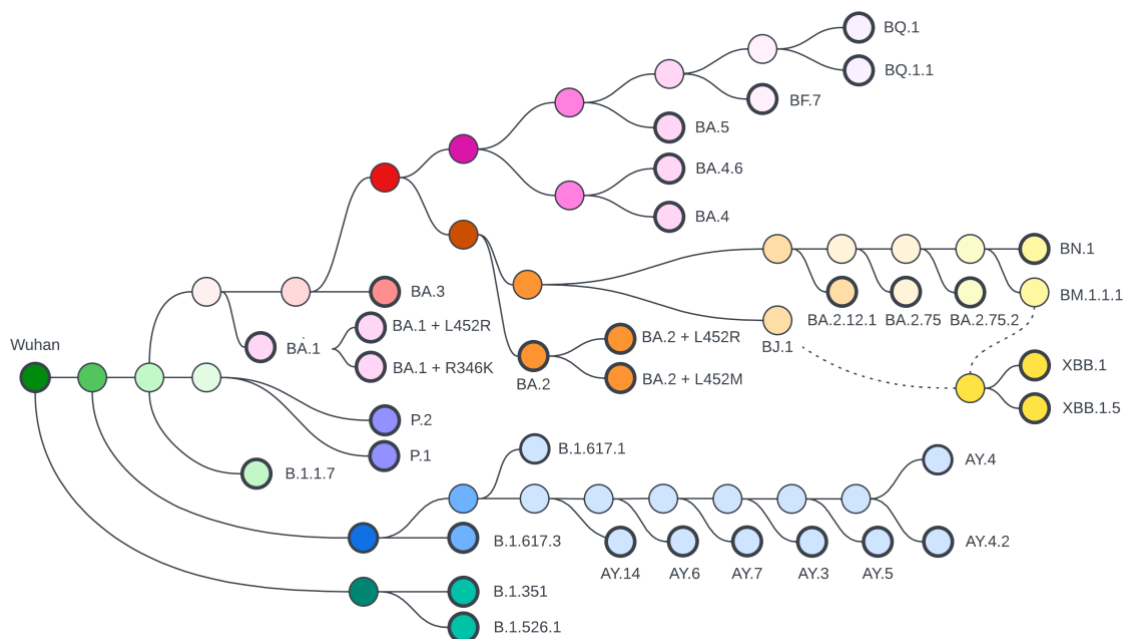
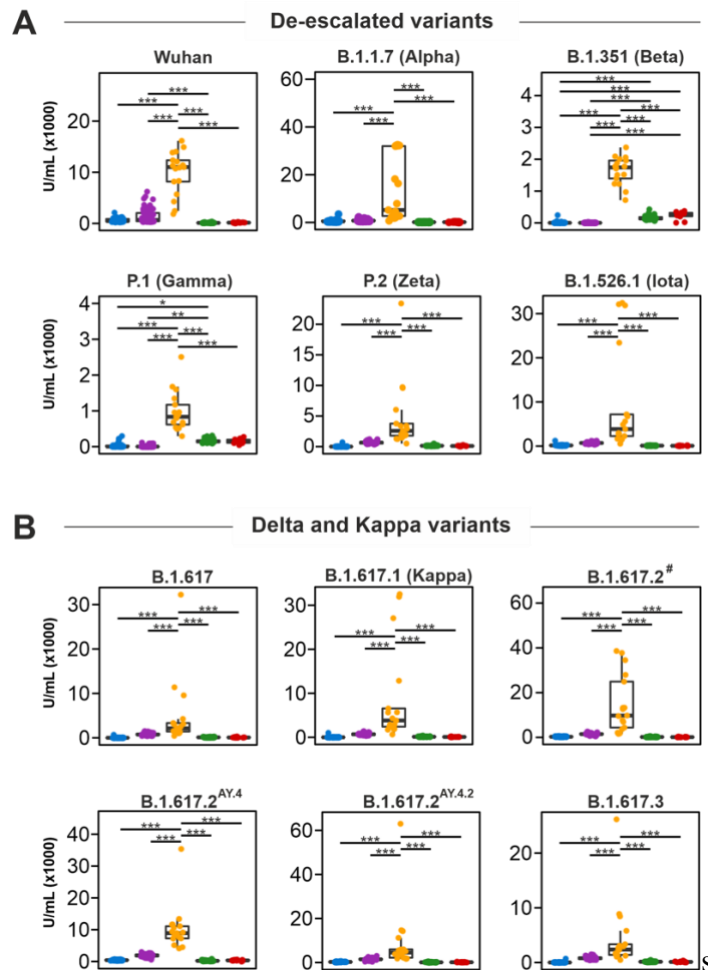


Figure 2. Evolution of SARS-CoV-2 viral variants. Phylogenetic tree built using Nextclade software depicting evolutionary relationships between SARS-CoV-2 variants. SARS-CoV-2 variants that were analyzed in the neutralization assays are highlighted in bold. Dotted line depicts evolution of XBB lineage, which resulted from the recombination between BJ.1 and BM.1.1.1.

Interestingly, we pinpointed several mutations that drove the resistance of certain variants to neutralization with specific mAbs. For example, BA.2 variant with L452R mutation became resistant to neutralization with casirivimab/imdevimab, while L452M mutation did not have a similar effect

(Figure 3). Similarly, BA.4 and BA.4.6 differed by only two mutations (R346T and N658S in BA.4.6), however, BA.4.6 had much more susceptibility to the neutralisation capacities of casirivimab/imdevimab. Additionally, BA.2.75 and BA.2.75.2 variants differing by seven mutations in the Spike protein (del25/27, G142D, K147E, W152R, F157L, R346T, and F486S in the BA.2.75.2 variant), expectedly showed a significantly lowered neutralization potential by both casirivimab/imdevimab and tixagevimab/cilgavimab mAb combinations for BA.2.75.2.

Given the varying efficacy of mAbs in neutralizing the most commonly circulating Omicron sub-variants, we created a recommendation table for choosing a mAb, given the prevalence of circulating VOCs. For this purpose, we stratified neutralisation responses into six equal groups based on the neutralization capacity (**Table 1**). This recommendation table could be used for point-of-care decision making in respect to the choice of the therapeutic mAb. This recommendation table also highlights the fact that tixagevimab/cilgavimab can be very efficient for pre-exposure prophylaxis as highlighted by its efficiency at Day 28, but should not be used off-label for the treatment of COVID-19 patients.



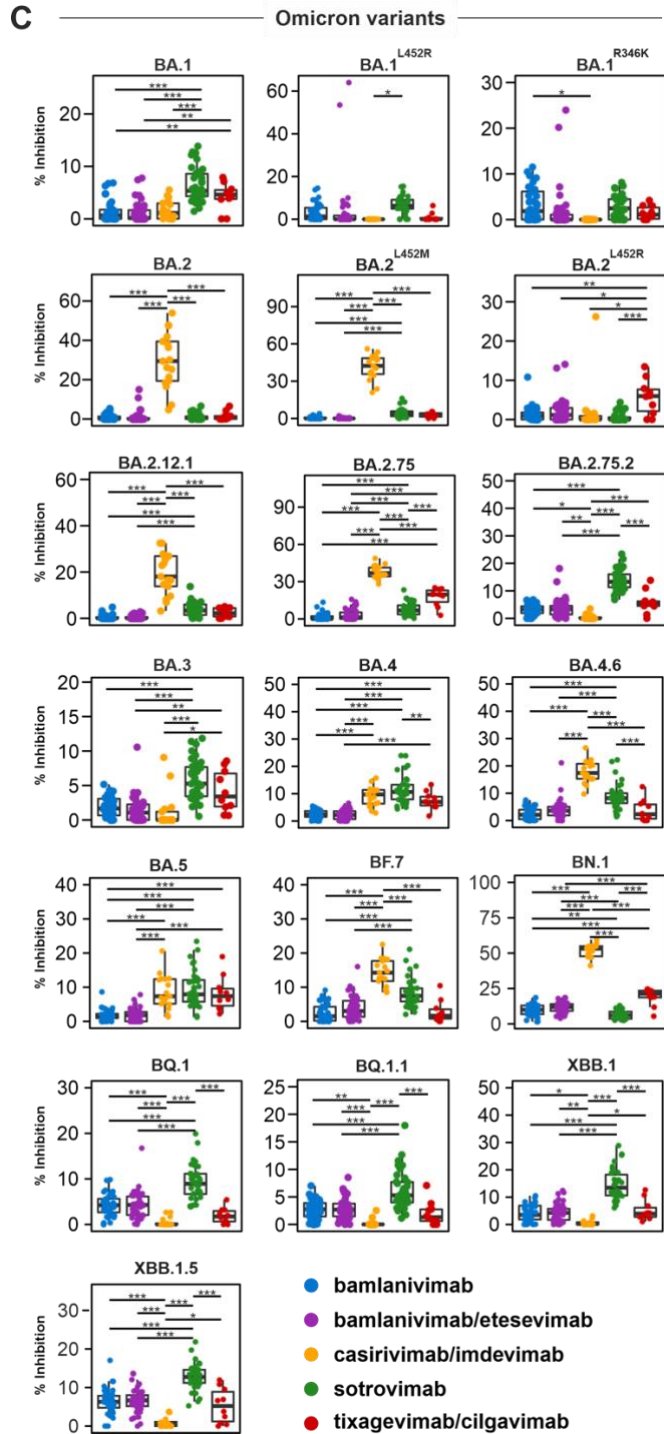


Figure 3. Seroneutralisation analysis following mAb administration. Anti-Spike neutralization capacity of bamlanivimab, bamlanivimab/etesevimab, casirivimab/imdevimab, sotrovimab, and tixagevimab/cilgavimab was measured immediately after mAb administration at Day 2 against de-escalated (A), Delta and Kappa variants (B), and Omicron variants (C), compared to other mAbs. #AY.3.AY.5.AY.6.AY.7.AY.14. Box plots indicate median (middle line), 25th, 75th percentile (box), and the 5th and 95th percentile (whiskers). All data points, including outliers, are displayed. *: $p < 0.05$. **: $p < 0.01$. ***: $p < 0.001$

Table 1. Recommended mAbs for the treatment of infections with or after exposure to different Omicron sub-variants. Studied mAbs were given a score based on the mean %Inhibition as: very poor (“±”; < 12.5%), poor (“+”; 12.5 – <25%), good (“++”; 25 – 37.5%), strong (“+++”; 37.5 – <50%), very strong (“++++”; 50 – <62.5%), excellent (“+++++”; >62.5%). The therapeutic mAb of choice for each Omicron VOC is highlighted in green. When there is no preferred mAb of choice due to poor neutralization capacity, mAbs are highlighted in light green. In case tixagevimab/cilgavimab at D28 was superior to other mAbs, it is highlighted in blue.

	bamlanivimab	bamlanivimab/ etesevimab	casirivimab/ imdevimab	sotrovimab	tixagevimab/ cilgavimab	
	D2	D2	D2	D2	D2	D28
Wuhan	+++++	+++++	+++++	++	++	++++
BA.1	±	±	±	±	±	±
BA.1^{L452R}	±	±	±	±	±	±
BA.1^{R346K}	±	±	±	±	±	±
BA.2	±	±	++	±	±	±
BA.2^{L452M}	±	±	+++	±	±	+
BA.2^{L452R}	±	±	±	±	±	+
BA.2.12.1	±	±	+	±	±	+
BA.2.75	±	±	+++	±	+	++
BA.2.75.2	±	±	±	+	±	+
BA.3	±	±	±	±	±	±
BA.4	±	±	±	±	±	++
BA.4.6	±	±	+	±	±	+
BA.5	±	±	±	±	±	++
BF.7	±	±	+	±	±	+
BN.1	±	±	++++	±	+	++
BQ.1	±	±	±	±	±	+
BQ.1.1	±	±	±	±	±	+
XBB.1	±	±	±	+	±	+
XBB.1.5	±	±	±	+	±	+

Macrophage-associated metabolism of mAbs affects neutralisation by casirivimab/imdevimab

MAbs pharmacokinetics could be affected by the metabolism mechanisms, such as proteolysis by the phagocytic cells of the immune system and the liver, target-mediated elimination through binding to the target and nonspecific endocytosis¹¹. Given the variance among neutralization responses between different variants, we studied the viral and host factors that can affect mAb metabolism. Specifically, we have looked into the casirivimab/imdevimab treatment group, since it demonstrates the most promising neutralization of the majority of variants, including de-escalated Wuhan variant.

Given that mAbs can be removed from the circulation by binding to their target, which in this case is the SARS-CoV-2, we assessed the correlation between Ct values for ORF1ab and N proteins and neutralization titres two days after mAb administration (**Figure 4A**). No correlation was observed for the ORF1ab, while a low insignificant correlation was observed between the N protein and

casirivimab/imdevimab neutralization titres. This suggests a low importance of viral load in the metabolism of mAbs.

Next, we looked into the role of phagocytic immune cells, specifically macrophages, in the metabolism of mAb. Correlation analysis demonstrated that multiple macrophage-secreted cytokines demonstrate a negative correlation trend with casirivimab/imdevimab neutralization titres, with IL-1Ra demonstrating significant correlation (**Figure 4B**). Additionally, we observed a negative correlation trend with a macrophage-stimulating cytokine IFN- γ (**Figure 4C**) and a positive correlation trend with macrophage-inhibiting cytokines IL-13 and IL-4 (**Figure 4D**). This highlights the importance of mAb metabolism by phagocytic immune cells, such as macrophages.

Discussion

This study highlights the importance of carefully monitoring circulating variants and making informed critical decisions on a case-by-case basis when selecting mAb therapy. The withdrawal of mAb therapies from clinical use have led to increasing concerns for managing at-risk patient groups who have shown some benefit from mAbs¹⁻⁴. The mutation prone nature of SARS-CoV-2 presents a new challenge to drug development to keep up with the rapidly emerging variants. Our findings demonstrate that although different mAbs neutralize different variants of concern (VOCs), there is only a minor overlap between their neutralization profiles. This makes point-of-care decision-making crucial in selecting the most appropriate mAb for a given patient.

We identify the range of neutralizing ability of different mAb therapies and support the possibility of re-using previously inefficient mAbs, such as casirivimab/imdevimab and sotrovimab, since their efficiency might be improved with further evolution of VOCs. The results of this study also suggest that it may be necessary to develop mAbs that target a broader range of VOCs to provide optimal therapeutic benefits. This could involve the oligoclonal combination of multiple mAbs with complementary neutralization profiles to ensure a more comprehensive coverage of variants. However, additional clinical studies are needed to evaluate safety and efficacy of these combination therapies.

While we show that further characterization is needed in mAb development, we also identify the pharmacokinetics of mAbs up to 28 days post mAb administration and factors that affect mAb metabolism. The majority of mAbs, except tixagevimab/cilgavimab, reach the highest concentration immediately after administration, ensuring that sufficient mAbs titres are achieved during the most critical phase of the disease – in the beginning of infection. However, a different kinetics trend was observed for tixagevimab/cilgavimab, a combination of intramuscularly administered mAbs, for which the titres continued to increase throughout the study period. Therefore, consistently with the recommendations of the manufacturer, the off-label use of intramuscularly administered tixagevimab/cilgavimab should not be recommended for post-exposure treatment of COVID-19.

Additionally, we identify several viral and host factors that drive faster metabolism of mAbs including, viral load and macrophage-associated cytokines, are indicative of stronger macrophage responses, and correlate with faster metabolization followed by elimination of mAbs. These factors could be used to identify fast-metabolizing patients and adjust the dosing of the mAb treatment to achieve comparable neutralization in all patients. In particular, this observation is important for pre-

exposure prophylaxis in fragile patients, where sufficient protection needs to be maintained for a prolonged period of time^{14,15}.

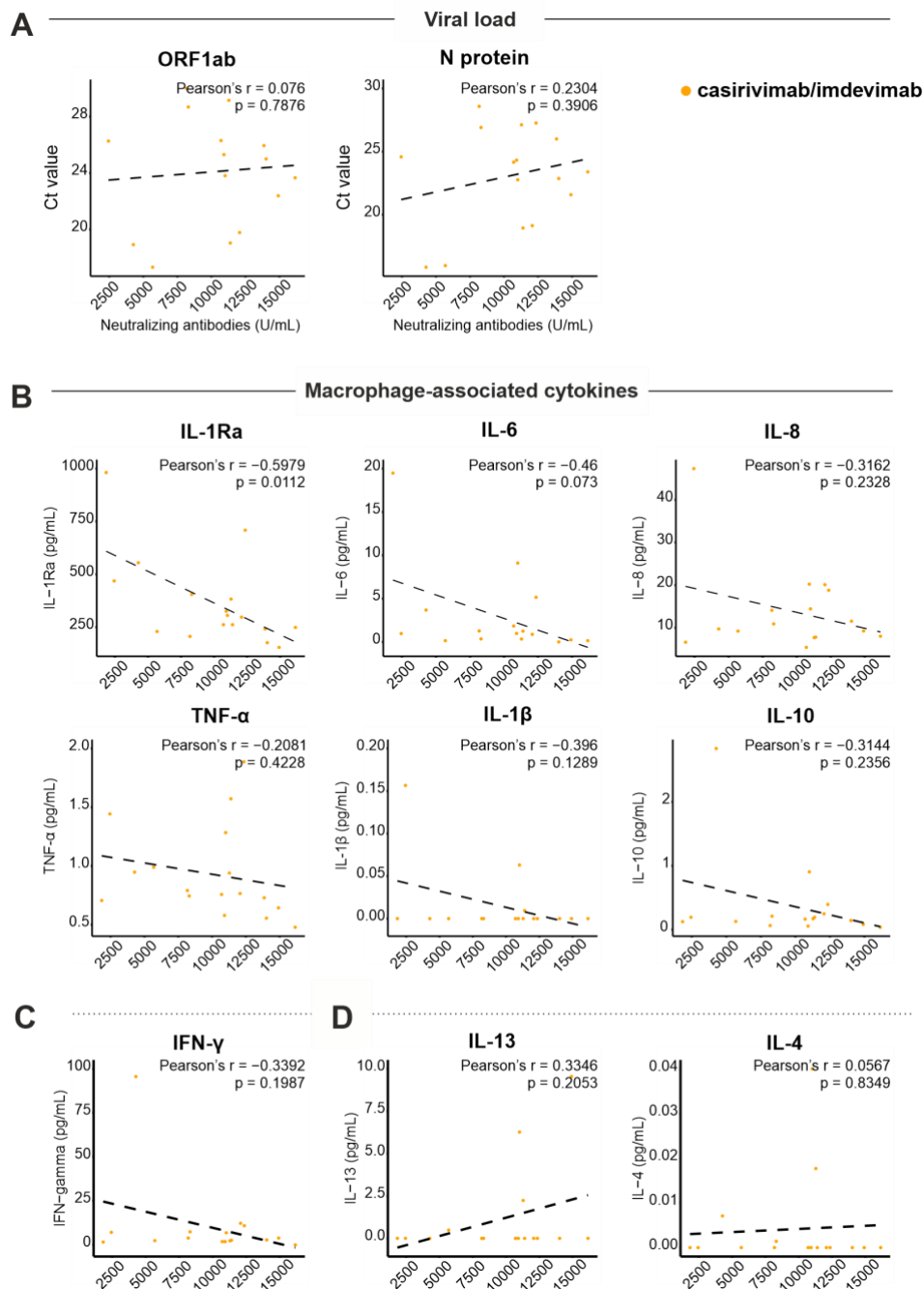
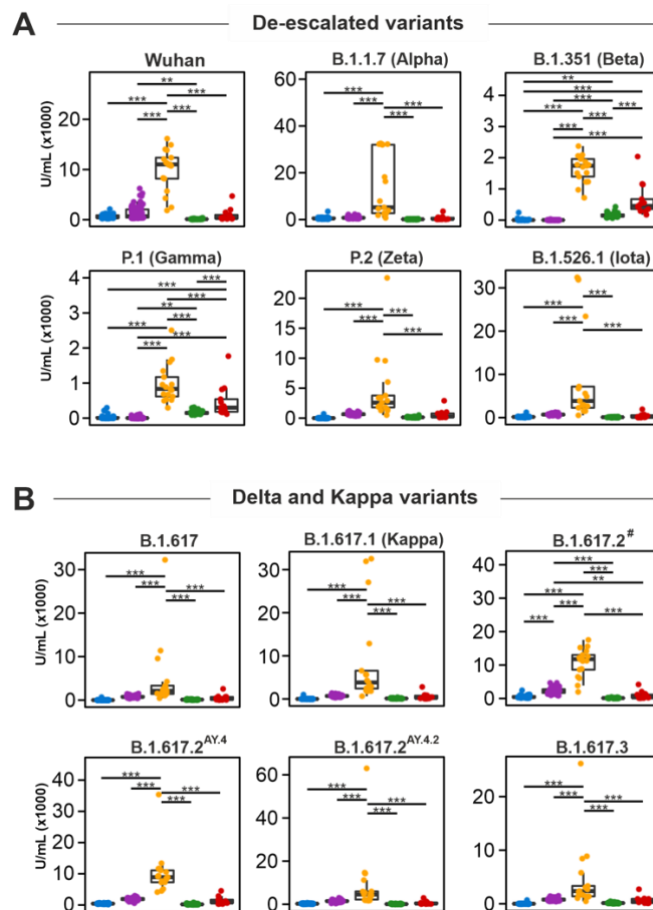


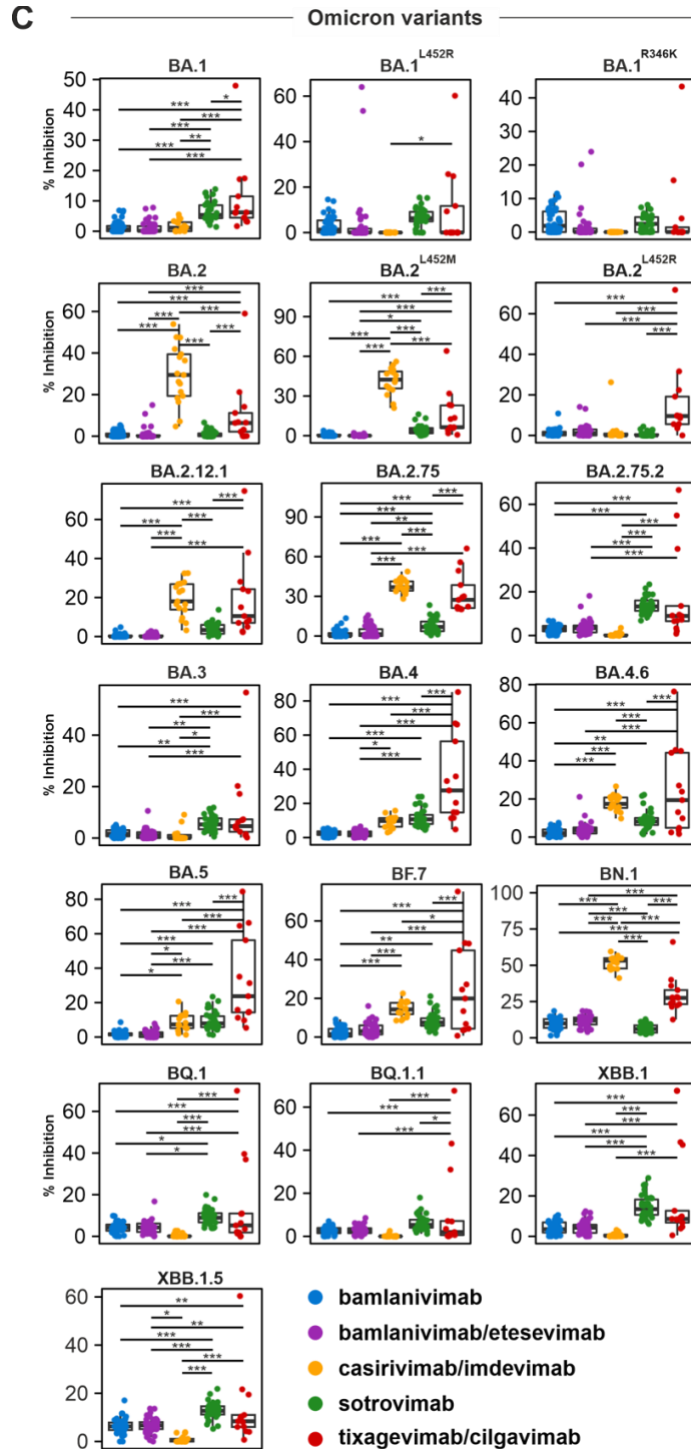
Figure 4. Correlation between seroneutralization and macrophage-associated cytokines. Anti-Spike neutralization capacity of casirivimab/imdevimab was correlated at Day 2 with viral Ct values (A) macrophage-secreted cytokines IL-1Ra, IL-6, IL-8, TNF- α , IL-1 β , and IL-10 (B), macrophage-stimulating cytokine IFN- γ (C) and macrophage-inhibiting cytokines IL-13 and IL-4 (D). Box plots indicate median (middle line), 25th, 75th percentile (box), and the 5th and 95th percentile (whiskers). All data points, including outliers, are displayed.

This study is limited by its varying sample sizes for different therapeutic groups from a monocentric cohort within a European project. The sampling also continued over an extended period of time alongside newly emerging VOCs, however this enables representation of real-world data and accounts for the rapid changes in epidemiological scenarios typical of the SARS-CoV-2 pandemic. Being a prospective monocentric cohort within a European project, this study is limited by heterogenous sampling and lacks validation on a combination of cohorts.

Our study raises concerns about the emergence of new VOCs and highlights the need for ongoing surveillance and development of new mAbs to keep pace with the evolving landscape of the pandemic. These important insights into the use of mAbs for COVID-19 treatment emphasizes the need for careful monitoring and informed decision-making to optimize treatment efficacy. As SARS-CoV-2 becomes a part of the circulating respiratory virus repertoire, ongoing research and development of mAbs will be critical to effectively manage the disease and reduce its impact on public health.

Supplementary Figures





Supplementary Figure 1. Seroneutralisation analysis at the peak day of IgG titres. Anti-Spike neutralization capacity of bamlanivimab, bamlanivimab/etesevimab, casirivimab/imdevimab and sotrovimab was measured at Day 2 and of tixagevimab/cilgavimab at Day 28. Neutralisation capacity was measured against de-escalated (A), Delta and Kappa variants (B), and Omicron variants (C), compared to other mAbs. #AY.3.AY.5.AY.6.AY.7.AY.14. Box plots indicate median (middle line), 25th, 75th percentile (box), and the 5th and 95th percentile (whiskers). All data points, including outliers, are displayed. *: $p < 0.05$. **: $p < 0.01$. ***: $p < 0.001$

References

1. Taylor, P.C., *et al.* Neutralizing monoclonal antibodies for treatment of COVID-19. *Nat Rev Immunol* **21**, 382-393 (2021).
2. Gupta, A., *et al.* Early Treatment for Covid-19 with SARS-CoV-2 Neutralizing Antibody Sotrovimab. *N Engl J Med* **385**, 1941-1950 (2021).
3. Savoldi, A., *et al.* Clinical efficacy of different monoclonal antibody regimens among non-hospitalised patients with mild to moderate COVID-19 at high risk for disease progression: a prospective cohort study. *Eur J Clin Microbiol Infect Dis* **41**, 1065-1076 (2022).
4. Savoldi, A., *et al.* Clinical Impact of Monoclonal Antibodies in the Treatment of High-Risk Patients with SARS-CoV-2 Breakthrough Infections: The ORCHESTRA Prospective Cohort Study. *Biomedicines* **10**, 2063 (2022).
5. Gupta, A., *et al.* Host immunological responses facilitate development of SARS-CoV-2 mutations in patients receiving monoclonal antibody treatments. *J Clin Invest* (2023).
6. Cao, Y., *et al.* BA.2.12.1, BA.4 and BA.5 escape antibodies elicited by Omicron infection. *Nature* **608**, 593-602 (2022).
7. Touret, F., *et al.* In vitro activity of therapeutic antibodies against SARS-CoV-2 Omicron BA.1, BA.2 and BA.5. *Sci Rep* **12**, 12609 (2022).
8. Ai, J., *et al.* Antibody evasion of SARS-CoV-2 Omicron BA.1, BA.1.1, BA.2, and BA.3 sub-lineages. *Cell Host Microbe* **30**, 1077-1083.e1074 (2022).
9. Wang, Q., *et al.* Alarming antibody evasion properties of rising SARS-CoV-2 BQ and XBB subvariants. *Cell* **186**, 279-286.e278 (2023).
10. Planas, D., *et al.* Resistance of Omicron subvariants BA.2.75.2, BA.4.6, and BQ.1.1 to neutralizing antibodies. *Nat Commun* **14**, 824 (2023).
11. Keizer, R.J., Huitema, A.D., Schellens, J.H. & Beijnen, J.H. Clinical pharmacokinetics of therapeutic monoclonal antibodies. *Clin Pharmacokinet* **49**, 493-507 (2010).
12. Dragoni, F., *et al.* Impact of SARS-CoV-2 omicron BA.1 and delta AY.4.2 variants on the neutralization by sera of patients treated with different authorized monoclonal antibodies. *Clin Microbiol Infect* **28**, 1037-1039 (2022).
13. Bruel, T., *et al.* Serum neutralization of SARS-CoV-2 Omicron sublineages BA.1 and BA.2 in patients receiving monoclonal antibodies. *Nat Med* **28**, 1297-1302 (2022).
14. Konnova, A., *et al.* Predictive model for BNT162b2 vaccine response in cancer patients based on blood cytokines and growth factors. *Front Immunol* **13**, 1062136 (2022).
15. Monin, M.B., *et al.* SARS-CoV-2 PrEP complicates antibody testing after vaccination: a call for awareness. *Ann Hematol* **101**, 2089-2090 (2022).

Chapter 7:

Conclusions and Future Perspectives

The overarching goal of this thesis was to expand the knowledge about immune responses to COVID-19 and COVID-19 vaccination with the focus on understanding how host immune responses, especially the ones driven by cytokines, chemokines, and growth factors, pre-determine or affect the course of the disease and vaccination. This thesis builds on the continuing research line of the Molecular Pathology Group in the field of viral and bacterial pneumonias with focus on immune biomarkers [1]. The research work in each chapter significantly contributes to our understanding of COVID-19 treatment and prevention strategies and lays the groundwork for future advancements in the field.

I start this thesis with a comprehensive overview of recent advances in the field of COVID-19 research as well as the roles of different cytokines, chemokines, and growth factors in COVID-19 and COVID-19 vaccination. In **Chapter 1 (Part B)**, I focus on a vulnerable population, specifically cancer patients, since the interplay between cancer-dysregulated and COVID-19-affected immune system compartments remains poorly studied. By reviewing currently available literature, I provide insights into how both acute and long-term COVID-19-related immune dysregulation may affect cancer progression and therapy resistance. This review chapter provides evidence that despite the wide range of cytokines and signalling pathways involved in the immune response, the majority of studies still focus on the most “well-described” cytokines. As the field of cytokinomics has progressed and so have methodologies precisely assessing them, this chapter concludes by suggesting to also incorporate lesser-known cytokines and their signalling pathways to gain a more comprehensive understanding of the immune response to COVID-19 in cancer patients.

Recent advances in the fields of COVID-19 research and cancer also emphasise the urgent need to investigate the potential link between post-COVID-19 syndrome (PCS) and cancer. Patients diagnosed with PCS develop an extended range of persistent symptoms and/or complications from COVID-19, which have a more pronounced effect on the quality of life than advanced or metastatic cancers [2]. Up to 60% of patients with solid or haematological malignancies have long-term sequelae of COVID-19 [3, 4], impacting both their survival and compliance with cancer-specific treatments [3]. However, little is known about molecular and immunological determinants of PCS in cancer patients, leading to the need for the development of prognostic and diagnostic markers in this vulnerable population.

The detrimental effects of COVID-19 infections highlight the importance of effective prevention strategies. COVID-19 vaccination strategies were proven to be very effective in healthy volunteers, but there are still concerns about their ability to protect vulnerable populations, such as cancer patients, solid organ transplant (SOT) recipients, patients living with HIV (PLWH), patients with cystic fibrosis (CF), pregnant women, and children. Previous studies performed by our group [5, 6] have demonstrated diminished antibody responses in cancer patients and SOT recipients. While the data on PLWH/HIV is not a part of this thesis, within the ORCHESTRA consortium, we have also demonstrated a diminished antibody responses in patients with CF and PLWH, in which serological data was complemented by cellular immunity analysis. In **Chapters 3 and 4**, we focus on

understanding molecular and clinical determinants of sufficient post-vaccine antibody response in immunocompromised patients with the focus on patients with solid and haematological malignancies and SOT recipients, respectively.

Specifically, in **Chapter 3** and published as [7], we identify a persistent blood-based signature consisting of dysregulated C-reactive protein (CRP), interleukin (IL)-15, IL-18, and placental growth factor (PIGF) that correctly classifies patients with a diminished antibody response with more than 80% accuracy. This signature remains robust at all studied timepoints and was not majorly affected by different anti-cancer treatments, highlighting the importance of pro-inflammatory cytokines and growth factors in dictating the inherent immune response in cancer patients and determining post-vaccine protection. Given the accessibility of blood biomarker measurements, particularly CRP measurements, we believe that this unique signature would not only be useful for clinicians in identifying cancer patients at high risk of developing COVID-19, but also would be able to guide health policies in terms of categorising cancer patients in need of booster vaccine doses or pre-exposure prophylaxis with monoclonal antibodies to protect potential non-responders to the COVID-19 vaccine.

In **Chapter 4** and published as [8] and [9], we studied antibody responses in SOT transplant recipients after the administration of up to three doses of the COVID-19 vaccine and determined that almost one fourth of patients do not respond to vaccination. Together with our study group (EU H2020 ORCHESTRA), we identify clinical factors that could be predictive of diminished antibody response (measured at the University of Antwerp), such as age, metabolites and steroid treatments, type of transplantation, and time since transplantation. However, machine learning models utilising these parameters were only able to reach moderate level of prediction accuracy, suggesting that the clinical covariates provide only limited information. Nevertheless, understanding clinical determinants of vaccination response in fragile populations is essential for patient management and allocation of resources, such as vaccines and prophylactic treatments. We are going to utilize CCG profiling of this patient population to investigate whether adding immune-related variables are able to increase the prediction accuracy.

Given the importance of pre-exposure prophylaxis or effective COVID-19 treatment in non-responders to COVID-19 vaccines, we continue with the investigation into monoclonal antibody (mAb) treatments in **Chapter 5** that was published as [10]. Together with colleagues from my second promotor's group (Laboratory of Medical Microbiology), we demonstrate that patients treated with different mAb combinations, such as bamlanivimab, bamlanivimab/etesevimab, casirivimab/imdevimab, and sotrovimab, developed evasive Spike mutations with remarkable speed and high specificity to the targeted mAb-binding sites. We specifically demonstrate that downregulated pro-inflammatory cytokines are linked with higher SARS-CoV-2 mutation rates, likely due to decreased viral clearance and increased replicative cycles of the virus, which give SARS-CoV-2 a higher chance to adapt evolutionarily. Additionally, we describe an upregulation of key host growth factors, such as angiogenic growth factors and their receptors, which could be a consequence of SARS-CoV-2-induced lung damage. A variant reparative milieu, likely also genetically driven, while facilitating a rapid recovery of patients, could allow boosted cell infection cycles enabling the virus to adapt. MAb pharmacokinetic evaluation further showed that levels of all mAbs were retained at more than one million BAU/mL over 4 weeks, suggesting a sustained longstanding environment wherein mutant SARS-CoV-2 could be sheltered and mutate further,

posing threats for viral rebound infections and dissemination of novel mutants. Lastly, this chapter suggests that assessment of CRP or Serum amyloid A (SAA) in blood with a set of specific pro-inflammatory and reparative growth factors in high-risk patients with SARS-CoV-2 infection receiving mAbs therapies could identify patients who are also at high risk of developing escape mutations against therapeutic mAbs. This or similar biomarker-based stratification could also benefit clinical decision making. For example, identification of immunocompromised patients who are at high risk of developing *de novo* mutations could benefit from alternative strategies such as anti-viral treatments or convalescent plasma containing high titres of polyclonal antibodies [11-13].

Chapter 6 focuses on a different aspect of mAb treatment, specifically ability of bamlanivimab, bamlanivimab/etesevimab, casirivimab/imdevimab, sotrovimab, and tixagevimab/cilgavimab combinations to neutralize different SARS-CoV-2 variants of concern (VOCs), including currently circulating Omicron variants. Our findings support the possibility of re-using previously inefficient mAbs, such as casirivimab/imdevimab and sotrovimab as their efficiency improved with further evolution of VOCs. However, none of the currently available mAb combinations are able to effectively neutralize all circulating VOCs, suggesting that it might be necessary to develop mAbs that target a broader range of VOCs to provide optimal therapeutic benefits. This could involve the oligoclonal combination of multiple mAbs with complementary neutralization profiles to ensure a more comprehensive coverage. Overall, this study underscores the importance ongoing surveillance for new variants and the concurrent development of novel mAbs to keep pace with the evolving landscape of the pandemic.

Future perspectives and deep cytokine profiling

Although the bulk of the COVID-19 pandemic is behind us, several fragile populations of patients remain at high risk of developing severe COVID-19 or dying from COVID-19. Within the ORCHESRA consortium and this thesis, we have demonstrated that patients with solid and haematological malignancies, SOT recipients, PLWH, patients with CF, and patients with rheumatological conditions are at a higher risk of developing insufficient responses to COVID-19 vaccines and therefore contracting a more severe disease. Currently, these patients are being followed-up up to 12 months after the administration of the 3rd booster dose, however, continuous monitoring is required to ensure sufficient protection and vaccination and prophylaxis policies guidance. Additionally, antibody response monitoring should continuously be adjusted based on the circulating SARS-CoV-2 variants in order to assess humoral responses correctly. Insufficient responses to the vaccines in these fragile patient populations are caused by their immunocompromised status, which results from either the immunological effect of the underlying condition, or therapy needed for the effective management of the condition, or the combination of both. It is frequently reflected in the dysregulation of CCGs and can therefore be used to predict vaccine response prior to vaccine administration. In this thesis, we developed a CCG signature predictive of vaccination response in cancer patients, but predictive signatures for other fragile populations of patients remain to be studied. In fact, due to the nature of the immunocompromising state being different between the studied patient populations, it might be expected to have different CCG signatures predictive of vaccination response in these patients. Additionally, antibody response signatures could be developed vaccines targeting other diseases, such as Influenza and RSV. We believe that these biomarker signatures would not only be useful for clinicians in identifying patients

at increased risk of developing a severe disease for better patient care, but also be able to guide health policies in categorizing patients in need of enhancer vaccine doses or pre-exposure prophylaxis with antivirals or synthetic monoclonal antibodies to protect potential non-responders to the vaccines.

Additionally, while there is a growing body of literature on the role of cytokines in COVID-19 infection and vaccination, there is still much to be learnt. Despite the wide range of cytokines and signalling pathways involved in the immune responses, the majority of studies still focus on rather well-described cytokines and ignoring many other potentially important CCGs and signalling pathways, the role of which in the immune response to COVID-19 remains unknown. While focusing on known CCGs, such as those identified in patients with acute COVID-19 or post-COVID-19 patients with PCS, future research should also explore lesser-known cytokines and signalling pathways to gain a more comprehensive understanding of the immune response to COVID-19 that would help to understand and tackle consequences of COVID-19. Deep cytokine profiling could eventually play a crucial role in developing personalised treatment plans, improving patient outcomes and treatment compliances.

In conclusion, much like an orchestra, where the contributions of each instrument may seem minimal and indistinguishable among others, the influence of cytokines, chemokines and growth factors on COVID-19 is also subtle and may not be overtly noticeable, however, they play a crucial role in coordinating and orchestrating various immune responses important in COVID-19 disease and its prevention and treatment. Research findings described in this thesis utilise these variables to understand the molecular pathology of COVID-19 and hopefully would provide a lasting impact on ongoing efforts to combat this global health crisis and its aftermath.

References

1. De Winter, F.H.R., et al., Blood Cytokine Analysis Suggests That SARS-CoV-2 Infection Results in a Sustained Tumour Promoting Environment in Cancer Patients. *Cancers (Basel)*, 2021. **13**(22).
2. Walker, S., et al., Impact of fatigue as the primary determinant of functional limitations among patients with post-COVID-19 syndrome: a cross-sectional observational study. *BMJ Open*, 2023. **13**(6): p. e069217.
3. Pinato, D.J., et al., Prevalence and impact of COVID-19 sequelae on treatment and survival of patients with cancer who recovered from SARS-CoV-2 infection: evidence from the OnCovid retrospective, multicentre registry study. *Lancet Oncol*, 2021. **22**(12): p. 1669-1680.
4. Dagher, H., et al., Long COVID in cancer patients: preponderance of symptoms in majority of patients over long time period. *Elife*, 2023. **12**.
5. Giannella, M., et al., Evaluation of the Kinetics of Antibody Response to COVID-19 Vaccine in Solid Organ Transplant Recipients: The Prospective Multicenter ORCHESTRA Cohort. *Microorganisms*, 2022. **10**(5).
6. Peeters, M., et al., Reduced humoral immune response after BNT162b2 coronavirus disease 2019 messenger RNA vaccination in cancer patients under antineoplastic treatment. *ESMO Open*, 2021. **6**(5): p. 100274.

7. Konnova, A., et al., Predictive model for BNT162b2 vaccine response in cancer patients based on blood cytokines and growth factors. *Front Immunol*, 2022. **13**: p. 1062136.
8. Savoldi, A., et al., Clinical Impact of Monoclonal Antibodies in the Treatment of High-Risk Patients with SARS-CoV-2 Breakthrough Infections: The ORCHESTRA Prospective Cohort Study. *Biomedicines*, 2022. **10**(9).
9. Giannella, M., et al., Using machine learning to predict antibody response to SARS-CoV-2 vaccination in solid organ transplant recipients: the multicentre ORCHESTRA cohort. *Clin Microbiol Infect*, 2023. **29**(8): p. 1084.e1-1084.e7.
10. Gupta, A., et al., Host immunological responses facilitate development of SARS-CoV-2 mutations in patients receiving monoclonal antibody treatments. *J Clin Invest*, 2023.
11. Ripoll, J.G., et al., Vaccine-boosted convalescent plasma therapy for patients with immunosuppression and COVID-19. *Blood Adv*, 2022. **6**(23): p. 5951-5955.
12. Estcourt, L.J., et al., Clinical Practice Guidelines From the Association for the Advancement of Blood and Biotherapies (AABB): COVID-19 Convalescent Plasma. *Ann Intern Med*, 2022. **175**(9): p. 1310-1321.
13. Agarwal, A., et al., A living WHO guideline on drugs for covid-19. *Bmj*, 2020. **370**: p. m3379.

Academic CV – Angelina Konnova

Contact information

ORCID: 0000-0001-9353-8026

LinkedIn: <https://www.linkedin.com/in/angelina-konnova-60508910a/>

Tel: +32 477 04 74 95 | Email: konnovaangelina@gmail.com

Education

- 2020 – 2023 PhD in Medical Sciences – University of Antwerp, Belgium
PhD thesis: Immunological biomarkers of COVID-19: response to vaccination and monoclonal antibody treatments in immunocompromised patients
- 2019 – 2020 PhD in Biomedical Sciences – KU Leuven, Belgium
PhD thesis: Exploiting the “dark matter” of the genome to defeat melanoma
- 2017 – 2019 MSc in Biomedical Sciences - KU Leuven, Belgium
Master’s thesis: Treating melanoma as an infectious disease
- 2014 – 2017 BA in Biological Sciences - University of Oxford, UK
Bachelor’s thesis: The influence of progesterone, testosterone, dexamethasone and tuftsin on the expression of the endogenous retrovirus HLM2 in the NCCIT cells
- 2012 – 2014 School of Young Politicians - Gymnasium 1306, Russia
IB Diploma Program and Russian Diploma Program

Publications

1. **Konnova A***, De Winter FHR*, Gupta A, Verbruggen L, Hotterbeekx A, Berkell M, Teuwen L-A, Vanhoutte G, Peeters B, Raats S, Massen IVd, De Keersmaecker S, Debie Y, Huizing M, Pannus P, Neven KY, Ariën KK, Martens GA, Van Den Bulcke M, Roelant E, Desombere I, Anguille S, Berneman Z, Goossens ME, Goossens H, Malhotra-Kumar S, Tacconelli E, Vandamme T, Peeters M, van Dam P and Kumar-Singh S (2022) Predictive model for BNT162b2 vaccine response in cancer patients based on blood cytokines and growth factors. *Front. Immunol.* 13:1062136. doi: 10.3389/fimmu.2022.1062136
2. Gupta A*, **Konnova A***, Smet M*, Berkell M*, Savoldi A, Morra M, Van averbeke V, De Winter F, Peserico D, Danese E, Hotterbeekx A, Righi E, De Nardo P, Tacconelli E,

- Malhotra-Kumar S and Kumar-Singh S (2022). *Host immunological responses facilitate development of SARS-COV-2 mutations in patients receiving monoclonal antibody treatments*. J Clin Invest <https://doi.org/10.1172/JCI166032>
3. Giannella M, Huth M, Righi E, Hasenauer J, Marconi L, **Konnova A**, Gupta A, Hotterbeekx A, Berkell M, Palacios-Baena ZR, Morelli MC, Tamè M, Busutti M, Potena L, Salvaterra E; Work Package 4.ORCHESTRA study group; Feltrin G, Gerosa G, Furian L, Burra P, Piano S, Cillo U, Cananzi M, Loy M, Zaza G, Onorati F, Carraro A, Gastaldon F, Nordio M, Kumar-Singh S, Baño JR, Lazzarotto T, Viale P, Tacconelli E. *Using machine learning to predict antibody response to SARS-CoV-2 vaccination in solid organ transplant recipients: the multicentre ORCHESTRA cohort*. Clin Microbiol Infect. 2023 May 6:S1198-743X(23)00201-X. doi: 10.1016/j.cmi.2023.04.027
 4. Savoldi A, Morra M, De Nardo P, Cattelan AM, Mirandola M, Manfrin V, Scotton P, Giordani MT, Brollo L, Panese S, Lanzafame M, Scroccaro G, Berkell M, Lippi G, **Konnova A**, Smet M, Malhotra-Kumar S, Kumar-Singh S, Tacconelli E; mAb Working Group. *Clinical efficacy of different monoclonal antibody regimens among non-hospitalised patients with mild to moderate COVID-19 at high risk for disease progression: a prospective cohort study*. Eur J Clin Microbiol Infect Dis. 2022 Jul;41(7):1065-1076. doi: 10.1007/s10096-022-04464-x
 5. Savoldi A*, Morra M*, Castelli A, Mirandola M, Berkell M, Smet M, **Konnova A**, Rossi E, Cataudella S, De Nardo P, Gentilotti E, Gupta A, Fasan D, Gibbin E, Puviani FC, Hasenauer J, Gusinow R, Tami A, Kumar-Singh S, Malhotra-Kumar S, mAb Orchestra Working Group, Tacconelli E. *Clinical Impact of Monoclonal Antibodies in the Treatment of High-Risk Patients with SARS-CoV-2 Breakthrough Infections: The ORCHESTRA Prospective Cohort Study*. Biomedicines. 2022 Aug 24;10(9):2063. doi: 10.3390/biomedicines10092063
 6. Gentilotti E, Górska A, Tami A, Gusinow R, Mirandola M, Rodríguez Baño J, Palacios Baena ZR, Rossi E, Hasenauer J, Lopes-Rafegas I, Righi E, Caroccia N, Cataudella S, Pasquini Z, Osmo T, Del Piccolo L, Savoldi A, Kumar-Singh S, Mazzaferri F, Caponcello MG, de Boer G, Hara GL; **ORCHESTRA Study Group**; De Nardo P, Malhotra S, Canziani LM, Ghosn J, Florence AM, Lafhej N, van der Gun BTF, Giannella M, Laouénan C, Tacconelli E. *Clinical phenotypes and quality of life to define post-COVID-19 syndrome: a cluster analysis of the multinational, prospective ORCHESTRA cohort*. EClinicalMedicine. 2023 Jul 21;62:102107. doi: 10.1016/j.eclinm.2023.102107. PMID: 37654668; PMCID: PMC10466236
 7. Giannella M, Righi E, Pascale R, Rinaldi M, Caroccia N, Gamberini C, Palacios-Baena ZR, Caponcello G, Morelli MC, Tamè M, Busutti M, Comai G, Potena L, Salvaterra E, Feltrin G, Cillo U, Gerosa G, Cananzi M, Piano S, Benetti E, Burra P, Loy M, Furian L, Zaza G, Onorati F, Carraro A, Gastaldon F, Nordio M, Kumar-Singh S, Abedini M, Boffetta P, Rodríguez-Baño J, Lazzarotto T, Viale P, Tacconelli E, On Behalf Of The **Orchestra Study Group Workpackage**. *Evaluation of the Kinetics of Antibody Response to COVID-19 Vaccine in Solid Organ Transplant Recipients: The Prospective Multicenter ORCHESTRA Cohort*. Microorganisms. 2022 May 12;10(5):1021. doi: 10.3390/microorganisms10051021

8. De Winter FHR*, Hotterbeekx A*, Huizing MT, **Konnova A**, Fransen E, Jongers B, Jairam RK, Van Averbeke V, Moons P, Roelant E, Le Blon D, Vanden Berghe W, Janssens A, Lybaert W, Croes L, Vulsteke C, Malhotra-Kumar S, Goossens H, Berneman Z, Peeters M, van Dam PA, Kumar-Singh S. *Blood Cytokine Analysis Suggests That SARS-CoV-2 Infection Results in a Sustained Tumour Promoting Environment in Cancer Patients*. *Cancers* (Basel). 2021 Nov 15;13(22):5718. doi: 10.3390/cancers13225718
9. Bouvy S*, Ceulemans L*, **Konnova A***, Mennens R*, Nankova M*, Nguyen T*, Sandler JP*, Van Laere T*, Vandamme AM, Baelen J, Langeret J, Thyssen P. *Uprooting Deeper Causes of Belgium's Lack of Pandemic Preparedness in the Covid-19 Crisis*. *Transdisciplinary Insights*, 5(1), pp. 7–8. doi:10.11116/tdi2021.5.1.4.
10. Vendramin R, Katopodi V, Cinque S, **Konnova A**, Knezevic Z, Adnane S, Verheyden Y, Karras P, Demesmaeker E, Bosisio FM, Kucera L, Rozman J, Gladwyn-Ng I, Rizzotto L, Dassi E, Millevoi S, Bechter O, Marine JC, Leucci E. *Activation of the integrated stress response confers vulnerability to mitoribosome-targeting antibiotics in melanoma*. *J Exp Med*. 2021 Sep 6;218(9):e20210571. doi: 10.1084/jem.20210571
11. Jacobs L*, Kattumana T*, **Konnova A***, Obasa M*, Smlatic E*, Vandendriessche V*, Voragen F*, Boey L, Vandermeulen C. *How Storytelling Can Combat Vaccine Hesitancy: a Transdisciplinary Approach*. *Transdisciplinary Insights*, 2(1), pp. 92–103. doi:10.11116/tdi2018.2.4.

Manuscripts in preparation/Abstracts submitted

1. **Konnova A***, Gupta A*, Savoldi A, Morra M, Berkell M, Smet M, Hotterbeekx A, Righi E, mAb ORCHESTRA working group, Malhotra-Kumar S, De Nardo P, Tacconelli E, and Kumar-Singh S. *Serological and seroneutralization analyses of five monoclonal antibodies, including tixagevimab/cilgavimab (Abstract submitted to ECCMID 2023)*
2. **Konnova A***, De Winter FHR*, Hotterbeekx A, van Dam P and Kumar-Singh S. *The misuse of the immune system by tumours might affect how cancer patients deal with infections such as the SARS-CoV-2 virus (Review)*.
3. Righi E*, Gupta A*, **Konnova A**, Sciammarella C, Spiteri G, Wouters S, Berkell M, Sartor A, Mirandola M, Malhotra-Kumar S, Azzini A, Pezzani D, Lourdes Monaco MG, Porru S, Tacconelli E and Kumar-Singh S. *Longitudinal humoral and cellular responses after SARS-CoV-2 vaccination in people living with HIV (Abstract submitted to ECCMID 2023)*
4. Hotterbeekx A, Lebourgeois S, **Konnova A**, Menidjel R, Tubiana S, Gupta A, Berkell M, Laouénan C, Gentilotti E, Gorska A, Malhotra-Kumar S, Tacconelli E, Ghosn J, Charpentier C and Kumar-Singh S. *Cytokine dynamics in the acute and post-acute phase of hospitalized COVID-19 patients and their link to disease severity, mortality, and Long COVID (Abstract submitted to ECCMID 2023)*
5. Hotterbeekx A*, De Winter FHR*, Vujkovic A*, Theunissen C, **Konnova A**, van Petersen L, Lammens M, van Rafelghem B, Jacobs W, Kumar Jairam R, 's Jongers B, Brosius I, Van Ierssel S, van Frankenhuijsen M, Berkell M, Malhotra-Kumar S, Vlieghe E, Vercauteren K

and Kumar-Singh S. *Predicting ARDS development in hospitalized patients with high accuracy utilizing machine learning approach based on TGFβ, IL-10, VEGF-C and CX3CL1*

6. Tagarro A, **Konnova A**, Gastesi I, Gupta A, Salso S, Berkell M, Villanueva S, Guillén R, Manzanares A, Giaquinto C, Dominguez S, Ballesteros A, Kumar-Singh S and Moraleda C. *Neutralisation of SARS-CoV-2 variants after BNT162b2 in children from 5 to 11 years* (Abstract submitted to CROI 2023)
7. Tagarro A, **Konnova A**, Gastesi I, Gupta A, Salso S, Berkell M, Villanueva S, Guillén R, Manzanares A, Giaquinto C, Dominguez S, Ballesteros A, Aguilera-Alonso D, Kumar-Singh S and Moraleda C. *Cellular and Humoral response correlation after SARS-CoV-2 mRNA vaccine in children* (Abstract submitted to CROI 2023)
8. Caponcello MG, Palacios Baena ZR, Olivares Navarro P, Gutierrez Campos D, Huth M, Alvarez Garavito C, Hasenauer J, Garcia-Sancez MI, Hidalgo AB, Hrom I, **Konnova A**, Berkell M, Kumar-Singh S, Cataudella S, Rodriguez-Fernandez A, Palazon-Carrion N, Caroccia N, Giannella M, Taconelli E, Rodriguez Bano J. *Evolution of antibody responses after vaccination against SARS-CoV-2 in a cohort of immunosuppressed patients* (Abstract submitted to ECCMID 2023 and SEIMC 2023)

Oral and poster presentations

1. **Konnova A***, De Winter FHR*, Gupta A, Verbruggen L, Hotterbeekx A, Berkell M, Teuwen L-A, Vanhoutte G, Peeters B, Raats S, Massen IVd, De Keersmaecker S, Debie Y, Huizing M, Pannus P, Neven KY, Ariën KK, Martens GA, Van Den Bulcke M, Roelant E, Desombere I, Anguille S, Berneman Z, Goossens ME, Goossens H, Malhotra-Kumar S, Tacconelli E, Vandamme T, Peeters M, van Dam P and Kumar-Singh S. *Predictive model for BNT162b2 vaccine response in cancer patients treated with anti-neoplastic drugs based on blood cytokines and growth factors* (Poster presentation at BelCoVac 2023)
2. **Konnova A***, Gupta A*, Savoldi A, Morra M, Berkell M, Smet M, Hotterbeekx A, Righi E, mAb ORCHESTRA working group, Malhotra-Kumar S, De Nardo P, Tacconelli E, and Kumar-Singh S. *Serological and seroneutralization analyses of five monoclonal antibodies, including tixagevimab/cilgavimab* (Oral presentation at ECCMID 2023)
3. **Konnova A***, De Winter FHR*, Gupta A, Verbruggen L, Hotterbeekx A, Teuwen L-A, Vanhoutte G, Peeters B, Raats S, Massen IVd, De Keersmaecker S, Debie Y, Huizing M, Pannus P, Neven KY, Ariën KK, Martens GA, Van Den Bulcke M, Roelant E, Desombere I, Anguille S, Berneman Z, Goossens ME, Malhotra-Kumar S, Goossens H, Vandamme T, Peeters M, van Dam P and Kumar-Singh S. *A predictive model for development of immune response based on cytokines, chemokines and growth factors in blood of cancer patients receiving BNT162b2 mRNA COVID-19 vaccine* (Oral presentation at ECCMID 2022)

Guidance in Master and Bachelor Dissertations

Lise Van Der Heyden	Bachelor dissertation: The immune response to SARS-CoV-2 in transplant patients
Luca Degreef	Bachelor dissertation: Immunoprofiling of patients infected with SARS-CoV-2 (Breakthrough infections)
Amber Willemsen	Bachelor dissertation: Immunoprofiling of patients infected with SARS-CoV-2 (Omicron infections)
Shahla Mamoudi	Master dissertation: Host immune response in patients infected with SARS-CoV-2 with or without anti-SARS-CoV-2 treatment

Grants/Awards

1. 33rd ECCMID 2023 Travel Grant (15 – 18 April 2023, Copenhagen, Denmark)

Acknowledgements

The completion of this PhD thesis has been a significant milestone in my academic journey, and it would not have been possible without the collective support and collaboration of numerous individuals. As the world faced the challenges imposed by the COVID-19 pandemic, it also witnessed the power of unity and the establishment of collaborations that have shaped the research presented in this thesis. I am immensely grateful to all those who have offered their guidance, encouragement, and assistance throughout this journey.

I would like to express a special thank you to my best friend **Iria**, whose unwavering support and encouragement played a crucial role in setting me on the path of this PhD journey. Despite 668 kilometres that separate us, you have been by my side every day from the very beginning, offering support and motivation whenever it was needed the most. Your constant presence during the most challenging moments (and 30-minute food recipes that you are always happy to share with me) provided me with the energy and strength I needed to walk till the finish line. As you are about to finish your own PhD, I want to take this opportunity to wish you the very best of luck in the next step of your career. May this part of your life be filled with personal growth, success, fulfilment, and happiness.

There is one more person, without whom this PhD would not have been possible. That person is my exceptional co-PhD and friend, **Akshita**. Akshita, your journey in this lab started directly with a 20-hour experiment with me, but it did not scare you and you did not give up. As a result, we had many more sleepless nights in the lab, but also co-authored multiple publications and travelled all over the world, including Portugal, Luxemburg, the Netherlands, Germany, Switzerland, Croatia, Italy, France, Denmark, India and the UK. Our duet is now highly efficient, to the point where we often joke that together we form one functioning human being. In the beginning of this PhD, I have promised you one big thank you at the end, so here it is: THANK YOU! I am also extending this thank you to your partner **Steven**, without whom I would have never discovered esquissy or Ascension.

I want to extend a big thank you to **Matthias** for supporting me during the last leg of this incredible journey. Your constant validation, guidance and positivity have been beyond amazing. Your faith in me has truly been a driving force, and I'm so lucky to have had you by my side. Here's to the exciting adventures ahead – couldn't have done it without you!

My sincere gratitude goes to my promotor **Prof. Samir Kumar-Singh** and my co-promotor **Prof. Surbhi Malhotra-Kumar** for providing me with the exceptional opportunity to work on the ORCHESTRA project. Within ORCHESTRA, we managed to revolutionize our understanding of COVID-19 treatments and vaccination, creating a tangible impact on patients. I would also like to extend my gratitude to **Prof. Evelina Taconelli**, the coordinator of ORCHESTRA, and other dedicated ORCHESTRA partners involved in this collaborative effort. I would also like to thank **Prof. Peter van Dam, Timon, Lise** and **Yana** for a successful collaboration in the B-Voice project, which started as a side project and ended with two chapters of this thesis. Their collective expertise, relentless dedication, and unwavering commitment to advancing our knowledge of infectious diseases have been truly inspiring.

I would also like to thank my jury members, **Prof. Annemieke Smet**, **Prof. Ingrid De Meester**, **Prof. Lieve Naesens**, **Prof. Charlotte Charpentier**, and **Prof. Wim Adriansen**, for their invaluable feedback, time, and expertise. Your contributions have significantly enhanced the quality of this thesis.

To all my colleagues at the Molecular Pathology Group, past and present, I am incredibly grateful for your invaluable contributions that have significantly shaped my research journey. I am deeply appreciative of daily support provided by **Dr. An Hotterbeekx** and **Dr. Matilda Berkell**, who have taken the burden of the ORCHESTRA project almost completely off my shoulders. I would also like to extend a special thank you to fellow PhD students that greeted me in this group in the beginning of my PhD. **Fien**, **Vincent**, **Ravi** and **Bart**, thank you for guiding me through my first experiments and manuscripts, successes and disappointments. I can list numerous moments with you that I will never forget: mouse experiments in the middle of the night, exploring the beautiful city of Lisbon, driving through the winding roads of Croatia and chilling on its beaches afterwards, filming and editing Fien's graduation video as well as the defence itself, heartfelt conversations during Akshita's birthdays, and many more to remember. I am also grateful to **Shari**, a PhD student who joined us full-time last year, for bringing structure and balance to our everyday lives. I am fully convinced that you are strong and smart enough to also finish this journey. **Proesha** and **Vincent**, thank you for taking over experiments during the last leg of my PhD journey. Without you, I would not have been able to focus on finishing my thesis and would also not have been able to enjoy such a friendly and supporting atmosphere in the lab. Finally, I would like to thank **Jasper**, who despite not officially belonging to our group, has been unofficially adopted by us. Thank you for bringing humour to everyday situations and providing support in the most challenging times. Altogether we had a lot of fun inside and outside of the lab!

I am also grateful to all the students that I had a chance to work with during the past three years. **Bato**, you were able to bring your authentic self and remind us to enjoy life in the middle of the pandemic. **Shahla**, you have helped us tremendously by organizing and processing an incredible number of patient samples. **Amber**, **Lise** and **Luca**, you were able to form such a well-functioning team that we sometimes had to question whether you can replace all of us. You also set extremely high standards for the next generations of students joining the lab. **Sofia**, your kindness, positivity and willingness to learn were truly inspiring. **Celestine**, despite the change of the project, you managed to set very high standards for yourself and achieve them to the fullest. **Dizzy** and **Luna**, you managed to demonstrate incredible maturity and knowledgeability, despite being in the very beginning of your scientific journey. **Ana**, **Genis** and **Yoel**, you formed another brilliant team that took over all of the last experiments in the lab, allowing me to finish this thesis. **Talar**, your kind, supportive and understanding personality definitely has definitely helped me throughout the perturbations of the last steps of this process. I am immensely grateful and can already see a very bright future ahead of all of you and wish you the best of luck in your future endeavours.

My gratitude also goes to all the people of the Laboratory of Cell Biology and Histology, including **Sarah DB**, **Sarah P**, **Lauren**, **Lana**, **Robin**, **Lenny**, **Freya**, **Marlies**, **Roxane**, **Rosanne**, **Nouchine**, **Johanna**, **Peter**, **Tim**, **Samuel**, **Isabel**, **Sofie**, **Inge**, **Margot**, **Karen**, and **Elien** as well as **Prof. Jean-Pierre Timmermans**, **Prof. Winnok De Vos**, **Prof. Sales Ibiza Martinez**, and **Prof. John-Paul Bogers**. Together, you have made this lab feel like one big family that is always ready to support all of its members. From the joyous piñatas to the lunches in the "put" in the summer, we have shared

laughter and created lasting memories. And during the difficult moments, I always knew that I could talk to anyone of you. Additionally, a special thank you goes to **Sofie** for finding us absolutely anything that was needed and fixing everything that we broke along the way (including an enormous number of pipettes).

A special thank you also goes to my horses **Klara, Funky, and Royal**, as well as to the exceptional individuals at the stables who have been an integral part of our journey. **Laurens** and **Emily**, thank you for the devoted care and unwavering commitment over the past five years that have allowed us to grow and thrive each day. I am immensely grateful to **Catherine** for providing invaluable help with Klara, enabling me to focus on completing this thesis. Thank you to "The Rescue Team" consisting of **Iria, Anja, Ellen** and **Alexis**, for the delightful evenings filled with talking and laughter that have brought so much joy. Additionally, I want to thank **Emma** for taking care of my horses when I couldn't be there and for patiently listening to my occasional complaints. Thank you to everyone else, including **Inne, Nathalie, Anne-Sophie, Sandrina, Marina, Karlien, Charlotte, Sarah, Siemon, Alexis, Annie, Zdenka, Githa**, and **Tine** for your presence, friendship, and dedication have made this journey all the more meaningful, and I am forever grateful for the role each of you has played in my life.

As the new chapter in my life is now starting, I want to thank the organisation called A Seat At The Table (ASATT) and personally **Mariam** for their invaluable support and for fostering an environment that encourages personal and professional growth. I am immensely grateful to my exceptional mentors, **Daniel** from McKinsey and **Joke** from AstraZeneca, for their guidance, wisdom, and shared expertise. I can say for sure that without these people I would not have had such a clarity about what the next chapter is going to be about.

Lastly, but certainly not least, I want to express my deepest gratitude to my **family** for their unwavering support throughout my entire journey. Their unconditional love, encouragement, and belief in me have been the bedrock of my success. They have stood by me through the challenges, celebrated my achievements, and provided a constant source of strength and inspiration. I am forever grateful for their faith in my abilities, from getting into Oxford to getting a PhD. Their presence in my life has been a source of immense motivation, and I am truly blessed to have such an incredible family by my side.

Thank you for everything!

Angelina